Mangrove ecosystems as a key to understand Late Quaternary climate and sea-level changes

Von der Fakultät für Georessourcen und Materialtechnik der
Rheinisch-Westfälischen Technischen Hochschule Aachen

zur Erlangung des akademischen Grades eines

Doktors der Naturwissenschaften

genehmigte Dissertation

vorgelegt von

M.Sc. Valeska Decker

Berichtende: **Herr PD Dr. rer. nat. Gösta Hoffmann**

Herr Univ.-Prof. Peter Kukla, PhD

Tag der mündlichen Prüfung: 30.01.2026

Diese Dissertation ist auf den Internetseiten der Universitätsbibliothek online verfügbar.

a) Decker, V., Falkenroth, M., Lindauer, S., Landgraf, J., Al-Lawati, Z., Al-Rahbi, H., Franz, S. O. & Hoffmann, G. (2021). Collapse of Holocene mangrove ecosystems along the coastline of Oman. *Quaternary Research, 100*, 52–76. https://doi.org/10.1017/qua.2020.96 [1]

Copyright: © University of Washington. Published by Cambridge University Press, 2020. Reprinted with permission, license number: 6074831486197.

b) Decker, V., Gee, C. T., Schucht, P. J., Lindauer, S., & Hoffmann, G. (2022). Life on the Edge: A Powerful Tsunami Overwhelmed Indian Ocean Mangroves One Millennium Ago. *Forests, 13(6)*, 922. https://doi.org/10.3390/f13060922

Copyright: © 2022 by the authors. Licensee MDPI, Basel, Switzerland. This article is an open access article distributed under the terms and conditions of the Creative Commons Attribution (CC BY) license (https://creativecommons.org/licenses/by/4.0/).

c) Decker, V., Falkenroth, M., & Hoffmann, G. (2024). Sedimentological evidence of Late Pleistocene shorelines in Oman. *Marine Geology, 477*, 107407. https://doi.org/10.1016/j.margeo.2024.107407

Copyright: © 2024 The Authors. Published by Elsevier B.V. This is an open access article under the CC BY license (http://creativecommons.org/licenses/by/4.0/).

Examination Board / Prüfungskommission
Herr PD Dr. habil. Gösta Hoffmann
Herr Univ.-Prof. Peter Kukla, PhD
Herr Univ.-Prof. Dr. Klaus Reicherter

Reviewer/Berichter
Herr PD Dr. habil. Gösta Hoffmann
Herr Univ.-Prof. Peter Kukla, PhD

[1] This publication was extended by a Corrigendum: *Quaternary Research, 100,* 260–262. https://doi.org/10.1017/qua.2021.6 ; reprinted with permission, license number: 6074831486197.

Statutory Declaration

Declaration of Generative AI and AI-assisted technologies in the writing process: During the preparation of this work I used ChatGPT in order to improve the language and readability. After using this tool, I reviewed and edited the content as needed and I take full responsibility for the content of this thesis.

Hereby, I declare that I have written this thesis on my own and have not used any aids other than those stated. All passages that are quoted or paraphrased from other sources have been clearly marked as such.

Meckenheim, 14. May 2026

_____

(Valeska Decker)

"Alles hängt mit allem zusammen." – Everything is linked.

[Alexander von Humboldt, 1769-1859]

Content

List of Abbreviations I
Abstract II
Kurzfassung III
1. Introduction and aim of this thesis 13
2. Study Area 4
2.1 Landscape characteristics 4
2.2 Geological overview 6
3. State of the art 8
3.1 Late Quaternary Climate Variabilities and Sea-Level Changes 8
3.1.1 Study-area-specific climate research 11
3.1.2 Study-area-specific sea-level research 14
3.2 Mangroves as climate and sea-level indicators 17
4. Study sites, applied methods and co-working – a short overview 20
5. Publications 22
5.1.1 Collapse of Holocene mangrove ecosystems along the coastline of Oman (Decker et al. 2021) 22
5.1.2 Collapse of Holocene mangrove ecosystems along the coastline of Oman – *Corrigendum* 48
5.2 Life on the Edge: A Powerful Tsunami Overwhelmed Indian Ocean Mangroves One Millennium Ago (Decker et al. 2022) 52
5.3 Sedimentological evidence of Late Pleistocene Shorelines in Oman (Decker et al. 2024) 65
6. Resumée 85
6.1 Discussion 85
6.2 Conclusions 88
6.3 Future research directions 89
7. Acknowledgements 91
8. References 93
APPENDIX 106
I. LIST OF PUBLICATIONS 106
II. PERSONAL CONFERENCE CONTRIBUTIONS 106

List of Abbreviations

BP = Before Present (before 1950 CE)

cal y BP = calibrated years Before Present

CE = Common Era, secular alternative to AD (Anno Domini)

ka = kilo annum = 1,000 years

Ma = million years

M_w = Moment magnitude scale; a logarithmic scale used to measure the magnitude of earthquakes

Abstract

The Late Quaternary period on the Arabian Peninsula exhibits considerable variability in both climatic regimes and sea-levels. Generally, cooler and drier conditions accompanied by lower sea-levels prevailed during Marine Isotope Stage (MIS) 6, MIS 5d and 5b, MIS 4, and MIS 2. In contrast, warmer and wetter phases with rising sea levels and sea-level highstands occurred during MIS 5e, 5c, and 5a, MIS 3, and MIS 1 (the Holocene). In general, periods of climatic amelioration, marked by moderate temperatures and increased precipitation, are referred to as Windows of Opportunity – such intervals were particularly favorable for human dispersal and the exploration of new migration routes.

MIS 5e, also known as the Last Interglacial, holds particular significance for paleo-climate and sea-level studies. Occurring around 120,000 to 130,000 years ago, this period was characterized by global mean surface temperatures 0.5 to 1 °C higher than today and sea levels approximately 3 to 4 m above current levels. Owing to its relative recency, MIS 5e is well-represented in global geological archives. Although the driving forces behind MIS 5e warming, such as solar insolation and orbital variations differ from those of modern climate change, which is mostly driven by greenhouse gas emissions, studying this period offers valuable insights into Earth system responses to warming and serves as a crucial analogue for anticipating future sea-level rise.

This thesis focuses on three distinct time periods, each characterized by specific climatic and sea-level indicators derived from geological archives along the northeastern coast of Oman. The research was conducted between 2017 and 2024. Fieldwork involved identifying signs of past climate and sea-level across the coastline, ultimately leading to the detailed investigation of 16 localities. These findings contribute to three peer-reviewed publications, one Master's thesis, and three Bachelor's theses. The investigations employed an interdisciplinary approach, integrating sedimentology, micropaleontology, geochemistry, and biology to thoroughly analyze the study sites. The primary outcomes are as follows:

a) **Late Pleistocene, Last Interglacial**: tentatively 125,000-year-old marine sediments exposed along the northern and eastern Omani coastline document a sea-level highstand of about 3 to 4 meters above present mean sea level. These findings align with global MIS 5e records and are therefore attributed to this interglacial period.

b) **Mid-Holocene**: about 6,000 year old paleo-lagoon deposits along the northern and eastern coastlines of Oman contain remnants of paleo-mangrove ecosystems in their basal layers. These are sharply overlain by aeolian sands and sabkha deposits, reflecting a sudden collapse of mangrove communities within decades, due to aridification processes. The transition marks the surpassing of a critical ecological threshold during the Mid-Holocene. Because mangroves exhibit a distinct zonation within the intertidal zone, centimeter-precise elevation measurements of mangrove-horizons can serve as reliable indicators of paleo-sea level. Based on this study, these horizons suggest that sea level was near or at present-day levels at the time of deposition.

c) **Late Holocene**: Sedimentary records from the lagoon of Sur reveal evidence of a tsunami event that led to the destruction of a local mangrove stand around 1,000 years ago. Incorporated wood

remains, histologically identified as *Avicennia marina*, provided suitable dating material. This represent the only known record of mangrove wood remains in this area during that time.

These findings contribute to a better understanding of past climate and sea-level fluctuations, the dynamics of Earth system processes, and the response of coastal ecosystems to changing conditions. This knowledge is particularly relevant for modern coastal risk management and can inform adaptation strategies for vulnerable areas, especially under the accelerating impacts of anthropogenic-driven climate change and sea-level rise.

Kurzfassung

Die Arabische Halbinsel ist im späten Quartär von signifikanten klimatischen Veränderungen und Meeresspiegelfluktuationen geprägt. Im Allgemeinen sind kühlere und trockenere Klimabedingungen verknüpft mit niedrigeren Meeresspiegelständen. Das ist während der Marinen Isotopenstadien (MIS) 6, MIS 5d und 5b, MIS 4 und MIS 2 zu erkennen. Wärmere und feuchtere Bedingungen gehen hingegen oft einher mit steigenden Meeresspiegeln und Meeresspiegelhochständen, zu sehen während MIS 5e, 5c und 5a und während MIS 3 und MIS 1, dem Holozän. Generell sind solche klimatisch günstigen Zeiten mit wärmeren Temperaturen und mehr Niederschlag sogenannte „Windows of Opportunity“, Zeitfenster der Möglichkeiten für Menschen neue Migrationsrouten auszuprobieren und neues Land zu erschließen.

Das MIS 5e, auch bekannt als Letztes Interglazial, ist besonders bedeutend hinsichtlich der Klima- und Meeresspiegelforschung. Während dieser Zeit, vor ca. 120.000 bis 130.000 Jahren, war die globale durchschnittliche Temperatur der Landoberfläche ca. 0,5 bis 1 °C wärmer als heute und der globale Meeresspiegel etwa 3 bis 4 Meter über dem heutigen Stand. Das Letzte Interglazial ist aus heutiger Perspektive gesehen der nächstgelegene Zeitabschnitt mit höheren Temperaturen und Meeresspiegelständen und wird dadurch oft als Analogbeispiel hergenommen, um mögliche Zukunftsszenarien zu konstruieren. Dabei ist jedoch wichtig zu beachten, dass die Erwärmung während des MIS 5e auf orbitale Veränderungen und dadurch bedingt auf eine veränderte Insolation zurückzuführen ist, während die rezente Erwärmung der anthropogenbedingten Treibhausgasemission zuzuschreiben ist.

Diese Arbeit fokussiert drei Zeiträume und deren besondere Klima- und Meeresspiegelbedingungen im Nordosten Omans anhand geologischer Untersuchungen. Geländearbeiten und Analysen der Proben fanden im Zeitraum zwischen 2017 und 2024 statt. Die Geländearbeiten umfassten eine Exploration der Nordost-Küste auf Paläo-Klima- und Meeresspiegel-Hinweise. Insgesamt wurden final 16 Lokalitäten eingehend untersucht. Die Ergebnisse der Forschungen sind als drei Peer-Reviewed-Publikationen veröffentlicht. Außerdem entstanden eine Masterarbeit und drei Bachelorarbeiten. Die Untersuchungen bauen auf einem interdisziplinären Ansatz auf und inkludieren sedimentologische, mikropaläontologische, geochemische und biologische Analyseverfahren. Die Hauptergebnisse sind im Folgenden aufgeführt:

a) Spätes Pleistozän, Letztes Interglazial: In etwa 3 bis 4 Meter Höhe über dem heutigen Meeresspiegel sind entlang der omanischen Nordostküste Ablagerungen zu finden, die eindeutig

einem marinen Umweltraum zuzuordnen sind. Da direkte Altersdatierungen noch ausstehen, wurden sie stratigraphisch zu umliegenden, datierten Ablagerungen in Bezug gesetzt und lassen so auf eine Entstehung während des Meeresspiegelhochstands während des MIS 5e, dem Letzten Interglazial vor etwa 125.000 Jahre schließen.

b) Mittleres Holozän: Etwa 6.000 Jahre alte Paläo-Lagunen sind entlang der Nord- und Ostküste nachweisbar. In den unteren Sedimentschichten heutiger Küstensabkhas finden sich Lagunensedimente mit Hinweisen auf Mangrovenbestände entlang der Uferzone. Der Übergang von Lagune zu Sabkha stellt sich in den Profilanschnitten äußerst scharf dar und spiegelt die Überschreitung eines Kipppunktes mit folgendem Kollaps der Mangrovenökosysteme entlang der Küste wider. Da Mangroven artspezifisch eine ganz bestimmte Zone innerhalb des Intertidals besiedeln, ist ein zentimeter-genaues Einmessen der Höhe der Paläo-Mangroven aussagekräftig bezüglich des damaligen Meeresspiegels. Unsere Ergebnisse zeigen, dass der Meeresspiegel im Untersuchungsgebiet vor etwa 6.000 Jahren mit maximal wenigen Zentimetern Abweichung, in etwa auf heutigem Niveau war.

c) Spätes Holozän: Sedimentologisch analysierte Ablagerungen in der Lagune von Sur zeigen Hinweise auf einen Tsunami, der vor etwa 1.000 Jahren den damaligen Mangrovenbestand in der Lagune zerstörte. In die tsunamigene Muschelschicht eingeregelte, lange Hölzer, die histologisch der Art *Avicennia marina* zugeordnet werden konnten, boten entscheidendes Datierungsmaterial. Solch ein Nachweis eines Mangrovenbestandes ist dort einzigartig für diesen Zeitraum.

Die Ergebnisse dieser Forschungen tragen zu einem verbesserten Verständnis vergangener Klima- und Meeresspiegelveränderungen bei und helfen, Zusammenhänge zwischen Erdprozessen und deren Auswirkungen auf Ökosysteme entlang der Küsten aufzuzeigen. Das kann vor allem den modernen Küstenschutz unterstützen und helfen, Anpassungsstrategien zu entwickeln, insbesondere vor dem Hintergrund des anthropogen-bedingten Klimawandels und Meeresspiegelanstiegs.

1. Introduction and aim of this thesis

The aim of this thesis was to identify and investigate evidence of Quaternary climate history, as well as long- and short-term sea-level changes, in the region of northeastern Oman on the eastern Arabian Peninsula (Figs. 1, 2). The results contribute to the global effort to reconstruct past climate and sea-level dynamics and to draw conclusions about ongoing processes and environmental changes. The necessity and importance of such efforts arise from the fact that coastal areas are the most densely populated regions on Earth, and even minor sea-level changes, just a few centimetres, can have significant impacts on millions of people (IPCC 2023; Bange et al. 2017). Currently, a global rise in sea level is being observed and has been verified by the Intergovernmental Panel on Climate Change (IPCC), with *high confidence* that it is predominantly anthropogenic in origin (Oppenheimer et al. 2019). The scientific consensus on anthropogenic climate change in peer-reviewed literature exceeds 99% agreement (Lynas et al. 2021). Importantly, sea-level rise is not occurring at a constant rate but is exponential: while the average rate was 1.4 mm per year between 1902 and 1990, it increased to 2.1 mm/year between 1970 and 2015, 3.2 mm/year between 1993 and 2015, and 3.6 mm/year between 2006 and 2015 (Oppenheimer et al. 2019). The discourse on climate and sea-level change is no longer limited to the academic sphere but now plays a prominent role in public and political discussions. It is present in both digital social media and face-to-face conversations. Therefore, it is even more important that scientists feel the responsibility to ensure that these debates are informed by well-substantiated, evidence-based scientific facts.

Research on past climate and sea-level changes also holds significant archaeological relevance, given that climate has always shaped human activity, and that early settlements were commonly established along coasts, rivers, and lake shores (Erlandson 2017; Petraglia 2003; Small & Nicholls 2003). The reconstruction of the paleo-environment helps us to better understand our human history: which lifestyles people chose, the availability of raw materials and natural resources, how people were influenced by environmental change — and, conversely, how much influence they had, and still have, on the environment. While modern climate and sea-level changes are well recorded by global measuring networks, information becomes increasingly scarce the further back we look in time. Only the geoscientific archive can shed light on the paleo-habitat, and highlight intervals that were characterized by conditions favourable to early human dispersal and the exploration of new migration routes. In this context, paleo-climatic and paleo-shoreline reconstructions are of particular importance.

This doctoral thesis is submitted as a cumulative dissertation, comprising three peer-reviewed publications published in international journals (cf. chapters 5.1 (Decker et al. 2021), 5.2 (Decker et al. 2023) and 5.3 (Decker et al. 2024)). The cover illustrations for the individual publications depict the environmental settings, highlighting key features related to climate and sea-level history, as well as the associated biota of the given periods (Figs. 3-5). The publications integrate research across the disciplines of sedimentology, paleo-botany, and sediment geochemistry, with support from radiocarbon dating methods. This interdisciplinary approach is essential for understanding the interconnected processes of the Earth system and for comprehending our planet as a whole.



Fig. 1: Overview maps of the broader study area. a) Regional map indicating major geographic locations and geological features referenced in the text, as well as the tracks of significant recent tropical cyclones. b) Detailed map highlighting the investigated sites and their corresponding publications included in this thesis (basemaps: ESRI World Imagery, visualized using QGis 3.16).

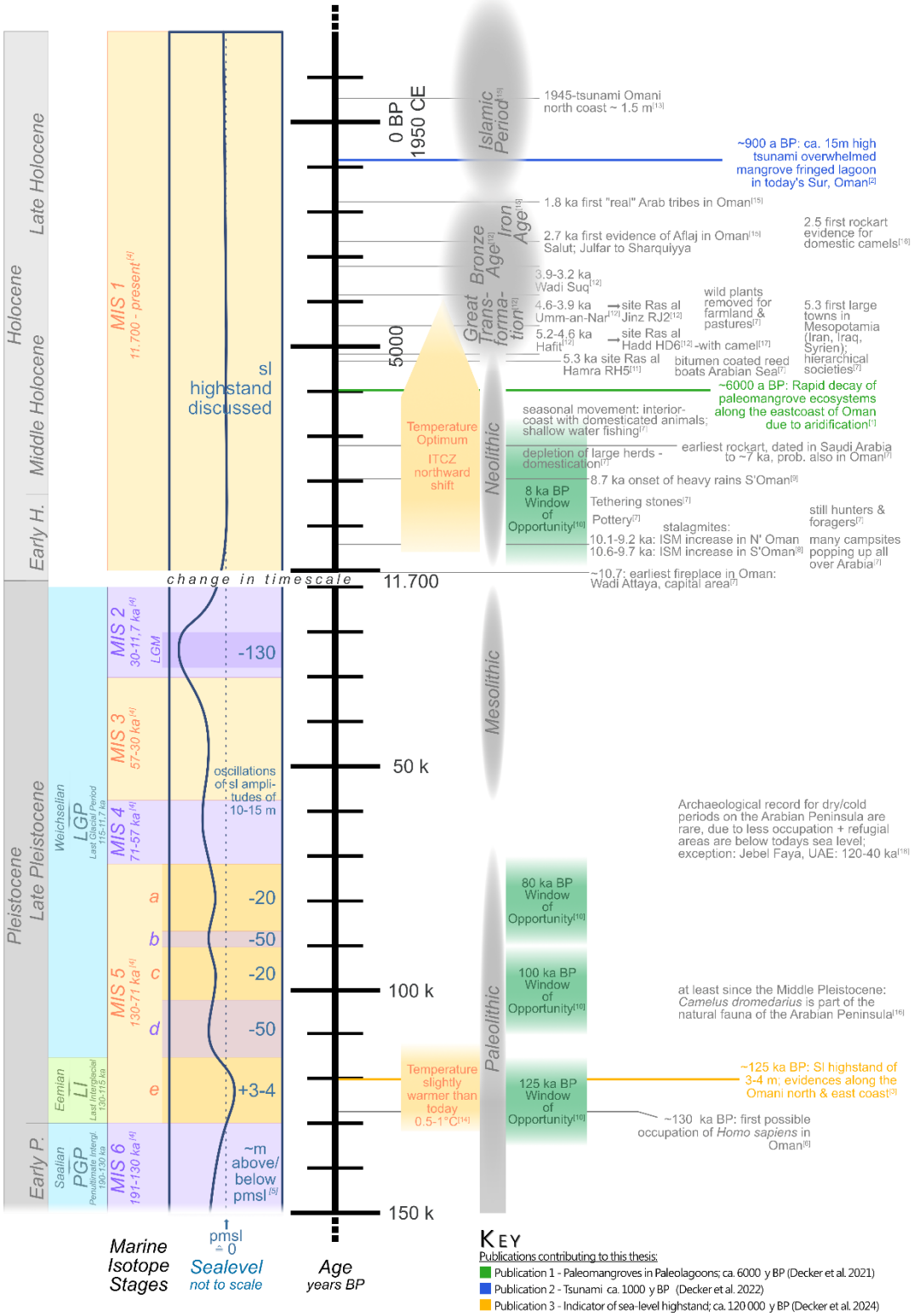

Fig. 2: Chronological timeline from the Late Pleistocene to the present, illustrating significant site-specific geological and archaeological events, phases, and processes. An additional section visualizes estimated sea-level fluctuations over time. The research contributions forming the basis of this thesis are highlighted in green (Decker et al. 2021), blue (Decker et al. 2022), and orange (Decker et al. 2024). (References: [1] Decker et al. 2021; [2] Decker et al. 2022; [3] Decker et al. 2024; [4] Cohen et al. 2013; [5] Lambeck et al. 2002; [6] Armitage et al. 2011; [7] Cleuziou & Tosi 2007; [8] Fleitmann et al. 2007; [9] Cremaschi & Negrino 2005; [10] Rosenberg et al. 2011; [11] Biagi & Nisbet 1999; [12] Azzarà 2009; [13] Hoffmann et al. 2013a; [14] Oppenheimer et al. 2019; [15] Wilkinson 2002; [16] Zarins 1978; [17] Curci et al. 2014; [18] Bretzke et al. 2022).

2. Study Area

2.1 Landscape characteristics

Location, geomorphology and recent climate

The study area is located in the eastern part of the Arabian Peninsula, within the Sultanate of Oman. Oman is bordered to the north by the Gulf of Oman, and to the east and south by the Arabian Sea, which is part of the Indian Ocean. It shares land borders with Yemen to the southwest, Saudi Arabia to the west, and the United Arab Emirates to the northwest (Fig. 1a). Additionally, Oman includes the Musandam Peninsula, an exclave strategically positioned along the Strait of Hormuz, the maritime corridor connecting the Gulf of Oman with the Persian Gulf (Figs. 1a, 1b).

Muscat, the capital, spans approximately 60 km along the northern coastline and has expanded westward from its historic core in Muttrah over the last couple of decades. The city is located on the Batinah Plain, a coastal lowland north of the Hajar Mountain range (Fig. 1a). This plain represents the distal zone of a large alluvial fan system, which was primarily active during earlier pluvial periods when erosional debris from the Hajar Mountains was transported to the coast. Today, Oman's shorelines are mostly sandy beaches, although gravel beaches, such as those near Tiwi, and pocket beaches in more rugged coastal settings (e.g., As Sifah, Ras Madraka), also occur. A notable geomorphological setting is the lagoonal environment at Bandar Khayran, which supports mangrove habitats. These mangrove forests are now under protection and subject to reforestation through government programs. Larger mangrove stands occur in the intertidal zone in sheltered locations like in Sawadee, Qurum, Sur, and Filim. Oman’s coastline experiences a mesotidal regime, with spring tides reaching up to 3 m, and generally low to moderate wave energy (McLachlan et al. 1998). Significant coastal upwelling enhances marine productivity, supporting a rich ecosystem that has sustained human populations since prehistoric times (Cleuziou & Tosi 2007).

Inland, the Hajar Mountains, Oman's most prominent geomorphological feature, run for about 650 km, from the Musandam Peninsula in the northwest to Ras Al Hadd in the east (Fig. 1a). The highest peak, Jebel Shams, the “Mountain of the Sun”, reaches approximately 3,000 m in elevation (Kwarteng et al. 2009). Numerous wadis dissect mainly the northern flank of the mountain range, forming drainage systems that transfer water and sediment toward the coast. While many wadis remain dry for long periods, a few maintain perennial flows, such as Wadi Al Ansab, Wadi Shab, and Wadi Bani Kharus. The majority, however, function as ephemeral channels, characterized by flash floods following heavy rainfall events. Their morphology and coarse sedimentary infill, including large boulders, indicate episodic high-energy fluvial transport.

In general, the climate in Oman is arid, marked by erratic precipitation, high temperatures, and significant evaporation rates. The Batinah Plain and Muscat region receive an average of ca. 80 mm of rainfall annually (Kwarteng et al. 2009). Summers are extremely hot and humid, with temperatures nearing 50 °C and humidity levels up to 90%, while winters are warm, with average temperatures around 30 °C (Kwarteng et al. 2009). During winter, moist Mediterranean air masses reach the region, leading to orographic rainfall when they meet the Hajar Mountains (Hoffmann et al. 2016). The mountains receive 250–400 mm of annual precipitation, making them the most

humid area in Oman (Kwarteng et al. 2009). However, due to the steep topography, limited soil cover, and short infiltration time, a significant proportion of this rainfall is converted to surface runoff (Abdel-Fattah et al. 2018). On plateau areas such as the Selma Plateau, precipitation infiltrates through joints and fractures into the extensively karstified limestone, recharging the underlying karst aquifer systems. Mountain-derived runoff is predominantly directed northward toward the Batinah Plain, where partial infiltration occurs within the coarse-grained alluvial fan deposits, either naturally or supported by artificial recharge structures. Ultimately, discharge pathways include subsurface groundwater flow and ephemeral surface flow through wadis toward the Gulf of Oman or the Arabian Sea (Zekri 2020). These wadi flows often cause severe flash floods and urban inundation (Hadidi et al. 2020).

South of the Hajar Mountains, the rain shadow zone is characterized by arid to hyper-arid conditions, where limited runoff accumulates in saline playas like Umm al-Samim, meaning the "Mother of Poisons". This extensive sabkha system is dominated by waterlogged sediments, extreme evaporation, and surface salt precipitation, making it inhabitable to most vegetation (Ghazanfar et al. 2019). Additionally, these arid conditions led to the formation of extensive sand deserts. Oman hosts two major sand fields (Fig. 1a). The Rub al Khali, also known as the Empty Quarter, the largest sand desert on the Arabian Peninsula, is primarily located in Saudi Arabia, but extends over 37,000 km² into Oman. The Sharqiyyah Sands, covering around 12,000 km², stretch southeast toward the Indian Ocean. Longitudinal dunes dominate the north, while barchans prevail in the south, with isolated star dunes in peripheral zones. Most dunes are now inactive, although smaller parasitic dunes remain active (Hoffmann et al. 2016).

South of the Sharqiyyah Sands lies the Dhofar region, encompassing the Dhofar Mountains and Oman's second-largest city, Salalah (Fig. 1a). This area has an exceptional climate, remaining warm year-round (ca. 30-35 °C) and experiencing seasonal monsoonal summer rainfall influenced by the northern extent of the Indian Summer Monsoon (ISM) (Kwarteng et al. 2009). Moist air masses condense along the 250 km-long Dhofar Mountains, generating seasonal precipitation that supports lush vegetation, distinct from the rest of the Arabian Peninsula (König 2016).

To the north, the Sharqiyyah Sands are bordered by a vast wadi system draining eastward from the Hajar Mountains. Wadis such as Wadi Bani Khalid merge and eventually reach the sea, supporting both sediment transport and ephemeral flood events.

The floodings in Oman can originate from strong winter rainfall events but can also derive from convective rainstorms and tropical cyclones (Kwarteng et al. 2009). Major recent examples include Cyclone Gonu in 2007 (Al-Maskari 2012), Cyclone Phet in 2010 (Haggag & Badry 2012), and Cyclone Shaheen in 2021 (Terry et al. 2022) (Fig. 1a). These cyclones brought extreme rainfall in few hours, leading to enormous flashfloods; combined with storm surges, extreme waves, and high winds, resulting in catastrophic flooding and considerable damage along the coasts of Oman, Iran, and Pakistan (Pourkerman et al. 2023; Hoffmann & Reicherter 2014). Cyclone Gonu was especially devastating due to a lack of historical precedent in living memory and thus, insufficient preparedness (Fritz et al. 2010). Rainfall peaked at 943 mm at the Asfar Mountain near Quriyat (Al-Maskari 2012). Resulting flash floods and coastal inundation led to several fatalities ("at least 49" (Fritz et al. 2010), "49 people dead, 22 missing" (Al-Maskari 2012)), and economic losses exceeding 1.5 billion Omani Rial (about 4 billion USD) (Al-Maskari 2012). While tropical cyclones frequently occur in the Arabian Sea, mainly pre- or post-monsoonal (Fritz et al. 2010), only 21% affect Oman,

mostly along the southeastern coast between Masirah and Salalah (Najah et al. 2024). Cyclone landfalls along the northeastern coast are rare but not unprecedented, with historic recorded events on 2nd May 865 CE and 4th-5th June 1890 (Fritz et al. 2010). Reliable satellite tracking and monitoring have been in place since 1979. The frequency of tropical cyclones has increased in recent years, thereby raising the likelihood of landfall events. This trend is attributed to ongoing climate change, which has led to higher sea surface temperatures (SST) which in turn shifts the land-sea-gradient that finally alters atmospheric circulation patterns (Najah et al. 2024; Pourkerman et al. 2023). Generally, recent climate trends show a rise in temperature (mean +0.27 °C per decade) and a decline in precipitation (mean −9.42 mm per decade) between 1979 and 2012 in the Jebel Akhdar region (Al-Kalbani et al. 2015). Mountain communities, historically reliant on agriculture and freshwaterdistributed via the traditional aflaj irrigation systems, now report decreasing flow rates and drying of once-reliable springs (Hamed, personal communication). Some aflaj have ceased flowing entirely. This is due to aridification and, additionally, to groundwater abstraction from new wells in the source areas of the historic aflaj (Zekri 2020). In response, Oman has restricted the establishment of new wells near old aflaj (Zekri 2020) and has launched a de-aridification initiative involving artificially enhanced rainfall through cloud-seeding technologies (Al Harrasi & Labib 2022; Chambers et al. 2016).

2.2 Geological overview

The geology of Oman is exceptional and encompasses a variety of enigmatic features. It has significantly influenced the country's settlement history; through its abundance of natural resources such as gold, copper and manganese and also, most importantly in earlier times, through the year-round availability of freshwater in the mountains. This played a crucial role especially around 6-5 ka BP, when the climate became increasingly arid (Cleuziou & Tosi 2007).

The numerous spring outflows along the mountain slopes, early settlers relied upon, are of geological origin. The Hajar Mountains consist primarily of water-soluble limestone. During pluvial climatic phases, intense karstification of the limestone layers occurred, resulting in the formation of extensive cave systems such as Majlis al Jinns and Al Hoota Cave (Hoffmann et al. 2016). Even today, rainfall infiltrates the limestone via small channels and fractures, feeding water flows that eventually emerge as springs. Those occur either within the limestone or, more commonly, at the boundary with underlying, relatively impermeable rock units (Hoffmann et al. 2016). This geological setting occurs in different parts of the mountain range, involving various lithological compositions. In the central part of the Hajar Mountains, the oldest rocks, Precambrian formations such as tillites, are exposed and form a relatively impermeable layer. Overlying these with an unconformity, is the Permian-Mesozoic strata, consisting almost entirely of limestone. These units are autochthonous (Searle 2007). Today, the Permian-Mesozoic sequence is particularly well exposed in Wadi Nakhr, the "Grand Canyon of Arabia,". Viewed from Jebel Shams it spans the Triassic, Jurassic and Cretaceous periods (Hoffmann et al. 2016; Searle 2007). A good example of a setting with spring emergence along the Precambrian–Permian unconformity, is found in the village of Wakan, within the Ghubrah Bowl, western Hajar Mountains (Hoffmann et al. 2016). A second, analogous configuration with strata-bound springs, is found in the northeastern part of the

mountain range. Here, the impermeable layer is composed of allochthonous ophiolite, while the overlying, karstified limestones are autochthonous Eocene deposits. A striking example of this setting can be observed in Wadi Tiwi, where the lithological transition is exposed (Hoffmann et al. 2016; Glennie et al. 1973).

The exposure of ophiolite in this region is geologically exceptional and results from the emplacement of allochthonous thrust sheets, or geological nappes. These were transported from the northeast and obducted onto autochthonous rocks approximately 90-70 Ma ago (Ali et al. 2018; Searle 2007). The overthrusted nappe units represent remnants of the Neotethys ocean floor, which was in the process of closing at the time (Searle 2007). The basal unit is the Hawasina Nappe, comprising sediments that range from shallow marine deposits at the continental shelf to abyssal and deep-sea formations such as radiolarites. Associated with these deep-marine facies are atolls, now uplifted and known as the "Oman Exotics," which form prominent landmarks (Glennie et al. 1973). Above these sedimentary strata lies the Semail Ophiolite, consisting of oceanic crust and lithosphere and exposing peridotite and gabbroic units to sheeted dikes and pillow basalts (Searle 2007). Such sequences typically remain hidden beneath the seafloor at depths of 12 to 50 km. Most remarkably, the complete ophiolitic sequence includes exposure of the Mohorovičić discontinuity (Moho), the transition between oceanic crust and upper mantle, visible in Wadi Al Abyadd (Hoffmann et al. 2016).

The main structural culminations of the Hajar Mountains, namely the Jebel Akhdar and Saih Hatat domes, formed from the Late Eocene to Early Miocene (Hansmann et al. 2017; Glennie et al. 1973). These domes were heavily eroded during pluvial periods. All limestone units underwent significant karstification, while the ophiolitic units experienced serpentinization due to fluid–rock interactions and chemical processes. In core areas such as the Saih Hatat Dome and the Ghubrah Bowl, erosion has exposed the basement rocks (Searle 2007). The exact mechanisms driving mountain uplift in northern Oman remain a matter of scientific debate (Hansmann et al. 2021). Possible contributors include karstification, which leads to mass loss and promotes isostatic rebound, and serpentinization, which increases volume and induces uplift (Hoffmann et al. 2020b). These uplift processes occurred in a stepwise and spatially variable manner and are, in part, still active today, as indicated by the recent incision of wadi terraces (Scharf et al. 2019). The uplift of the Saih Hatat Dome is attributed to intense isostatic rebound of the Arabian foreland after subduction into the eclogite facies beneath the overriding Hawasina and Semail nappes (Scharf et al. 2021). Subsequent uplift of the Jebel Akhdar Dome occurred during continued convergence in the Late Miocene to Eocene (Scharf et al. 2021). Despite these insights, uplift rates and tectonic processes within the Hajar Mountains remain understudied (Woor et al. 2023). The third major culmination, the Musandam Mountains, has experienced a dynamic history of uplift and subsidence. Its tectonic evolution may have influenced the broader uplift history of the Hajar Mountains (Ali et al. 2018). Presently, the Musandam region in the far northwest is subsiding (Ali et al. 2018), while the Sur area at the eastern tip of Oman is considered tectonically stable, at least since the Late Pleistocene (Falkenroth et al. 2020). Nevertheless, signs of recent uplift are evident along the coast. A notable example occurs between Quriyat and Qalhat, where a rising tectonic block and ongoing erosion have carved deep canyons. Particularly striking are the uplifted marine abrasion platforms formed during past sea-level highstands. This block shows regionally variable

uplift rates, ranging from 0.01 ± 0.06 mm/year near Quriyat to 0.89 ± 0.09 mm/year near Qalhat (Hoffmann et al. 2020b). These fossilized marine terraces provide valuable insights into paleo-coastal processes and tectonic activity (Hoffmann et al. 2020b; 2013b).

The Arabian Peninsula as a whole is in motion as part of the Arabian Plate, which is currently colliding with the Eurasian Plate. This interaction has created major tectonic features such as the Makran Subduction Zone (MSZ) in the Gulf of Oman and the Zagros Fold-and-Thrust Belt in the Persian Gulf, extending into Iran, Iraq and Turkey (Faheem et al. 2025). The Arabian Plate rifted from the African Plate during the Early Miocene with the initiation of the Dead Sea Fault System (Segev et al. 2024; Lyakhovsky et al. 1994). Today, it is bounded by the sinistral strike-slip Dead Sea (Pre-)Transform Fault (Segev et al. 2024) to the west and by the extensional Red Sea and Gulf of Aden Rift Systems to the southwest. Its eastern boundary is marked by the strike-slip Owen Fracture Zone (Fig. 1a). The Arabian plate undergoes a slight counter-clockwise rotation, reflected in the variable spreading rates along its margins: from 0.9 cm/year in the northern Red Sea Rift to 1.5 cm/year in the central part and 1.4 cm/year in the western Aden Rift System, increasing to 2.4 cm/year at the Sheba Ridge (DeMets et al. 2010). The dextral-lateral motion rate of the Owen Fracture Zone is 3 mm/year, while subduction rates at the MSZ range from 4.2 cm/year in the east to 3.7 cm/year in the west (DeMets et al. 2010). The MSZ is separated in an eastern and a western part, separated by the Sonne Fault (Kukowski et al. 2000), and extends nearly 1000 km across the Gulf of Oman and terminates near Musandam, where it is truncated by the Minab Fault. The ongoing subduction of oceanic crust generates significant seismic activity and poses a major geohazard, including the potential for tsunamis (Faheem et al. 2025; Al-Habsi et al. 2022). Offshore northeastern Oman, this tectonic setting threatens the most densely populated parts of the country, including the capital Muscat and cities such as Quriyat and Sur. Much of Oman's critical infrastructure, including desalination facilities, a gas liquefaction plant, petroleum operations, and the international airport, is located along this vulnerable coastal plain (Aguirre-Ayerbe et al. 2018). In response to the geohazard potential, Oman has implemented a tsunami early warning system and conducts public awareness programs in schools (Aguirre-Ayerbe et al. 2018). Despite its significance, the MSZ remains poorly understood due to its thick sedimentary cover, which obscures the underlying structures and processes. However, recent geophysical studies have begun to unravel its architecture (Penney et al. 2017).

3. State of the art

3.1 Late Quaternary Climate Variabilities and Sea-Level Changes

Climate variability on Earth is primarily influenced by the amount and distribution of solar radiation received at the surface, which follows long-term cyclic patterns known as Milankovitch cycles (Milankovitch 1941). These cycles, operating on timescales of tens to hundreds of thousands of years, modulate global climate through changes in orbital eccentricity, axial tilt and precession. In addition to these astronomical drivers, extraterrestrial phenomena such as solar storms can also trigger significant climate fluctuations (Karl & Trenberth 2005). Regarding terrestrial effects,

volcanic eruptions, the albedo effect of extensive ice sheets, and, more recently, anthropogenic influences play crucial roles in climate change (Karl & Trenberth 2005). In contemporary climate science, interdisciplinary approaches are increasingly employed to identify linkages among various Earth system processes.

Reconstructions of past climate and sea-level conditions and their impacts on environmental changes rely on multiple proxies derived from geological, biological, and geochemical archives (Heine 2024). Some of the most significant approaches include the study of paleo-lake and wetland deposits, cave deposits, marine sediment cores, and ice cores. Climatic transitions often are accompanied by shifts in eustatic sea-level (Yokoyama & Esat 2011). The warming trend of the 20th and 21st centuries has been closely associated with an accelerating eustatic sea-level rise (IPCC 2023; Kemp et al. 2011). To enhance the reliability of future climate and sea-level projections, paleo-climate data are essential.

Evidence of past pluvial phases is preserved in freshwater deposits, paleo-lake and -bog sediments, as well as in alluvial, fluvial and lacustrine formations (Lüning & Vahrenholt 2018; Bradley 1999). Palynological studies, for instance, allow the reconstruction of past vegetation and by this of climate through species composition and distribution (Li et al. 2010; Bradley 1999). These sedimentary deposits, along with geomorphological features such as channels or ponds, provide valuable insights into past climate variability. Speleothem research also plays a vital role in paleo-climate studies (Overpeck et al. 2005; Bradley 1999). Stalagmites and stalactites in cave systems serve as natural archives, preserving high-resolution records of precipitation, temperature, and hydrological variability through changes in stable isotopes, trace elements, and growth rates (Fleitmann et al. 2022). Sedimentological and geochemical analyses of marine sediment cores , along with microfossil and isotopic studies, help reconstruct past climate and atmospheric circulation patterns (DeMenocal et al. 2000). Ice cores offer one of the most detailed and continuous records of past climate providing data reaching back up to 800 ka (Hannah et al. 2005). The $\delta^{18}O/\delta^{16}O$ isotope ratio in the ice layers indicates past temperature shifts. Moreover, ice cores provide insight into past atmospheric compositions, including variations in greenhouse gas concentrations across glacial-interglacial cycles (Hannah et al. 2005; Overpeck et al. 2005). The study of global mean temperatures during the Last Interglacial (LIG) is of particular relevance, as it represents the most recent warmer period in Earth's history. This temperature shift is primarily attributed to a change in Earth's obliquity, with the axial tilt being about 1.23° greater than today (Otto-Bliesner et al. 2013). In general, mean surface temperature was 0.5 to 1 °C higher than today. However, temperature deviations from present-day values varied significantly across the globe, particularly with respect to latitude, and also during the LIG. Climate models indicate a marked increase in seasonality and, most notably, summer mean temperatures in parts of the Northern Hemisphere were up to +5 °C higher at the onset of the LIG, leading to significant melting of the ice sheets (Otto-Bliesner et al. 2013).

A key aspect of sea-level research involves identifying so-called sea-level indicators, deposits that are demonstrably linked to the coastline, ideally to a specific elevation within the intertidal zone. Hijma et al. (2015) defined sea-level index points (SLIPS) and established a protocol to standardize the collection of (paleo-) sea-level associated data, aiming to enhance comparability and reduce

uncertainties. SLIPs may include beachrock sediments, fossils of sessile organisms such as oysters or barnacles, or trace fossils like grazing marks and crab boreholes (Falkenroth et al. 2020). Geomorphological features such as marine terraces also serve as SLIPs (Cerrone et al. 2021; Hoffmann et al. 2020b). Archaeological remains can additionally contribute to paleo-shoreline reconstruction, ranging from small ancient settlements (Nirgi et al. 2020) to large-scale infrastructure like submerged or elevated harbours or fishponds (Auriemma & Solinas 2009).

In sea-level reconstructions, the LIG is frequently used as an analogue for projecting future sea-level scenarios, given that global temperatures during this period were slightly higher than today, leading to substantial melting of continental ice sheets (Otto-Bliesner et al. 2013). Reconstructions indicate a significantly higher global mean sea level (GMSL) during the LIG. According to the CAPE Last Interglacial Project, the melting of Northern Hemisphere continental ice sheets contributed approximately 2.2 to 3.4 m to the GMSL rise during the LIG (Otto-Bliesner et al. 2006). This rise occurred in at least two distinct phases, with average rates of 2.8 and 2.3 cm a^{-1}, respectively (Rohling et al. 2019). The initial phase, leading to the GMSL peak at approximately 127 ka BP, was dominated by meltwater from the Antarctic Ice Sheet, followed later by contributions from the Greenland Ice Sheet. Rohling et al. (2019) propose that similar processes could be triggered by ongoing anthropogenic climate change. By the end of the LIG, GMSL had fallen to approximately present-day levels (Rohling et al. 2019). Notably, the PALSEA project (PALeo constraints on SEA-level rise) aims to synthesize global findings on past sea-level fluctuations (Rovere & Dutton 2021). Its broad geographic scope is essential due to site-specific influences, including glacial isostatic adjustment (GIA), equatorial ocean syphoning (Mitrovica & Peltier 1991), tectonics uplift and subsidence and sediment influx and compaction. These factors result in significant site-specific variations, which are reflected in what is known as relative sea level (Rovere et al. 2016b). The ongoing PALSEA project aims to compile as much relative sea-level data from the LIG as possible, progressively enhancing our global understanding of sea-level fluctuations during this period.

Following minor sea-level fluctuations after glacial and interglacial phases, the GMSL rose to near-present levels after the Last Glacial Maximum (LGM) (Lambeck et al. 2002). During the Mid-Holocene, a sea-level highstand of <10 m above current levels was reached in many regions globally between 8 and 4 ka BP, although timing and amplitude vary by location (Khan et al. 2015).

However, climate and sea-level signals are complex, both spatially and temporally. Sea-level rise may result from single melting events, such as post-LGM deglaciation (Lambeck 2002). Variability in sea-level fluctuation behaviour during the Holocene differs by proximity to former ice sheets – categorized as near-field, intermediate-field, and far-field regions. These differences largely result from isostatic adjustment processes within the Earth's mantle. Additionally, the redistribution of water within ocean basins leads to dynamic shifts in sea level. Mitrovica and Peltier (1991) introduced the concept of equatorial ocean siphoning, which describes the gravitational redistribution of ocean water due to ice-sheet melting and isostatic processes, influencing sea level in far-field locations.

Paleo-sea-level reconstructions are crucial for refining flood-risk assessments and supporting civil protection. This includes studying long- as well as short-term sea-level changes caused by storms or tsunamis. To support both civil protection and scientific research, Ramírez-Herrera and Coca

(2024) compiled a global database of past tsunamis. Water level fluctuations during such events occur rapidly and are typically short-lived, lasting only a few hours to days in the case of storms, and mere minutes in the case of tsunamis (Morton et al. 2007). While storms result from meteorological extremes, tsunamis are triggered by terrestrial forces such as submarine earthquakes or landslides, anthropogenic detonations, or even extraterrestrial events like meteorite impacts. Despite their distinct origins and durations, both storms and tsunamis generate high-energy wave events capable of generating similar geological deposits, which are challenging to differentiate from each other (Morton et al. 2007).

By integrating diverse data sources, researchers can refine models of past climate and sea-level variability, enhance our understanding of Earth system dynamics, and help to improve forecasts of future changes under ongoing global warming.

3.1.1 Study-area-specific climate research

Significant variations in precipitation patterns and temperatures are evident throughout the Quaternary on the Arabian Peninsula. In general, climate is characterized by colder phases with decreased precipitation during the Marine Isotope Stage (MIS) 6, MIS 5d and 5b, MIS 4 and MIS 2. In contrast, warmer phases with enhanced precipitation occurred during MIS 5e, 5c and 5a, MIS 3 and MIS 1 (the Holocene) (Parton et al. 2015; Fleitmann & Matter 2009). These more temperate and humid periods, referred to as Windows of Opportunity for human dispersal, offered favourable conditions for human migration and exploration. Lower sea levels at the onset of these phases facilitated movement by exposing land bridges or narrowing maritime straits, such as the Bab al-Mandab; these features were subsequently submerged as sea levels rose (Beyer et al. 2021; Rosenberg et al. 2011). The climatic and sea-level history of present-day Oman, together with major cultural-historical periods and events, is illustrated in Figure 2.

On the Arabian Peninsula, and particularly in Oman, several paleo-environmental archives contribute to paleo-climatic reconstructions. These include paleo-lakes (Rosenberg et al. 2012; Preusser et al. 2005), sabkha deposits (Matter et al. 2015) and speleothems such as stalagmites, stalactites and flowstones with visible annual growth bands (Fleitmann & Matter 2009; Burns et al. 1998, 2001). Additionally, fluvial terraces and alluvial fans provide insight into ancient drainage systems, evident in satellite imagery and indicate phases of past hydrological activity. However, securing precise chronological control over these features remains challenging. Parton et al. (2015) investigated alluvial fans in northeastern Oman and identified pluvial phases during MIS 6, MIS 5e, 5c and 5a and during early MIS 3. They interpreted these as potential Windows of Opportunity for human dispersals out of Africa. Parton et al. (2015) employed OSL dating and various paleo-environment-reconstruction methodologies, including geochemical, carbonate isotope and magnetic susceptibility analyses, as well as phytolith analyses. Phytoliths are microscopic silica particles in vascular plants, that appear to be familiy-specific in morphology. They serve as an archaeobotanical tool to reconstruct paleo-vegetation. Their analyses indicate continuous freshwater supply during MIS 6, and MIS 5e, 5c and 5a with grassland and woody elements, the latter especially developed during MIS 5e. Pluvial periods are well documented in the geological record, with one prominent example from MIS 5e being Lake Saiwan, located in present-day

eastern Oman. The presence of an escarpment and lacustrine sediments indicates the former existence of a lake, with deposits indicating a lake phase between 132 and 104 ka BP (Rosenberg et al. 2012). This timeframe corresponds to the Palaeolithic in the archaeological record. The paleo-lake deposits are associated with lithic artefacts such as hand axes and scrapers, suggesting human presence during the humid phase (Rosenberg et al. 2012; Biagi 1994).

The high-resolution speleothem records also prove a pluvial period at that time (Chen et al. 2022). $\delta^{18}O$ values provide insight into the freshwater source and confirm an intensified ISM, driven by enhanced solar radiation and a heightened thermal land-ocean gradient (Chen et al. 2022).

Further insights into climatic conditions during MIS 3 were obtained by Hoffmann et al. (2015b), who investigated freshwater sediments in the western Hajar Mountains. These sediments were deposited in an ephemeral water body that emerged more than a hundred times after intense rainfalls because a rockfall had obstructed the outflow. Analyses and dating of these sediment layers suggest climatic conditions similar to today. This extends findings of Parton et al. (2013) who document the activation of drainage systems, fluvial channels and the establishment of a lake at the western Hajar Mountain flank, Aqabah, UAE at that time. These paleo-lake deposits reveal at least four distinct lake phases and in between a water body with varying water level, interpreted as evidence of an enhanced monsoonal activity in this region with strong periodic rainfalls that may have benefitted Mesolithic human communities (Parton et al. 2013).
The subsequent MIS 2 was characterized by a global temperature decline and the expansion of continental ice sheets, culminating in the LGM, during which GMSL dropped by approximately 130 m (Lambeck et al. 2002). For this time interval, Preusser (2009) documented hyper-arid conditions along the eastern coast of Oman, accompanied by the exposure of extensive shelf areas. Strong winds, particularly immediately before and after the LGM, transported sediments from the exposed shelf northward, contributing to the formation of the Sharqiyya Sand dunes. These aeolian processes were also active during earlier glacial periods and stadials, specifically during MIS 6, MIS 5d and MIS 4 (Preusser 2009). According to pedogenic analyses, the consolidation of these dune systems occurred during a significantly more humid phase in the Early Holocene (Preusser et al. 2005). Paleo-lacustrine sediments and interdune strata reflect hydrological conditions wetter than those of today, attributed to an intensified and northward-displaced monsoonal system (Preusser et al. 2005). These findings are corroborated by Lézine et al. (2002), who reconstructed a humid climatic phase during the Early to Mid-Holocene based on palynological data from paleo-lagoonal archives. The identified species assemblages, particularly the presence of diverse mangrove taxa, point to enhanced freshwater influx, reflecting a sustained period of increased precipitation. Speleothem records further confirm a pluvial phase during Early to Mid-Holocene (Tian et al. 2023; Fleitmann et al. 2022; 2007). Using a new multi-proxy approach, Tian et al. (2023) analyzed speleothem records from the Qunf-Cave in southern Oman and compared these with $\delta^{18}O$ records from the Hoti-Cave in the northern Oman. Their results indicate that the intensified precipitation during this interval was driven by an enhanced ISM and a concurrently strengthened North African Summer Monsoon (NASM), which is suggested to have functioned as a unified monsoonal system during the LIG (Tian et al. 2023; Chen et al. 2022). Despite general agreement on a wetter climate in the Early to Mid-Holocene (Fleitmann et al. 2022; Preusser et al. 2005; Lézine et al. 2002), the quantity of precipitation remains a subject of

debate (Enzel et al. 2017, 2015; Engel et al. 2017). The so-called "How wet is wet?" debate dates back at least to the 1990s, when Woods and Imes (1995) addressed this question and explored this issue by examining paleo-capillary surfaces in the UAE. The challenge of quantitatively reconstructing past precipitation levels continues to be a key obstacle in paleo-climatic research. One of my research topics addressed this issue by aiming to refine our understanding of spatial precipitation patterns through the use of an additional proxy: mangroves. Because mangroves are sensitive to soil salinity, their species composition can serve as an indicator of regional precipitation. Building on the work of Lézine et al. (2002), I replaced palynological analysis with a combination of satellite-based remote sensing, core sampling, and a sedimentological–geochemical approach, and extended the study area to the entire north-eastern Omani coastline. The corresponding study is published as Decker et al. (2021) and is included in Chapter 5.1 of this thesis. An environmental reconstruction of the paleo-lagoons and their associated biota, including human presence, according to the archaeological record, is presented as the cover illustration of the publication reproduced in Chapter 5.1 (Fig. 3).

Marine sediment cores provide valuable information on atmospheric circulation patterns and SST (Bradley 1999). However, the Arabian Sea and particularly the Gulf of Oman remain relatively understudied in this context (Clemens et al. 1991; Sirocko et al. 1991). In an effort to address this gap, Rodrigues et al. (2023) analyzed pollen grains and non-pollen palynomorphs to investigate variability in monsoonal patterns across the Pleistocene–Holocene transition. The inclusion of non-pollen palynomorphs represents an innovative methodological advancement. Recent work by Maier et al. (2025) has further contributed to closing this research gap. Using alkenone-derived SST as a proxy, and compiling new and previously published datasets from the region, they produced a comprehensive reconstruction of SST and monsoonal circulation over the past 43 ka. Their results indicate that SSTs fluctuated between 20.1 °C and 27.4 °C throughout this period. During the LGM, an intensification of the northeasterly winter monsoon is inferred, transporting cold, dry air masses from the Tibetan Plateau to the Arabian Sea. Although this wind regime still persists today, its intensity has declined in favour of the southwesterly ISM, which strengthened during the onset of the Early Holocene Humid Period (EHHP) (Maier et al. 2025). During that time, air temperature and SST increased and climate circulation patterns changed globally (Lüning and Vahrenholt 2018; Kuhlmann et al. 2004). Among other effects, this resulted in northward displacements and intensifications of two monsoonal systems: of the NASM, today affecting eastern and northern Africa, and of the ISM, influencing the Horn of Africa, the Arabian Peninsula and western India (Axelsson 2024; Lüning & Vahrenholt 2018; Fleitmann et al. 2007). Zaki et al. (2025) discuss a northeastward shift of the NASM, identifying it as the primary moisture source behind the greening of the Rub al Khali Desert during the Early to Mid-Holocene. Enhanced precipitation in northern Africa led to the so-called “Green Sahara” and “African Humid Period” (AHP) (e.g., Duque-Villegas et al. 2025; Knight 2023). The Arabian counterpart is known as the EHHP (e.g., Zaki et al. 2025; Lézine et al. 2014). The durations of these humid phases vary: the AHP lasted roughly from 14.8 to 5.5 ka BP (Knight 2023), while the Arabian EHHP spanned approximately 10.5 to 5.5 ka BP (Lézine et al. 2014) with climate optima between 11 and 7 ka BP in both cases (Lézine et al. 2014). Similarly, the western Indian region experienced enhanced rainfall during this time, evidenced by fluvial and lacustrine deposits peaking around 8 and 6 ka BP, while marine records align more

closely with the 11–7 ka BP interval (Lézine et al. 2014). Notably, marine data (Lézine et al. 2014, and references therein) and speleothem investigations (Fleitmann et al. 2022) suggest a rather abrupt termination of the wetter conditions and shift to an arid climate within decades. The Mid-Holocene shift from a summer monsoon-dominated precipitation regime (ISM) toward a more arid climate influenced by Mediterranean Westerlies and winter rainfall, inevitably had a profound impact on the societies that thrived in these regions. (Fleitmann et al. 2022; Anderson et al. 2007). Studying the past several millennia, the traditional irrigation systems known as aflaj also serve as valuable indicators of increasing aridification in southeastern Arabia. These community-managed systems provided perennial water supplies for domestic use and agriculture. By this, they always have played a critical role in enabling permanent human settlement and the development of sedentary lifeways in an environment that became progressively more arid after approximately 6 ka BP (Cleuziou & Tosi 2007). Given that Oman's annual rainfall is insufficient to support agriculture without supplemental irrigation (Al-Marshudi, 2007), the emergence and long-term maintenance of aflaj underscore the adaptive strategies employed by human societies in response to climatic stress. The origins of the aflaj remain a subject of debate, though archaeological evidence from the site of Salut in northern Oman suggests their use dates back to at least 2.7 ka BP (Chakraborty 2012; Wilkinson 2002). These systems are gravity-fed, meaning that any significant decline in the source-water table requires the realignment of the entire channel network, involving vertical adjustments of centimeters to meters, as observed, for example, in Wadi Tanuf (Walsh 2013). Today, more than 4000 aflaj systems, both active and abandoned, are distributed throughout Oman (Walsh 2013). With a use history exceeding two millennia, they constitute an underutilized but highly promising archive for paleo-hydrological and geoarchaeological research. Carbonate deposits formed within these channels, commonly referred to as aflaj travertine, can be dated using uranium-series methods, offering potential for establishing high-resolution chronologies of water availability and climatic variability (Cremaschi et al. 2018).

3.1.2 Study-area-specific sea-level research

This chapter highlights sea-level variations along the northeastern coastline of Oman during the Late Pleistocene and Holocene. This region has been inhabited for thousands of years (Cleuziou & Tosi 2007) and is particularly vulnerable to coastal inundation today, as several major urban centers, including the capital, Muscat, are situated directly along the shoreline. Moreover, critical infrastructure is concentrated near the coast as well, including the country's main international airport, a major gas liquefaction facility, and multiple desalination plants essential for freshwater supply.

Multiple geodynamical and climatic drivers influence the sea level along this coastline. Firstly, long-term natural processes, influenced by orbital forcing, GIA and local tectonic activity have shaped sea-level dynamics throughout the Late Quaternary. In the contemporary context, anthropogenic climate change contributes to global sea-level rise, compounding these natural trends. Secondly, the proximity of the MSZ, located offshore in the Gulf of Oman, poses a significant tectonic hazard, designating the coastline tsunamigenic (Hoffmann et al. 2020a). Thirdly, the regional atmospheric circulation systems periodically generate tropical cyclones over the Indian Ocean and the Arabian

Sea, some of which make landfall along the Omani coast, causing heavy rainfall, episodic flooding and coastal erosion (Pourkerman et al. 2023).
To address the range of influences on sea-level fluctuations along the northeastern Omani coastline, this chapter is divided into two sections: long-term (millennial-scale) variations, driven by tectonics, GIA and orbital forcings; and short-term (hours to days) changes, reflecting extreme wave events such as tsunamis and tropical cyclones. The former is examined through paleo-environmental proxies and sedimentary archives, while the latter also includes historical records and instrumental observations.

Long-term sea-level fluctuations in northeastern Oman

During the Late Quaternary, the Omani coastline was repeatedly affected by sea-level fluctuations associated with glacial–interglacial cycles. During colder periods, such as MIS 6, MIS 5d and 5b, MIS 4, and particularly MIS 2, global sea levels regressed, exposing broad shelf areas (Lambeck et al. 2002). The LGM, around 21 ka BP, marked the most pronounced lowstand, with GMSL approximately 130 m below present mean sea level (pmsl) (Lambeck et al. 2014, 2002). These lowstands subjected the exposed continental shelf to aeolian deflation and sediment mobilization, as discussed in the previous chapter.
Subsequent warming phases triggered glacio-eustatic sea-level rise due to the melting of continental ice sheets (Lambeck et al. 2002). These transgressive phases often resulted in the formation of coastal erosional and depositional features, such as marine terraces and beachrock platforms; notably, such features are well-preserved in tectonically uplifting areas along the northeastern Omani coastline, particularly around Fins and Tiwi (Hoffmann et al. 2020b; Falkenroth et al. 2019). Here, sequential marine terraces represent past highstands and often contain fossil assemblages and beachrock deposits that mark the position of former shorelines. The preservation of these features is facilitated by ongoing Quaternary uplift, which progressively raises older shoreline indicators above current sea level (Hoffmann et al. 2020b). Falkenroth et al. (2019), using the standardized methodology proposed by Hijma et al. (2015), analyzed beachrock and paleo-marine sediments in the Sur lagoon area. Their results demonstrate a transgressive event associated with a sea-level highstand of 3.93 ± 0.12 m above pmsl during the MIS 5e highstand (ca. 125 ka BP), a period globally recognized for elevated sea levels and warmer climatic conditions (Rovere et al. 2016a; Lambeck et al. 2002). During my fieldwork, particular attention was given to identifying deposits indicative of paleo-sea-level highstands, with the aim of detecting a possible Holocene highstand or verifying the well-documented Last Interglacial highstand at as many locations as possible. The findings are presented in Decker et al. (2024) and detailed in Chapter 5.3 of this thesis. The cover illustration for Chapter 5.3 presents two comparative depictions of sea-level positions: the present-day level and a stand the Last Interglacial, around 125,000 years ago (Fig. 5).

A Holocene sea-level highstand is also postulated for the Omani coast, particularly around 6 ka BP; however, its magnitude and extent remain debated. Proposed highstand estimates range from minor seawater incursions (Lézine et al. 2002) to elevations of 2–3 m (Teillet et al. 2025) and even up to 9 m above pmsl (Berger et al. 2013). While these studies suggest the possible magnitude of

sea-level rise, conclusive geomorphological or sedimentological evidence remains limited, and further research is needed to confirm the extent and drivers of this proposed Mid-Holocene highstand. My study of mangroves in paleo-lagoons also contributes to this discussion, as mangroves are reliable shore-line indicators, given that they exclusively grow within the intertidal zone. In the course of my research, I recorded both modern and paleo-mangrove horizons with centimetre accuracy using a differential GPS, providing valuable data for the reconstruction of sea level around 6,000 years ago. The results are presented in Chapter 5.1 and have been published as Decker et al. (2021).

Short-term sea-level fluctuations and coastal hazards in northeastern Oman

The northeastern Omani coastline is exposed to short-term sea-level fluctuations driven by extreme events such as tsunamis and tropical cyclones (Hoffmann et al. 2020a, 2015a; Fritz et al. 2010). These events, though temporally brief, can cause profound inundation and pose significant risks to coastal infrastructure and populations. Tsunamis represent a particularly acute hazard due to their short onset time and potentially devastating impacts. The primary source of tsunamigenic activity in this region is the MSZ, located offshore in the northeastern Gulf of Oman (Fig. 1a). Tsunami waves in this setting may be generated by submarine earthquakes, successive submarine landslides, or even non-seismic processes (Haider et al. 2023). The MSZ is capable of generating very large earthquakes (≥M_w 9.0), which could result in tsunami wave run-ups of up to 15 m along the adjacent coastlines (Haider et al. 2024, 2023).

Geological and archaeological records provide multiple lines of evidence for past tsunamis. At the archaeological site HD6 at Ras Al Hadd, a shell layer up to 10 cm thick, intercalated between two mudbrick building phases, is interpreted as the result of a major marine inundation event, potentially a tsunami, dated to ca. 4,450 cal y BP (Hoffmann et al. 2015a). In the coastal zone near Fins, Tiwi, and Ras Al Hadd, imbricated boulder and block deposits suggest deposition by a high-energy tsunami. Some of these boulders weighing ca. 100 tonnes and appear to have been transported from the base on top of a 15 m-high cliff (Hoffmann et al. 2020a). Chronological constraints are derived from associated *Lithophaga* and oyster shells, interpreted as having died due to the impact of the event, and dated to approximately 1,000 y BP. Comparable tsunami deposits from this time period have been reported along the coasts of northwestern India (Prizomwala et al. 2018) and southern Iran (Shah-Hosseini et al. 2011), supporting a regional high-energy wave event, likely tsunami-induced, with reconstructed run-ups of 4 to 15 m. More recent tsunamis are also documented: for example, the 1819 CE event in northwest India caused significant fatalities and destruction (Murty & Rafiq 1991), though no run-up height was recorded. The 1945 tsunami, generated by a M_w 8.1 earthquake along the MSZ, caused wave heights of 13.0 m in Pasni and Ormara, Pakistan, while waves of 1.98 m height were recorded in Mumbai (Haider et al. 2024; Murty & Rafiq 1991). For Oman specifically, Hoffmann et al. (2013a) reconstructed the 1945 tsunami based on eyewitness reports, which described two waves 2–3 m in height that caused only minimal property damage. A more recent tsunami event occurred in 2013, following a M_w 7.7 inland earthquake in Pakistan. Though small in magnitude, this event generated wave heights of 15 cm in Dibba and up to 100 cm in Quriyat, affecting the eastern Arabian Peninsula from Musandam to Al Ashkara (Heidarzadeh & Satake 2014). Additional possible tsunami evidence

includes an undated shell layer in the Sur lagoon, attributed to tsunami activity based on sedimentological, taphonomic, and micropaleontological analyses (Pilarczyk & Reinhardt 2012; Donato et al. 2009, 2008). Although not yet conclusively dated, this deposit is frequently associated with the 1945 tsunami. During a renewed sedimentological investigation conducted as part of a field exercise, wood was discovered embedded within the tsunamigenic shell layer. This provided an valuable basis for radiocarbon dating and, through anatomical analysis of the wood, allowed inferences about the local vegetation at the time. The analyses and results are presented in Chapter 5.2 and were published in Decker et al. (2023). The cover page (Fig. 4) of Chapter 5.2 reconstructs the state of the lagoon shortly before the tsunami inundation approximately 1,000 years ago.

In addition to tsunamis, tropical cyclones represent another major short-term sea-level hazard. Unlike tsunamis, cyclones allow for longer response times, with hours to days for preparation and evacuation. However, their impact is compounded by dual sources of flooding—coastal storm surges and inland flash floods from overflowing wadis. Notably destructive cyclones made landfall in Oman in 2007 (Gonu), 2010 (Phet), and 2021 (Shaheen) (Fig. 1a).

Despite the critical importance of understanding these hazards, historical records of marine inundation events along the Omani coast remain sparse, particularly prior to the 20th century. Systematic data collection began only in recent decades, primarily with the involvement of the Ministry of Agriculture, Fisheries, and Water Resources (MAFWR). This agency has developed flood risk maps, emergency response protocols, and an early warning centre. While these efforts are now effective for tropical cyclone preparedness (Al-Zaabi & Al-Zadjali, 2022), tsunami early warning remains a challenge due to the rapid onset and unpredictable nature of such events.

3.2 Mangroves as climate and sea-level indicators

General mangrove specifications

Mangroves are halophytic plants that thrive in saline and brackish water environments, enabling them to occupy one of the most challenging ecological niches: the estuarine and intertidal zones. This unique adaptation has evolved convergently, resulting in approximately 80 species across 30 genera and 17 families globally, predominantly woody angiosperms and one palm species (Saenger et al. 2019; Tomlinson 2016). The earliest mangroves date back to the Late Cretaceous to Early Paleogene, with the evolutionary emergence of angiosperms along the southeast Asian coastlines. Although their precise origin remains debated (Saenger et al. 2019), the so-called Indo-West-Pacific mangroves harbour the highest mangrove biodiversity today. In contrast, the later-developing Atlantic-East-Pacific mangroves own fewer species. Modern mangroves are distributed pantropically and in some subtropical areas, ranging from 32° N to 38° S (Saenger et al. 2019). This distribution is primarily constrained by aridity and winter air temperature and SST (Chen et al. 2017; Tomlinson 2016), forming a global zone of potential mangrove distribution that is further shaped by local biotic and abiotic factors (Saenger et al. 2019). The coastlines of Oman lie at the margins of this distribution range, resulting in particularly harsh conditions for mangroves. Consequently, Oman hosts only a single extant mangrove species: *Avicennia marina*, one of the

most salt- and cold-tolerant species (Chen et al. 2017; Tomlinson 2016). Although the fossil record for mangrove diversity and distribution in Oman is limited, paleo-ecological data indicate the historical presence of at least one additional species, which is *Rhizophora mucronata*, alongside *Avicennia marina* during the Early to Mid-Holocene (Lézine 2009; Lézine et al. 2002). Present-day *A. marina* in Oman displays significant morphological variation across environmental gradients. Along the arid northern coast, such as in Qurum and Bandar Khayran, west of Muscat, the species often forms dwarf, shrub-like stands due to more stressful conditions. In contrast, in the wetter southern regions around Dhofar, it can develop into trees several meters in height.

In general, mangroves colonize sheltered intertidal zones, with species-specific preferentially zonation patterns dictated by tolerance to salinity, which in turn depends on freshwater availability. Where multiple species coexist, this creates a structured gradient from the seaward edge to the landward margin. Mangrove adaptations are diverse: for example, some species own salt-blocker microfilters directly on the root endodermis, *Rhizophora* utilizes salt-excreting glands on its stems, while *Avicennia* excretes salt through glands on both leaf surfaces. Their complex root systems are adapted to diurnal tidal inundation and oxygen deprivation. Species like *Avicennia* developing a cable-root system with pneumatophores, vertical root structures, that facilitate sediment accumulation and prevent erosion and enables gas exchange (Tomlinson 2016). Reproduction is similarly adapted to the intertidal environment. Mangroves are typically semi-viviparous: their propagules develop on the parent plant and are ready to root immediately upon contact with suitable substrate, reducing the risk of dispersal to unfavourable sites (Clarke 1993). Mangrove forests, or "mangals," are unique ecosystems and provide essential ecosystem services. They support diverse animal communities, some of which rely on mangroves for specific life stages, such as some fish and prawns that use them as nurseries, or for their entire life cycles, as in the case of some crabs and the mangrove snail *Terebralia palustris*. Mangroves also support migratory birds and create intricate ecological networks that enhance biodiversity and benefit adjacent ecosystems (Arceo-Carranza et al. 2021; Kathiresan 2021).

Mangroves act as natural coastal barriers, mitigating the impact of storm surges, strong winds, and tsunamis (Ragavan et al. 2021). They stabilize shorelines and even promote land formation by trapping sediment (Ragavan et al. 2021). Their complex root systems and high biomass make mangrove forests highly effective carbon sinks: Their wood and leaves possess some of the highest calorific values among tree species, and their roots facilitate the burial of organic matter, further enhancing carbon sequestration (Wirabuana et al. 2025; Kathiresan 2021; Islam et al. 2019). In fact, mangroves sequester carbon at rates which exceeds the carbon sequestration potential of terrestrial neo-tropical forests by two to five times (Murdiyarso et al. 2015). Crabs also contribute by burying leaf litter, and sediment deposition seals organic debris, reducing erosion and aiding long-term carbon storage (Donato et al. 2011).

Despite their ecological importance, mangroves are increasingly vulnerable to human activities (Ragavan et al. 2021). Between 2000 and 2016, 47% of global mangrove loss was attributed to land reclamation for agriculture, particularly rice and oil palm cultivation, and aquaculture, e.g. shrimp farming (Goldberg et al. 2020; Martinez-Alier 2001). Coastal urbanization, tourism infrastructure, salt ponds, and desalination facilities further exacerbate degradation (Saenger et al. 2019).

Mangrove wood is still harvested, often illegally, for firewood, charcoal, and construction. Grazing pressure is another issue, especially from camels and other livestock that consume seedlings and impede regeneration. Additionally, in ancient times as well as today, mangrove foliage is often harvested as fodder for goats, sheep, and cattle (Kathiresan 2021; Cleuziou & Tosi 2007).

Pollution from plastics, oil, and industrial waste poses another major threat (Sandilyan & Kathiresan 2014). Climate change introduces further challenges: declining regional rainfall reduces freshwater input and increasing soil salinity, which particularly hampers the growth of seedlings and young plants. Rising sea levels present a more complex issue. Mangroves can adapt by vertically accreting sediment, but this capacity is generally limited to around 6.1 mm per year (Saintilan et al. 2020), and only in areas that allow for landward migration and peat accumulation. Without such conditions, even the most resilient mangals face submergence. In response to these threats, there has been growing global momentum to conserve, restore, and sustainably manage mangrove ecosystems. This is driven not only by environmental concern but also by economic opportunity. Mangroves are among the most effective natural systems for carbon capture and storage (Murdiyarso et al. 2015; Donato et al. 2011). This has sparked rising interest in mangrove conservation within science, policy, and business (Macreadie et al. 2019). Carbon offset projects increasingly target mangroves, incentivizing their protection and restoration while generating economic benefits for coastal communities. These efforts support ecosystem services such as shoreline stabilization, fisheries enhancement, beekeeping including mangrove honey production, and ecotourism. Despite ongoing pressures, these initiatives contribute to the expansion and recovery of mangrove forests worldwide (Saenger et al. 2019).

Mangroves as paleo-sea-level indicators

Beyond their role as significant carbon sinks, mangrove ecosystems offer valuable insights across various research fields, particularly in climate and sea-level reconstruction (Tomlinson 2016). The species-specific sensitivity of mangroves to soil salinity allows their assemblages to be used as proxies for past salinity levels and, by extension, freshwater input. Comparative analyses over time can thus inform about relative precipitation changes. Although mangrove composition is also influenced by multiple other factors, including increasing anthropogenic pressures during the Holocene, both mangrove distribution and species assemblages remain robust environmental indicators (Pimple et al. 2022; Blasco et al. 1996). Additionally, the morpho-anatomical plasticity of mangrove leaves reflects environmental parameters such as pH and salinity (Arrivabene et al., 2014).

While individual mangrove species occupy distinct zones within the intertidal range, reconstructing centimeter-scale sea-level changes from paleo-mangrove records remains challenging, primarily due to difficulties in identifying precise paleo-surfaces. Attempts to derive high-resolution sea-level reconstructions from paleo-mangrove material, such as those reported by Sefton et al. (2021), have generally been unsuccessful. Nonetheless, remnants of ancient mangrove forests, including root penetration structures, preserved roots, stems, branches, leaves, and pollen, remain reliable indicators of former intertidal zones. Wood and pollen offer particular advantages, as they allow taxonomic identification to genus or even species level. Wood anatomical investigations employ

three section planes: transverse, radial, and tangential, to analyze xylem and phloem structures and distinctive characteristics like the arrangement of vessel elements (Jagiella & Kürschner 1987). Pollen exoskeletons also exhibit distinct features enabling precise taxonomic attribution. These exoskeletons are remarkably durable and can persist longtime under anoxic conditions (Tomlinson, 2016; Bradley, 1999). Mangrove-associated faunal remains also function as paleo-mangrove indicators. For instance, fossil oysters that once colonized aerial roots and the mangrove-dwelling gastropod *Terebralia palustris* [Linnaeus], which only inhabits zones from the landward margin to the seaward fringe of mangrove ecosystems, can signal the past presence of mangroves (Fratini et al. 2004). Mangrove wood, snail shells, and oyster shells are datable using radiocarbon (^{14}C) techniques. However, the radiocarbon dating of marine mollusk shells must account for the marine reservoir effect, which can result in a considerable dating uncertainty. Bulk sediment, commonly used for dating, only provides averaged ages and is prone to contamination from younger root intrusion or reworked older material (Sefton et al. 2021).

While such methods may constrain the general timeframe of mangrove ecosystem presence, they often fail to pinpoint precise environmental transitions or abrupt ecological collapse events - key elements in geo-biological studies. High-resolution chronological reconstructions therefore require reliable datable material such as mangrove wood, ideally embedded within a stratigraphically well-defined sedimentary context.

4. Study sites, applied methods and co-working – a short overview

The study area encompasses the northeastern Omani coastal zone stretching from the Batinah Plain, including the capital city Muscat in the north, to Cape Ras Madraka in the southeast (Fig. 1b). The research period for this thesis spans the years 2017 to 2024. The entire coastal strip was surveyed for potential paleo-environmental and sea-level archives. This included the evaluation of previous publications, satellite imagery analysis, and classical geological fieldwork including sediment coring and test drilling. A total of 16 localities were examined in detail. Several of these sites were used for multiple types of analyses and appear in two or all three of the resulting publications (Fig. 1b). The research culminated in three peer-reviewed publications, accompanied by one Master's thesis and three Bachelor's theses.

Parts of this work were conducted within the framework of the project "Mangrove ecosystems as indicators for environmental change (Oman, Indian Ocean)", funded by the German Research Foundation (Deutsche Forschungsgemeinschaft, DFG) (grant number HO2550/15-1). Additionally, this work contributed to the IGCP Project 639, “Sea-level change from Minutes to Millennia” which is part of the UNESCO International Geoscience Programme (IGCP).

This project required close interdisciplinary collaboration, involving researchers across disciplines, departments and institutions, as well as several universities:

Dr. Sven Oliver Franz (University of Bonn, Germany) supported the geochemical analyses of selected sediment samples and their interpretation.

Prof. Carole Gee and Pia Schucht (both University of Bonn) assisted with the identification and verification of wood samples, which required elaborate histological preparation.
For the analysis of foraminiferal assemblages from one of the sediment profiles, Prof. Martin Langer (University of Bonn) provided both laboratory equipment and his expertise.
Dr. Michaela Falkenroth (now Darmstadt University, Germany), an expert in sedimentology, provided critical input particularly for the facies analyses. She has previously conducted fieldwork in Oman herself and continues to work there. She also recently supervised a Bachelor's thesis in the region: Hannah Wiesenthal (2025), “Facies and cyclicity of Quaternary coastal sediments in Ra’s ar Ru’ays, Oman”.
Chronological constraints were established through radiocarbon dating (^{14}C), primarily on mollusc shells, and, where possible, on terrestrial plant remains. The radiocarbon analyses and age interpretations were conducted in collaboration with Dr. Susanne Lindauer (Curt Engelhorn Centre for Archaeometry, Mannheim, Germany).
The research findings were regularly presented and discussed at national and international geological meetings and conferences throughout this period.
The following section presents the three peer-reviewed publications resulting from this research.

5. Publications

5.1.1 Collapse of Holocene mangrove ecosystems along the coastline of Oman (Decker et al. 2021)



Fig. 3: Environmental reconstruction of a lagoon on the eastern coast of present-day Oman around 6,000 years ago, showing the mangrove species *Avicennia marina* with pneumatophores and *Rhizophora mucronata* with stilt roots. Human populations practiced a pastoral lifestyle, seasonally moving between the mountains and the coast, utilized the mangrove forests for subsistence, and left behind shell middens that are preserved in the archaeological record today.

Quaternary Research
Copyright © University of Washington. Published by Cambridge University Press, 2020.
doi:10.1017/qua.2020.96

Collapse of Holocene mangrove ecosystems along the coastline of Oman

Valeska Decker[a]*, Michaela Falkenroth[b], Susanne Lindauer[c], Jessica Landgraf[a], Zahra Al-Lawati[d], Huda Al-Rahbi[d], Sven Oliver Franz[a], Gösta Hoffmann[a,b]

[a]Geology Section, Institute of Geosciences, Bonn University, Nussallee 8, 53115 Bonn, Germany
[b]Neotektonik und Georisiken, RWTH Aachen University, 52056 Aachen, Germany
[c]Curt-Engelhorn-Centre Archaeometry, C4, 8, 68159 Mannheim, Germany
[d]Department of Applied Geosciences, German University of Technology in Oman, PO Box 1816, PC 130, Muscat, Oman
*Corresponding author at: e-mail address: v.decker@uni-bonn.de (V. Decker).

(Received April 24, 2020; Accepted September 11, 2020)

Abstract

Sedimentological, geochemical, and paleontological investigations of the coastline of northeastern Oman have provided the authors with an in-depth insight into Holocene sea levels and climate conditions. The spatial distribution and species assemblage of mangrove ecosystems are analyzed. These ecosystems are sensitive to changes in sea level and precipitation and thus reflect ecological conditions. The close proximity to archaeological sites allows us to draw conclusions regarding human interaction with the mangrove ecosystems. Our interdisciplinary inquiry reveals that the mangrove ecosystems along the east coast of Oman collapsed ~6000 cal yr BP on a decadal scale. There is no sedimentological evidence for a mid-Holocene sea-level highstand. The ecosystem collapse was not caused by sea-level variation or anthropogenic interferences; rather, it was the consequence of reduced precipitation values related to a southward shift of the Intertropical Convergence Zone. This resulted in a decrease of freshwater input and an increase in soil salinity. Further, the aridification of the area caused increased deflation and silting up of the lagoons.

Keywords: Arabian Sea; Indian Ocean; Sea level; Climate change; Intertropical Convergence Zone; Coast; Monsoon; Geoarchaeology; Mangrove

INTRODUCTION AND AIMS

Climate change is affecting the world's coastlines; the sea level is rising and the intensity and frequency of climatically induced extremes are increasing (Mitchell et al., 2006; Seneviratne et al., 2012). Coastal communities are vulnerable, as coastal systems are highly dynamic. Globally, 2.8 billion people live at a distance of less than 100 km from the coastline; 200 million live within areas less than 5 m above the present sea level (Bollmann et al., 2010; Bange et al., 2017). Processes that control coastal systems are related to changes in climate circulation patterns and relative sea level (RSL). The latter reflects local to regional variations of the coastline, influenced by the volume of the oceans as well as vertical land movements (Rovere et al., 2016). Changes in climate and sea level affect not only humans but also ecosystems (McGowan et al., 1998). However, uncertainties remain regarding the response of marine and terrestrial ecosystems to RSL change (Lovejoy and Hannah, 2005). Local studies in selected key areas are therefore necessary to understand the processes that control ecosystem changes. Here, we demonstrate that mangrove-fringed coastal lagoons serve as sedimentary archives that can be used to reveal an ecosystem's reaction to physical stress.

Globally, mangroves are declining rapidly (Polidoro et al., 2010). As much as 35% of mangrove area has been lost since the 1980s (Curnick et al., 2019). Mangrove forests are threatened by urban development, agriculture, aquaculture, tourism, and other developments in coastal areas. In addition to physical habitat destruction, global warming-related process changes are another factor to be considered (Ellison and Stoddart, 1991).

Our study area is the coastline of northeastern Oman, along the shore of the northern Indian Ocean. Here, human activities have been documented in the archaeological record since the Neolithic period (Cleuziou and Tosi, 2007). Neolithic archaeological evidence indicates that lagoons must have existed along the coastline, which is characterized by hyper-arid conditions today. Studies show that these lagoons

Cite this article: Decker, V., Falkenroth, M., Lindauer, S., Landgraf, J., Al-Lawati, Z., Al-Rahbi, H., Franz, S. O., Hoffmann, G. 2021. Collapse of Holocene mangrove ecosystems along the coastline of Oman. *Quaternary Research* 100, 52–76. https://doi.org/10.1017/qua.2020.96

https://doi.org/10.1017/qua.2020.96 Published online by Cambridge University Press

CrossMark

were fringed by mangroves (Lézine et al., 2002; Berger et al., 2013, 2020; Marrast et al., 2020). Owing to their sensitivity to salinity and temperature, and also to their intertidal position, mangrove ecosystems are excellent archives of environmental changes in climate and sea level. Moreover, mangrove-fringed lagoons are exceptional natural records, as they serve as sediment traps with anoxic conditions. Therefore, we focus on the localization of the spatial distribution of mangrove forests along the shoreline of the Arabian Sea during the Holocene. Our study addresses three main topics, as outlined below.

Holocene sea-level variation

We shed light on the development of the RSL from the mid-Holocene until today. We center our attention on whether there is field evidence for a mid-Holocene sea-level highstand in the study area. By investigating mangrove ecosystems as a sea-level indicator as well as some nonmangrove coastal profiles we hope to make a valuable contribution to this research field.

Climatic change

We contribute to the ongoing discussion on climate change in the region during the mid-Holocene (Fleitmann et al., 2003). Climate conditions are arid today, but there are various lines of evidence showing that the climate was substantially wetter during the early and mid-Holocene (Lézine et al., 2002, 2017; Enzel et al., 2015, 2017; Engel et al., 2017). We hypothesize that the effects of climate change are documented in mangrove sediments.

Relationship between humans and coastal ecosystems

In our study area, archaeological evidence indicates that hunter-and-gatherer populations exploited mangrove ecosystems during the Neolithic period and the Bronze Age (Lézine et al., 2002, Berger et al., 2020). Thus, archaeological investigation is an appropriate way to localize paleo-mangrove settings. We aim to reconstruct the environmental conditions during the mid-Holocene.

STUDY AREA

Regional setting

Oman represents the most eastern part of the Arabian Peninsula. Today, most of this peninsula is dominated by desert environments, and the climate is semi-arid to arid, and even hyper-arid, locally (Glennie and Singhvi, 2002). In the northern part of Oman, moisture is received from winter rainfall supplied by the westerlies, a wind regime that transports rain from the Mediterranean. Humid air masses from the Mediterranean reach the Hajar Mountains from the northwest. This mountain chain is up to 3000 m high and acts as a topographical obstacle and initiates rainfall on the windward side. The southernmost part of the peninsula, namely parts of Yemen and the Dhofar region in southern Oman, receives considerable amounts of precipitation throughout the summer months. This rainfall is associated with the seasonal northward movement of the Intertropical Convergence Zone (ITCZ) and the accompanying Indian summer monsoon (ISM) (Hoffmann et al., 2016). The ITCZ is the main component of the global atmospheric circulation pattern that significantly influenced the climatic variability in the area of the northwest Indian Ocean during the Quaternary (Fleitmann et al., 2003). With some local exceptions, other parts of southern Arabia receive between 50 and 200 mm of annual precipitation. Precipitation events are often sporadic and can be intense, with a high erosional potential and regional flooding. Our main study area is located on the east coast of northern Oman. This part of the coast is dominated by arid conditions and aeolian processes. Former marine lagoons are silted up and form *sabkhas* (salt pans). Precipitation values are below 80 mm per year (Enzel et al., 2015). Flooding occurs due to episodic rainfall events when water fills the plain areas, leaving interlayered deposits of silt and evaporates. Today, Oman witnesses sporadic landfall of tropical cyclones, including Cyclones Gonu in 2007 and Phet in 2010 (Fritz et al., 2010).

The coastline is characterized by a mesotidal regime, with a maximum tide range of 3 m during spring tide (McLachlan et al., 1998). The sandy beaches face low to moderate wave-energy levels, with wave heights of up to 1 m (McLachlan et al., 1998). The water level and wave height can increase significantly during storms events like Gonu (Fritz et al., 2010).

The sea surface temperature (SST) of the Gulf of Oman is as low as 23°C in January. The coastline of northeastern Oman shows SSTs of 24–25°C (Luis and Kawamura, 2002). The atmospheric forcing is the northeast monsoon/winter monsoon, which influences the SST in this location. Wind turbulences can additionally diminish SST up to 2°C (Luis and Kawamura, 2002). The wind patterns switch twice a year, influenced by the ISM in summer and the Mediterranean westerlies in winter. The wind influences seawater currents, which leads to a current from the southwest to northeast in summer and from the northwest to southeast in winter. The latter activates an upwelling of cold, nutrient-rich water masses (Piontkovski et al., 2012).

Mangrove ecosystems in Oman

Mangrove habitats are scattered along the Omani shoreline, with approximately 30 small sites commonly not exceeding 2–3 km^2 (Al-Hashmi et al., 2013). These are locally called *khawrs*. Oman is located at the outer margin of the potential mangrove distribution area. Mangroves inhabit intertidal areas in tropical to subtropical regions, roughly between 35°N and 35°S. Global expansion is mainly restricted by the SST during winter months. Although SST tolerance

https://doi.org/10.1017/qua.2020.96 Published online by Cambridge University Press

shows an intraspecific variation, a general threshold for the more tolerant species can be correlated with the 24°C SST isotherm (Tomlinson, 2016). The SST is highly influenced by ocean currents, which leads to an irregular-shaped potential distribution pattern of mangroves (Ricklefs and Latham, 1993). A mean SST of about 23°C in the winter months along the northern coastline of the Arabian Peninsula reduces species variation to robust mangroves like *Rhizophora mucronata* and *Avicennia marina* (Ward et al., 2016). Because of arid to semi-arid climate conditions with low precipitation of <120 mm/yr (Kwarteng et al., 2009), mangrove forests in Oman are made up solely of the more salt-tolerant species of *A. marina*. Physical stresses like low temperature and high salinity inhibit plant growth, which results in a plant cover of scrubby bushes instead of large trees (Tomlinson, 2016). The spatial distribution of mangrove forests is limited to sheltered environments such as lagoons. Mangroves develop in brackish lagoons and are fed by fresh water, either through input of wadis or by underground fresh water. Examples of recent mangrove habitats depending on fluvial input are Qurum and Quriyat to the east of Muscat. The lagoons of Sur and Khawr al Jaramah belong to the groundwater-fed type (Lézine et al., 2002). They are located in the most eastern part of the country, next to the eastern tip of the Arabian Peninsula, which is called Ras al Hadd. Lagoonal embayments near Bandar al Khayran are surrounded by steep hillsides from which fresh water flows directly to the mangrove-fringed lagoons. South of Ras al Hadd, along the eastern coast of northern Oman, up to the peninsula of Bar al Hikman, no suitable habitats for mangrove settlement exist.

During the Neolithic, mangrove forests were popular spots, as they guaranteed fresh water, food, and wood. Archaeological evidence in the form of debitage and food leftovers is preserved as shell middens (Biagi, 1994). Fossil species compositions of these shell middens reflect the source of food supply (Waselkov, 1987). This can be open sea or lagoonal fauna. At some sites, the latter includes mangrove-associated species like the gastropod *Terebralia palustris* (Martin, 2005; Berger et al., 2013, 2020).

Today, the population in Oman is encroaching on coastal areas; increasing human activities are therefore endangering the marine environment, including mangrove forests. In Oman, mangrove ecosystems are protected areas, which restrict anthropogenic destruction, the major threat that mangroves currently face. Chopping down mangrove forests was very common and still is in some places. People use mangrove wood for cooking, livestock fodder, and construction (Cleuziou and Tosi, 2007). It is used because alternative wood supplies are insufficient (Fouda and Al-Muharrami, 1995), as the terrestrial vegetation cover is sparse and dominated by grasses and small bushes.

Awareness campaigns by governmental institutions are showing some initial positive results. Efforts are being undertaken to protect, recover, and spread mangrove ecosystems (e.g., reforestation programs initiated by the Omani Ministry of Environment and Climate Affairs [MECA], in cooperation with the Japan International Cooperation Agency, whereby a new environmental information center has been established in Qurum (Japan International Cooperation Agency, 2014).

Holocene sea level along the coastline of Oman

Quaternary RSL variation along the coastline of Oman has not been thoroughly investigated. Differential movement of the lithosphere during the Quaternary along the Omani coastline is reported by Hoffmann et al. (2013). Falkenroth et al. (2020) identified a coastal notch in Sur, associated with the last interglacial sea-level highstand, at an elevation of 3.9 m, and confirm the tectonic stability of this area. The elevation of the paleo-shoreline testifies to differential crustal movement, as the coastal area north of Sur shows uplift for at least 800 ka (Mattern et al., 2018; Moraetis et al., 2018; Hoffmann et al., 2020).

Holocene sea-level research along the coastline of Oman is very limited. To our knowledge, no study has focused on the reconstruction of Holocene sea-level variability; only individual reports on Holocene marine deposits exist. Mid-Holocene sea-level estimates range from decimetres (Lézine et al., 2002) to several meters above present values (Berger et al., 2013). In one location, Preusser et al. (2005) report Holocene ages for marine deposits well above the recent sea level. In contrast, Beuzen-Waller et al. (2019) postulate a stable RSL for the Quriyat area, based on sea-level index points (SLIPS) at least from 7416 to 7183 cal yr BP.

Detailed sea-level studies have been undertaken in adjacent areas, mainly in the Persian Gulf. Lokier et al. (2015), for example, report a possible sea-level highstand in excess of 1 m by 5290–4570 cal yr BP and a regression to recent levels by 1440–1170 cal yr BP. Bernier et al. (1995) investigated Holocene shoreline variations and found these to vary up to 2 m. Parker et al. (2018) were the first to use SLIPS in this area to find the variations significant but slightly reduced.

Knowledge about sea level, especially about a potential sea-level highstand, is important for reconstructing the paleo-coastal morphology. The latter is essential for archaeological research, as communities were living along the coastline during the Late Neolithic.

Holocene climate variability

The climate of the Arabian Peninsula has shown considerable variation throughout the Quaternary, resulting in drastic arid–humid transitions and fundamental environmental deviations that had an important impact on past human societies (Parker and Rose, 2008; Petraglia et al., 2020). As in most arid zones, the preservation potential of sediments that serve as terrestrial archives is poor; hence, detailed information on past environmental conditions is scarce.

Aeolian sediments have often been interpreted as indicators of phases of aridity in Arabia (Preusser et al., 2002, 2005; Bray and Stokes, 2004; Radies et al., 2004; Stokes and Bray, 2005; Atkinson et al., 2011). Aeolian deposition also reflects other factors, such as sediment availability and

preservation (e.g., Preusser, 2009; Bailey and Thomas, 2014). Past humid periods in Arabia have been identified by analyzing speleothems (Burns et al., 1998, 2001; Neff et al., 2001; Fleitmann et al., 2003, 2007) and relict lake deposits (Radies et al., 2005; Rosenberg et al., 2011, 2012). These pluvials concur with maxima in fluvial activity and alluvial fan generation (Maizels, 1990; Rodgers and Gunatilaka, 2003; Blechschmidt et al., 2009; Parker, 2009). The climate variability recorded in terrestrial archives of southern Arabia, notably the change in moisture supply, is apparently controlled by changes in the location of the ITCZ and the associated rainfall belt of the Indian Ocean monsoon (IOM). During times of increased summer season insolation, the mean latitudinal position of the summer ITCZ shifts northward, and the IOM is drawn into the continent. Precipitation in Oman is estimated to have been 100–160 mm higher than the present owing to the shift of the summer rain impact of about 100–150 km northward, creating paleo-wetlands in Arabia (Enzel et al., 2015). Periods with a stronger monsoon circulation and increased humidity in the interior of the Arabian Peninsula are recorded for the early to mid-Holocene as well as for Marine Isotope Stages (MIS) 5a, 5c, 5e, 7a, and 9 (Burns et al., 2001; Fleitmann et al., 2003; Rosenberg et al., 2011).

Holocene climate variability in Arabia is comparable to changes observed in northern Africa (Tierney et al., 2017; Lüning et al., 2018). The poleward-shift of the ITCZ led to significantly more rainfall in the Sahara between ~11 and 6 ka ago (Tierney et al., 2017). This period is known as the African Humid Period (AHP) in Africa (deMenocal and Tierney, 2012) and is contemporaneous with the Early Holocene Humid Period (EHHP) in Arabia (Lézine et al., 2017). Both are caused by a northward shift of the ITCZ, which affected the atmospheric circulation patterns of the African monsoon (Bonfils et al., 2001) as well as the ISM. During this period, lakes existed in, for example, the central Sahara (Gasse, 2002) and the Rub al Khali (Awafi Lake), where falling lake levels indicate the onset of climatic aridity ~5900 cal yr BP (Preston et al., 2012). Griffiths et al. (2020) investigated the relationship between the end of the AHP and an aridification of mainland Southeast Asia. They refer to a correlation of orbital forcing factors, less vegetation, and increased dust-load that influenced atmospheric circulation patterns and cooled the Indian Ocean during this time. By examining stalagmites in North Oman (Hoti cave) and South Oman (Qunf cave), Fleitmann et al. (2007) reconstructed the shift to drier conditions to be gradual and a consequence of a long-term trend of decreasing monsoon precipitation. This is supported by Lézine et al. (2017).

A significant change in wind patterns along the coast of northeastern Oman around the 4.2 ka event was identified by Watanabe et al. (2019). Sr/Ca ratios and stable oxygen isotopes of fossil *Porites* spp. corals collected from this location indicate abrupt colder and wetter winter seasons ~4.1 ka. This change was caused by a shift in the winter *shamals*, also known as the Mediterranean northwesterlies. On the one hand, this led to an increased precipitation in the Gulf of Oman; on the other hand, it led to aridification in Mesopotamia, which according to Watanabe et al. (2019), finally caused the collapse of the Akkadian Empire. Kathayat et al. (2017) see a long-term decreasing trend in the ISM over the last 5700 years for northern India and relate it to the decline of the Harappan civilization in the Indus Valley.

Archaeological investigations in eastern Arabia reveal a socioeconomic change marking the transition from the Late Neolithic to the Early Bronze Age. Evidence from the fourth millennium BC indicates that people in Oman changed from a mainly nomadic to a mainly sedentary way of life beginning in 3400 BC, based on a higher proportion of remains relating to a sedentary lifestyle (Biagi and Nisbet, 1999; Cleuziou and Tosi, 2007). This corresponds to a climate change during that time. The socioeconomic transition results in what is known as the Great Transformation and is documented by the appearance of various settlements and the evolution of new cultures in the Early Bronze Age, namely the Hafit (3200–2700 BC) and the Umm an-Nar (2700–2000 BC) (Cleuziou, 2009; Gregoricka, 2016).

In summary, it can be concluded that wetter conditions are indisputable for the mid-Holocene in Arabia as well as in northern Africa (Staubwasser and Weiss, 2006). However, there is ongoing debate about the quantity of precipitation (Enzel et al., 2017 [and references therein]). Further, the transition to more arid conditions has not been fully resolved, with both the ISM and the North African summer monsoon discussed as moisture sources (Enzel et al., 2015 [and references therein]).

METHODS

Site investigation and sampling

In total, five different localities along the northern and eastern coastline of Oman were investigated, with the focus on paleo-mangroves. The northernmost site is Sawadi, west of the Muscat city area. Following the coastline to the southeast, two sites are near Ar Rumays and Quriyat. South of Ras al Hadd, we found two outcrops near Al Haddah and As Sulayb that reveal coastal marine deposits. With a sedimentological profile analysis, we attained more information about sea-level variation in our study area. At the east coast, south of Ras al Hadd, we also found paleo-mangrove sites and cored *sabkhas* near Suwayh and Ras ar Ru'ays (Fig. 1). Coring was carried out at 48 sites in total, in order to get an overview of the paleo-lagoon spatial distribution. The core depth ranged from 28 to 320 cm, and coring was conducted using an Edelman clay auger. At those localities where paleo-lagoonal deposits were revealed by coring, trenches were dug to study the structure of the layers. In the trenches, the focus was on the documentation of structures like bioturbation and cross-lamination. The profile descriptions follow the standard protocol according to DIN EN ISO 14688-1 (Deutsches Institut für Normung e.V, 2011). The trenches allowed a proper sampling to be taken from uncontaminated material. Overall, 10 trenches were dug during this field campaign. The most

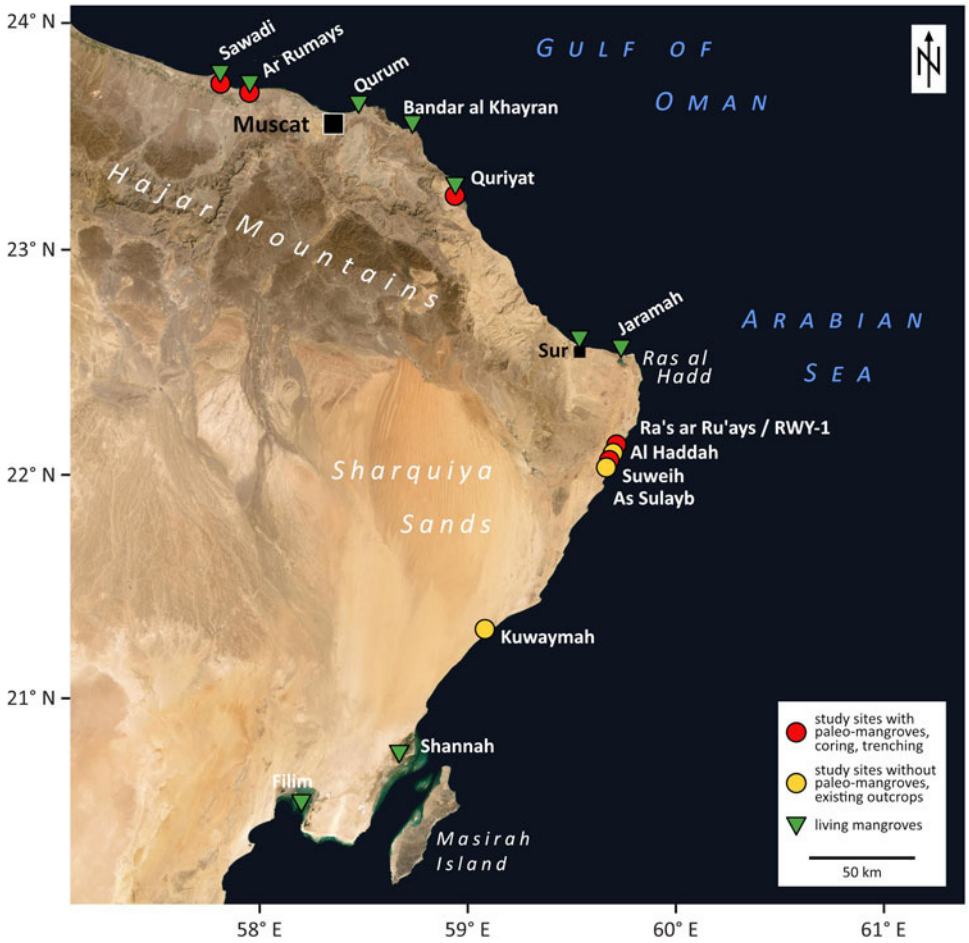

Figure 1. (color online) Map of northeastern Oman showing the study area and the distribution of recent and paleo-mangroves (source: ESRI data, map created using ArcGIS 2015).

promising sites are located on the eastern coastline. The coring and trenching in the *sabkhas* near Suwayh and Ras ar Ru'ays allowed us to construct cross sections. Trenches were 70 to 185 cm deep and were sampled every 2, 5, or 10 cm, depending on the stratigraphy. Where sediment was promising for pollen preservation, the profile was sampled every 2 cm for high-resolution analyses. Overall, 168 samples were taken.

Sedimentological analyses

Granulometric analyses were performed by sieving and laser diffractometry, and 100 g of each sample was presorted by wet sieving using sieves measuring 2 and 0.063 mm. Material <0.063 mm in size was collected for further preparation and analysis with the laser particle sizer. The measurements were executed with a Horiba Partica LA 950V2 laser at the Department of Geography, University of Bonn. The Fraunhofer theory was used to convert the light-intensity patterns into grain size. Material >0.063 mm in size was stored in a compartment drier at 105°C for 24 h and then sieved dry. Sieves with mesh sizes of 2, 1, 0.5, 0.25, 0.125, and 0.063 mm were used. During the gradation test, a sieving loss ranging from 0 to 0.24% was determined. Sieving processes with a sieving loss of <1% (Deutsches Institut für Normung e.V, 1987a, 1987b) are valid, thereby rendering the gradation of this study valid.

Geochemical analyses

We carried out carbon, nitrogen, and sulfur (CNS) measurements (total carbon [TC], total nitrogen [TN], and total sulfur [TS]). A total of 40 ml of the sample was ground using the vibratory disc mill RS 200 from Retsch equipped with a tungsten carbide jar. The CNS measurements were carried out with the CNS analyzer vario EL cube by Elementar. A total of 20 mg of ground material from the sample was pyrolyzed at 1800°C, with O_2 supply and He as a carrier gas. Detection limits are 0.23% for carbon, 0.04% for nitrogen, and 0.11% for sulfur. The total organic carbon (TOC) content was determined using the indirect muffle furnace method (Hirota and Szyper, 1975; Keefe, 1994; Steinbeiss et al., 2008). To determine the total inorganic carbon (TIC) content, the organic substance must be removed (Bisutti et al., 2004). This was done by double determination of a 2-g sample in a muffle furnace at 450°C for 16 h. The TIC content of the rest of the sample was determined by the CNS analyzer. The loss on ignition

(450°C) was taken into account to relate the TIC content to the starting substance. The organic carbon concentration was then calculated as the difference between the TC and the TIC content. The TOC content helps to differentiate the source of carbon. The carbon/nitrogen ratio should help distinguish between the terrestrial and the aquatic organic matter (Perdue and Koprivnjak, 2007). The TS content is used as a proxy for marine influence (Berner and Raiswell, 1984).

Topographic survey

In the *sabkhas* near Ras ar Ru'ays, at the sites of Quriyat and Ar Rumays, and in recent mangrove ecosystems near Sawadi, Sur, and Ras al Hadd, we conducted differential-GPS (D-GPS) measurements. This is a standard technique to precisely evaluate the height of a certain point above the present mean sea level to centimetre accuracy. Here, we aimed to detect Holocene sea-level variations. We used a Leica GS15 in real-time kinematic mode with two paired antennas. The elevations were measured relative to the base station, with an accuracy of 0.02 m or less. Coordinates were presented as meters in the Universal Transverse Mercator (UTM) projection, Zone 40Q, using the WGS 1984 reference ellipsoid. To calculate the absolute height, the sea level was first measured at different tidal datums and normed to mean sea level, with sea-level data derived from the web-based service of the Intergovernmental Oceanographic Commission.

By acquiring data about the modern vertical distribution of *A. marina*, we obtained more information about living mangroves in Oman to better interpret the findings from paleo-mangroves, particularly indicative meanings. We chose these three different places because the mangrove distribution is not limited by infrastructure or geomorphological obstacles, and the sites provide different ecological conditions. Mangroves in Sawadi grow in a creek system, Sur Lagoon is densely populated and attached to larger Wadi systems, and Ras al Hadd is a rather small, remote lagoon.

Shell midden investigations

We investigated shell middens next to the *sabkhas* to shed light on the human-environment interaction. We focused on the species assemblage, especially on the occurrence of the mangrove gastropod *T. palustris*. A suitable shell midden for taking samples was found next to the *sabkha* south of Ras ar Ru'ays. Here, gravel mining created a 2.3-m profile, and we sampled it every 50 cm to analyze the species assemblage. The species were identified according to Bosch et al. (1995). Three molluscs, specifically two oysters and one unspecified bivalve, were dated using radiocarbon.

^{14}C AMS dating

We used the ^{14}C method to date the sediment profiles and focused on the paleo-lagoon layers and the transition to the following sedimentological settings. We dated nine shells, one piece of wood, and five bulk sediment samples. The shell sampling material consisted of gastropods and bivalves. The latter were articulated shells to ensure a sample of in situ organisms. The piece of wood was found in a layer without carbonate macrofossils. To determine the reservoir effect, we needed carbonate and terrestrial material for comparison. We did not find molluscs or macrofossil terrestrial material in the same layer in any of the trenches. To better understand the reservoir effect, we decided to also date the bulk sediment samples after the carbonates were removed.

The bulk sediments samples were pretreated using a standard acid-base-acid solution to remove carbonates and humic acids (Lindauer et al., 2017). Shells were pretreated with diluted acid (HCl) to remove the outer, most probably contaminated, part of the shell material. After pretreatment, sediments were combusted in an elemental analyzer (MicroCube, Elementar) and the CO_2 collected and reduced to graphite. The shells were hydrolyzed with phosphoric acid, and the emerging CO_2 was collected and graphitized. Samples were then measured in a MICADAS-type AMS (Kromer et al., 2013), and fractionation was corrected. It should be noted that isotope data from ^{13}C measured with an AMS system cannot be used for interpretation in the same way as stable isotope measurements. They only serve the fractionation correction of the measurement. Calibration and reservoir effect modeling were done with Oxcal 4.3 (Ramsey and Lee, 2013) and the IntCal13 (Reimer et al., 2013) dataset. We used a phase model in Oxcal, with undetermined reservoir effect ΔR, as presented by Zazzo et al. (2012). Data are presented as 2-sigma values, which represent a 95.4% confidence interval of finding the true age.

Radiocarbon dating of marine organisms requires determining a local reservoir effect. As these organisms mainly incorporate carbon provided in the marine environment, their ages often do not correspond to calendar ages. The difference is then called a reservoir age, known as R(t). These age differences can vary locally and over time, depending on marine conditions like upwelling and ocean circulation. Because of differences in habitat and diet, the reservoir age also has a strong species-specific component that must be considered. To determine the reservoir ages and the reservoir effect, it is necessary to take paired values of a marine sample and a contemporary terrestrial sample without any reservoir effect. If this is not possible, literature values might provide some help but usually are not suitable for determining precise chronologies. We determined preliminary reservoir effects for the shells that were dated in this study by using the sediments from the cores. Although of marine origin, no other terrestrial material was found. Hence, we decided to remove carbonaceous material and soluble humic acids. As we encountered a lot of root-penetration structures in the paleo-lagoonal sediment, we presume that the main content of the remaining organic material in the sediment should originate from mangroves. It was already shown in another study (Lindauer et al., 2016) that mangrove leaves measured with radiocarbon provide atmospheric ages without influence from the marine environment because of photosynthesis. Younger

sediment ages can be a result of bioturbation or younger mangrove roots growing into older sediment (Woodroffe et al., 2015). Accordingly, bioturbation can transport older carbon into younger layers. Or, conversely, infaunal carbonate macrofossils bring younger carbon into older layers. For a precise chronology, the sediment must be checked for other indicators, such as pollen or foraminifera, which can also be dated.

RESULTS

Trenches south of Ras ar Ru'ays

The sediment sequences in the *sabkhas* near Suwayh and Ras ar Ru'ays on the east coast all show a similar pattern: dark gray fine-grained deposits at the base and overlying beige coarser sediments. The surface of the *sabkhas* is characterized by a salty crust and sometimes authigenic gypsum crystals. Often, mollusc shells cover the surface.

The *sabkha* south of Ras ar Ru'ays (40Q 781980, 2452862) is representative for this area and is thus described here in detail. It has a maximum length of 3 km from west to east and 1.5 km from north to south. Five core sites, each spaced 50 m apart, were located along a transect crossing the *sabkha* in the south (Fig. 2). The surface of the *sabkha* is featureless, except for some minor dunes of decimeter height. D-GPS measuring of the *sabkha* surface gave results ranging from -25 cm a msl at core site 4 to 15 cm a msl at core site 1 (Table 1). Two trenches, A and B, measuring 113 and 150 cm deep, respectively, were dug and sampled next to core sites 2 and 5. The stratigraphic sequences of profiles 1–5 in the transect are similar, hence the layers can be correlated. The basal layer is represented by at least 40 cm of dark gray, fine-grained, shell-rich sediments. The mollusc remains belong to both bivalves and gastropods, indicating marine to brackish environmental conditions. Some bivalves are thin-shelled, others are hard-shelled, and some are articulated and were found fossilized in situ in the sediment. This layer is overlain by a 7- to 18-cm-thick clay layer, followed by 41–104 cm of shell-less silt and 7–15 cm of clayey silt that shows bioturbation structures.

Trench B at core site 5 displays bioturbation in the form of tubes measuring 2–3 cm in diameter (Fig. 3). They are filled with light greenish gray silt. The tubes have an inner channel with organic plant remains and are therefore identified as root-penetration structures. In some structures, a light brown-gray clayey silt between the inner channel and the greenish gray silt is present, and the contact to the overlying sand is sharp. The layers above are 34–64 cm thick, and the color shifts from beige to light reddish brown toward the top. Salt and gypsum crystals are present in the upper 1–5 cm of all profiles.

Trench A at core site 2 was analyzed for granulometry and geochemistry. The profile consists of a 113-cm-deep trench that was extended by 187 cm with coring to reach 300 cm in length. A total of 12 layers (L1–L12) were documented. The basal layer (L1: 300–256 cm below surface) is a dark gray color and rich in millimeter- to centimeter-sized shell fragments. The sediment grain size fines upward, from fine sand at the base to silt at the top. The dark gray silt continues in L2 (256–213 cm), but no shell fragments are observed. Finer sediment on top (L3: 213–195 cm) includes a dark gray silty clay with millimeter-sized shell and plant fragments. This sequence is overlain by dark gray fine sandy silt (L4: 195–182 cm). L5 (182–170 cm) is a dark gray silty clay layer with millimeter-sized plant remains. L6 extends from 170 to 66 cm below the surface and was explored by coring (170–113 cm) and trenching (113–66 cm). It is a fining upward sequence, with silt to fine sand at the base to light clayey silt to fine sand at the top, all dark gray in color. The upper 10 cm are bioturbated with tubelike disturbances of 1–2 cm in diameter. These are filled with light gray fine sand from the overlaying sequence. L7 (66–48 cm) is composed of grayish fine sand containing silt and medium sand. A significant change in color to L8 (48–17 cm) is evident, and this layer consists of light beige light silty fine to medium sand with millimeter-sized orange layers in the upper 22 cm of the sequence. L9 (17–8 cm) is an orange-beige fine- to medium-sand layer. It is overlain by 2 cm of reddish brown clayey fine sand (L10: 8–6 cm) and 3 cm of reddish brown clay with black algal mats (L11: 6–3 cm). These mats display desiccation cracks filled with reddish brown clay. On top, a slightly reddish brown layer rich in salt crystals forms a salt crust (L12: 3–0 cm). Scattered gypsum crystals and mollusc shells are found on the surface. The dominating species is the gastropod *Cerithidea cingulata*, but other species and bivalves are also present.

Trench A was sampled every 5 cm. Granulometric and geochemical analyses were conducted using five samples, at depths of 105 cm (L6), 85 cm (L6), 55 cm (L7), 30 cm (L8), and 10 cm (L9) below the surface. Figure 4 displays the results of the granulometric analyses. The two samples from L6 indicate a very positive skewness and a bimodal grain-size distribution, with two almost equal peaks at the medium silt and the fine sand fraction of 26% and 10% (>0.0063 mm) and 31% and 12% (>0.063 mm). This fine-grained layer is overlain by coarser sediments that deviate from the underlying layer mainly in terms of grain-size distribution. As Figure 4 shows, sediments of L7 and L8 are still very positively skewed. L7 is less well sorted and has a main peak of 48% in the fine sand (>0.125 mm), a smaller one of 16% in the medium sand (>0.25 mm), and a small one of 6% in the fine silt fraction (>0.002 mm). L8 also shows larger peaks of 49% in the fine sand (>0.125 mm) and 19% in the medium sand (>0.25 mm) fraction and displays an amount of 6% each in the fine and medium silt (>0.002–0.02 mm). L9 consists of >90% fine and medium sand (58% and 31%, respectively) and lacks a peak at finer particle sizes. These sediments are moderately sorted and show a negative skewness. Geochemical analyses (Supplementary Table 1) reveal a TC content of 2.5% and 2.3% for the silty layers and a 5.1%, 5.7%, and 5.5% for the upper fine sand layers. In these sequences, a significant difference is present in the amount of TOC and TIC content. The TOC content is the main component of the TC in the lower

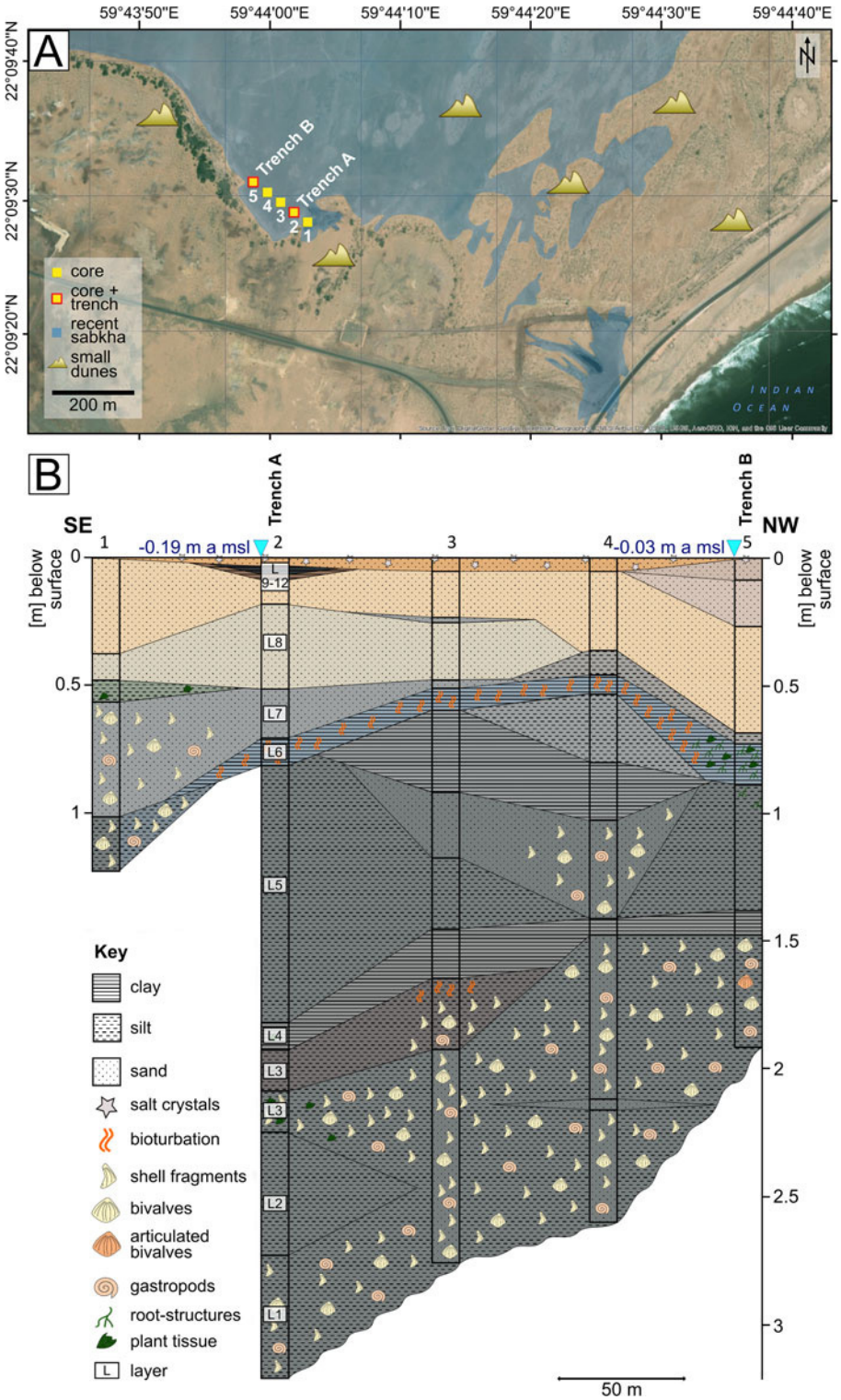

Figure 2. Transect in the southern part of a *sabkha*, south of Ras ar Ru'ays. (A) The yellow square and red-outlined yellow square show the coring and trenching locations, respectively; the blue area shows the extension of the recent *sabkha*, mostly limited by smaller dunes (map created using ArcGIS [2015] basemap imagery). (B) A correlated profile, including grain size and fossil content of the corings and trenches in the *sabkha*; the colors reflect those of the sediment, the blue triangles show the D-GPS measurements. (For interpretation of the references to color in this figure legend, the reader is referred to the web version of this article.)

https://doi.org/10.1017/qua.2020.96 Published online by Cambridge University Press

Table 1. D-GPS measurements of surface height a msl of selected investigated locations in the study area. Mean sea level is taken from the web-based service of the Intergovernmental Oceanographic Commission. Coordinates are presented as meters in the UTM projection, Zone 40Q, using the WGS 1984 reference ellipsoid.

location, site	North East	Longitude Latitude	meter a msl
Ar Rumays			
Top profile	2622646.095	23°42′41.1″N	0.68
	603585.091	58°00′58.1″E	
Top shell midden	2622751.921	23°42′44.5″N	5.10
	603566.681	58°00′57.5″E	
Quriyat			
Top profile	2569251.434	23°13′13.2″N	0.1
	699709.647	58°57′06.0″E	
Top shell midden	2569688.575	23°13′26.9″N	10.86
	700751.446	58°57′42.8″E	
Central Ras ar Ru'ays			
Top core site	2453529.437	22°09′50.1″N	0.25
	783076.600	59°44′41.5″E	
South of Ras ar Ru'ays			
Top core site 1	2452862.840	22°09′29.1″N	0.15
	781980.568	59°44′02.8″E	
Top core site 2 -	2452895.427	22°09′30.2″N	-0.19
Trench A	781941.206	59°44′01.5″E	
Top core site 3	2452929.250	22°09′31.3″N	-0.18
	781899.920	59°44′00.0″E	
Top core site 4	2452961.128	22°09′32.3″N	-0.25
	781862.501	59°43′58.8″E	
Top core site 5 -	2453000.490	22°09′33.6″N	-0.03
Trench B	781815.958	59°43′57.2″E	
Top shell midden	2453361.439	22°09′44.4″N	11.56
	783432.916	59°44′53.8″E	
Al Haddah			
Top L5	2450131.011	22°08′00.6″N	2.64
	781443.103	59°43′42.3″E	

part (76% and 78%) and reaches 24% of TC content in L7 at a 55-cm depth, 19% in L8, and 7% in L9. Similar to the TC, TS content decreases from 0.62% at the base to 0.22% at the top (Fig. 5). All results for TN were below the detection limit of 0.04%. Creating carbon/nitrogen ratios was therefore impossible.

For our radiocarbon data we had to consider the reservoir effect. We calculated reservoir effects for the shell samples, which showed a significantly older age than the sediments. In some cases, the uncalibrated sediment ages were younger than the shells, which is not to be expected from marine organisms. Along the coast of Oman, we found strong upwelling conditions of old carbon to the surface; hence, the shells must be older than the terrestrial counterparts. We therefore used the reservoir effect determined for *Marcia* sp. (MAMS 37279, MAMS 37380) for the other bivalves as well as for the oyster samples. We are aware that the reservoir effect determined as $\Delta R = -185 \pm 101$ yr can differ from the true value, but it should account better for the local effects than literature values from other lagoons. We were also able to derive a reservoir effect as $\Delta R = 72 \pm 90$ yr for two gastropod samples. With respect to calibration, negative reservoir effects mean that the value must be subtracted from the general marine calibration curve that is shifted from the atmospheric curve by a mean value of 405 ± 20 yr. Positive values need to be added to the marine calibration curve data. This is automatically done by software such as Oxcal when assigning a reservoir effect value to the samples.

The ^{14}C dating results of the *sabkha* sediments near Ras ar Ru'ays indicate the fine-grained basal layers as mid- to late Holocene depositions. The oldest sediments were found in the *sabkha* south of Ras ar Ru'ays and are dated to 6617–6497 cal yr BP (MAMS 37271) (Table 2). The dating material was bulk sediment at a depth of 140 cm below the surface. An articulated bivalve (*Marcia* sp.) collected at the same depth gave an uncalibrated age of 5710 ± 25 ^{14}C yr BP (MAMS 37281). The top of these silt layers is dated at a depth of 69 cm with bulk sediment to 5991–5835 cal yr BP (MAMS 37270). Unspecified bivalve shell fragments revealed uncalibrated ages of 5197 ± 24 (MAMS 37279) and 5180 ± 25 ^{14}C yr BP (MAMS 37280). The ^{14}C dating of bulk sediment from a profile 1.5 km to the northeast (40Q 782922, 2453641) indicates the transition of gray fine-grained sediments to beige coarser-grained sediments at 5920–5815 cal yr BP (MAMS 37267). Dating of two gastropods (*C. cingulata*) shows uncalibrated ages of 5648 ± 25 (MAMS 37273) and 5663 ± 25 ^{14}C yr BP (MAMS 37274).

Shell midden south of Ras ar Ru'ays

A shell midden is located adjacent to the investigated *sabkha* south of Ras ar Ru'ays (Fig. 6). It is situated on the sea side of the paleo-lagoon, on top of a ridge. The shell midden was partly removed by mining activities, exploiting an underlying fluvial gravel deposit. Graves were found in the deposits. The time of burial must have been during the shell accumulation, as indicated by the stratigraphy. Berger et al. (2020) date the burials to the Middle Neolithic period. Mining activities were stopped, and the site was declared an archaeological heritage site by the Ministry of Heritage and Culture. According to Google Earth satellite images taken in 2003, the shell midden had an extension of 350 x 150 m.

The profile accessible in the remaining deposits is 283 cm in height, and the top is at 11.56 m amsl (Table 1). The outcrop can be divided into two main layers consisting of a conglomerate overlain by shell midden deposits. The matrix-supported conglomerate (L1) is 55 cm thick and composed of semiconsolidated silt to coarse sand. Clasts are 1–10 cm in length and well rounded. The sorting is good, and layers show decimeter-scale cross stratification. Clast lithology differs, including granite and gabbro derived from the crystalline basement as well as various sedimentary rocks (e.g., Jurassic radiolarian chert). The top of L1 is at an elevation of 9.28 cm a msl. The layer is interpreted as a fluvial-deltaic deposit. Berger et al. (2020) give an OSL age of >400 ka for this layer. Given the close relation to the recent shoreline, these deposits probably formed during a sea-level highstand

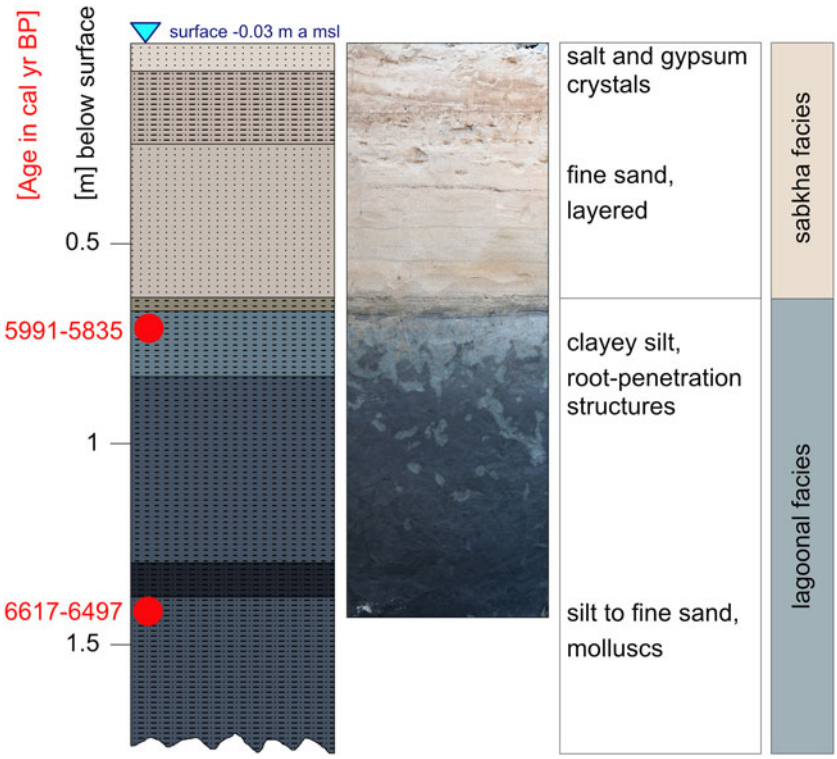

Figure 3. (color online) The sediment profile of Trench B in the *sabkha* south of Ras ar Ru'ays. The ^{14}C dates are based on bulk sediment dating.

(e.g., MIS 5e). The contact between the conglomerate (L1) and the shell midden deposits (L2) is erosive.

L2 consists of broken mollusc shells, in a silty to sandy matrix. The whole profile is layered and shows interbedded pure sand layers and ash lenses. The latter are often combined with millimeter-sized unspecified fish bones. Very few angular to subrounded pebbles and cobbles up to 15 cm in length are present in L2. The mollusc shells derive from edible organisms originating from marine and brackish environments. The species assemblage is similar throughout the profile.

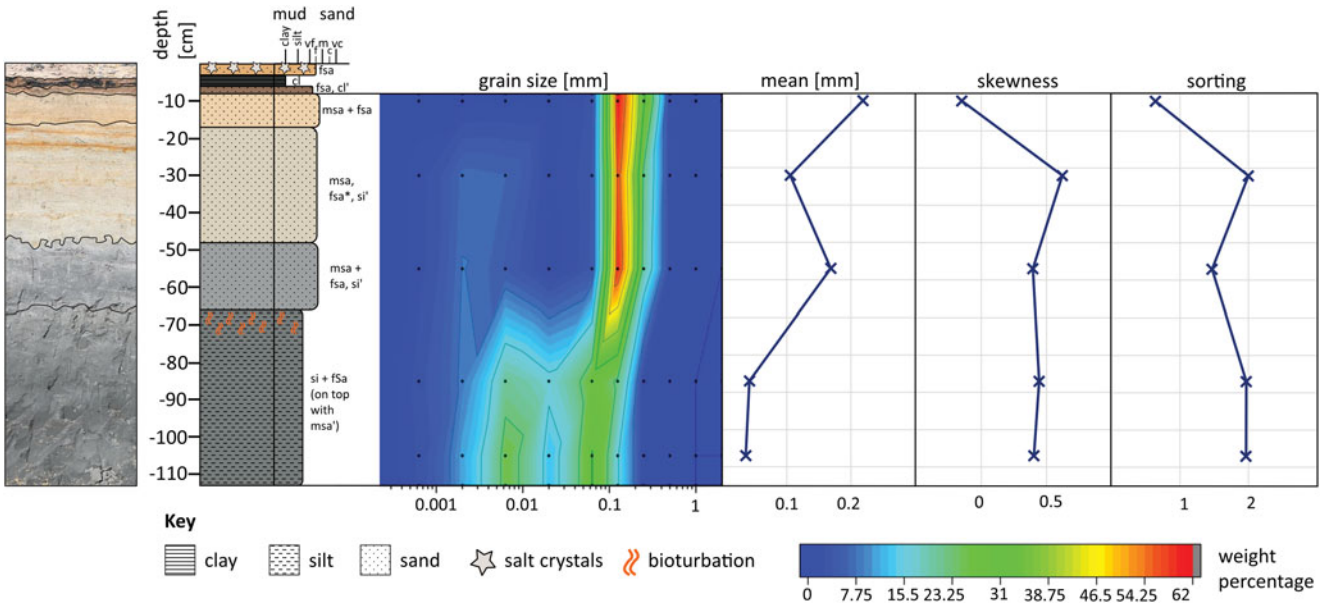

Figure 4. (color online) Sediment profile of Trench A in the *sabkha* south of Ras ar Ru'ays, and the granulometric results, including grain size distribution, mean, skewness, and sorting.

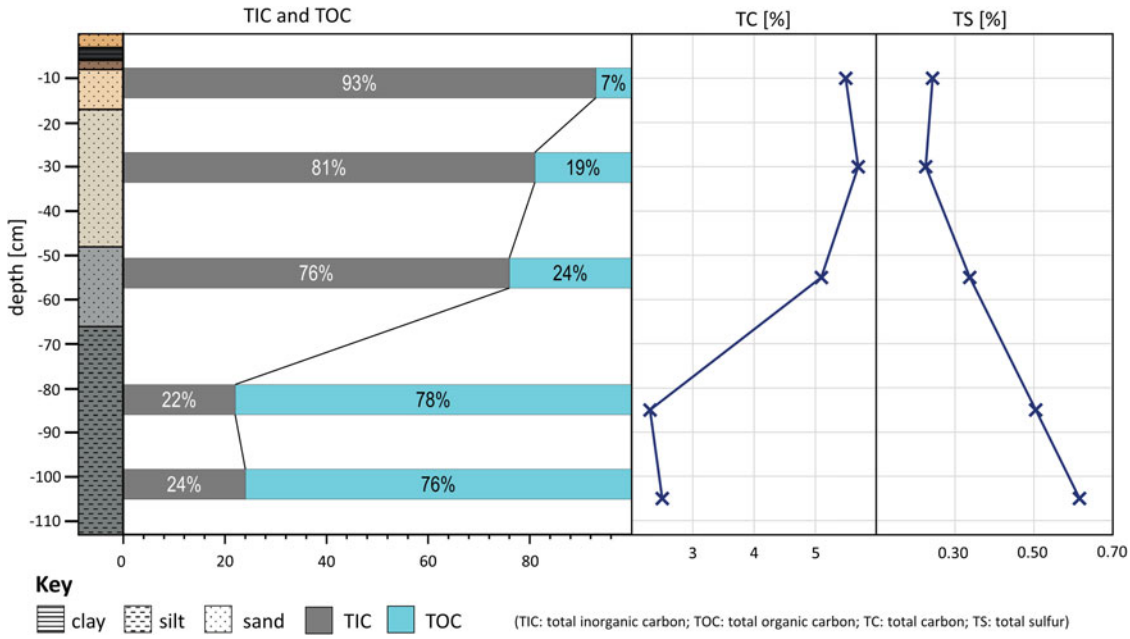

Figure 5. (color online) Geochemical results of Trench A in the *sabkha* south of Ras ar Ru'ays, including TOC and TIC cumulative content (left), TC (center), and TS content (right).

The most abundant species are oysters: *Anadara* sp., *Marcia* sp., and *T. palustris* among others, as depicted in Figure 7. Most important in the context of our research is the mangrove ecosystem indicating gastropod *T. palustris*. The ^{14}C dating revealed ages of 7319–6838 cal yr BP (COL1172.1.1) at the bottom of L2, and 7539–7151 cal yr BP (COL1173.1.1) and 5977–5546 cal yr BP (COL1174.1.1) below the top (Fig. 6, Table 2). Berger et al. (2020) detail a stratigraphic analysis of this shell midden.

Profiles near Al Haddah and As Sulayb

Along the east coast, marine deposits are present that clearly indicate a different RSL at some time. We include the results of these profile analyses because they play a part in contributing to the investigation of Oman's sea-level history.

A 4-m-high coastal cliff of semiconsolidated marine sediments crops out close to the town of Al Haddah (Fig. 8). The sediments discordantly overlay radiolarian mudstones and pelagic limestones of the Triassic Sal Formation (Peters et al., 2001).The outcropping succession consists of conglomerates and sandstones that were deposited in a marine nearshore environment. A weak coarsening upward trend from the sand-dominated lower half of the profile to the matrix-supported conglomerates of the upper half is observed. The whole succession dips seaward at a 6° angle.

Clasts in the lower part, below 1.5 m, consist almost exclusively of angular radiolarian cherts and shell debris. In the upper conglomeratic part, above 1.5 m, the number of well-rounded clasts increases significantly. This indicates a change from a locally supplied, wave-dominated depositional system to a deltaic coast fed by a feeder alluvial system that supplies sediment from the hinterland.

The beach facies of the lower part are variable, consisting of typical swash-dominated foreshore facies with steeply seaward dipping beds that vary in grain size between sand and granules but also of fine to medium sandstone that is intensely burrowed. The succession is interrupted by lenses of coarse-grained material, which indicates extreme wave events.

The deltaic facies, above 1.5 m in Al Haddah, shows large-scale cross-bedding as well as channel structures. Clast sizes range from pebbles to large cobbles. This facies also crops out in a 2-m-high coastal cliff near As Sulayb, where it discordantly overlays radiolarian chert as well. At both outcrops, the conglomerates contain a large number of oyster shells that were identified as *Crassostrea gryphoides* (Hoffmann et al., 2016). The shells are up to 30 cm in length and are elongated and have a round diameter. They usually occur as single valves but are otherwise well preserved, which indicates transportation but not over a long distance. A shell from the profile in As Sulayb was dated using radiocarbon, but the result was inconclusive, as the age of the shell material exceeds the age limit of the ^{14}C method, indicating an age of >43.5 ka (Beta-318819).

Ar Rumays site

The granulometric and geochemical investigations of a profile near Ar Rumays, on the northern coastline of Oman, reveal an alteration similar to the profiles near Ras ar Ru'ays and Suwayh. However, the transition is less sharp than that observed in the profiles on the east coast.

Near Ar Rumays, a 140-cm profile was investigated (40Q 603587, 2622641). It is located at a distance of 100 m from the open sea, in a small depression. This profile is divided

https://doi.org/10.1017/qua.2020.96 Published online by Cambridge University Press

Table 2. ^{14}C dating results showing uncalibrated and calibrated ages BP whenever applicable. It should be noted that isotope data from Delta13C measured with an AMS system cannot be used for interpretation in the same way as stable isotope measurements. They only serve the fractionation correction of the measurement. Coordinates are presented as meters in the UTM projection, Zone 40Q, using the WGS 1984 reference ellipsoid.

sample	lab ID	North East	Longitude Latitude	conv. age (BP)	cal yr BP 2σ	$^{13}C/^{12}C$ (‰)	elevation [m a msl]	material	remark
Shell midden south of Ras ar Ru'ays - 1	COL1172.1.1	2453413 783151	22°01′37.5″N 59°40′14.4″E	6399±23	7319-6838	-1.2	ca. 9.6	oyster shell	assumption ΔR = -185±101
Shell midden south of Ras ar Ru′ays - 2	COL1173.1.1	2453413 783151	22°01′37.5″N 59°40′14.4″E	6641±23	7539-7151	0.8	ca. 9.9	oyster shell	
Shell midden south of Ras ar Ru'ays - 3	COL1174.1.1	2453413 783151	22°01′37.5″N 59°40′14.4″E	5191±21	5977-5546	-0.1	ca. 10.8	bivalve	assumption ΔR = -185±101
As Sulayb	Beta-318819	2438235 775689	22°01′37.5″N 59°40′14.4″E	>43500	na	-1.5	ca. 1.8	oyster shell	
Central Ru'ays 94 cm depth	MAMS 37267	2453567 783012	22°09′51.4″N 59°44′39.2″E	5200±25	5920-5815	-15.2	-0.69	organic remains	
Central Ru'ays 94 cm depth	MAMS 37273	2453567 783012	22°09′51.4″N 59°44′39.2″E	5648±25	6190-5739	1.6	-0.69	gastropode	ΔR = 72±90
Central Ru′ays 94 cm depth	MAMS 37274	2453567 783012	22°09′51.4″N 59°44′39.2″E	5663±25	6202-5753	1.6	-0.69	gastropode	
Central Ru'ays 125 cm depth	MAMS 37272	2453567 783012	22°09′51.4″N 59°44′39.2″E	4682±23	5391-5262	-12.8	-1.0	wood	
Central Ru'ays 164cm depth	MAMS 37268	2453567 783012	22°09′51.4″N 59°44′39.2″E	5485±30	6256-6141	-27.6	-1.39	bulk sediment	
Central Ru'ays 164cm depth	MAMS 37275	2453567 783012	22°09′51.4″N 59°44′39.2″E	5472±26	6285-5840	0.1	-1.39	bivalve	assumption ΔR = -185±101
Central Ru'ays 164cm depth	MAMS 37276	2453567 783012	22°09′51.4″N 59°44′39.2″E	5490±26	6295-5859	-2.6	-1.39	bivalve	
Central Ru'ays 170 cm depth	MAMS 37269	2453567 783012	22°09′51.4″N 59°44′39.2″E	5398±32	6178-5997	-27.5	-1.45	bulk sediment	
Central Ru'ays 170 cm depth	MAMS 37277	2453567 783012	22°09′51.4″N 59°44′39.2″E	5528±26	6323-5889	1.6	-1.45	bivalve	ΔR = -185±101
Central Ru'ays 170 cm depth	MAMS 37278	2453567 783012	22°09′51.4″N 59°44′39.2″E	5546±25	6344-5902	-1.2	-1.45	bivalve	
South of Ras ar Ru'ays 69 cm depth	MAMS 37270	2453003 781816	22°09′33.7″N 59°43′57.2″E	5238±36	5991-5835	-29.5	-0.71	bulk sediment	
South of Ras ar Ru'ays 69 cm depth	MAMS 37279	2453003 781816	22°09′33.7″N 59°43′57.2″E	5197±24	5983-5549	0.9	-0.71	bivalve	assumption ΔR = -185±101
South of Ras ar Ru'ays 69 cm depth	MAMS 37280	2453003 781816	22°09′33.7″N 59°43′57.2″E	5180±25	5966-5526	0.3	-0.71	bivalve	
South of Ras ar Ru'ays 140 cm depth	MAMS 37271	2453003 781816	22°09′33.7″N 59°43′57.2″E	5841±19	6617-6497	-17.2	-1.42	bulk sediment	
South of Ras ar Ru'ays 140 cm depth	MAMS 37281	2453003 781816	22°09′33.7″N 59°43′57.2″E	5710±25	6557-6064	0.2	-1.42	bivalve	assumption ΔR = -185±101

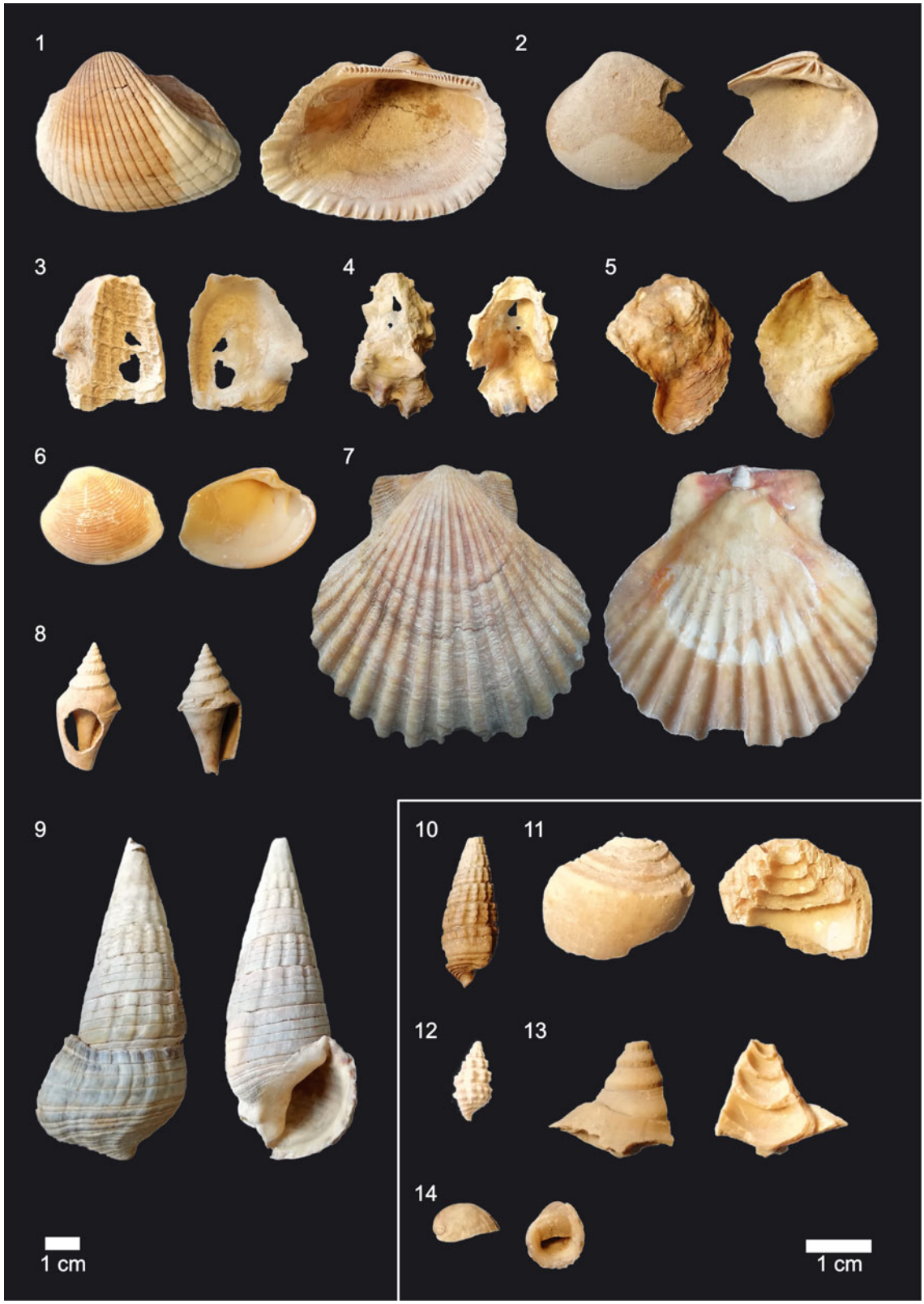

Figure 6. The shell midden south of Ras ar Ru'ays showing the underlying fluvial deposits. The stars mark the ^{14}C dates of molluscs; the blue triangle indicates the D-GPS measured height a msl. (For interpretation of the references to color in this figure legend, the reader is referred to the web version of this article.)

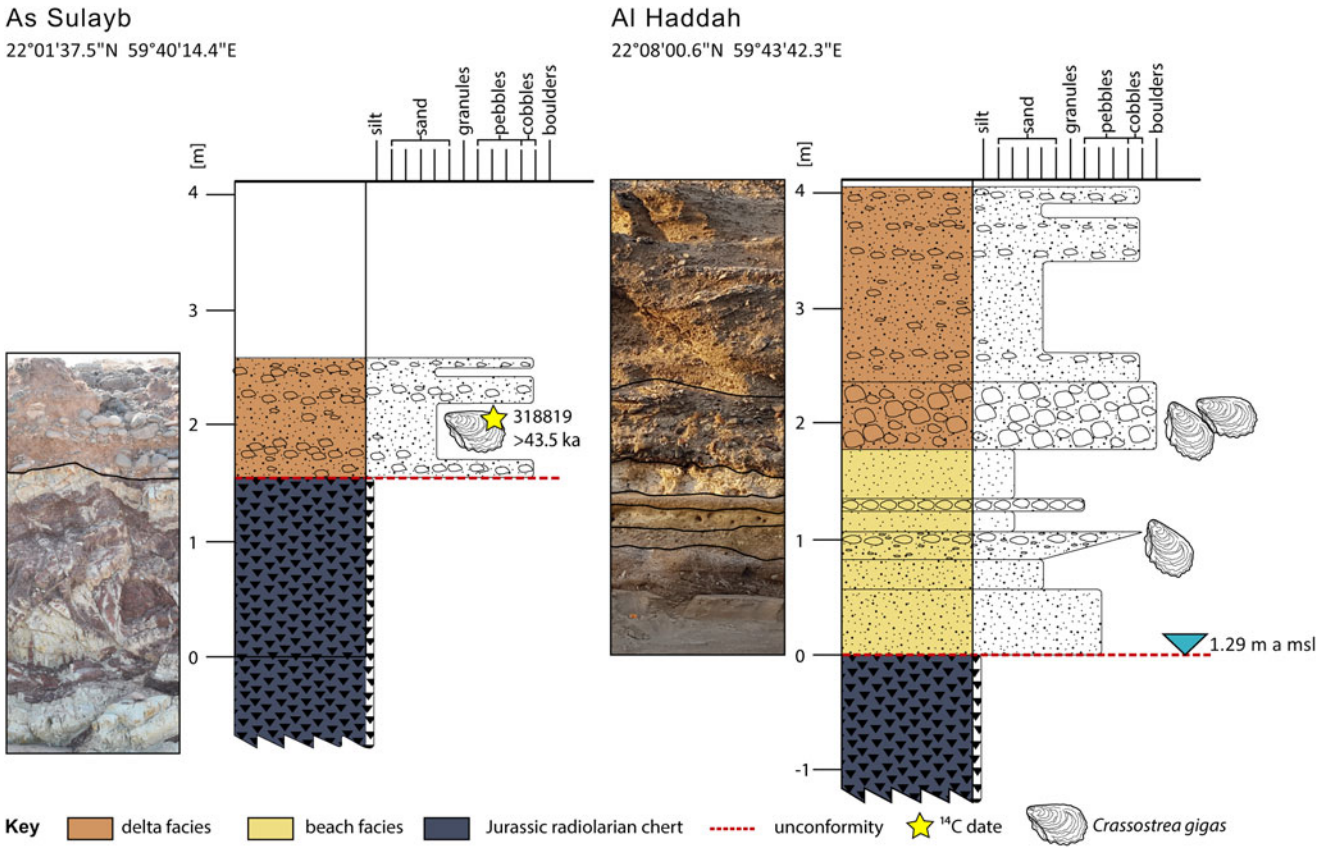

Figure 7. (color online) Bivalve shells were the most abundant species found in the shell midden of Ras ar Ru'ays (exterior shown at left, interior shown at right): 1, *Anadara* cf. *antiquata*; 2, *Marcia* sp.; 3–5, oyster; 3, imprint of a *Terebralia palustris* shell in an oyster shell; 6, *Marcia* sp.; 7, *Chlamys townsendi;* 8, *Strombus* sp.; 9, *Terebralia palustris*; 10, *Cerithidea cingulata*; 11, broken *Conus* sp.; 12, *Cerithidium* sp.; 13, broken *Strombus* sp.; 14, *Nerita* sp.

into three main layers that vary in color and grain size: The mainly black layer (L1) at the base is made up of fine sand. On top, a reddish fining upward sequence (L2) from silty fine sand to clayey silt is present. This is overlain by brown fine sand, shifting to beige toward the top (L3). The 28-cm-thick basal layer that lies at a depth of 140–112 cm below the surface consists of black to reddish brown silt to fine sand and contains a few pieces of wooden remains and various mollusc shells. The latter includes the mangrove-adapted gastropod *T. palustris* and some remains of unspecified gastropods and fragile bivalves. This basal layer is poorly sorted and enriched in carbon. The TC content is 5.7%, of which 1.9% is TOC. L1 is covered by a reddish fining upward sequence from silty fine sand to clayey silt (L2: 112–71 cm). No fossils are preserved in the reddish section. The sediment of L2 is also poorly sorted. The TC content is verified in these sediments, with a value of 3.1%, of which 1.7% is TOC. L3, from a depth of 71 cm to the surface, is made up of fine sand; the sediment's color shifts from brown to light beige. At a depth of 18–24 cm, an interbedded layer is enriched in salt crystals. Sorting is moderate. The TC content varies from below detection limit (<0.23%) to 6.1%. The TOC is below 1% (0.6 and 0.9%, respectively).

A shell midden is located on Ar Rumays' coastline, situated next to the profile (40Q 603562, 2622757), at a distance of 20 m. On top of this shell midden, we found remains of the mangrove indicator taxa *T. palustris* next to marine species like *Anadara* sp. and *Ostrea* sp. A small patch of recent *A. marina* shrubs was found (40Q 601127, 2622512) 2.5 km west of this site.

Rhizoliths at Sawadi

Besides the findings of *T. palustris* in Ar Rumays and the root structures in the sediment at Ras ar Ru'ays, other evidence of paleo-mangroves is noted in the form of root casts near Sawadi and organic root remains near Quriyat.

The morphological coastal setting in Sawadi, to the west of Muscat, is characterized by an estuary with a perennial creek that has a subsurface water supply. Satellite images show a 2-km^2 subaerial drainage system forming a seasonal wetland. Owing to the short pathway of 3 km, the creek's sediment load is low. Coastal dynamics lead to a longshore sediment transport toward the northwest. A group of small islands less than 1 km off the coast interrupts the sediment flow, resulting in the formation of a spit and a tombolo. Beach

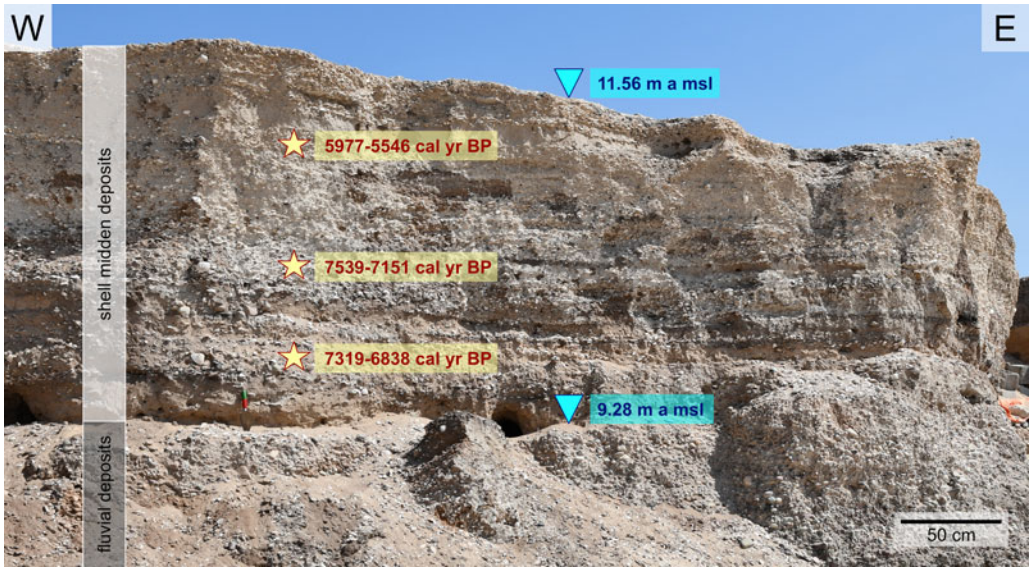

Figure 8. (color online) Coastal cliff outcrops near As Sulayb and Al Haddah showing a succession of radiolarian chert unconformly overlain by coastal deposits. The sediments indicate that the last sea-level highstand was before 43.5 ka.

ridges are observed along the western coast of the spit. The terminal course of the creek shifts and progrades in short periods due to the dynamic processes, as shown by satellite image analyses (Fig. 9). Evidence of paleo-mangroves were observed on the creek bank (40Q 580444, 2629084). The remnants are casts, of the outer structure of stems, roots, and pneumatophores that resemble those of *A. marina*. All structures are composed of cemented sediment and are void, with no organic macromaterial preserved. These kinds of structures are known as rhizoliths (Cramer and Hawkins, 2009). The casts in Sawadi consist of cemented silt to medium sand, and some have attached gastropod shells of *C. cingulata*. Some pneumatophore casts are irregularly shaped, with ball-like structures around them (Fig. 10). A 1-m-deep trench was dug through these structures toward the inland. At the level of the rhizoliths, orange to reddish brown redoximorphic features are present in a fine sand matrix, but no consolidated casts are preserved. We tracked this layer through coring, with orange sediment spots about 100 m inland. Two additional cores beside the lagoon bank (40Q 580435, 2628960 and 580552, 2628750) revealed orange discoloring at a depth of 50–60 cm below the surface.

A recent mangrove forest of about 12 ha is located 500 m to the east (Japan International Cooperation Agency, 2014). Crabs were highly active, and living *T. palustris* were found. This forest originated from several afforestation campaigns that have taken place here since 2001, as part of the mangrove afforestation program of the MECA (Japan International Cooperation Agency, 2014).

Preserved root material at Quriyat

Salt-evaporation ponds of 2 x 3 m in size are located about 6 km southeast of Quriyat; these are dug in clayey sediments, which make the ponds watertight at the base and toward the sides. An unused, empty pond provided a profile of 75-cm depth (40Q 699707, 2569250). Overlying fluvial deposits of about 2 m were removed by the salt miners. The profile displays two layers. The basal layer consists of 40 cm of dark gray clay with redoximorphic features, which indicate root-penetration structures and organic plant material in the upper part. Millimeter-sized black plant fragments and compressed roots of 1–4 cm in diameter are preserved. This sequence is overlain by 35 cm of silty sediment that shifts in color from light grayish green to light brown and contains fragments of unspecified shells. Shell middens (Khor Milk I and II) located almost 1 km to the northeast include *T. palustris* shells.

Modern mangrove vertical distribution

The D-GPS investigation of living *A. marina* in recent lagoons in Sawadi, Sur Lagoon, and Ras al Hadd showed a vertical distribution of -0.31–1.1 m a msl. Sawadi shows a more seaward mangrove vegetation, which begins at -0.31 and ends at 0.4 m a msl; mangroves in Ras al Hadd grow at higher elevations, from about 0.3 to 1.1 m a msl (Table 3). In all sites, a clear zonation of mangroves was encountered in the intertidal area, which is a belt without—or with only sparse—vegetation and a succulent plant zone that includes *Halopeplis perfoliata* and *Tetraena qatarensis*.

DISCUSSION

Rise and fall of mangrove ecosystems in Oman

The recent mangrove ecosystems along the coast of Oman are patchy and restricted to isolated, mostly lagoonal, sites. *A. marina*, which is known to be the most robust mangrove (Tomlinson, 2016), is the only living species. The spatial

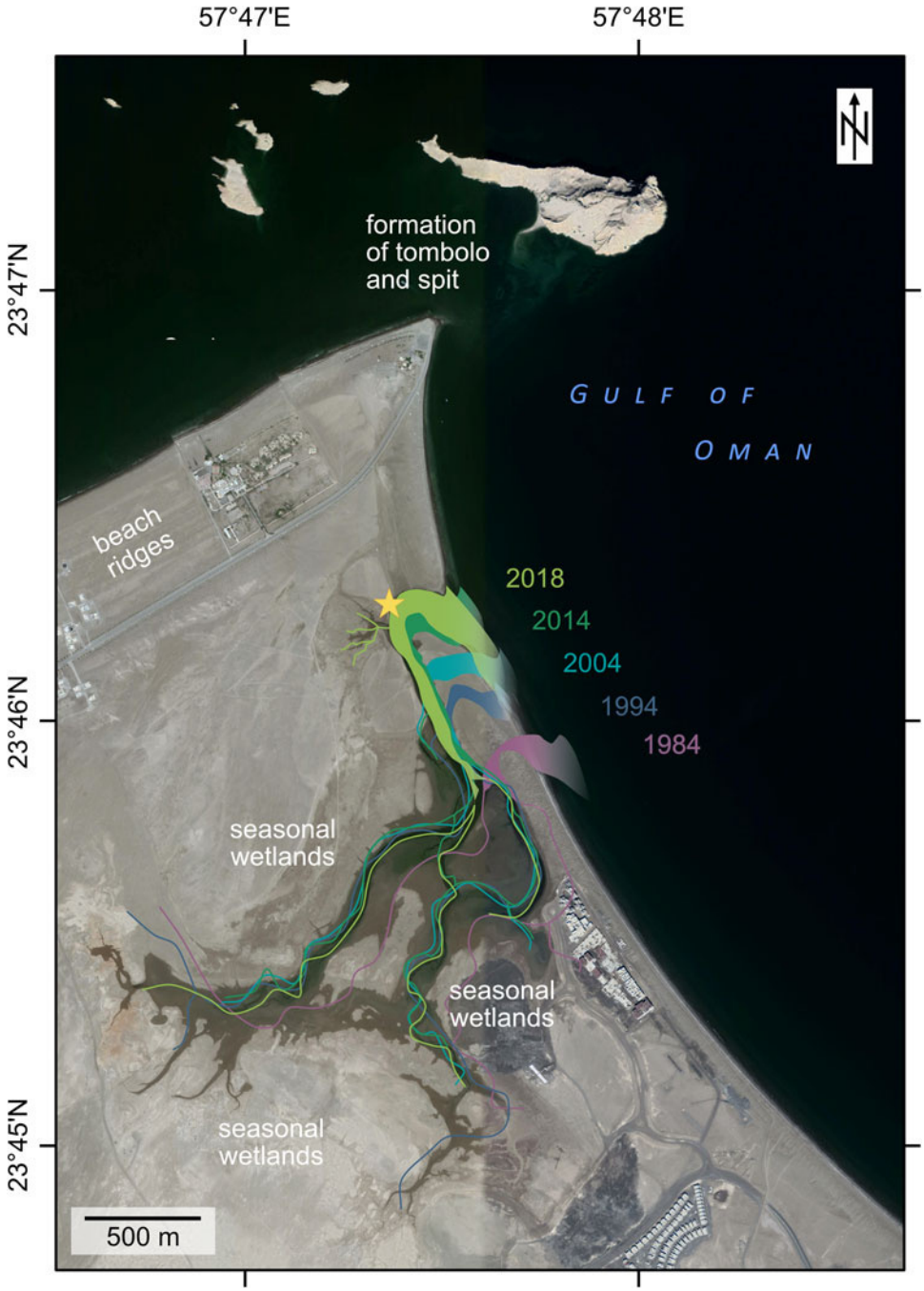

Figure 9. (color online) The satellite image from March 2018 showing the area around Sawadi with its prograding creek. The different colors depict the progradation from 1984 to 2018. The star marks the location where rhizoliths were found in 2018 (map created using Google Earth).

distribution of the recent mangroves apparently reflects the precipitation pattern and coastal geomorphology. The precipitation is comparatively high along the Batinah coastal plain owing to Mediterranean winter rains, but the coastline is straight. Thus, only mangroves in an estuarine setting are present near Sawadi, and isolated individual trees are present in similar settings to those near Ar Rumays. To the east, precipitation values are comparable, but there are more sheltered lagoons. Mountains are close to these lagoons, which lead to a direct freshwater input following rainfall. There are several mangrove-fringed lagoons (e.g., Qurum, Bandar Khayran, Sur, and Ras al Hadd). However, most of the larger current mangrove forests are the result of afforestation programs carried out by MECA. Toward the south, environmental conditions are not suitable for mangrove ecosystems today; precipitation values are low, and appropriate geomorphological settings like lagoons are missing.

The mid-Holocene mangrove distribution apparently was much larger. Paleo-mangrove ecosystems were identified in the subsurface of *sabkhas* along the east coast. These have



Figure 10. Mangrove rhizolith structures in the intertidal zone at the creek shore near Sawadi. The arrows indicate the different parts of the plant: orange = trunk; blue = pneumatophore; yellow = ball structure attached to the pneumatophore. (For interpretation of the references to color in this figure legend, the reader is referred to the web version of this article.)

already been described by Berger et al. (2013) and Lézine et al. (2002), who also identify a second mangrove species, *R. mucronata*. Rhizophoraceae are known to be less tolerant toward saline soil and SST (Chen and Twilley, 1998).

Available archives of Holocene coastal records along the coastline of Oman cover the mid- and late Holocene. Early Holocene coastal deposits are not expected, as global sea level was well below present levels (Woodroffe and Horton, 2005). According to paleontological and palynological records, the oldest published ^{14}C results related to mangrove ecosystems cluster ~7000 cal yr BP (Lézine et al., 2002, Berger et al., 2020). Following the archaeological investigations by Charpentier et al. (2000, 2003), the existence of a lagoon near Suwayh is proven for 7500 cal yr BP, but a mangrove ecosystem did not develop before 7000 cal yr BP.

When, how fast, and why the mangrove ecosystems vanished is still under discussion (Berger et al., 2020). Our sediment profiles display a collapse in 6000 cal yr BP, as shown by an abrupt change that is detectable in all paleo-lagoons along the east coast. The lower layers represent paleo-lagoonal facies, as indicated by the bimodal grain-size distribution that reflects two different sediment sources. These are interpreted as a marine and a terrestrial input. Additionally, the TS content is rather high, which documents a strong marine influence. The TOC content visualizes a high bioproductivity in the paleo-lagoonal area. This is supported by the undetectability of nitrogen. The growth of mangrove trees is limited by nitrogen and phosphorus (Twilley et al., 2019); as a consequence, mangrove soils are usually depleted in these (Reef et al., 2010). Though performing a high net primary production, mangrove ecosystems are often oligotrophic. Values of nutrients like nitrogen and phosphorus can vary significantly between different geomorphological settings, types of mangroves, and in a single mangrove wetland. This is due to highly dynamic nitrification-denitrification processes. Reducing conditions inhibit nitrification and enhance denitrification

Table 3. The D-GPS measurements show the spatial distribution of recent *Avicennia marina* mangrove ecosystems in the intertidal zone along the northern coastline of Oman. The values are averages out of 3 to 16 measurements. In the creek of Sawadi, no distal single mangrove trees are present. In Sur Lagoon, only proximal extent was measurable owing to high tide. Coordinates are presented as meters in the UTM projection, Zone 40Q, using the WGS 1984 reference ellipsoid.

	Sawadi	Sur	Ras al Hadd 1	Ras al Hadd 2
North	2628492.460	2495981.605	2493513.317	2492887.637
East	580581.834	757866.430	786508.761	785821.777
longitude	23°45′55.9″N	22°33′03.6″N	22°31′26.9″N	22°31′07.0″N
latitude	57°47′27.0″E	59°30′26.8″E	59°47′06.9″E	59°46′42.5″E
mangrove distal (seaside) extent, single trees [m a msl]	-	-	0.07	0.31
mangrove distal (seaside) extent [m a msl]	-0.31	none	0.3	0.37
mangrove proximal (landward) extent [m a msl]	0.3	0.21	0.62	1.1
mangrove proximal (landward) extent, single trees [m a msl]	0.4	0.41	0.82	1.1
begin of succulent plants [m a msl]	0.44	1.1	1.26	1.2

(Twilley et al., 2019). The overlying layers in the profile of Ras ar Ru'ays show a much lower TOC and TS content and a different granulometric pattern. The well-sorting of the sediment and its positive skewness at around 30 cm in depth reveals the sediment input to be aeolian (Das, 2015; Alharbi et al., 2016). These upper layers display a *sabkha* environment, with sporadic floods after heavy rainfall in the mountain areas. There is no fluvial sediment input because there is no open Wadi system. Subsurface water flow and groundwater level rise after rainfall can cause an inundation of such sinks. The depression has no natural drainage, so the water enters and flattens the aeolian sediments. This is indicated by planar layered deposits and a lack of characteristic aeolian sedimentological structures like cross-bedding. The water is highly saline because of the lagoonal deposits underneath. It evaporates slowly, taking up to several weeks. During this process, salt and gypsum crystallize; this can be seen in the profile and on top of the *sabkha* surface. The shift from the lagoonal facies toward the *sabkha* facies is sharp in the investigated profiles. There is a lack of evidence for erosional surfaces; thus, we presume a continuation of the sedimentation and an ecosystem collapse on a decadal scale, as the facies shift is identical in all investigated paleo-lagoons.

Our interpretation is therefore a rapid change in environmental setting. Ecosystems show a sensitive threshold regarding the precipitation/evaporation balance. If a certain threshold is reached, it leads to an abrupt collapse of the whole system (Ratajczak et al., 2018). Lézine (2009) emphasizes that in arid areas, thresholds rather than long-term shifts are more likely for vegetation communities. A pollen profile revealed a *Rhizophora* sp. population in the lagoon of Jaramah, in the northeast of Oman, which disappeared abruptly ~4500 cal yr BP. The limnic interdune lake ecosystems of the Wahiba (Radies et al., 2005) are good examples of a whole collapsing ecosystem in Oman. Sedimentological and paleontological analyses of these lake deposits indicate an abrupt change of the surrounding ecosystems due to aridification 9 ka ago. This collapse seems to be similar to what we see in the sedimentological record of the 6000-year-old paleo-lagoons we investigated on the east coast. Our interpretation is currently based on sedimentological evidence. Further research must focus on the dating of this facies shift.

Possible forcing factors

There are three main forcing factors that can lead to such environmental changes: sea-level variability, climate variation, and human impact. In the following section, we discuss each of these scenarios and their plausibility.

Relative sea-level fall and/or continental uplift

Mangrove vertical development is directly influenced by RSL variation, and effects depend on its rate (Saintilan et al., 2020). Most investigations focus on RSL rise due to recent climate change and inundation hazards. The rate of RSL rise is the limiting factor that decides whether the ecosystem keeps pace with the change or fails and declines (Lovelock et al., 2015). Saintilan et al. (2020) recently published an upper threshold of 6.1 mm RSL rise/yr, revealed by reviewing responses of mangrove ecosystems toward RSL rise after glacial ice melt between 10 and 7 cal ka BP. The threshold serves as a benchmark. Additionally, local environmental conditions have to be considered, such as geomorphological setting, tidal range, and sediment accumulation rate (Ellison and Stoddart, 1991; Saintilan et al., 2020). Mangrove ecosystems' responses toward RSL rise and fall cannot be considered as analogous processes. Mangrove forests keep up with RSL rise mainly by vertical accretion of sediment, allochthonous as well as autochthonous (Krauss et al., 2014; Woodroffe et al., 2016). As this natural accretion of organic and inorganic sediment positively influences the progradation landward, calculated mangrove survival rates during sea-level rise cannot be projected to those of sea-level fall (Ellison, 2019). Ellison and Farnsworth (1997) conducted a long-term laboratory experiment investigating physiological parameters of Rhizophoraceae seedlings until the reproduction phase during a simulated sea-level rise, stable sea level, and sea-level fall. Rise and fall were realized by a 16-cm higher or lower tide, respectively. The authors observed some differences. The best physiological values were represented by the stable sea-level group. Mangroves of the sea-level rise group were notably fast growing at the beginning. Those of the sea-level fall group showed a retarded growth and a compact canopy. This indicates that Rhizophoraceae are able to keep up with a sudden sea-level fall of 16 cm. The forming seedlings could then inhabit a more suitable zone. During continuous sea-level fall, these mangroves would still struggle or vanish. As far as we know, there is no threshold rate published specifically related to sea-level fall. Thus, with the data at our disposal, we are not able to accurately reconstruct a RSL fall rate in the paleo-lagoons we investigated.

In a situation where sea-level variation causes the decline of the mangrove ecosystem, a sea-level fall would provoke the silting up of the former intertidal lagoon with material brought in by fluvial or aeolian processes. According to Das (2015) and Alharbi et al. (2016), sorting and skewness of the granulometric analyses of the paleo-lagoons reveal aeolian input. These sediments would have embedded intertidal-related facies above the present sea level, which is not the case in the investigated paleo-lagoons. Nevertheless, sea-level models predict a mid-Holocene highstand in mid-latitudes (Mitrovica and Milne, 2002) followed by a sea-level fall.

To our knowledge, only one study defines SLIPS along the coastline of Oman, following the guidelines of Hijma et al. (2015): Beuzen-Waller et al. (2019), who investigated the Quriyat area. The mandatory data are a well-constrained age, the indicative meaning consisting of elevation a msl, a reference water level, and an indicative range as an error estimate. Individual local profiles are described that are in most cases only tentatively assigned to a potential mid-Holocene sea-level highstand. Preusser et al. (2005) describe a profile

near Kuwaymah (40Q 715569.98; 2355040.05), 115 km south of our sites, which they interpret as Holocene coastal *sabkha* deposits, IRSL dated to BC 1650 ± 400 but with an unclear relation to sea level. We reexamined the site and could not find sea level–related facies. The gastropod *Melanoides tuberculata* identified by Preusser et al. (2005) is not tolerant of high salinities. Bolaji et al. (2011) suggest *M. tuberculata* does not tolerate a salinity level higher than 25‰. Salinity tolerance tests performed by Farani et al. (2015) support this, and reveal that 50% of adult gastropods survive 22.8‰ salinity, and juveniles are even less robust. All *M. tuberculata* in this tolerance test were motionless at 30‰. This species does survive in a *sabkha* environment. The deposits found near Kuwaymah likely originate from a freshwater lake near the coast, with limited marine influences like sea spray or flooding due to storm events. These deposits are not reliable sea-level indicators.

Berger et al. (2013) assign to their models a mid-Holocene sea level up to 9 m above the recent mean sea level. Besides a global sea-level highstand of 2–3 m a msl and postsedimentary effects of 2–3 m, Berger et al. (2013) take regional tectonic uplift into account. This is in contrast to Hoffmann et al. (2013), who show that the northern part of the east coast is tectonically stable, excluding any noneustatic sea-level change. The topic of neotectonic movements in northern Oman is currently being researched (Mattern et al., 2018; Moraetis et al., 2018, 2020; Ermertz et al., 2019; Hoffmann et al., 2020).

In our study area, no evidence exists for vertical displacement since the mid-Holocene. According to our D-GPS measurements, the uppermost layer of the paleo-mangrove deposits in the *sabkha* south of Ras ar Ru'ays is located 71 cm below recent mean sea level. We refrain from a significant postdepositional lowering. This is not reasonable because root penetration and other bioturbation structures seem to be well preserved and undeformed. Additionally, the sediment predominantly consists of uncompactable siliciclastic material and not easily compactable organic mud or peat, which would have made it necessary to conduct a decompaction calculation (Schmedemann et al., 2008). Taking little postdepositional lowering into account, the paleo-mangrove layers found at a depth of 70 cm are within recent tidal range, where mangroves are still growing today. Based on our measurements, mangroves near Sawadi, Sur Lagoon, and Ras al Hadd grow between -30 and 100 cm a msl, depending on environmental conditions (Table 3). Our dataset does not allow us to quantify the sea-level development in detail, but our findings suggest that sea level never exceeded modern levels during the Holocene.

There is ongoing research on mangrove sediments for centimeter- to decimeter-scale RSL reconstructions (Sefton, 2020). This contributes to our attempt to calculate an indicative meaning that would help interpret our findings much better. However, Sefton (2020) could not find a suitable approach that we could use in our investigations. The difficulty for Sefton (2020) seemed to be finding indicative characteristics for vegetation and elevation zones in recent mangroves. We face the same problem: we cannot correlate the paleo-mangrove layers to a specific elevation within recent mangroves. There is a lack of information on granulometric patterns of mangrove sediments and root-system expansion of living *A. marina* in Oman. Thus, more data of recent mangroves in this region must be acquired for statistically valid and comparable analyses. Currently, the calculation of an indicative meaning is difficult with the material at hand (Lorscheid, T., personal communication, 2020), although it may be used as a starting point for further sea-level studies.

There is, however, evidence for Pleistocene sea-level highstands along the coastline under investigation. Three outcrops are important in this context: profiles in Ras ar Ru'ays, Al Haddah, and As Sulayb. All three profiles show gravel accumulations that are interpreted as alluvial fan deposits, with a transition into deltaic deposits where the fan reaches the coastline. The gravel deposits below the shell midden south of Ras ar Ru'ays represent the proximal part of the fan. These gravel deposits are found at an elevation of up to 9 m a msl. These sediments are interpreted as representing a fluvial environment, as they show no sign of wave reworking, bioerosion, or marine fossils. The boundary to the overlying shell midden is sharp and partly erosional, indicating a paleosurface and a depositional hiatus. This is supported by an OSL date by Berger et al. (2020), which indicates fluvial activity and deposition of the gravel during the mid-Pleistocene, while the shell midden is Holocene in age.

The profiles at Al Haddah and As Sulayb are both located on the recent coastline and show deltaic sediments deposited under marine influence, as beach and shoreface facies indicate a wave-dominated setting. At As Sulayb, the distal part of the alluvial system was dated using ^{14}C (Beta-318819). The dating results indicate sediment deposition beyond the dating limit (e.g., >43.5 ^{14}C ka BP), precluding a Holocene formation of these sediments.

Evidence for last interglacial shorelines in the area is published by Falkenroth et al. (2020), where a coastal notch in Sur is described. This notch mapped at an elevation of 3.93 ± 0.12 m a msl correlates well with the deltaic sediments in Al Haddah that are found between 0 and 4 m a msl and those in As Sulayb that are mapped at approximately 1.8 m a msl. The initial formation of the alluvial fan predates the last interglacial, as evidenced by the age of the fluvial gravel in Ras ar Ru'ays. A higher RSL after this period is not indicated along the northern part of the east coast of Oman.

Forcing factor climate change

The climatically driven scenario would be caused by a decrease in precipitation owing to a shift of the ITCZ toward the south. This is followed by a transregional loss of vegetation or shift to a different vegetation community, as indicated by pollen analyses (Lézine, 2009). In arid areas, such a loss of vegetational cover leads to increasing deflation and aeolian sediment transport. The windblown sand is trapped in depressions such as lagoons, which soon become silted up. During wetter times a small river flow could have flushed the lagoon

continuously and kept it open. We presume this river flow became too weak, and incoming sediment accumulated. Sporadic floods—both flash floods and marine inundations—blanket the sand in the former lagoon.

According to our dating, the paleo-mangroves on the east coast vanished ~6000 cal yr BP. This is in agreement with the results published by Berger et al. (2020), who date some of the upper paleo-lagoonal layers of the same *sabkha* south of Ras ar Ru'ays 500 years younger. Lézine et al. (2017) outline two main aridification phases: after 4500–5000 cal yr BP and after 2700 cal yr BP. Dating and palynological analyses of a paleo-lagoon in Suwayh, 13 km south of Ras ar Ru'ays, show a decline of mangroves and replacement by a brackish to freshwater lagoon without mangroves ~5000 cal yr BP (Lézine et al., 2002). Lézine et al. (2017) demonstrate that in some areas a continuous mangrove forest has existed from ~7000 cal yr BP until today. These areas are Jaramah (22°29′N, 59°43′E), west of Ras al Hadd, and Filim (20°61′N, 58°17′E), located in the southeast, in a bay next to the peninsula of Bar al Hikman. The mangrove species assemblage has changed over time. *A. marina* and *R. mucronata* were present first; the latter vanished in Jaramah ~4500 cal yr BP and in Filim ~2500 cal yr BP. Lézine et al. (2017) correlate the disappearance of the *R. mucronata* mangroves in Filim and Jaramah with the shift of the ITCZ. Beuzen-Waller et al. (2019) show that mangroves in a lagoon near Quriyat, on the north coast, disappeared ~4000 cal yr BP. This fits with the 4.2 aridification event that mainly triggered the fall of the Akkadian Empire in Mesopotamia, as documented by Watanabe et al. (2019), and the Harappan civilization in India (Giosan et al., 2012).

We postulate an earlier onset of the ITCZ shift and change in precipitation patterns that led to a collapse of the mangrove ecosystems on the east coast of Oman 6 ka ago. Other studies support this. Lindauer et al. (2017) reveal a change in the reservoir effect between 7000 and 6500 cal yr BP and ~4000 cal yr BP. This indicates a shift in sea currents, which are mainly influenced by climate circulation patterns and may show an alteration of those. Studies from northwest India depict an alteration in monsoonal patterns beginning 7000–7500 cal yr BP (Singh et al., 1990). Singh et al. (1990) investigated sediments of a mid-Holocene deep, permanent freshwater lake and revealed a significant lowering of the lake level ~6000 cal yr BP. In addition to the reduced precipitation, a cooling of the Indian Ocean due to vegetation-dust climate feedbacks from the Sahara (Griffiths et al., 2020) worsened the living conditions for the temperature-sensitive mangroves. Cooler SSTs can explain the final decline of Rhizophoraceae and the persistence of the more robust *A. marina* that inhabits Oman's coastline today.

The remaining mangroves in Jaramah and Filim are seen as relict areas, where Rhizophoraceae mangroves struggled with unfavorable conditions for a longer time compared to the mangroves on the east coast. Both Jaramah and Filim are very sheltered lagoons; Jaramah is protected from open sea currents by the tip of Ras al Hadd; Filim is protected by the peninsula to the east. Both sites are still suitable for mangroves and are inhabited with *A. marina* today. These places provided a kind of safe haven for mangroves in times of climate change 6 ka ago.

The east coast is more exposed, on the one hand to the open sea and is thus affected by currents. On the other hand, large sand dunes along the east coast were reactivated because of aridification and the resulting lack of vegetation. The sand of the dunes could easily provide material to silt up the lagoons in this location.

Human impact

According to the archaeological record, the human impact on mangrove ecosystems was not significant and thus negligible 6 ka ago. The ancient way of life during the EHHP is still under discussion. Cleuziou and Tosi (2007) postulate a sustainable nomadic lifestyle, with seasonal migration and campsites at the foot of the Hajar Mountains and along the coast. Berger et al. (2020) hypothesize that the migration tracks were used only by hunters and pastoral communities and that there were settlements all year round along the coast. The shell midden near Ras ar Ru'ays was identified as a production site for drills and net sinkers as well as a place for the processing of beads (Berger et al., 2020). The workers lived there with their families and exploited the sea and the paleo-lagoon for the needs of daily living. Based on their way of life, these people are often called "Fish-eaters," or *Ichthyophagi*, which relates to ancient texts as far back as Plinius (Charpentier, 2002). Their diet mainly consisted of small fish, like sardines and herring, as well as large fish such as tuna and shark. It also contained *Chelonia mydas* (the green turtle), its eggs, and crustaceans and molluscs (Biagi and Nisbet, 1999).

The mangrove ecosystems provided for all the needs of the people living there: fresh water, edible molluscs such as *T. palustris* and oysters, and wood for construction purposes and for making fires for cooking. According to charcoal analyses from fireplaces in the Ras ar Ru'ays shell midden strata (Berger et al., 2020), *A. marina* wood was one of the most popular firewoods during the Neolithic. Other archaeological sites show similar results. Several of them are located near Qurum. Ras al Hamra (RH)-5 was settled ~8450–7150 cal yr BP and is dated by various *A. marina* charcoals taken from fireplaces (Biagi, 1994). In RH-5 and RH-6 (7450–6150 cal yr BP) charcoal fragments from *Ziziphus* sp., *Tamarix* sp., and *Acacia* sp. were found. The most common firewood at both sites was *A. marina* (Biagi and Nisbet, 1999). It was popular because of its high calorific value (Maundu and Tengnäs, 2005) and because it burns with neither smell nor smoke (Biagi and Nisbet, 1999). Determinations of calorific values of wood show variations between mangrove species (Sathe et al., 2013). *R. mucronata* shows the highest calorific values, reaching 6739.95 cal/g. Subspecies of *A. marina* follow the Rhizophoraceae, with values around 5000 cal/g. These high calorific values made mangroves of Oman's coastline a popular charcoal wood for copper production. Evidence exists of long-distance transport of

A. marina charcoal from 4850 to 4650 cal yr BP (Deckers et al., 2019). Charcoal fragments of *A. marina* were found in a building near Al Khasbah, south of the Hajar Mountains, 100 km from the coast. This charcoal is ~1000 years younger than the silting up of the paleo-lagoon at Ras ar Ru'ays.

The *A. marina* charcoal near Al Khasbah correlates with the Great Transformation (Cleuziou and Tosi, 2007) period. At the end of the fourth millennium, people left most of the coastal campsites and moved to the mountains, where they began sophisticated farming and metalworking (Cleuziou and Tosi, 2007). The oldest evidence for large-scale copper production dates to 5250–5050 cal yr BP, which is the beginning of the Hafit period (Deckers et al., 2019). Human interaction with the environment changed from this time. Approximately 4000 years ago, copper smelting was common, and humans exploited the environment to produce charcoal. There is evidence that high-calorific mangrove wood was used; in Al Khasbah, up to 60% of all charcoal fragments were identified as *Rhizophora* sp. and 10% as *A. marina* (Deckers et al., 2019). We tentatively suggest that this is the reason why *Rhizophora* sp. disappeared in some places where *A. marina* survived (e.g., in Jaramah and Filim). Our interpretation is that variation in mangrove species assemblages is an anthropogenic signal, commencing with the beginning of charcoal production. We abstain from the hypothesis that the disappearance of the mangroves was due to charcoal production, as there is no evidence for this along the east coast as early as 6 ka ago. Nevertheless, human activities did assert additional pressure and inhibited natural recovery of the mangrove ecosystems, which suffered in times of aridification.

CONCLUSIONS

The Holocene sedimentological record along the coastline of Oman indicates that mangrove ecosystems were more widespread in the past. Based on radiocarbon dating, the oldest mangrove-related sediments are dated to ~7000 cal yr BP.

An abrupt facies change was observed in paleo-lagoons along the east coast, mainly in the Ja'alan area. This change was dated to 6000 cal yr BP, and it represents a rapid collapse of the mangrove ecosystem. We interpret this collapse to be the consequence of climate change rather than sea-level fall or anthropogenic influence. The climate change led to a decline in precipitation values. The most likely reason is a southward shift of the ITCZ. Further research efforts will concentrate on the quantification of paleo-precipitation.

ACKNOWLEDGMENTS

Decker would like to acknowledge with gratitude the Ph.D. scholarship received from the Studienstiftung des deutschen Volkes. Falkenroth acknowledges the valuable support by Graduiertenförderung, RWTH Aachen University. The project is funded by the German Research Foundation; without it, this work would not have been possible (DFG 2550/15-1, "Mangrove ecosystems as indicators for environmental change [Oman, Indian Ocean]"). This paper is a contribution to the IGCP project 639 "Sea-level change from minutes to millennia." We would also like to thank the team of Golden Highlands in Oman for perfect field support, and Kim Hußmann for her help conducting the fieldwork. Eva Heumann-Lange is acknowledged for her organizational work that is essential to the smooth running of the project. We are grateful to Stefani Clark for the English review. The constructive feedback by Tara Beuzen-Waller and one anonymous reviewer helped improve the manuscript significantly.

SUPPLEMENTARY MATERIAL

The supplementary material for this article can be found at https://doi.org/10.1017/qua.2020.96

REFERENCES

Al-Hashmi, K., Al-Azri, A., Claereboudt, M.R., Piontkovski, S., Amin, S.M.N., 2013. Phytoplankton community structure of a mangrove habitat in the arid environment of Oman: the dominance of Peridinium quinquecorne. *Journal of Fisheries and Aquatic Science* 8, 595–606.

Alharbi, O.A., Williams, A.T., Phillips, M.R., Thomas, T., 2016. Textural characteristics of sediments along the southern Red Sea coastal areas, Saudi Arabia. *Arabian Journal of Geosciences* 9, 735.

Atkinson, O.A., Thomas, D.S., Goudie, A.S., Bailey, R.M., 2011. Late Quaternary chronology of major dune ridge development in the northeast Rub'al-Khali, United Arab Emirates. *Quaternary Research* 76, 93–105.

Bailey, R.M., Thomas, D.S., 2014. A quantitative approach to understanding dated dune stratigraphies. *Earth Surface Processes and Landforms* 39, 614–631.

Bange, H.W., Bathmann, U., Behrens, J., Dahlke, F., Ebinghaus, R., Ekau, W., Emeis, K.-C., *et al.*, 2017. Coasts – A Vital Habitat Under Pressure. *World Ocean Review: Living with the Oceans* 5. Maribus, Hamburg, Germany.

Berger, J.F., Charpentier, V., Crassard, R., Martin, C., Davtian, G., López-Sáez, J.A., 2013. The dynamics of mangrove ecosystems: changes in sea level and the strategies of Neolithic settlements along the coast of Oman (6000–3000 cal. BC). *Journal of Archaeological Science* 40, 3087–3104.

Berger, J.F., Guilbert-Berger, R., Marrast, A., Munoz, O., Guy, H., Barra, A., López-Sáez, J.A., *et al.*, 2020. First contribution of the excavation and chronostratigraphic study of the Ruways 1 Neolithic shell midden (Oman) in terms of Neolithisation, palaeoeconomy, social-environmental interactions and site formation processes. *Arabian Archaeology and Epigraphy* 31, 32-49.

Berner, R.A., Raiswell, R., 1984. C/S method for distinguishing freshwater from marine sedimentary rocks. *Geology* 12, 365–368.

Bernier, P., Dalongeville, R., Dupuis, B., de Medwecki, V., 1995. Holocene shoreline variations in the Persian Gulf: example of the Umm al-Qowayn Lagoon (UAE). *Quaternary International* 29–30, 95–103.

Beuzen-Waller, T., Stéphan, P., Pavlopoulos, K., Desruelles, S., Marrast, A., Puaud, S., Giraud, J., Fouache, É., 2019. Geoarchaeological investigation of the Quriyat coastal plain (Oman). *Quaternary International* 532, 98–115.

Biagi, P., 1994. A radiocarbon chronology for the aceramic shell-middens of coastal Oman. *Arabian Archaeology and Epigraphy* 5, 17–31.

Biagi, P., Nisbet, R., 1999. The shell-midden sites of RH-5 and RH-6 (Muscat, Sultanate of Oman) in their environmental setting. *Archaeologia Polona* 37, 31–47.

Bisutti, I., Hilke, I., Raessler, M., 2004. Determination of total organic carbon: an overview of current methods. *TrAC Trends in Analytical Chemistry* 23, 716–726.

Blechschmidt, I., Matter, A., Preusser, F., Rieke-Zapp, D., 2009. Monsoon triggered formation of Quaternary alluvial megafans in the interior of Oman. *Geomorphology* 110, 128–139.

Bolaji, D.A., Edokpayi, C.A., Samuel, O.B., Akinnigbagbe, R.O., Ajulo, A.A., 2011. Morphological characteristics and salinity tolerance of Melanoides tuberculatus (Muller, 1774). *World Journal of Biological Research* 4, 1–11.

Bollmann, M., Bosch, T., Colijn, F., Ebinghaus, R., Froese, R., Güssow, K., Khalilian, S., *et al*., 2010. *World Ocean Review: Living with the Oceans* 1. Maribus, Hamburg, Germany.

Bonfils, C., de Noblet-Ducoudré, N., Braconnot, P., Joussaume, S., 2001. Hot desert albedo and climate change: mid-Holocene monsoon in North Africa. *Journal of Climate* 14, 3724–3737.

Bosch, D.T., Dance, S.P., Moolenbeek, R.G., Oliver, P.G., 1995. *Seashells of Eastern Arabia*. Motivate Publishing, Dubai.

Bray, H.E., Stokes, S., 2004. Temporal patterns of arid-humid transitions in the south-eastern Arabian Peninsula based on optical dating. *Geomorphology* 59, 271–280.

Burns, S.J., Fleitmann, D., Matter, A., Neff, U., Mangini, A., 2001. Speleothem evidence from Oman for continental pluvial events during interglacial periods. *Geology* 29, 623–626.

Burns, S.J., Matter, A., Frank, N., Mangini, A., 1998. Speleothem-based paleoclimate record from northern Oman. *Geology* 26, 499–502.

Charpentier, V., 2002. Archéologie de la côtes des ichtyophages coquilles, squales et cétacés du site IVe-IIIe millénaire de Ra's al-Jinz. [Coastal archaeology of shellfish, sharks and cetaceans from the 4th to the 3rd millennium at Ra's al Jinz]. In: Cleuziou, S., Tosi, M., Zarins, J. (Eds.), *Essays of the Late Prehistory of the Arabian Peninsula*. Serie Orientale Roma XCIII, Rome, pp. 73–99.

Charpentier, V., Angelluci, D., Méry, S., Saliège, J.-F., 2000. Autour de la mangrove morte de Suwayh, l'habitat VIe–Ve millénaire de Suwayh SWY-11. [Around the dead mangroves of Suwayh and the environment of Suwayh SWY-11 in the 6th to the 5th millennium]. *Proceedings of the Seminar for Arabian Studies* 30, 69–85.

Charpentier, V., Marquis, P., Pellé, É., 2003. La nécropole et les derniers horizons Ve millénaire du site de Gorbat al-Mahar (Suwayh, SWY-1, Sultanat d'Oman): premiers résultats. [The necropolis and the last horizons 5th millennium of the Gorbat al-Mahar site (Suwayh, SWY-1, Sultanate of Oman): first results]. *Proceedings of the Seminar for Arabian Studies* 33, 11–19.

Chen, R., Twilley, R.R., 1998. A gap dynamic model of mangrove forest development along gradients of soil salinity and nutrient resources. *Journal of Ecology* 86, 37–51.

Cleuziou, S., 2009. Extracting wealth from a land of starvation by creating social complexity: a dialogue between archaeology and climate? *Comptes Rendus Geoscience* 341, 726–738.

Cleuziou, S., Tosi, M., 2007. The great transformation. In: Cleuziou, S., Tosi, M. (Eds.), *In the Shadow of the Ancestors*. Al Nahda Printing Press, Muscat, pp. 61–97.

Cramer, M.D., Hawkins, H.-J., 2009. A physiological mechanism for the formation of root casts. *Palaeogeography, Palaeoclimatology, Palaeoecology* 274, 125–133.

Curnick, D.J., Pettorelli, N., Amir, A.A., Balke, T., Barbier, E.B., Crooks, S., Dahdouh-Guebas, F., *et al*., 2019. The value of small mangrove patches. *Science* 363, 239–239.

Das, G.K., 2015. *Estuarine Morphodynamics of the Sunderbans*. Springer, Cham, Switzerland..

Deckers, K., Döpper, S., Schmidt, C., 2019. Vegetation, land, and wood use at the sites of Bat and Al-Khashbah in Oman (fourth–third millennium BC). *Arabian Archaeology and Epigraphy* 30, 1–14.

deMenocal, P.B., Tierney, J.E., 2012. Green Sahara: African humid periods paced by Earth's orbital changes. *Nature Education Knowledge* 3, 12.

Deutsches Institut für Normung e.V., 1987a. *DIN 66165-1: Partikelgrößenanalyse; Siebanalyse; Grundlagen*. [Particle size analysis; Sieving analysis; Fundamentals]. Beuth Verlag, Berlin.

Deutsches Institut für Normung e.V., 1987b. *DIN 66165-2: Partikelgrößenanalyse; Siebanalyse; Durchführung*. [Particle size analysis, Sieving analysis; Procedure]. Beuth Verlag, Berlin.

Deutsches Institut für Normung e.V., E. *14688-1: 2011-06. Geotechnische Erkundung und Untersuchung: Benennung, Beschreibung und Klassifizierung von Boden. Teil 1: Benennung und Beschreibung (ISO 14688-1:2002); Deutsche Fassung EN ISO 14688-1:2002*. [Geotechnical Investigation and testing - Identification and classification of soil - Part 1: Identification and description (ISO 14688-1:2002); German version EN ISO 14688-1:2002]. Beuth Verlag, Berlin.

Ellison, A.M., Farnsworth, E.J., 1997. Simulated sea level change alters anatomy, physiology, growth, and reproduction of red mangrove (Rhizophora mangle L.). *Oecologia* 112, 435–446.

Ellison, J.C., 2019. Biogeomorphology of mangroves. In: Perillo, G.M.E., Wolanski, E., Cahoon, D., Hopkinson, C.S. (Eds.), *Coastal Wetlands: An Integrated Ecosystem Approach*. Elsevier, Amsterdam, pp. 687–715.

Ellison, J.C., Stoddart, D.R., 1991. Mangrove ecosystem collapse during predicted sea-level rise: Holocene analogues and implications. *Journal of Coastal Research* 7, 15.

Engel, M., Matter, A., Parker, A.G., Parton, A., Petraglia, M.D., Preston, G.W., Preusser, F., 2017. Lakes or wetlands? A comment on "The middle Holocene climatic records from Arabia: reassessing lacustrine environments, shift of ITCZ in Arabian Sea, and impacts of the southwest Indian and African monsoons" by Enzel et al. *Global and Planetary Change* 148, 258–267.

Enzel, Y., Kushnir, Y., Quade, J., 2015. The middle Holocene climatic records from Arabia: reassessing lacustrine environments, shift of ITCZ in Arabian Sea, and impacts of the southwest Indian and African monsoons. *Global and Planetary Change* 129, 69–91.

Enzel, Y., Quade, J., Kushnir, Y., 2017. Response to Engel et al. (in press): Lakes or wetlands? A comment on "The middle Holocene climatic records from Arabia: reassessing lacustrine environments, shift of ITCZ in Arabian Sea, and impacts of the southwest Indian and African monsoons" by Enzel et al. (2015). *Global and Planetary Change* 148, 268–271.

Ermertz, A., Kázmér, M., Adolphs, S., Falkenroth, M., Hoffmann, G., 2019. Geoarchaeological evidence for the decline of the medieval city of Qalhat, Oman. *Open Quaternary* 5, 1–14.

Falkenroth, M., Adolphs, S., Cahnbley, M., Bagci, H., Kázmér, M., Mechernich, S., Hoffmann, G. 2020. Biological indicators reveal small-scale sea-level variability during MIS 5e (Sur, Sultanate of Oman). *Open Quaternary* 6, 1–20.

Farani, G.L., Nogueira, M.M., Johnsson, R., 2015. The salt tolerance of the freshwater snail Melanoides tuberculata (Mollusca,

Gastropoda), a bioinvader gastropod. *Pan-American Journal of Aquatic Sciences* 10, 212–221.

Fleitmann, D., Burns, S.J., Mangini, A., Mudelsee, M., Kramers, J., Villa, I., Neff, U., *et al*., 2007. Holocene ITCZ and Indian monsoon dynamics recorded in stalagmites from Oman and Yemen (Socotra). *Quaternary Science Reviews* 26, 170–188.

Fleitmann, D., Burns, S.J., Mudelsee, M., Neff, U., Kramers, J., Mangini, A., Matter, A., 2003. Holocene forcing of the Indian monsoon recorded in a stalagmite from southern Oman. *Science* 300, 1737–1739.

Fouda, M.M., Al-Muharrami, M., 1995. *An Initial Assessment of Mangrove Resources and Human Activities at Mahout Island, Arabian Sea, Oman*. Asia-Pacific Symposium on Mangrove Ecosystems. Springer, Dordrecht, Netherlands, pp. 353–362.

Fritz, H.M., Blount, C., Albusaidi, F.B., Al-Harthy, A.H.M., 2010. Cyclone Gonu storm surge in the Gulf of Oman. In: Charabi, Y. (Ed.), *Indian Ocean Tropical Cyclones and Climate Change*. Springer, Dordrecht, Netherlands, pp. 255–263.

Gasse, F., 2002. Diatom-inferred salinity and carbonate oxygen isotopes in Holocene waterbodies of the western Sahara and Sahel (Africa). *Quaternary Science Reviews* 21, 737–767.

Giosan, L., Clift, P.D., Macklin, M.G., Fuller, D.Q., Constantinescu, S., Durcan, J.A., Stevens, T., *et al*., 2012. Fluvial landscapes of the Harappan civilization. *Proceedings of the National Academy of Sciences* 109, E1688–E1694.

Glennie, K.W., Singhvi, A.K., 2002. Event stratigraphy, paleoenvironment and chronology of SE Arabian deserts. *Quaternary Science Reviews* 21, 853–869.

Gregoricka, L.A., 2016. Human response to climate change during the Umm an-Nar/Wadi Suq transition in the United Arab Emirates. *International Journal of Osteoarchaeology* 26, 211–220.

Griffiths, M.L., Johnson, K.R., Pausata, F.S., White, J.C., Henderson, G.M., Wood, C.T., Yang, H., Ersek, V., Conrad, C., Sekhon, N., 2020. End of green Sahara amplified mid- to late Holocene megadroughts in mainland Southeast Asia. *Nature Communications* 11, 1–12.

Hijma, M.P., Engelhart, S.E., Törnqvist, T.E., Horton, B.P., Hu, P., Hill, D.F., 2015. A protocol for a geological sea-level database. In: Shennan, I., Long, A.J., Horton, B.P. (Eds.), *Handbook of Sea-Level Research*. doi:10.1002/9781118452547.ch34.

Hirota, J., Szyper, J.P., 1975. Separation of total particulate carbon into inorganic and organic components. *Limnology and Oceanography* 20, 896–900.

Hoffmann, G., Meschede, M., Zacke, A., Al Kindi, M., 2016. *Field Guide to the Geology of Northeastern Oman*. Schweizerbart, Stuttgart.

Hoffmann, G., Rupprechter, M., Mayrhofer, C., 2013. Review der langfristigen Küstenentwicklung Nordomans: Senkung und Hebung. *Zeitschrift der Deutschen Gesellschaft für Geowissenschaften* 164, 237–252.

Hoffmann, G., Schneider, B., Mechernich, S., Falkenroth, M., Dunai, T., Preusser, F., 2020. Quaternary uplift along a passive continental margin (Oman, Indian Ocean). *Geomorphology* 350, 106870.

Japan International Cooperation Agency, 2014. *The Qurum Environmental Information Center Project: Final Report*. Ministry of Environment and Climate Affairs, Muscat, Oman.

Kathayat, G., Cheng, H., Sinha, A., Yi, L., Li, X., Zhang, H., Li, H., Ning, Y., Edwards, R.L., 2017. The Indian monsoon variability and civilization changes in the Indian subcontinent. *Science Advances* 3,doi: 10.1126/sciadv.1701296.

Keefe, C.W., 1994. The contribution of inorganic compounds to the particulate carbon, nitrogen, and phosphorus in suspended matter and surface sediments of Chesapeake Bay. *Estuaries* 17, 122–130.

Krauss, K.W., McKee, K.L., Lovelock, C.E., Cahoon, D.R., Saintilan, N., Reef, R., Chen, L., 2014. How mangrove forests adjust to rising sea level. *New Phytologist* 202, 19–34.

Kromer, B., Lindauer, S., Synal, H.-A., Wacker, L., 2013. MAMS: a new AMS facility at the Curt-Engelhorn-Centre for Achaeometry, Mannheim, Germany. *Nuclear Instruments and Methods in Physics Research Section B: Beam Interactions with Materials and Atoms* 294, 11–13.

Kwarteng, A.Y., Dorvlo, A.S., Vijaya Kumar, G.T., 2009. Analysis of a 27-year rainfall data (1977–2003) in the Sultanate of Oman. *International Journal of Climatology: A Journal of the Royal Meteorological Society* 29, 605–617.

Lézine, A.-M., 2009. Timing of vegetation changes at the end of the Holocene Humid Period in desert areas at the northern edge of the Atlantic and Indian monsoon systems. *Comptes Rendus Geoscience* 341, 750–759.

Lézine, A.-M., Ivory, S.J., Braconnot, P., Marti, O., 2017. Timing of the southward retreat of the ITCZ at the end of the Holocene Humid Period in southern Arabia: data-model comparison. *Quaternary Science Reviews* 164, 68–76.

Lézine, A.-M., Saliège, J.F., Mathieu, R., Tagliatela, T.L., Mery, S., Charpentier, V., Cleuziou, S., 2002. Mangroves of Oman during the late Holocene: climatic implications and impact on human settlements. *Vegetation History and Archaeobotany* 11, 221–232.

Lindauer, S., Marali, S., Schöne, B.R., Uerpmann, H.-P., Kromer, B., Hinderer, M., 2016. Investigating the local reservoir age and stable isotopes of shells from southeast Arabia. *Radiocarbon* 59, 355–372.

Lindauer, S., Santos, G.M., Steinhof, A., Yousif, E., Phillips, C., Jasim, S.A., Uerpmann, H.-P., Hinderer, M., 2017. The local marine reservoir effect at Kalba (UAE) between the Neolithic and Bronze Age: an indicator of sea level and climate changes. *Quaternary Geochronology* 42, 105–116.

Lokier, S.W., Bateman, M.D., Larkin, N.R., Rye, P., Stewart, J.R., 2015. Late Quaternary sea-level changes of the Persian Gulf. *Quaternary Research* 84, 69–81.

Lovejoy, T.E., Hannah, L., 2005. *Climate Change and Biodiversity*. Yale University Press, New Haven, CT.

Lovelock, C.E., Cahoon, D.R., Friess, D.A., Guntenspergen, G.R., Krauss, K.W., Reef, R., Rogers, K., *et al*., 2015. The vulnerability of Indo-Pacific mangrove forests to sea-level rise. *Nature* 526, 559–563.

Luis, A.J., Kawamura, H., 2002. Mechanism for sea surface temperature cooling in the Gulf of Oman during winter. *Geophysical Research Letters* 29, 16-1–16-4.

Lüning, S., Gałka, M., Danladi, I.B., Adagunodo, T.A., Vahrenholt, F., 2018. Hydroclimate in Africa during the medieval climate anomaly. *Palaeogeography, Palaeoclimatology, Palaeoecology* 495, 309–322.

Maizels, J., 1990. Raised channel systems as indicators of palaeohydrologic change: a case study from Oman. *Palaeogeography, Palaeoclimatology, Palaeoecology* 76, 241–277.

Marrast, A., Béarez, P., Charpentier, V., 2020. Sharks in the lagoon? Fishing exploitation at the Neolithic site of Suwayh 1 (Ash Sharqiyah region, Arabian Sea, Sultanate of Oman). *Arabian Archaeology and Epigraphy* 31, 178-193.

Martin, C., 2005. Stratégies et statut de la collecte des mollusques marins sur les sites côtiers d'Oman du Néolithique à l'âge du

Bronze: apport des sites de Suwayh 1, Ra's al-Khabbah 1 et Ra's al-Jinz 2. [Strategies and status of the collection of marine molluscs at the coastal sites of Oman from the Neolithic to the Bronze Age: contributions of the sites Suwayh 1, Ra's al-Khabbah 1 and Ra's al-Jinz 2]. *Paléorient* 31, 169–175.

Mattern, F., Moraetis, D., Abbasi, I., Al Shukaili, B., Scharf, A., Claereboudt, M., Looker, E., Al Haddabi, N., Pracejus, B., 2018. Coastal dynamics of uplifted and emerged late Pleistocene near-shore coral patch reefs at Fins (eastern coastal Oman, Gulf of Oman). *Journal of African Earth Sciences* 138, 192–200.

Mattern, F., Scharf, A., Al-Sarmi, M., Pracejus, B., Al-Hinaai, A.-S., Al-Mamari, A., 2018. Compaction history of Upper Cretaceous shale and related tectonic framework, Arabian Plate, eastern Oman Mountains. *Arabian Journal of Geosciences* 11, 444.

Maundu, P., Tengnäs, B.O., 2005. *Useful Trees and Shrubs for Kenya*. ICRAF Technical Handbook No. 35. World Agro-Forestry Centre, Eastern and Central Africa Regional Programme, Nairobi.

McGowan, J.A., Cayan, D.R., Dorman, L.M., 1998. Climate-ocean variability and ecosystem response in the northeast Pacific. *Science* 281, 210–217.

McLachlan, A., Fisher, M., Al-Habsi, H.N., Al-Shukairi, S.S., Al-Habsi, A.M., 1998. Ecology of sandy beaches in Oman. *Journal of Coastal Conservation* 4, 181–190.

Mitchell, J.F.B., Lowe, J., Wood, R.A., Vellinga, M., 2006. Extreme events due to human-induced climate change. *Philosophical Transactions of the Royal Society A: Mathematical, Physical and Engineering Sciences* 364, 2117–2133.

Mitrovica, J.X., Milne, G.A., 2002. On the origin of late Holocene sea-level highstands within equatorial ocean basins. *Quaternary Science Reviews* 21, 2179–2190.

Moraetis, D., Mattern, F., Scharf, A., Frijia, G., Kusky, T.M., Yuan, Y., El-Hussain, I., 2018. Neogene to Quaternary uplift history along the passive margin of the northeastern Arabian Peninsula, eastern Al Hajar Mountains, Oman. *Quaternary Research* 90, 418–434.

Moraetis, D., Scharf, A., Mattern, F., Pavlopoulos, K., Forman, S., 2020. Quaternary Thrusting in the central Oman Mountains—novel observations and causes: insights from optical stimulate luminescence dating and kinematic fault analyses. *Geosciences* 10, 166.

Neff, U., Burns, S.J., Mangini, A., Mudelsee, M., Fleitmann, D., Matter, A., 2001. Strong coherence between solar variability and the monsoon in Oman between 9 and 6 kyr ago. *Nature* 411, 290–293.

Parker, A.G., 2009. Pleistocene climate change in Arabia: developing a framework for hominin dispersal over the last 350 ka. In: Petraglia, M.D., Rose, J.I. (Eds.), *The Evolution of Human Populations in Arabia*. Springer, Dordrecht, Netherlands, pp. 39–49.

Parker, A.G., Morley, M.W., Parton, A., Preston, G.W., Russ, H., Armitage, S.J., 2018. Chapter 2, geomorphology, geoarchaeology and palaeoenvironments. In: Drechsler, P. (Ed.), Dosariyah: Reinvestigating a Neolithic Coastal Community in the Eastern Arabia. British Foundation for the Study of Arabia Monograph No.19. Archaeopress, Oxford, pp. 21-55.

Parker, A.G., Rose, J.I., 2008. Climate change and human origins in southern Arabia. *Proceedings of the Seminar for Arabian Studies* 38, 25–42.

Perdue, E.M., Koprivnjak, J.F., 2007. Using the C/N ratio to estimate terrigenous inputs of organic matter to aquatic environments. *Estuarine, Coastal and Shelf Science* 73, 65–72.

Peters, T., Al Battashy, M., Bläsi, H., Hauser, M., Immenhauser, A., Moser, L., Al Rajhi, A., 2001. Geological Map of Sur and Al Ashkharah, Sheet NF 40-8F and NF 40-12C, Explanatory Notes. Ministry of Commerce and Industry, Muscat, Oman.

Petraglia, M.D., Groucutt, H.S., Guagnin, M., Breeze, P.S., Boivin, N., 2020. Human responses to climate and ecosystem change in ancient Arabia. *Proceedings of the National Academy of Sciences* 117, 8263–8270.

Piontkovski, S.A., Al-Gheilani, H.M.H., Jupp, B.P., Al-Azri, A.R., Al-Hashmi, K.A., 2012. Interannual changes in the Sea of Oman ecosystem. *The Open Marine Biology Journal* 6, 38–52.

Polidoro, B.A., Carpenter, K.E., Collins, L., Duke, N.C., Ellison, A.M., Ellison, J.C., Farnsworth, E.J., *et al*., 2010. The loss of species: mangrove extinction risk and geographic areas of global concern. *PLOS ONE* 5, e10095.

Preston, G.W., Parker, A.G., Walkington, H., Leng, M.J., Hodson, M.J., 2012. From nomadic herder-hunters to sedentary farmers: the relationship between climate change and ancient subsistence strategies in south-eastern Arabia. *Journal of Arid Environments* 86, 122–130.

Preusser, F., 2009. Chronology of the impact of Quaternary climate change on continental environments in the Arabian Peninsula. *Comptes Rendus Geoscience* 341, 621–632.

Preusser, F., Radies, D., Driehorst, F., Matter, A., 2005. Late Quaternary history of the coastal Wahiba Sands, Sultanate of Oman. *Journal of Quaternary Science* 20, 395–405.

Preusser, F., Radies, D., Matter, A., 2002. A 160,000-year record of dune development and atmospheric circulation in southern Arabia. *Science* 296, 2018–2020.

Radies, D., Hasiotis, S.T., Preusser, F., Neubert, E., Matter, A., 2005. Paleoclimatic significance of early Holocene faunal assemblages in wet interdune deposits of the Wahiba Sand Sea, Sultanate of Oman. *Journal of Arid Environments* 62, 109–125.

Radies, D., Preusser, F., Matter, A., Mange, M., 2004. Eustatic and climatic controls on the development of the Wahiba Sand Sea, Sultanate of Oman. *Sedimentology* 51, 1359–1385.

Ramsey, C.B., Lee, S., 2013. Recent and planned developments of the program OxCal. *Radiocarbon* 55, 720–730.

Ratajczak, Z., Carpenter, S.R., Ives, A.R., Kucharik, C.J., Ramiadantsoa, T., Stegner, M.A., Williams, J.W., Zhang, J., Turner, M.G., 2018. Abrupt change in ecological systems: inference and diagnosis. *Trends in Ecology & Evolution* 33, 513–526.

Reef, R., Feller, I.C., Lovelock, C.E., 2010. Nutrition of mangroves. *Tree Physiology* 30, 1148–1160.

Reimer, P.J., Bard, E., Bayliss, A., Beck, J.W., Blackwell, P.G., Ramsey, C.B., Buck, C.E., *et al*., 2013. IntCal13 and marine13 radiocarbon age calibration curves 0–50,000 years cal BP. *Radiocarbon* 55, 1869–1887.

Ricklefs, R.E., Latham, R.E., 1993. *Global Patterns of Diversity in Mangrove Floras.* In: Ricklefs, R.E., Schluter, D. (Eds.), *Species Diversity in Ecological Communities: Historical and Geographical Perspectives*. University of Chicago Press, Chicago, pp. 215–229.

Rodgers, D.W., Gunatilaka, A., 2003. Bajada formation by monsoonal erosion of a subaerial forebulge, Sultanate of Oman. *Sedimentary Geology* 154, 127–146.

Rosenberg, T.M., Preusser, F., Blechschmidt, I., Fleitmann, D., Jagher, R., Matter, A., 2012. Late Pleistocene palaeolake in the interior of Oman: a potential key area for the dispersal of anatomically modern humans out-of-Africa? *Journal of Quaternary Science* 27, 13–16.

Rosenberg, T.M., Preusser, F., Fleitmann, D., Schwalb, A., Penkman, K., Schmid, T.W., Al-Shanti, M.A., Kadi, K., Matter, A., 2011. Humid periods in southern Arabia: windows of opportunity for modern human dispersal. *Geology* 39, 1115–1118.

Rovere, A., Stocchi, P., Vacchi, M., 2016. Eustatic and relative sea level changes. *Current Climate Change Reports* 2, 221–231.

Saintilan, N., Khan, N.S., Ashe, E., Kelleway, J.J., Rogers, K., Woodroffe, C.D., Horton, B.P., 2020. Thresholds of mangrove survival under rapid sea level rise. *Science* 368, 1118–1121.

Sathe, S.S., Lavate, R.A., Bhosale, L.J., 2013. Mangrove as source of energy for rural development with special reference to Ratnagiri and Sindhudarg district (MS) India. *Bioscience Discovery* 4, 198–201.

Schmedemann, N., Schafmeister, M.T., Hoffmann, G., 2008. Numeric de-compaction of Holocene sediments. *Polish Geological Institute Special Papers* 23, 87–94.

Sefton, J.P., 2020. *Evaluating Mangrove Proxies for Quantitative Relative Sea-Level Reconstructions*. Master's thesis, Durham University, Durham, UK.

Seneviratne, S.I., N. Nicholls, D. Easterling, C.M. Goodess, S. Kanae, J. Kossin, Y. Luo, *et al*., 2012. Changes in climate extremes and their impacts on the natural physical environment. In: Field, C.B., Barros, V., Stocker, T.F., Qin, D., Dokken, D.J., Ebi, K.L., Mastrandrea, M.D., *et al*. (Eds.), *Managing the Risks of Extreme Events and Disasters to Advance Climate Change Adaptation: A Special Report of Working Groups I and II of the Intergovernmental Panel on Climate Change (IPCC)*. Cambridge University Press, Cambridge, UK, pp. 109–230.

Singh, G., Wasson, R.J., Agrawal, D.P., 1990. Vegetational and seasonal climatic changes since the last full glacial in the Thar Desert, northwestern India. *Review of Palaeobotany and Palynology* 64, 351–358.

Staubwasser, M., Weiss, H., 2006. Holocene climate and cultural evolution in late prehistoric–early historic West Asia. *Quaternary Research* 66, 372–387.

Steinbeiss, S., Beßler, H., Engels, C., Temperton, V.M., Buchmann, N., Roscher, C., Kreutziger, Y., Baade, J., Habekost, M., Gleixner, G., 2008. Plant diversity positively affects short-term soil carbon storage in experimental grasslands. *Global Change Biology* 14, 2937–2949.

Stokes, S., Bray, H.E., 2005. Late Pleistocene eolian history of the Liwa region, Arabian Peninsula. *Geological Society of America Bulletin* 117, 1466–1480.

Tierney, J.E., Pausata, F.S., deMenocal, P.B., 2017. Rainfall regimes of the green Sahara. *Science Advances* 3, doi: 10.1126/sciadv.1601503.

Tomlinson, P.B., 2016. *The Botany of Mangroves*. Cambridge University Press, Cambridge, UK.

Twilley, R.R., Rivera-Monroy, V.H., Rovai, A.S., Castañeda-Moya, E., Davis, S., 2019. Mangrove biogeochemistry at local to global scales using ecogeomorphic approaches. In: Perillo, G.M.E., Wolanski, E., Cahoon, D., Hopkinson, C.S. (Eds.), *Coastal Wetlands: An Integrated Ecosystem Approach*. Elsevier, Amsterdam, pp. 687–715.

Ward, R.D., Friess, D.A., Day, R.H., Mackenzie, R.A., 2016. Impacts of climate change on mangrove ecosystems: a region by region overview. *Ecosystem Health and Sustainability* 2, e01211.

Waselkov, G.A., 1987. Shellfish gathering and shell midden archaeology. In: Schiffer, M.B. (Ed.), *Advances in Archaeological Method and Theory*. Vol. 10. Academic Press, San Diego, pp. 93–210.

Watanabe, T.K., Watanabe, T., Yamazaki, A., Pfeiffer, M., 2019. Oman corals suggest that a stronger winter shamal season caused the Akkadian Empire (Mesopotamia) collapse. *Geology* 47, 1141–1145.

Woodroffe, C.D., Rogers, K., McKee, K.L., Lovelock, C.E., Mendelssohn, I.A., Saintilan, N., 2016. Mangrove sedimentation and response to relative sea-level rise. *Annual Review of Marine Science* 8, 243–266.

Woodroffe, S.A., Horton, B.P., 2005. Holocene sea-level changes in the Indo-Pacific. *Journal of Asian Earth Sciences* 25, 29–43.

Woodroffe, S.A., Long, A.J., Punwong, P., Selby, K., Bryant, C. L., Marchant, R., 2015. Radiocarbon dating of mangrove sediments to constrain Holocene relative sea-level change on Zanzibar in the southwest Indian Ocean. *The Holocene* 25, 820–831.

Zazzo, A., Munoz, O., Saliège, J.F., Moreau, C., 2012. Variability in the marine radiocarbon reservoir effect in Muscat (Sultanate of Oman) during the 4th millennium BC: reflection of taphonomy or environment? *Journal of Archaeological Science* 39, 2559–2567.

https://doi.org/10.1017/qua.2020.96 Published online by Cambridge University Press

5.1.2 Collapse of Holocene mangrove ecosystems along the coastline of Oman – *Corrigendum*

Quaternary Research (2021), **100**, 260–262
doi:10.1017/qua.2021.6

Corrigendum

Collapse of Holocene mangrove ecosystems along the coastline of Oman – Corrigendum

Valeska Decker, Michaela Falkenroth, Susanne Lindauer, Jessica Landgraf, Zahra Al-Lawati, Huda Al-Rahbi, Sven Oliver Franz and Gösta Hoffmann

Published online by Cambridge University Press 29 December 2020;
DOI: https://doi.org/10.1017/qua.2020.96

In the original publication of Decker et al. (2020), Figures 6, 7, and 8 were incorrectly labelled. The correct figures and their captions are reproduced below:

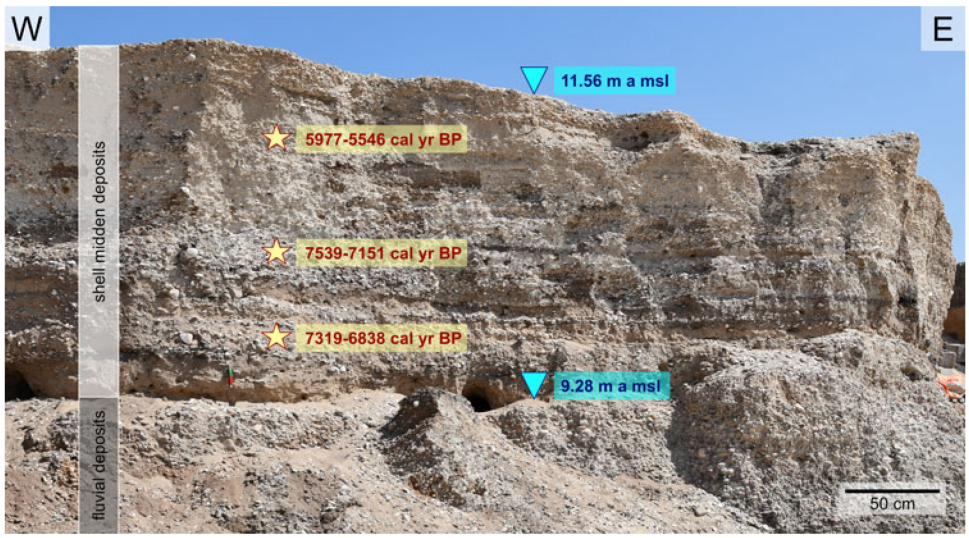

Figure 6. The shell midden south of Ras ar Ru'ays showing the underlying fluvial deposits. The stars mark the ^{14}C dates of molluscs; the blue triangle indicates the D-GPS measured height a msl. (For interpretation of the references to color in this figure legend, the reader is referred to the web version of this article.)

Cite this article: Decker V, Falkenroth M, Lindauer S, Landgraf J, Al-Lawati Z, Al-Rahbi H, Franz SO, Hoffmann G (2021). Collapse of Holocene mangrove ecosystems along the coastline of Oman – Corrigendum. *Quaternary Research* **100**, 260–262. https://doi.org/10.1017/qua.2021.6

© University of Washington. Published by Cambridge University Press, 2021

Downloaded from https://www.cambridge.org/core. IP address: 84.175.163.16, on 22 Mar 2021 at 19:05:21, subject to the Cambridge Core terms of use, available at https://www.cambridge.org/core/terms. https://doi.org/10.1017/qua.2021.6

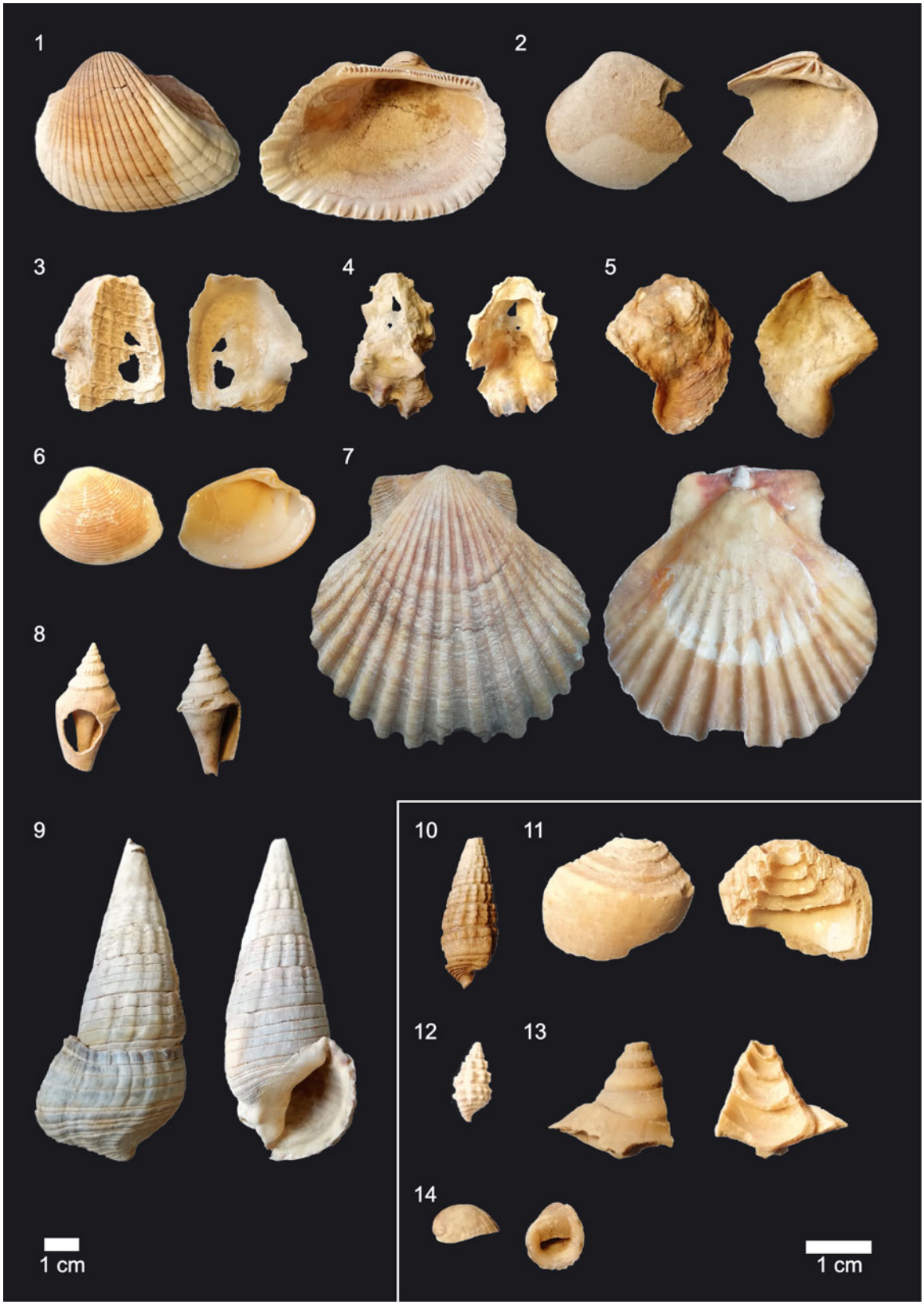

Figure 7. (color online) Bivalve shells were the most abundant species found in the shell midden of Ras ar Ru'ays (exterior shown at left, interior shown at right): 1, *Anadara* cf. *antiquata*; 2, *Marcia* sp.; 3–5, oyster; 3, imprint of a *Terebralia palustris* shell in an oyster shell; 6, *Marcia* sp.; 7, *Chlamys townsendi*; 8, *Strombus* sp.; 9, *Terebralia palustris*; 10, *Cerithidea cingulata*; 11, broken *Conus* sp.; 12, *Cerithidium* sp.; 13, broken *Strombus* sp.; 14, *Nerita* sp.

Downloaded from https://www.cambridge.org/core. IP address: 84.175.163.16, on 22 Mar 2021 at 19:05:21, subject to the Cambridge Core terms of use, available at https://www.cambridge.org/core/terms. https://doi.org/10.1017/qua.2021.6

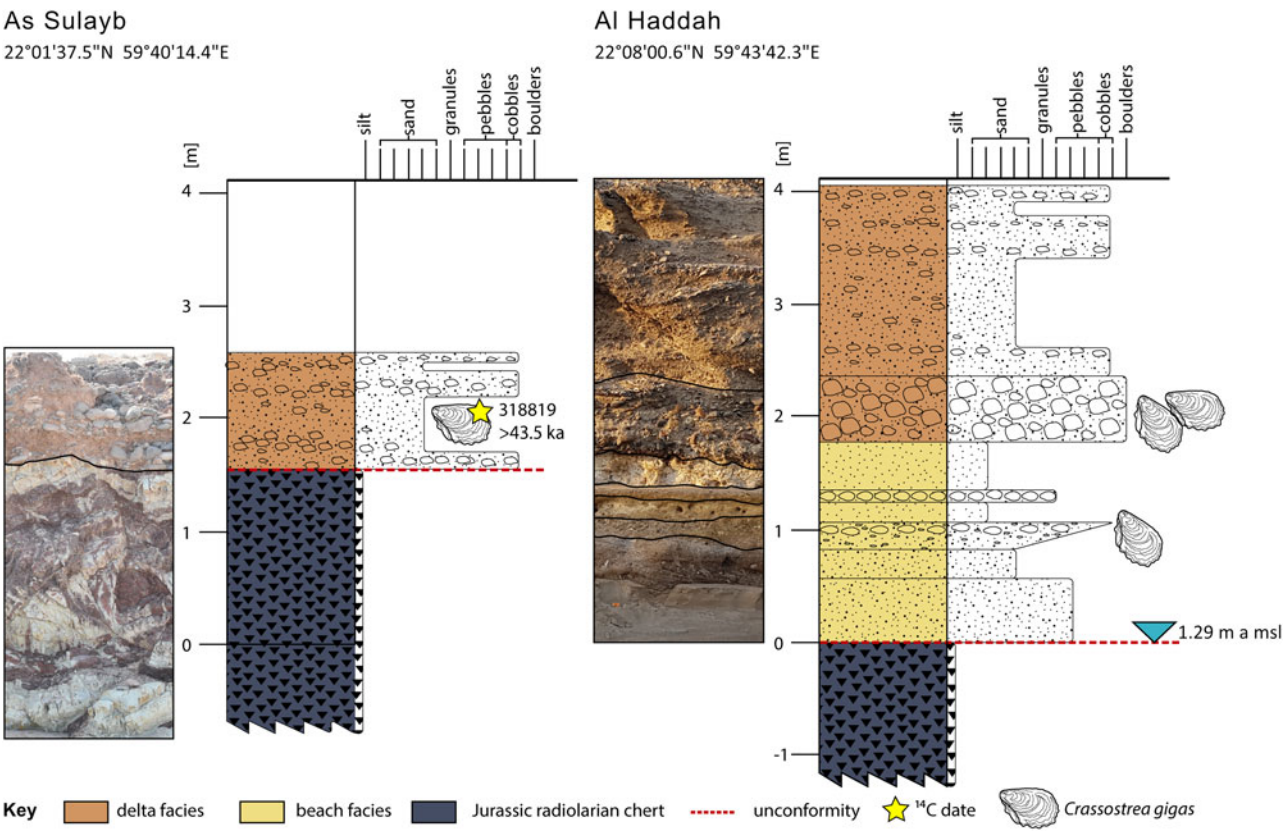

Figure 8. (color online) Coastal cliff outcrops near As Sulayb and Al Haddah showing a succession of radiolarian chert unconformly overlain by coastal deposits. The sediments indicate that the last sea-level highstand was before 43.5 ka.

REFERENCE

Decker, V., Falkenroth, M., Lindauer, S., Landgraf, J., Al-Lawati, Z., Al-Rahbi, H., Franz, S. O., Hoffmann, G. Collapse of Holocene mangrove ecosystems along the coastline of Oman. First published online 29 December 2020. *Quaternary Research*, doi: https://doi.org/10.1017/qua.2020.96.

Downloaded from https://www.cambridge.org/core. IP address: 84.175.163.16, on 22 Mar 2021 at 19:05:21, subject to the Cambridge Core terms of use, available at https://www.cambridge.org/core/terms. https://doi.org/10.1017/qua.2021.6

5.2 Life on the Edge: A Powerful Tsunami Overwhelmed Indian Ocean Mangroves One Millennium Ago (Decker et al. 2022)



Fig. 4: The Sur lagoon around 1,000 years ago, with shores vegetated by *Avicennia marina* mangroves, shortly before a 10–15 m high tsunami wave impacts the coast. The event deposits a tsunamigenic shell layer within the lagoon, embedding the mangroves that were destroyed by the wave's destructive force.

forests

MDPI

Article

Life on the Edge: A Powerful Tsunami Overwhelmed Indian Ocean Mangroves One Millennium Ago

Valeska Decker [1,*], Carole T. Gee [2,3], Pia J. Schucht [4], Susanne Lindauer [5] and Gösta Hoffmann [6]

1 Institute of Geology and Palaeontology, RWTH Aachen University, 52056 Aachen, Germany
2 Paleontology, Institute of Geosciences, University of Bonn, 53115 Bonn, Germany; cgee@uni-bonn.de
3 Huntington Botanical Gardens, San Marino, CA 91108, USA
4 Institute of Zoology, University of Bonn, 53115 Bonn, Germany; pschucht@uni-bonn.de
5 Curt-Engelhorn-Centre Archaeometry, C4, 8, 68159 Mannheim, Germany; susanne.lindauer@ceza.de
6 Neotectonics and Natural Hazards, RWTH Aachen University, 52056 Aachen, Germany; g.hoffmann@nug.rwth-aachen.de
* Correspondence: valeska.decker@rwth-aachen.de

Abstract: In this paper, we demonstrate how subfossil mangrove wood can be used to elucidate the timing of past tsunami events. Although tsunamis generated by submarine earthquakes along the Makran subduction zone in the Arabian Sea are not unusual, rigorous age documentation is generally lacking. The best known is the only instrument-recorded tsunami, which affected the coastlines of Iran, Pakistan, India, and Oman in November 1945. Eyewitness accounts of the effect along the Oman coastline assert that this tsunami was not destructive. However, a 25-cm-thick shell layer in the lagoon adjacent to the city of Sur was attributed to the 1945 tsunami, although dating of the shell deposit proved difficult, and the radiocarbon dates of mollusk shells were regarded as unreliable. Here, we reinterpret the age of this tsunamigenic layer based on the new discovery of parallel-oriented woody axes in the sedimentological context of the tsunami shell layer in the Sur lagoon. The woody axes were analyzed anatomically and identified as pertaining to the gray mangrove *Avicennia*. Radiocarbon dating of the wood (905–722 cal BP), along with sedimentological investigations, suggests that the deposition of the woody axes should be attributed to an older tsunami event that occurred ca. 1000 years ago, which has been documented at other locations along the Arabian Sea coastline. From this, we conclude that mangroves grew in this lagoon at that time. Very little is known about ancient mangrove distribution in this region and, so far, no records have been provided for this time window at this site. We also deduce that the tsunami event that occurred one millennium ago must have been substantially more severe than the one in 1945. More accurate dating of tsunamigenic events will aid in calculating the recurrence intervals and magnitude of tsunamis generated along the Makran subduction zone.

Keywords: mangrove wood anatomy; taphonomy; *Avicennia marina*; Sur lagoon; tsunami; Gulf of Oman; Arabian Sea; Makran subduction zone; Oman

check for updates

Citation: Decker, V.; Gee, C.T.; Schucht, P.J.; Lindauer, S.; Hoffmann, G. Life on the Edge: A Powerful Tsunami Overwhelmed Indian Ocean Mangroves One Millennium Ago. *Forests* **2022**, *13*, 922. https://doi.org/10.3390/f13060922

Academic Editor: Victor H. Rivera-Monroy

Received: 11 April 2022
Accepted: 11 June 2022
Published: 13 June 2022

Publisher's Note: MDPI stays neutral with regard to jurisdictional claims in published maps and institutional affiliations.

Copyright: © 2022 by the authors. Licensee MDPI, Basel, Switzerland. This article is an open access article distributed under the terms and conditions of the Creative Commons Attribution (CC BY) license (https://creativecommons.org/licenses/by/4.0/).

1. Introduction

Despite huge scientific advances in recent years [1], the vulnerability of coastal areas to the risk of tsunamis remains high [2]. Due to the rapid, unpredictable, wave-triggering geodynamic processes that can produce catastrophic geological events along coastlines, early warning systems for tsunamis are increasingly being installed within ocean basins to monitor seismic activity and to mitigate coastal and inland damage. Studies of recent extreme wave events and the devastation they cause on land show that mangrove stands can significantly reduce the energy of tsunami waves [3]. Although the degree of potential protection of mangroves is widely discussed in more recent reviews [4,5], large-scale reforestation programs and mangrove protection in many parts of the world are intended to make coasts safer again [6]. To estimate the risk of oceanic extreme wave events with

overpowering and often fatal outcomes on shore, recurrence intervals have come under archeological and sedimentological study [7,8]. The reconstruction of tsunami events becomes more uncertain the further back they occurred in the past, due to the nature of these archives, preservation potential, and dating uncertainties.

The Makran subduction zone (MSZ) in the Gulf of Oman marks the convergence of the Eurasian and Arabian Plates. Located on a narrow extension of the northeastern Indian Ocean, this subduction zone extends from west to east over a distance of at least 1000 km [9]. The Arabian Plate is subducting at a rate of ~4 cm/year and, at 4.5° [10], the dip angle of the incoming plate is shallow; the seismicity is low compared to other subduction zones. Concentrated seismicity is recorded in the eastern part, while it is seismically quiet to the west. The seismogenic potential of the MSZ is among the most enigmatic in the world [11]. The trench of the megathrust is filled with a sequence of organic-rich sediments of up to 7 km thickness [12], hampering geophysical investigations. Furthermore, historical seismicity along the MSZ is low [9]. Subduction earthquakes have resulted in tsunamis affecting adjacent coastlines. Another tsunami-triggering process in this area is submarine sliding [13].

The only tsunamigenic earthquake instrumentally recorded along the MSZ had a magnitude of M_W 8.1 and occurred on 27 November 1945. Eyewitness accounts collected along the coasts bordering the Arabian Sea in the Northern Indian Ocean [14] report that, while tsunami waves severely impacted the coastlines of today's Iran, Pakistan, and India, they only affected the coastline of Oman in a minor way. Sedimentological evidence attributed to this tsunami event by [15] includes a shell layer up to 25 cm thick in the Sur lagoon on the Oman shoreline. However, the deposition of such a thick shell layer contradicts the eyewitness reports that describe the tsunami as having very little impact in Oman.

Since the age of the tsunami layer in the Sur lagoon was poorly defined by previous studies, we revisited the site in search of material suitable for radiocarbon dating. Here, we present new sedimentological and paleontological evidence for the shell layer having originated from a powerful tsunami event, and offer a new interpretation of its age.

Located on the eastern edge of the Arabian Peninsula, the northeastern coast of Oman is directly exposed to the MSZ. A large city of historical importance, Sur (Figure 1), is situated here and borders a 5 km^2 horseshoe-shaped lagoon, Khor al Batah. The Sur lagoon is separated from the open sea by a Holocene beach barrier spit system. The oldest part of Sur is located on top of this spit, which is elevated 2–3 m above mean sea level. Tides are semi-diurnal, and the tidal range in the outer coast is 3 m. The sea is connected to the lagoon via a 1 km-long channel with a width of at least 110 m. Khor al Batah is microtidal, with a tidal range of 1.2 m [15], and is almost completely dry during low tide. A well-developed tidal channel system, which drains the large intertidal flats, exists within the lagoon (Figure 1). These intertidal flats are dominated by siliciclastic fine sand bearing mollusks and foraminifera, while coarser material is observed in the tidal channels.

The lagoon is fringed by stands of the gray mangrove *Avicennia marina* (Forssk.) Vierh. (family Acanthaceae), with greatest densities along the southern shores where freshwater input is highest.

During the Holocene Humid Period, a period of higher precipitation around 8000–6000 cal BP ago, mangroves of the species *Avicennia marina* and *Rhizophora mucronata* Lam. were common along the northern and eastern coastlines of Oman [16]. Climate change and accompanying aridification owing to a southward shift of the Intertropical Convergence Zone (ITCZ) led to the collapse of several mangrove ecosystems along the eastern coastline [17]. Some very sheltered mangrove stocks could survive this radical change in environmental conditions, e.g., those in the lagoon of Jaramah in the north and those near Filim in the east [18].

Archaeological evidence reveals the extensive exploitation of mangroves by humans from the beginning of the Bronze Age. Its extraordinarily high calorific value made it a popular firewood and a popular charcoal wood for copper production [19,20]. Additionally,

mangroves have always served as suitable livestock fodder and are also used as construction wood [21]. A growing population that mainly feeds on animal protein and adheres to pasturing methods causes ever-increasing grazing pressure. Charcoal production placed even more stress on the mangrove ecosystems.

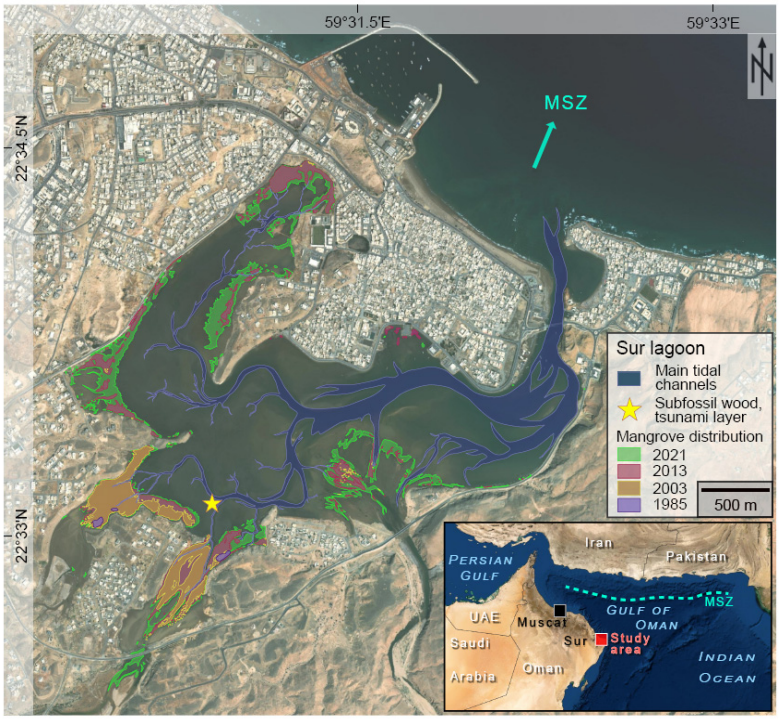

Figure 1. Aerial photo of the Sur lagoon, showing the recent tidal channel system in blue and the modern mangrove distribution in green. The pink, brown, and purple colors indicate mangrove distribution in 2013, 2003, and 1985, respectively. The star marks the trench site, and the turquoise arrow points towards the Makran subduction zone (MSZ) (source: satellite image from Google Maps). Inset: location of the study area in Oman on the northeastern Arabian Peninsula (source: ESRI data, map created using ArcGIS 2015).

Little is known about mangrove distribution from the end of this Holocene Humid Period to recent times. Palynological investigations document an extinction of *Rhizophora mucronata* and a continuous occurrence of *Avicennia marina* in northeastern Oman [16,18].

These species differ from one another in their tolerances towards ecological parameters. *A. marina* is known as the most robust mangrove species and is anatomically adapted to higher salinities and drier climate than *R. mucronata* [22,23]. It can also cope with different substrate types and can withstand cold temperatures and short freezing periods in the winter months [24]. *R. mucronata* is much more sensitive, especially towards salinity and temperature. Thus, expansion of mangroves is often limited by cold and dry climates [24]. Though humans have always exploited mangrove ecosystems, the disappearance of only *R. mucronata* and the continuous occurrence of *A. marina* in Oman mainly reflect a shift in climatic conditions [17,25].

From the 1980s onwards, we can monitor the development of mangrove cover via satellite images. According to these images, only solitary mangrove trees grew along the coastline of the lagoon in Sur in the 1980s (Figure 1). However, urban expansion and waste dumping since ancient times, and especially in the last few decades, have become enormous threats to the mangroves. According to [25], mangroves covered 2.06 km^2 of the northern Omani coastline towards the Gulf of Oman in 1977; their areal extent decreased during the 1980s, but then expanded to 5.3 km^2 in 2017 due to a governmental mangrove reforestation program. Today, only *Avicennia marina* mangroves are present in Oman. They grow as dwarf-shrub-like forms along the northern coastline, e.g., in Qurum and Sur, and

develop dense stands with up to 5 m high trees within a sheltered bay near Filim in the east. Expansion of mangrove habitats, as has been seen in Qurum, Sur, and Filim, is a consequence of environmental protection and reforestation programs.

The erosional processes during and after a tsunami event limit the preservation of ancient tsunami records [26–28]. The mangrove-fringed, lagoonal setting of Sur offers a protected depositional environment with good preservation potential.

2. Materials and Methods

2.1. Fieldwork

Fieldwork in the Sur lagoon was carried out in spring 2020. The southwestern part of the lagoon was targeted for trenching on the basis of earlier investigations and mapping campaigns by [15,29]. We expected to encounter a 10 to 25-cm-thick shell deposit at a 20 cm depth below the surface. Trenching and excavation were conducted manually during low tide, 190 m north of the lagoon's rim and 20 m west of a tidal channel, at 22.5515° N, 59.514818° E. The upper layers were removed, and the surface of the target horizon was prepared as a planum. Shells and wood found on the target horizon were collected for later study in the laboratory. Today, mangrove trees grow 110 m to the southwest. A piece of recent wood of *Avicennia marina* was collected from Khor Mahut on the west coast of Bar al Hikman in east Oman in 2019 and used for comparative study.

2.2. Wood Preparation

The study of all wood took place at the University of Bonn in Germany. The fragile and brittle trench wood was stored at 5–10 °C to prevent fungal growth prior to sectioning. The recent wood from Bar al Hikman was stored in a 1:1:2 mixture of water, glycerol, and ethanol for three months to soften it sufficiently for sectioning.

Wood anatomical sections were prepared following the method described by [30]; incubation times were adjusted for the larger, poorly impregnable samples. All wood samples were sectioned using a hand saw into ca. $1 \times 1 \times 1$ cm^3 pieces in the three planes of section needed for study, namely, in the transverse, radial, and tangential sections. The samples were fixed in 4% neutral buffered formalin for 2 days, rinsed under running tap water for 3 h, dehydrated in a graded series of isopropyl alcohol over the course of a week, and embedded in paraffin (Surgipath Paraplast, REF 39601006, LeicaBiosystems). The paraffin blocks were thin-sectioned at a thickness of 20–40 µm using a Microm HM 355 rotary microtome (Microm International GmbH, Dreieich, Germany). The thin sections were transferred into a drop of 20% ethanol on protein glycerol-coated glass slides and flattened on a hot plate. After drying overnight, the thin sections were then deparaffinized in 2 changes of xylene for a total of 10 min. Cover slips were placed over the sections using Roti® Histokitt II (Carl Roth GmbH + Co. KG, Karlsruhe, Germany).

The thin sections were analyzed and photographed at 1.25× or 5.0× magnification using a Leica® DM2500 compound light microscope equipped with a Leica® DFC240 camera (Leica Microsystems, Wetzlar, Germany). The images were processed using ImageAccess easyLab 7 (Version 1992–2007, iMagic, Glattburg, Switzerland) and Affinity Designer (Version 1.10.5.1342, ©Serif Europe LTD, Nottingham, UK).

In addition to the thin sections on glass slides, thick sections of the trench wood and recent wood of 15-mm-thickness were cut transversely with a handsaw and wet-ground with a manual grinding and polishing machine under running tap water with abrasive paper, using successive grain sizes of 400, 600, 800, and 1200.

Analyses of the thick sections were carried out with a Leica® SAPO stereo microscope equipped with a Leica® DFC240 camera (Leica Microsystems, Wetzlar, Germany). Digital images were taken at 1.0× or 5.0× magnification and processed using the integrated measurement software ImageAccess easyLab 7 (Version 1992–2007, iMagic, Glattburg, Switzerland) and Affinity Designer (Version 1.10.5.1342, ©Serif Europe LTD, Nottingham, UK). Figured wood sections are archived at the Division of Paleontology, University of Bonn, Germany. Anatomical descriptions follow the work of [24,31].

2.3. Age Dating

Radiocarbon dating of three bivalve shells and the trench wood was outsourced to a commercial lab (Beta Analytic, FL, USA). The conventional radiocarbon ages were adjusted for local reservoir correction and calibrated by us. We then adjusted the measurement results with respect to reservoir correction prior to calibrating the data.

Marine reservoir correction and calibration [32] was applied to the radiocarbon dates on the three bivalve samples using a local ΔR value of 79 ± 50 years, taken from the online Marine Reservoir Correction database (http://calib.org/marine/ accessed on 11 November 2021) as a mean value of reservoir effects of surrounding areas in the database. Bivalves and wood samples were calibrated with the Intcal20 dataset in Oxcal 4.4. Values from the database were determined using species from museum collections that were collected live before 1950.

3. Results

3.1. Measured Section at SW Sur Lagoon

The trench excavated in the southwestern part of the Sur lagoon measures 52 cm deep and exposes three layers, which are designated here as L1 to L3 (Figure 2). The lowermost layer (L1: 0–19 cm) is composed of a gray, silty, fine sand. Abundant redoximorphic features, such as centimeter-sized black spots and some light beige vertical bioturbation structures 1 mm in diameter, are found in the trench, in addition to some small, solitary fragments of mollusk shells.

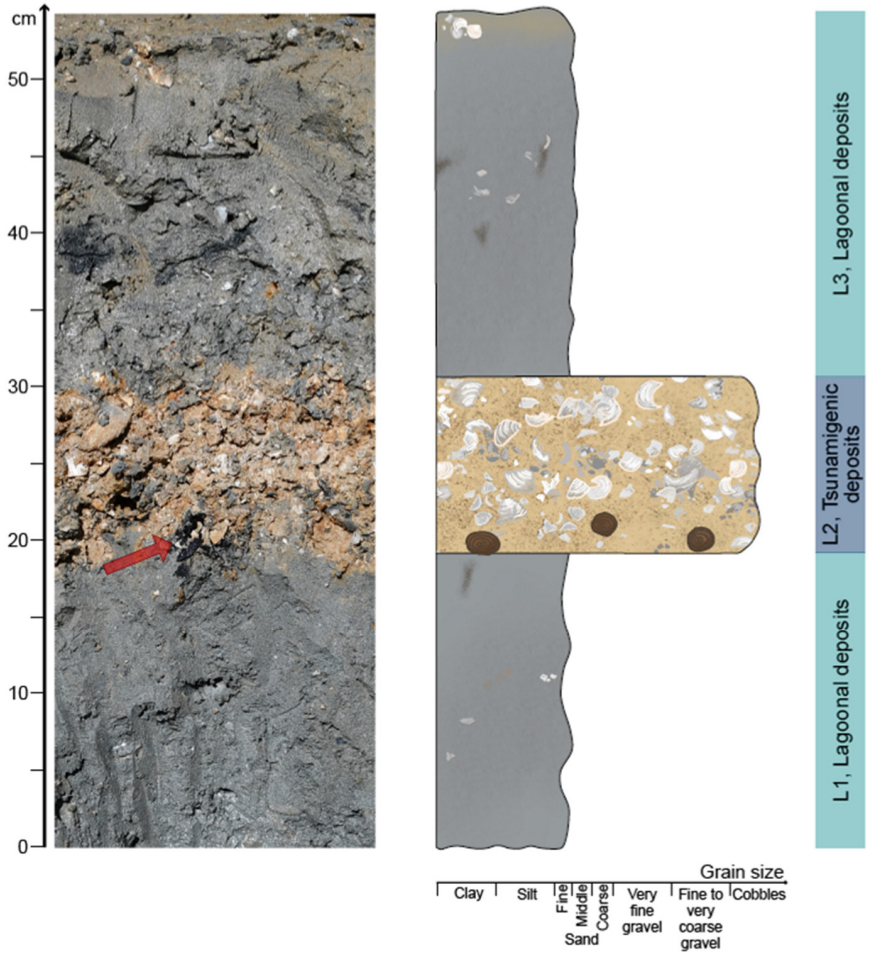

Figure 2. Vertical sections through the tsunamigenic deposits in the Sur lagoon. Left: photo of the trench. The red arrow indicates dark-colored wood remains. Right: measured section. Brown circles represent woody axes at the base of the tsunamigenic layer L2.

Layer L2 (19–29 cm) consists of an unsorted, clast-supported sediment with a variety of white mollusk shells, mainly articulated bivalves, and many angular shell fragments in an orange-beige, fine-to-medium sandy matrix. Woody axes occur at the base and in the lower part of L2 (Figures 2 and 3). The woody axes measure up to 4 cm in diameter and up to 1.4 m long, but are commonly broken into pieces of decimeter length. They are horizontally aligned subparallel to one another and oriented NNE–SSW. The woody axes are well-preserved with macroscopic features on the bark and represent branch or stem wood. No roots were discovered.



Figure 3. Block diagram showing the subfossil woody axes in situ, aligned NNE–SSW, and embedded at the base of the tsunamigenic layer (depicted in beige) in between gray lagoonal layers. Towards the top of the block are some redoximorphic features, living *Cerithidea cingulata* gastropods, a few bivalve shells, and small mats of seagrass on the surface.

The sequence is capped by L3 (29–52 cm), a gray, silty fine sand with some mollusk shells, such as the gastropod *Cerithidea cingulata*. This layer is bioturbated by bivalves, crabs, and worms. L3 shows some centimeter-sized black spots, similar to those in L1. The color changes to light brownish gray within the upper 1 cm of the sections. Abundant mollusk shells are scattered on the surface of the lagoon; living *Cerithidea cingulata* gastropods are very abundant locally. Some mats of seagrass can be found.

3.2. Age Dating

Radiocarbon dating of the three bivalve shells yielded reservoir-corrected ages of 95–0 cal BP (Beta-414721), 99–0 cal BP (Beta-414722) and 115–0 cal BP (Beta-414723). Radiocarbon dating of the trench wood from L2 produced an age of 905–722 cal BP (Beta-579069) and thus characterizes the plant remains as subfossil (Table S1).

3.3. Additional Observations

Observations made in the eastern part of the lagoon at 40Q 759186 m E, 2497192 m N reveal a different sedimentological situation. Here, the subsurface is characterized by silty fine sand, comparable to layer L1 in the trench in the southwestern part of the lagoon. A shell layer equivalent to L2 was not observed. Noteworthy are cobbles, bricks, and coral fragments of decimeter size scattered on the surface. This building material apparently originates from construction in the city of Sur, as the nearest modern houses are located only 90 m away. The size of the individual clasts of this coarse surface decreases towards the center of the lagoon.

3.4. Identification of the Trench Wood

The anatomy of the trench wood is highly comparable with the recent *Avicennia marina* wood. Of the three planes of section, the transverse and tangential sections are the most appropriate for comparison. In the transverse section, an extremely distinctive feature

found in recent *Avicennia* wood is a series of concentric rings which consist of alternating bands of xylem and phloem, but do not represent annual growth [31,33]. A thin band of sclerenchyma separates the rings from one another. Transverse sections of recent *Avicennia* wood also clearly show the occurrence of multiple, radially arranged vessel elements [24,31]. In the tangential section, another feature typically observed in recent *Avicennia* wood is the presence of medullary rays that are between two and five cells wide [31]. Both the recent wood of *Avicennia marina* and the wood from L2 show this suite of distinctive features (Figures 4 and 5). Thus, based on the distinctive anatomical features of its wood, it can be concluded that the woody axes found in L2 pertain to the mangrove *Avicennia*.

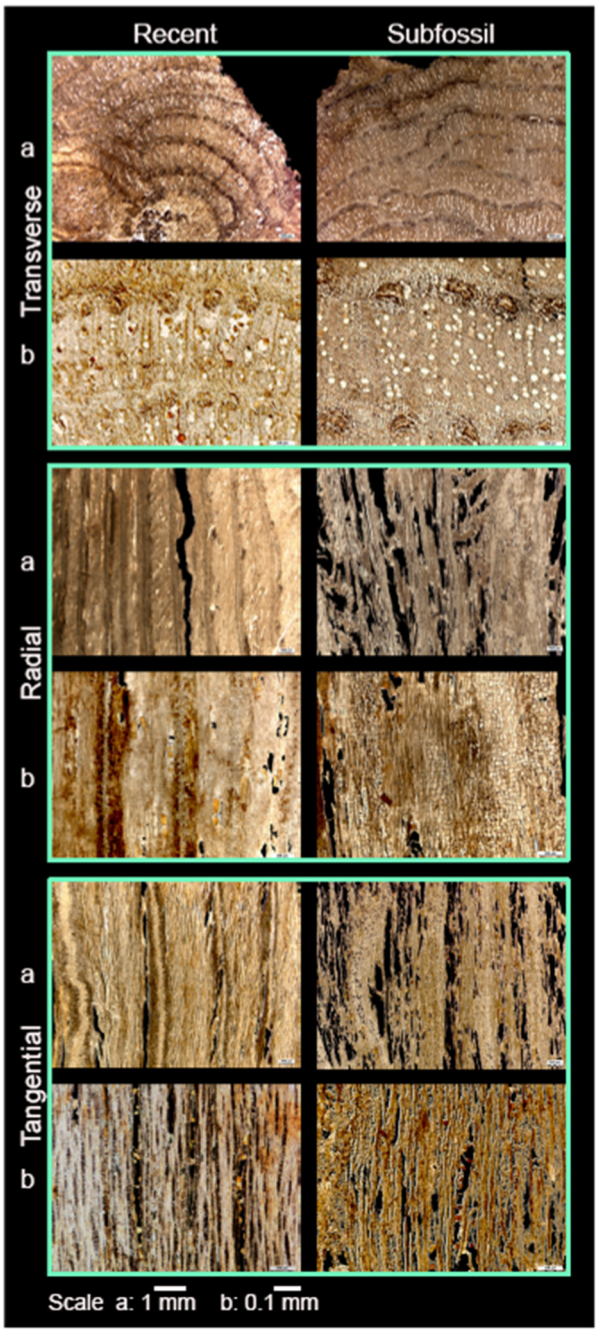

Figure 4. Thin sections of recent *Avicennia marina* wood (left column) for comparison with the subfossil trench wood (right column), in the transverse, radial, and tangential sections at 1.25× (**a**) or 5.0× (**b**) magnification. Section thickness is 20 µm. The letters a and b refer to the scale bars at the bottom of the figure.

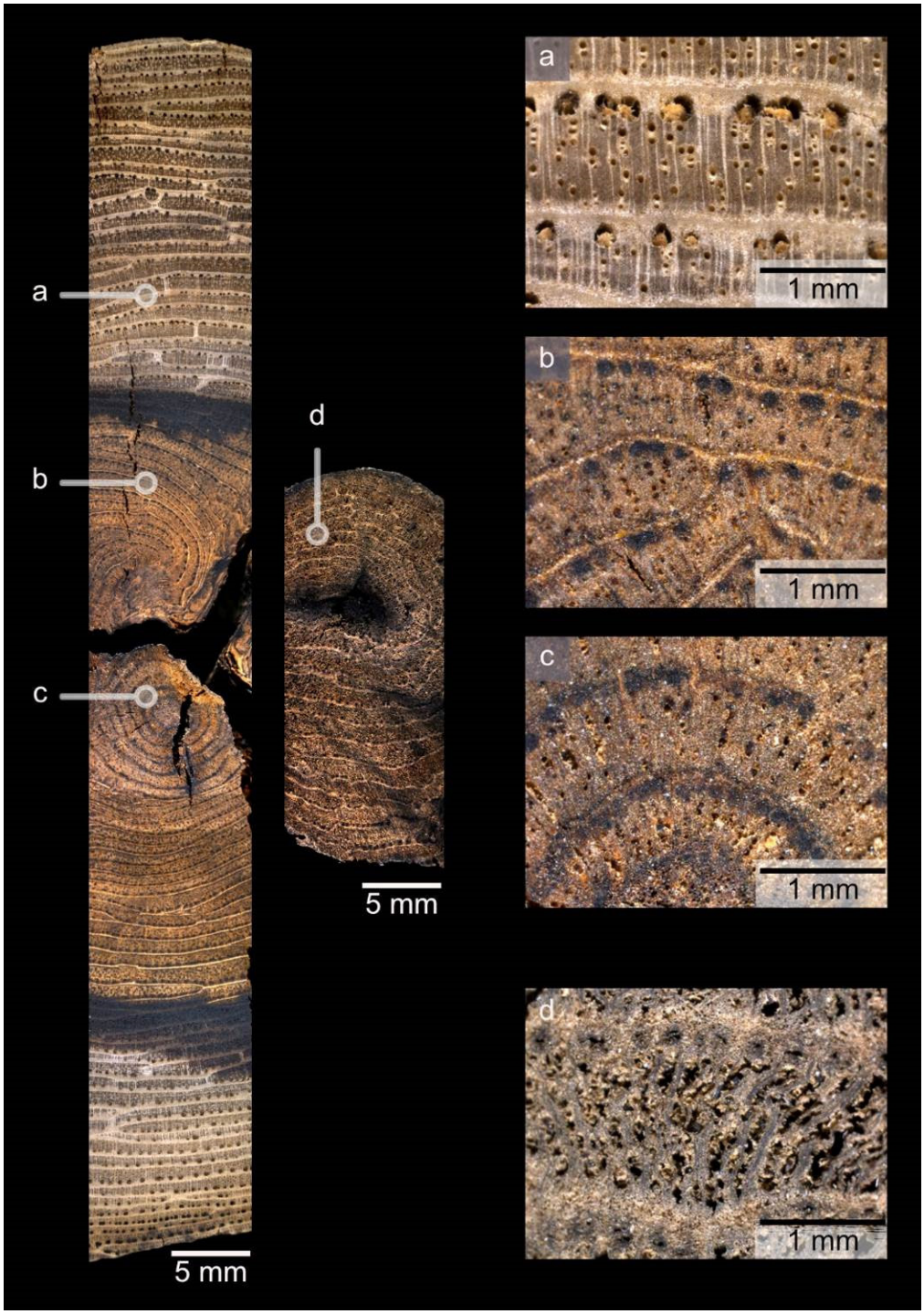

Figure 5. Thick sections in transverse section at 1.0× magnification of recent *Avicennia marina* wood (left) for comparison with the subfossil trench wood (center). The right column shows details of the recent *Avicennia marina* wood (**a**–**c**) and the subfossil trench wood (**d**), all at 5.0× magnification.

4. Discussion

The northeastern Omani coastline has witnessed several tsunamigenic inundations. The relatively recent event in 1945 had a minor effect along the coastline of Oman [14]. Elsewhere, there is weak historical evidence for a tsunami around the year 1008 [34], which is supported by growing geological and sedimentological evidence of a major inundation event at this time: tsunamigenic deposits related to this event are documented in western India [35], as well as along the coastline of Iran [36] and the northern coastline of Oman [37].

Investigations along the east African coast suggest that the 1000-year-old tsunami deposits [38] may have originated from two source areas, the MSZ and the Sumatra-Andaman trench. We exclude the Sumatra-Andaman subduction zone as the source for the Sur deposits, because the tsunami in 2004 affected neither the western Indian coast nor the coastline of Iran. Thus, the source of the tsunamis in 1945 and 1008 AD can be traced back to the MSZ.

Studies by [15,29,39] describe tsunamigenic deposits in the Sur lagoon. Detailed shell taphonomy and the state of shell preservation are indicative of live transport and high energy conditions without subsequent reworking. Our sedimentological investigation of the Sur lagoon deposits is in line with the observations and interpretations made in these earlier studies. Absolute dating of the tsunamigenic layer, which we call L2, could not, however, be carried out, and an attribution to the 1945 tsunami was inferred [15]. The supposed deposition of this layer in 1945 contradicts eyewitness reports that the waves were only about 2 m high and caused only minor effects along the coastline of Oman [14]. We postulate that the bricks in the northern part of the lagoon directly behind the inhabited beach barrier accumulated as a result of the 2-m-high tsunami waves in 1945.

Our dating results challenge the earlier suggestion that the distinct shell layer L2 resulted from the tsunami of 1945. This layer contains a number of woody mangrove axes at its base, incorporated into the 10 to 20 cm-thick unsorted shell deposit. Dating of shell material from L2 remains difficult. Using shells for chronologies is problematic if their association with contemporaneous terrestrial material is not straightforward [40–42]. Mollusks have a reservoir effect and may contain some live endobenthic; this can lead to the incorrect dating of the specific sediment layer. An initial dating approach towards the bivalve shells of L2 in the Sur lagoon supports their association with the tsunami event in 1945, but we regard the dating results of the mollusks as incorrect due to multiple methodological challenges. Instead, we consider the wood to be the most reliable basis for age dating. As mentioned earlier, a sample taken from a woody axis found in association with L2 provides a radiocarbon date of 905–722 cal BP, characterizing the plant remains as subfossil, not modern. The orientation of the woody axes in a north–northeast direction pointing towards the MSZ suggests that this subduction zone is the most likely source area.

Regarding the sedimentological data, layer L2 points to a single tsunami event that was more extreme than the tsunami of 1945. The ^{14}C age of the wood links the tsunamigenic deposits to the event that occurred around 1000 years ago, which is described as severe in historical [34] and geological [36,37] archives. A detailed discussion of the comparison of the impact of the tsunamis in 1945 and around the year 1000 can be found in [43].

As determined by wood anatomy, the meter-long woody axes are the remains of *Avi-cennia* mangroves. They offer insight into the environmental setting and details of the tsunami event that occurred roughly a millennium ago. A lack of roots means the woody axes are allochthonous or parautochthonous. While the subfossil wood can be identified as *Avicennia*, it could not be identified to the species level. However, it is certainly possible that the subfossil woody axes pertain to the species *Avicennia marina*, because this species has been known in northeastern Oman for the past few thousand years [44]. The small diameter of the woody axes, which reach a maximum diameter of 4 cm, is consistent with the size of the shrubby *Avicennia marina* mangrove plants that grow along the northeastern coast of Oman today.

Geological–sedimentological archives and investigations are essential to understanding tsunami dynamics and to developing good risk management and rapid emergency response. Mangrove forests reduce tsunami wave energy significantly. Similar approaches, where interdisciplinary research of geology, sedimentology, and botany prove valuable in reconstructing earthquake potential and tsunamigenic events, are presented by [28,45,46]. Recording mangrove occurrences in the geological record and monitoring them over time can, on one hand, make a major contribution to today's coastal protection and, on the other hand, are a valuable component of environmental reconstruction and possible tsunami risk assessment with regard to archaeological questions. Hence, our understanding of past

mangrove habitats, ancient coastal environments, and geological events is greatly enhanced when sedimentology, paleontology, and botany come together.

5. Conclusions

The tsunamigenic deposit in the Sur lagoon with its 25-cm-thick shell layer is reinterpreted as evidence of an extreme tsunami event that occurred almost 1000 years ago. Woody axes were newly discovered in the context of this layer. Anatomical analyses of this wood identify it as *Avicennia*, which attests to the presence of mangroves in the Sur lagoon one millennium ago. This tsunami event must have been more severe than the tsunami waves observed in AD 1945. A deeper understanding of the age and magnitude of tsunamigenic events will aid in understanding tsunamis generated along the Makran subduction zone. Hazard mitigation measurements along the coastline of the Arabian Sea should be reexamined today within the framework of our reinterpretation.

Supplementary Materials: The following supporting information can be downloaded at: https://www.mdpi.com/article/10.3390/f13060922/s1, Table S1: Dating results of shells and wood from the tsunamigenic layer in a trench in the Sur lagoon.

Author Contributions: Conceptualization, G.H. and V.D.; Methodology, V.D., C.T.G., S.L. and P.J.S.; Validation, G.H., C.T.G., S.L., V.D. and P.J.S.; Formal Analysis, S.L.; Investigation, G.H. and V.D.; Resources, C.T.G., P.J.S. and S.L.; Data Curation, C.T.G.; Writing—Original Draft Preparation, V.D.; Writing—Review and Editing, G.H., C.T.G., S.L. and P.J.S.; Visualization, V.D.; Supervision, G.H. and C.T.G.; Project Administration, G.H.; Funding Acquisition, G.H. All authors have read and agreed to the published version of the manuscript.

Funding: This research was funded by Deutsche Forschungsgemeinschaft, grant number HO2550/15-1. V.D. is grateful for a scholarship from the *Studienstiftung des deutschen Volkes*.

Data Availability Statement: Not applicable.

Acknowledgments: Dülfer, O., Shunn, K. and Lambertz, M. (University of Bonn) are thanked for providing technical assistance and equipment. This paper is a contribution to IGCP projects 639 and 725.

Conflicts of Interest: The authors declare no conflict of interest.

References

1. Costa, P.J.; Andrade, C. Tsunami deposits: Present knowledge and future challenges. *Sedimentology* **2020**, *67*, 1189–1206. [CrossRef]
2. Løvholt, F.; Setiadi, N.J.; Birkmann, J.; Harbitz, C.B.; Bach, C.; Fernando, N.; Kaiser, G.; Nadim, F. Tsunami risk reduction—Are we better prepared today than in 2014. *IJDRR* **2014**, *10*, 127–142.
3. Tanaka, N.; Sasaki, Y.; Mowjood, M.I.M.; Jinadasa, K.B.S.N.; Homchuen, S. Coastal vegetation structures and their functions in tsunami protection: Experience of the recent Indian Ocean tsunami. *Landsc. Ecol. Eng.* **2007**, *3*, 33–45. [CrossRef]
4. Alongi, D.M. Mangrove forests: Resilience, protection from tsunamis, and responses to global climate change. *Estuar. Coast. Shelf Sci.* **2008**, *76*, 1–13. [CrossRef]
5. Lee, S.Y.; Primavera, J.H.; Dahdouh-Guebas, F.; McKee, K.; Bosire, J.O.; Cannicci, S.; Diele, K.; Fromard, F.; Koedam, N.; Marchand, C.; et al. Ecological role and services of tropical mangrove ecosystems: A reassessment. *Glob. Ecol. Biogeogr.* **2014**, *23*, 726–743. [CrossRef]
6. Barbier, E.B. Natural barriers to natural disasters: Replanting mangroves after the tsunami. *Front. Ecol. Environ.* **2006**, *4*, 124–131. [CrossRef]
7. Minoura, K.; Imamura, F.; Sugawara, D.; Kono, Y.; Iwashita, T. The 869 Jogan tsunami deposit and recurrence interval of large-scale tsunami on the Pacific coast of northeast Japan. *J. Nat. Disaster Sci.* **2001**, *23*, 83–88.
8. Barnes, G.L. The search for tsunami evidence in the geological and archaeological records, with a focus on Japan. *Asian Perspect.* **2017**, *56*, 132–165. [CrossRef]
9. Byrne, D.E.; Sykes, L.R.; Davis, D.M. Great thrust earthquakes and aseismic slip along the plate boundary of the Makran subduction zone. *J. Geophys. Res. Solid Earth* **1992**, *97*, 449–478. [CrossRef]
10. DeMets, C.; Gordon, R.G.; Donald, F.A. Geologically current plate motions. *Geophys. J. Int.* **2010**, *181*, 1–80. [CrossRef]
11. Smith, G.L.; McNeill, L.C.; Wang, K.; He, J.; Henstock, T.J. Thermal structure and megathrust seismogenic potential of the Makran subduction zone. *Geophys. Res. Lett.* **2013**, *40*, 1528–1533. [CrossRef]
12. Kopp, C.; Fruehn, J.; Flueh, E.R.; Reichert, C.; Kukowski, N.; Bialas, J.; Klaeschen, D. Structure of the Makran subduction zone from wide-angle and reflection seismic data. *Tectonophysics* **2000**, *329*, 171–191. [CrossRef]

13. Hoffmann, G.; Al-Yahyai, S.; Naeem, G.; Kociok, M.; Grützner, C. An Indian Ocean tsunami triggered remotely by an onshore earthquake in Balochistan. *Geology* **2014**, *42*, 883–886. [CrossRef]
14. Kakar, D.M.; Naeem, G.; Usman, A.; Hasan, H.; Lohdi, H.A.; Srinivasalu, S.; Andrade, V.; Rajendran, C.P.; Beni, A.N.; Hamzeh, M.A.; et al. Elders recall an earlier tsunami on Indian Ocean shores. *Eos Trans. Am. Geophys. Union* **2014**, *95*, 485–486. [CrossRef]
15. Donato, S.V.; Reinhardt, E.G.; Boyce, J.I.; Rothaus, R.; Vosmer, T. Identifying tsunami deposits using bivalve shell taphonomy. *Geology* **2008**, *36*, 199–202. [CrossRef]
16. Lézine, A.M.; Saliège, J.F.; Mathieu, R.; Tagliatela, T.L.; Mery, S.; Charpentier, V.; Cleuziou, S. Mangroves of Oman during the late Holocene; climatic implications and impact on human settlements. *Veg. Hist. Archaeobot.* **2002**, *11*, 221–232. [CrossRef]
17. Decker, V.; Falkenroth, M.; Lindauer, S.; Landgraf, J.; Al-Lawati, Z.; Al-Rahbi, H.; Franz, S.O.; Hoffmann, G. Collapse of Holocene mangrove ecosystems along the coastline of Oman. *Quat. Res.* **2021**, *100*, 52–76. [CrossRef]
18. Lézine, A.M.; Ivory, S.J.; Braconnot, P.; Marti, O. Timing of the southward retreat of the ITCZ at the end of the Holocene Humid Period in Southern Arabia: Data-model comparison. *Quat. Sci. Rev.* **2017**, *164*, 68–76. [CrossRef]
19. Deckers, K.; Döpper, S.; Schmidt, C. Vegetation, land, and wood use at the sites of Bat and Al-Khashbah in Oman (fourth–third millennium BC). *Arab Arch Epig.* **2019**, *30*, 1–14. [CrossRef]
20. Tengberg, M. Les forêts de la mer. Exploitation et évolution des mangroves en Arabie orientale du Néolithique à l'époque islamique. *Paléorient* **2005**, *31*, 39–45. [CrossRef]
21. Cleuziou, S.; Tosi, M. The great transformation. In *In the Shadow of the Ancestors*; Cleuziou, S., Tosi, M., Eds.; Al Nahda Printing Press: Muscat, Oman, 2007; pp. 61–97.
22. Robert, E.M.; Koedam, N.; Beeckman, H.; Schmitz, N. A safe hydraulic architecture as wood anatomical explanation for the difference in distribution of the mangroves *Avicennia* and *Rhizophora*. *Funct. Ecol.* **2009**, *23*, 649–657. [CrossRef]
23. De Deurwaerder, H. How are Anatomical and Hydraulic Features of *Avicennia marina* and *Rhizophora mucronata* Trees Influenced by Siltation? Master's Thesis, University of Ghent, Brussels, Belgium, 2012.
24. Tomlinson, P.B. *The Botany of Mangroves*, 2nd ed.; Cambridge University Press: New York, NY, USA, 2016; p. 432.
25. Milani, A.S. Mangrove forests of the Persian Gulf and the Gulf of Oman. In *Threats to Mangrove Forests: Hazards, Vulnerability, and Risk Management*; Makowski, C., Finkl, C.W., Eds.; Springer: Cham, Germany, 2018; pp. 53–75.
26. Le Roux, J.P.; Vargas, G. Hydraulic behavior of tsunami backflows: Insights from their modern and ancient deposits. *Environ. Geol.* **2005**, *49*, 65. [CrossRef]
27. Dawson, A.G.; Stewart, I. Tsunami deposits in the geological record. *Sediment. Geol.* **2007**, *200*, 166–183. [CrossRef]
28. Rhodes, B.P.; Kirby, M.E.; Jankaew, K.; Choowong, M. Evidence for a mid-Holocene tsunami deposit along the Andaman coast of Thailand preserved in a mangrove environment. *Mar. Geol.* **2011**, *282*, 255–267. [CrossRef]
29. Pilarczyk, J.E.; Reinhardt, E.G.; Boyce, J.I.; Schwarcz, H.P.; Donato, S.V. Assessing surficial foraminiferal distributions as an overwash indicator in Sur Lagoon, Sultanate of Oman. *Mar. Micropaleontol.* **2011**, *80*, 62–73. [CrossRef]
30. Riedelsheimer, B.; Büchl-Zimmermann, S.; Welsch, U. Schnittpräparation für die Lichtmikroskopie. In *Romeis—Mikroskopische Technik*, 19th ed.; Mulisch, M., Welsch, U., Eds.; Springer: Berlin/Heidelberg, Germany, 2015; pp. 99–120.
31. Jagiella, C.; Kürschner, H. *Atlas der Hölzer Saudi Arabiens. Die Holzanatomie der Wichtigsten Bäume und Sträucher Arabiens mit Einem Holzanatomischen Bestimmungsschlüssel*; Beihefte zum TAVO; Ludwig Reichert: Wiesbaden, Germany, 1987; Volume 20, p. 176.
32. Reimer, P.J.; Bard, E.; Bayliss, A.; Beck, J.W.; Blackwell, P.G.; Ramsey, C.B.; Buck, C.E.; Buck, C.E.; Cheng, H.; Edwards, R.L.; et al. IntCal13 and Marine13 Radiocarbon Age Calibration Curves 0–50,000 Years cal BP. *Radiocarbon* **2013**, *55*, 1869–1887. [CrossRef]
33. Schmitz, N.; Verheyden, A.; Kairo, J.G.; Beeckman, H.; Koedam, N. Successive cambia development in *Avicennia marina* (Forskk.) Vierh. is not climatically driven in the seasonal climate at Gazi Bay, Kenya. *Dendrochronologia* **2007**, *25*, 87–96. [CrossRef]
34. Ambraseys, N.N.; Melville, C.P. *A History of Persian Earthquakes*; Cambridge University Press: Cambridge, UK, 1982; p. 219.
35. Prizomwala, S.P.; Gandhi, D.; Bhatt, N.; Winkler, W.; Kumar, M.R.; Makwana, N.; Bhatt, N. Geological evidence for AD 1008 tsunami along the Kachchh coast, Western India: Implications for hazard along the Makran Subduction Zone. *Sci. Rep.* **2018**, *8*, 16816. [CrossRef] [PubMed]
36. Shah-hosseini, M.; Morhange, C.; Beni, A.N.; Marriner, N.; Lahijani, H.; Hamzeh, M.; Sabatier, F. Coastal boulders as evidence for high-energy waves on the Iranian coast of Makran. *Mar. Geol.* **2011**, *290*, 17–28. [CrossRef]
37. Hoffmann, G.; Grützner, C.; Schneider, B.; Preusser, F.; Reicherter, K. Large Holocene tsunamis in the northern Arabian Sea. *Mar. Geol.* **2020**, *419*, 106068. [CrossRef]
38. Maselli, V.; Oppo, D.; Moore, A.L.; Gusman, A.R.; Mtelela, C.; Iacopini, D.; Taviani, M.; Mjema, E.; Mulaya, E.; Che, M.; et al. A 1000-yr-old tsunami in the Indian Ocean points to greater risk for East Africa. *Geology* **2020**, *48*, 808–813. [CrossRef]
39. Donato, S.V.; Reinhardt, E.G.; Boyce, J.I.; Pilarczyk, J.E.; Jupp, B.P. Particle-size distribution of inferred tsunami deposits in Sur Lagoon, Sultanate of Oman. *Mar. Geol.* **2009**, *257*, 54–64. [CrossRef]
40. Bezerra, F.H.R.; Vita-Finzi, C.; Lima-Filho, F.P. The use of marine shells for radiocarbon dating of coastal deposits. *Rev. Bras. Geociências* **2000**, *30*, 211–213. [CrossRef]
41. Culleton, B.J.; Kennett, D.J.; Ingram, B.L.; Erlandson, J.M.; Southon, J.R. Intrashell radiocarbon variability in marine mollusks. *Radiocarbon* **2006**, *48*, 387–400. [CrossRef]
42. Gillespie, R.; Polach, H.A. The suitability of marine shells for radiocarbon dating of Australian prehistory. In *Radiocarbon Dating*; Berger, R., Suess, H.E., Eds.; University of California Press: Berkeley, CA, USA, 2020; pp. 404–421.

43. Hoffmann, G.; Rupprechter, M.; Al Balishi, N.; Grützner, C.; Reicherter, K. The impact of the 1945 Makran tsunami along the coastlines of the Arabian Sea (Northern Indian Ocean)—A review. *Z. Für Geomorphol.* **2013**, *57* (Suppl. 4), 257–277. [CrossRef]
44. Lézine, A.M. Timing of vegetation changes at the end of the Holocene Humid Period in desert areas at the northern edge of the Atlantic and Indian monsoon systems. *Comptes Rendus Geosci.* **2009**, *341*, 750–759. [CrossRef]
45. Cisternas, M.; Atwater, B.F.; Torrejon, F.; Sawai, Y.; Machuca, G.; Lagos, M.; Eipert, A.; Youlton, C.; Salgado, I.; Kamataki, T.; et al. Predecessors of the giant 1960 Chile earthquake. *Nature* **2005**, *437*, 404–407. [CrossRef]
46. Monecke, K.; Finger, W.; Klarer, D.; Kongko, W.; McAdoo, B.G.; Moore, A.L.; Sudrajat, S.U. A 1000-year sediment record of tsunami recurrence in northern Sumatra. *Nature* **2008**, *455*, 1232–1234. [CrossRef]

5.3 Sedimentological evidence of Late Pleistocene Shorelines in Oman (Decker et al. 2024)

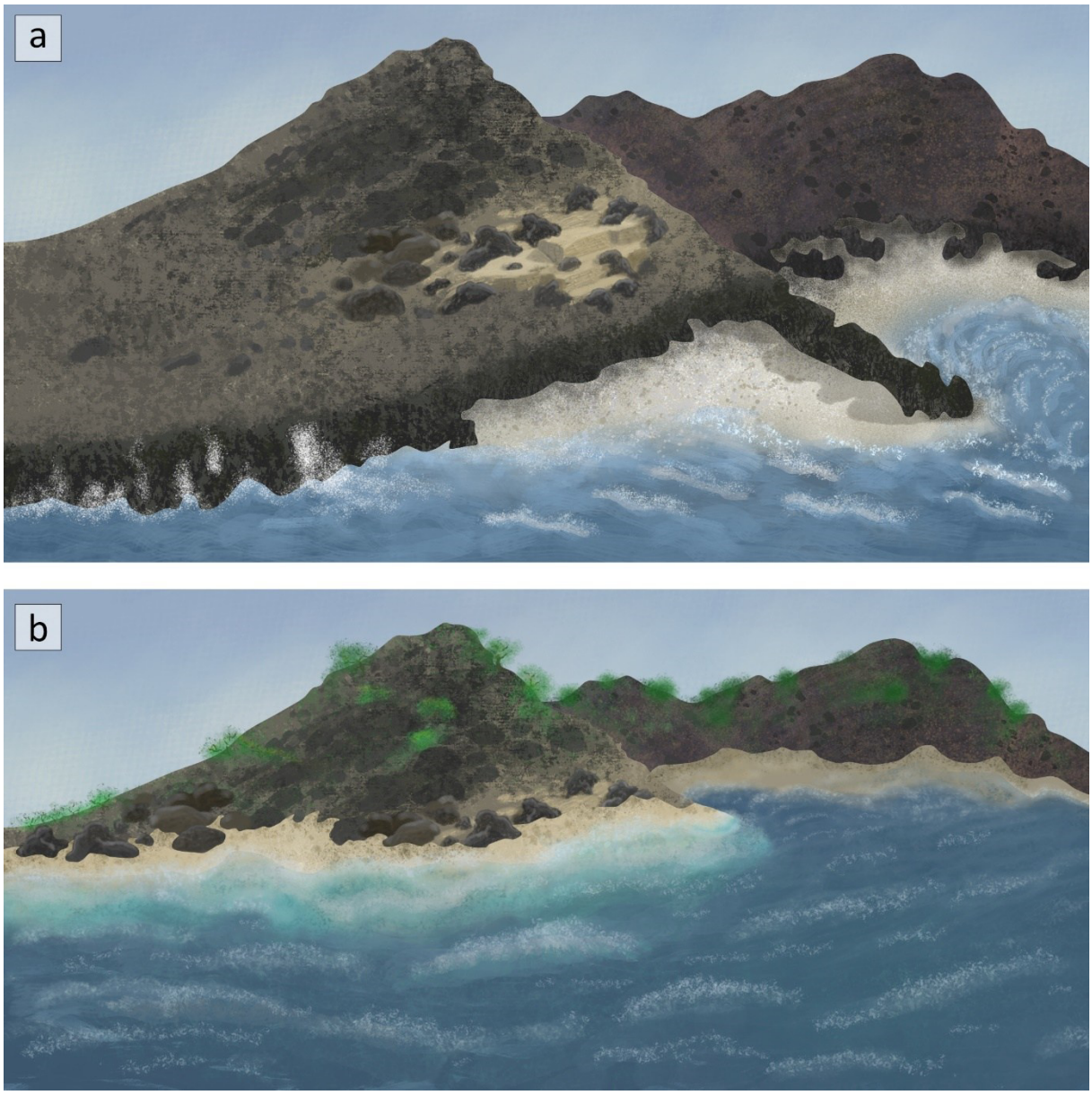

Fig. 5: Shoreline of Ras Madraka: (a) present-day view with light beige paleo-beach deposits; (b) ca. 125,000 years ago during the Last Interglacial, when global mean sea level was 3–4 m higher than today, likely also at this site, leaving beach deposits in the upper rock wall that are preserved today as paleo-beach rock.

Marine Geology 477 (2024) 107407

Contents lists available at ScienceDirect

Marine Geology

journal homepage: www.elsevier.com/locate/margo

Research Article

Sedimentological evidence of Late Pleistocene Shorelines in Oman

V. Decker [a,*], M. Falkenroth [b], G. Hoffmann [a,c]

[a] RWTH Aachen University, 52056 Aachen, Germany
[b] TU Darmstadt, 64287 Darmstadt, Germany
[c] German Commission for UNESCO, Global Geoparks Unit, 53175 Bonn, Germany

ARTICLE INFO

Editor: Edward Anthony

Keywords:
Last interglacial shorelines
Sea-level change
Beach processes
Foraminifera
Oman
Indian Ocean

ABSTRACT

As the climate crisis intensifies, estimating sea-level rise will become increasingly relevant, in particular assessing changes in the relative sea level in different regions. One key to comprehending global sea-level changes is the study of past sea-level highstands. Many regional studies help refine the reconstruction of paleo sea levels globally. Thus far, the Middle East remains understudied.

This paper presents evidence for Quaternary sea-level variations along the shores of the western Indian Ocean. Eight coastal outcrops along the northern and eastern coasts of Oman are presented in detail. The sedimentological evidence for sea-level highstands varies within the study area. However, in relation to recent sea-level conditions, all of these marine and beach deposits are now found well above the environments where such formations would typically form. Dating the timing of sea-level highstands remains a challenging task within the study area. In different studies, attempts to ^{14}C date samples from that area were unsuccessful, as the time of sediment deposition lies beyond the dating limit of ^{14}C, precluding a Holocene formation of these sediments. Thus, the sediments are regarded as deposits formed during Pleistocene sea-level highstands, presumably during MIS 5e. For some sections, optically stimulated luminescence dating could provide a solution, as igneous source rocks supply quartz and feldspar. This paper aims to localise eight sea-level related outcrops along the Omani coast and depict their potential for future work, which should include dating and elevation measurements. Through this, our work contributes to the ongoing effort to globally identify records of sea-level changes, as well as providing insights into the regional setting in Oman.

1. Introduction

Coastal zones have always been attractive for humans to settle (Erlandson, 2017; Small and Nicholls, 2003). This is due to the accessibility to freshwater and seafood, as well as the advantages for trade routes and eventually their attractiveness as sites for industries. Today, 75 % of the megacities are located directly at the coast (Bange et al., 2017). Concurrently, these areas are facing mounting challenges, chiefly due to the anthropogenic climate change causing global sea levels to rise at an unprecedented pace compared to the late Holocene (IPCC, 2023; Haigh et al., 2014; McGranahan et al., 2007). This is particularly relevant in that human societies evolved during a period of relative climate stability, where sea levels remained comparatively stable for an extended period (Steffen and Wu, 2011). A sea-level rise of 3.6 mm per year was observed during the period 1993–2015 (Oppenheimer et al., 2019) which threatens millions of people and leads to huge logistical challenges regarding humanitarian and economic aspects.

The study of Quaternary sea-level fluctuations is crucial for understanding the impact of recent sea-level changes. The main mechanisms behind Quaternary eustatic sea-level variations, which depict the global oscillations, are driven by changes in Earth's orbit, which affect insolation, leading to glaciation and melting of terrestrial-based ice masses (e.g., Rovere et al., 2016a, 2016b; Paillard, 2010; Church et al., 2001; Imbrie et al., 1984; Imbrie and Imbrie, 1980; Milankovitch, 1941). One important factor related to Quaternary sea-level changes is Glacial Isostatic Adjustment (GIA) (Peltier, 1999). This describes the post-glacial rebound of the Earth's crust when the ice mass on top of it is reduced, as well as all other associated processes (Li et al., 2023; Spada, 2017). The GIA affects sea levels worldwide (Mitrovica and Milne, 2002; Mitrovica and Peltier, 1991), even well beyond the time after glaciers have melted (Spada, 2017). The spatio-temporal variability of the mantle's response to deglaciation processes varies significantly and non-overlapping sea-level highstands may belong to a single deglaciation process. Therefore, it is advisable to consider site-specific signals of

* Corresponding author.
E-mail address: valeska.decker@rwth-aachen.de (V. Decker).

https://doi.org/10.1016/j.margeo.2024.107407
Received 9 January 2024; Received in revised form 22 September 2024; Accepted 27 September 2024
Available online 30 September 2024
0025-3227/© 2024 The Authors. Published by Elsevier B.V. This is an open access article under the CC BY license (http://creativecommons.org/licenses/by/4.0/).

relative sea level (rsl) (Lambeck et al., 2002).

In addition to these global processes, regional factors such as subsidence and uplift, sediment influx and compaction also apply. Thus, the site-specific rsl is the one that provides a real, measurable sea-level elevation at a specific location (Rovere et al., 2016b).

Past interglacial periods are highly relevant, as they enable the study of climate systems and sea-level conditions during times as warm as or slightly warmer than today (Rohling et al., 2019; Rovere et al., 2016a; Pedoja et al., 2014). The study of Pleistocene shorelines is essential to understand the fundamental processes in coastal geomorphology and coastal groundwater dynamics related to sea-level rise. The Last Interglacial (Marine Isotope Stage (MIS) 5e; 129–116 ka,e.g., Barlow et al. (2018), is of particular interest as it is one of the closest climatic analogues to the Holocene. During this period, the global mean surface temperature was 0.5–1.0 °C warmer as well as the global mean sea level (msl) was higher than today (Oppenheimer et al., 2019). How much higher it was is still under debate. Recent studies have reached a consensus of a MIS 5e sea level peaking around 1–5 m higher than present mean sea level (pmsl) (Dumitru et al., 2023; Dyer et al., 2021), whereas previous studies reconstructed sea-level highstands of up to 9 m during MIS 5e (e.g. Dutton and Lambeck, 2012). Insights from the study of sea-level variability during this period hold the potential to significantly enhance our understanding of future changes (Deiana et al., 2021). However, paleo-shorelines are the result of the interaction between eustatic changes and local isostatic, neotectonic and erosional processes (e.g. De Santis et al., 2023; Cerrone et al., 2021a, 2021b; Chauveau et al., 2021; De Giosa et al., 2019; Milne and Mitrovica, 2008; Lajoie, 1986). Local studies addressing the interaction of these forcings and processes provide a better understanding of coastal stratigraphies and rsl changes (e.g. Chauveau et al., 2024a; Pedoja et al., 2014).

The Middle East is of particular interest for past sea-level reconstructions because this area is located at a certain distance to the Pleistocene iceshields: it lies between the so-called near-field and far-field locations (Yokoyama and Purcell, 2021), where near-field locations are in direct proximity to the limits of Pleistocene ice sheets. However, in order to understand and model the glacio-hydro-isostatic adjustment, sea-level studies in far-field locations and intermediate areas are needed (Milne, 2009). Despite recent research efforts along the coastline of Oman (Hoffmann et al., 2020a; Ermertz et al., 2019; Falkenroth et al., 2019; Moraetis et al., 2018), little is known about the remains of past interglacial shorelines along the Indian Ocean's coastline of the Arabian Peninsula (Rovere et al., 2023). Thus, the broader picture remains elusive. This is in part due to a lack of suitable sea-level archives. Consequently, research on Arabian paleo sea level is challenging and often relies only on geomorphological evidence and limited outcrops that show marine or beach deposits. In addition to these challenges, the use of sea-level index points following the guidelines of Hijma et al. (2015) is outstanding in this region. These index points serve as crucial reference markers for reconstructing past sea levels and understanding the region's geological history. The guidelines provide a protocol for standardized field survey and sample investigation to create a sea-level database. The main advantage of these guidelines is the comparability with other findings worldwide and throughout different timescales (Hijma et al., 2015).

Another compelling incentive for studying sea-level changes lies in their relevance to archaeological issues. Potential migration routes of early human populations can be reconstructed based on ancient coastline configurations (Petraglia et al., 2015; Rose et al., 2011).

Here, we present sedimentological evidence for a significant sea-level highstand, most likely related to the Last Interglacial period along the coastline of Oman. The focus of this paper is the identification and documentation of locations in Oman where Pleistocene sea-level can be studied. This work can, therefore, provide a basis for future studies and modelling work.

2. Study area

2.1. Regional setting

Oman is situated in the eastern part of the Arabian Peninsula, with its coastline bordered by the Gulf of Oman to the north and the Arabian Sea to the east, both of which are part of the Indian Ocean (Fig. 1). Along its entire coastline, there is a narrow continental shelf, leading to a seamless

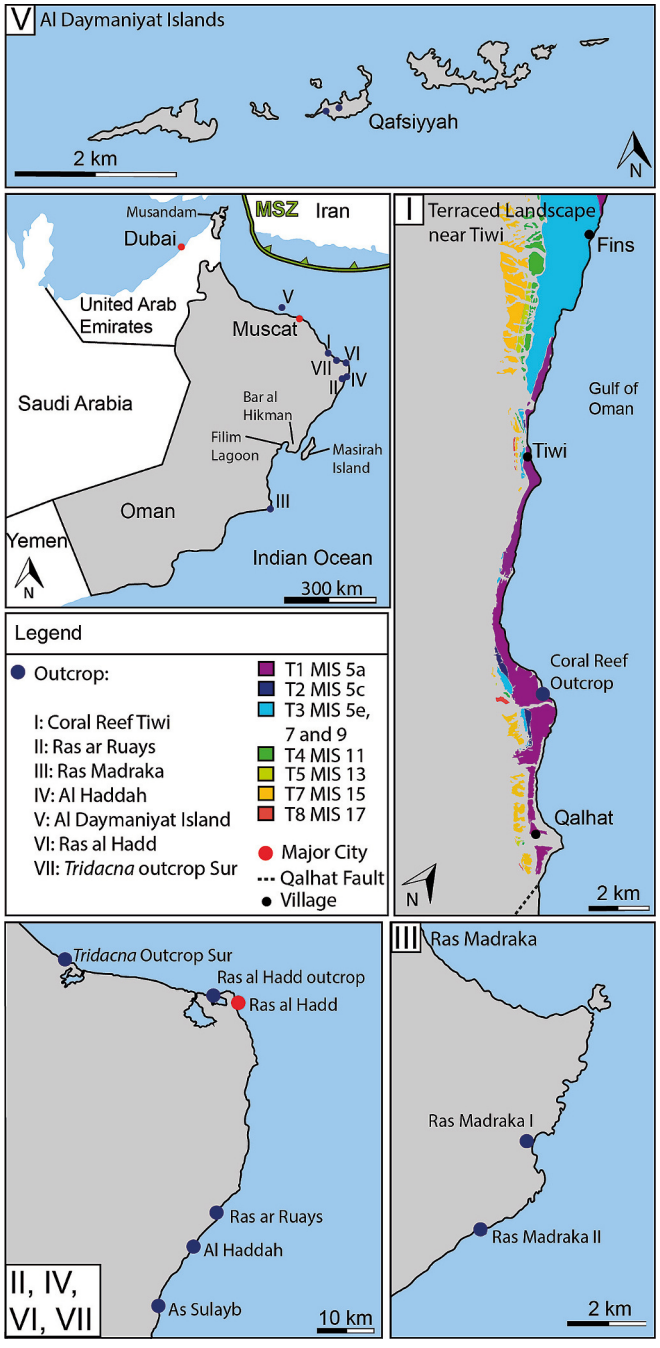

Fig. 1. Overview map of the study area in Oman. Major cities in this region are marked with a red dot, all eight outcrops with a blue dot. The upper map displays the location of outcrop V, Qafsiyya within the Daymaniyat Islands. The right map indicates the location of the coral reef near Tiwi and highlights the outcrop's position within the colourful marked marine terraces setting, which range in this section from ca. 15 m above pmsl (T1, purple) to ca. 250 m above pmsl (T8, orange). (For interpretation of the references to colour in this figure legend, the reader is referred to the web version of this article.)

transition from the shoreline to the deep sea. The Omani coastline, including the Musandam enclave and Masirah Island, spans over 2300 km. Approximately 1200 km of Oman's coastline consists of sandy beaches (McLachlan et al., 1998), while some tidal flats can be found in sheltered lagoons, such as in Sur, or in embayments, like the area west of Bar al Hikman (Fig. 1). These low-energy environments alternate with rocky shores, including steep cliffs in the northern region, such as those north of Ras ar Ru'ays. The entire eastern coast is exposed to the Indian Ocean with a mean swell of 0.4–0.8 m, however, with a frequency of less than 10 % waves can reach heights of up to 2 m (Sana et al., 2023). The study area is situated along the northern and eastern coastlines of Oman. The tide regime is mesotidal, with spring tides reaching up to 3 m in height. Wave energies are generally low to moderate (McLachlan et al., 1998) with mean wave heights of 0–0.8 m for this coast (Sana et al., 2023).

The northern Omani coast is dominated by the alluvial plain of the Hajar Mountains. The coastline here is flat and experiences mostly low wave energy due to the relatively narrow Gulf of Oman. However, despite its low energy, this coast is susceptible to tsunamis and has been impacted by several tsunami events over time: A severe tsunami hit the coastline ~1000 years ago (Decker et al., 2022; Hoffmann et al., 2020b) and several smaller tsunami waves reached the Omani coast in recent history. Most notably are the ones 1945, 2010 and 2013 with wave heights of less than 3 m (Hoffmann et al., 2013). This tsunamigenic potential is attributed to activities in the Makran Subduction Zone (MSZ), which runs semi-parallel to the coast northeast of Oman (Kukowski et al., 2000). Tsunamis can also be triggered or exacerbated by submarine slides within the Gulf of Oman (Heidarzadeh and Satake, 2017; Hoffmann et al., 2013).

The distal parts of the large alluvial fans that stretch along the northern coast are composed of sediments originating from the massive mountain chain located 30 km to the south. The Hajar Mountains consist mainly of highly karstified limestone, reaching heights of up to 3000 m and spanning over 600 km from Musandam in the northwest to Ras al Hadd in the east. Eastward, the alluvial fans disappear and autochthonous Eocene limestone forms the coastal area. Near Fins and Tiwi, wave-cut platforms are carved into this limestone (Fig. 1-I). Nine marine terraces were extensively described by Hoffmann et al. (2020a) who postulate that each terrace represents a Pleistocene sea-level highstand, ranging from MIS 5a to MIS 19 (82 to 790 ka). The various levels illustrate uplift in this area with different uplift rates varying in space and time from near zero in the northern part up to 0.85 mm per year in the southeast part of the marine staircase (Hoffmann et al., 2020a). This distinctive landform terminates to the southeast with the Qalhat fault, near Sur (Fig. 1I) (Ermertz et al., 2019). Several mangrove-fringed lagoons can be found between Sur and Ras al Hadd. Heading southward, the shoreline is predominantly characterized by semi-consolidated and active dunes as well as sabkha environments, characterized by their shallow basins without surface drainage meaning that they become temporarily water-filled after heavy rainfalls or spring tides (Al-Farraj, 2005). This shift in the environment is a result of a different geomorphological setting without uplift and without the direct influence of erosional processes and gravel deposits of the Hajar Mountains on one hand (Béchennec et al., 1993). On the other hand, a different rain pattern with fewer wet air masses lead to a more arid climate along the east coast (Enzel et al., 2015). Overall, Oman experiences a semi-arid to arid climate (Kwarteng et al., 2009). Due to steep slopes, limited soil, and sparse vegetation, rainfall often leads to significant surface runoff resulting in wadi flash floods with severe impact on human society as well as the environment (Saber et al., 2022). The rain shadow area to the south of the Hajar mountain chain is characterized by sand desert environments. Quaternary climate changes in the region have been reconstructed using various proxies (Decker et al., 2021; Engel et al., 2017; Enzel et al., 2015, Enzel et al., 2017; Lézine et al., 2002, 2017; Burns et al., 2001).

2.2. Regional Quaternary sea-level studies

Evidence of Quaternary sea-level fluctuations has been established in Saudi Arabia by Dullo (1990). He investigated terraces all along the Saudi Arabian coastline focussing on paleo reef facies. Three reef units were detected forming these steps and they were sampled for dating. U/Th-dating clustered ages of 86–118 ka for the lower reef unit and approximately 205 ka for the middle one which Dullo (1990) associates with sea-level highstands. The dating of the upper reef unit failed; the age is assumed to be 290–340 ka which correlates with the preceding sea-level highstand. The elevations of the terraces associated with the youngest reef unit vary significantly along the coast with 1.5–12 m above pmsl and up to 20 m pmsl in the Gulf of Aqaba in the north. The terraces belonging to the middle unit reach 26–57 above pmsl. As the tectonic setting remains unclear and quantitative uplift rates are missing, this work shows sea-level fluctuation evidence but lacks information for a quantitative analysis.

At the coasts of the Gulf of Suez, 125 ka old coral terraces at ~10 m elevation above pmsl indicate a sea-level highstand within the Last Interglacial (Bosworth and Taviani, 1996). Parker et al. (2012) pin two marine terraces at elevations of 0.5 to 8 m above pmsl at the coastline of the Sinai Peninsula, in the northern Red Sea, to MIS 5 (77–129 ka). Other evidence of former sea-level highstands is preserved in the form of emerged marine terraces documented along the Makran coast of Iran and Pakistan (Normand et al., 2019; Reyss et al., 1999; Harrison, 1941). These terraces stretch along the entire Iranian and Pakistani coastline of the Gulf of Oman. According to these investigations, the Makran terraces mainly formed during MIS 3, 5 and 7 and are found at elevations of ca. 5 to 70 m above pmsl. Some undated marine terraces can be found at elevations of up to ca. 160 m above pmsl and were linked to previous highstands up to MIS 17 by Normand et al. (2019). For this coast, they postulate uplift rates varying approximately from 0.05 to 1.2 mm per year (Normand et al., 2019).

Research on Oman's coasts (Hoffmann et al., 2020a) detected a similar morphological setting of marine terraces near Fins and Tiwi at the north eastern coast. These uplifted terraces were assigned to MIS 5, 7, 9, 11, 13, 15, 17 and 19 based on an age model with cosmogenic nuclide (^{10}Be ^{36}Cl) and OSL dating (Hoffmann et al., 2020a). Potential MIS 5e sea-level proxies in Oman, United Arab Emirates, Qatar and Iran are described by Falkenroth et al. (2019, 2020), Williams and Walkden (2002), Oveisi et al. (2007) and Pirazzoli et al. (2004).

Though indicating a relative sea-level highstand, uplifted marine terraces are not suitable for paleo sea-level reconstruction as uncertain uplift rates may lead to miscalculations in reconstructing sea-level elevations. Instead, paleo marine deposits in tectonically stable areas are of high value to refine the amplitude of sea-level oscillations (Pirazzoli, 1993). Tectonic stability is postulated for the study area east of the marine terraces block which is separated by the Qalhat fault (Fig. 1I) from the area around Sur (Falkenroth et al., 2020) and the northern part of the east coast (Decker et al., 2021; Hoffmann et al., 2013). Near Sur, Falkenroth et al. (2020) describe coastal notches with apexes at an elevation of 3.93 ± 0.12 m above pmsl. The elevation was measured using a Differential Global Positioning System (DGPS) and the pmsl was used as a reference point. The age model combines a maximum age that is the age of a fanglomerate that formed before the formation of the notches and a minimum age which is the age of a nearby beachrock. Cosmogenic radionuclide ^{10}Be dating on fanglomerate quartz pebbles reveals a maximum age for the notch of 371 ± 38 ka and a previously published OSL dating on quartz grains in a nearby beachrock reveals a minimum age of 80 ± 3 ka (Mauz et al., 2015). Falkenroth et al. (2020) associate the formation of the notches around Sur to the Last Interglacial and postulate a sea-level highstand of 3.93 ± 0.12 m during MIS 5e.

Holocene sea-level research activities are more widespread due to the higher preservation potential and interdisciplinary interest, as archaeological research for example addresses broad scientific issues like landscape evolution and paleoshorelines to identify migration or

trade routes (Berger et al., 2013). In Oman, some studies (Berger et al., 2020; Berger et al., 2013; Preusser et al., 2005; Lézine et al., 2002) document records like paleolake and paleolagoonal sediments of a potential Mid- or Late-Holocene sea-level highstand, however, the assumed sea-level elevations are highly inconsistent. Berger et al. (2013) postulate a sea-level of up to 9 m above pmsl ca. 7 ka BP, 2–3 m of which are assigned to an eustatic highstand and 2–3 m of post-sedimentary effects, namely tectonic uplift. Lézine et al. (2002) postulate a 'slight seawater incursion' around 5 ka BP. Contradictorily, investigations on paleo mangrove sediments by Decker et al. (2021) precludes a Holocene sea-level highstand and finds the region to be tectonically stable, which is supported by a study on paleo coastal notches in Sur (Falkenroth et al., 2020).

3. Methods

3.1. Fieldwork and sedimentological investigation

Fieldwork was conducted in 2021, 2022 and in 2023. Eight coastal outcrops were investigated along the north and east coast of Oman (Fig. 1, Table 1). The locations are presented as meters within the Universal Transverse Mercator (UTM) projection, Zone 40Q using the WGS 1984 reference ellipsoid.

For the sedimentological facies analysis, all eight outcrops are described including grain size, sedimentological textures, structures, ichnology and fossil content of the observed layers. The indicated heights of the specific layers were determined by using a measuring tape, we defined the base of a profile as zero. The layers are then grouped into lithofacies based on their sedimentological properties. Facies associations are defined by lithofacies and facies architecture as well as stratigraphical relationship. Each outcrop is interpreted regarding its depositional realm taking also microfossil data into account.

3.2. Microfossil analysis

Two samples (S1 and S2) from Ras ar Ru'ays were collected for microfossil analysis. The two lowermost layers of the profile seemed especially suitable for microfossil analysis as their clay to silt grain size provides good preservation potential. To loosen the cemented sediments, they were washed and then dried in an oven at 50 °C. Material smaller than 0.063 mm was removed by wet sieving. Afterwards, the foraminifera were extracted by using a microscope.

Quantity, species assemblage, biodiversity and relative abundance of the three different foraminiferid test types are indicative for specific environmental conditions (Murray, 1991; Brasier, 1980). Eutrophic conditions and biodiversity are determined by the relationship of quantity and number of species, this is displayed in the Fisher-α-index. The Shannon-Weaver-index (*H*) is a measure for species diversity within a given ecosystem. It is calculated by the total amount of each species, the proportion each species is out of the sum of specimen, and sums the proportion multiplied by the natural log of that proportion. The Shannon-Weaver index provides a single value that reflects both the number of different species present (species richness) and their relative abundances (species evenness) within the ecosystem. Higher values of the index indicate greater species diversity, while lower values indicate lower diversity. It is a useful tool in ecology and conservation biology for comparing the diversity of different ecosystems and assessing the impact of environmental changes on biodiversity. Our interpretation of environmental conditions is based on the relation of the Fisher-α- and the Shannon-Weaver-indices. The different foraminiferid test types are presented in a ternary diagram. The distributional patterns can already be indicative for different milieus (Murray, 1991). Thus, foraminiferal analyses are appropriate to estimate subjects like environmental setting, salinity and wave energy and can help to complete the sedimentological description.

4. Observations and interpretation

Along the northeastern coastline of Oman, between Muscat in the north and Ras Madraka in the south (Fig. 1), a number of outcrops reveal marine facies occurring at elevations of approximately 1–18 m above pmsl. For a summary of all outcrops described in this study with locations, observed lithofacies and samples see Table 1. Additional data related to this article can be found at (https://data.mendeley.com/datasets/6yx52x7cvv/1), an open source online data repository hosted at Mendeley Data (Decker et al., 2024).

4.1. Outcrop I: Profile fossil coral reef in Tiwi

A roughly 300 m wide and 10 to 15 m high coastal cliff section 5 km south of the village Tiwi (Fig. 1) exposes fossil coral reefs. The modern beach at the foot of the cliff is a gravel beach with a steep profile, a high berm and no considerable backbeach. The cliff itself consists of two

Table 1
General overview of all described outcrops in this paper including name, their location with different coordinate systems, findings and sample site where applicable.

		location (WGS84)								
		Decimal degrees		Degree/Min/Sec		UTM-Coordinates				
	Name Outcrop	Latitude (°N)	Longitude (°E)	Latitude (N)	Longitude (E)	Z	E	N	Observed lithofacies	Samples
1	Coral-Outcrop Tiwi	22.751618	59.328755	22°45′5.8248"	59°19′43.518"	40Q	739135.258	2517904.534	Coral reef/debris flow deposits	Thin sections 30 cm + 160 cm: forams
2	Profile Ras ar Ru'ays	22.181339	59.768410	22°8′31.6644"	59°39′20.7432"	40Q	773926.700	2450952.744	Tidal flat facies and fluvial deposits	
3	Profile Ras Madraka I	18.9823096	57.8098511	18°58′56.31456"	57°48′35.46396"	40Q	585247.998	2099066.029	Paleobeach	
4	Profile Ras Madraka II	18.969326	57.787767	18°58′09.5736"	57°47′15.9612"	40Q	582929.647	2097618.775	Paleobeach	
5	Profile Al Haddah	22.133500	59.728417	22°08′00.6"	59°43′42.3"	40Q	781441.845	2450129.720	Marine facies with *Crassostrea*	
6	Daymaniyat Island Qafsiyyah	23.855013	58.085087	23°51′18.0468"	58°5′6.3132"	40Q	610493.135	2638597.785	Beachrock with bioturbation and cross bedding	
7	Profile Ras al Hadd	22.531255	59.760664	22°31′52.518"	59°45′38.3904"	40Q	783962.656	2494254.145	Beachrock with bioturbation	
8	*Tridacna*-outcrop Sur	22.5878170	59.5081819	22°35′16.1412"	59°30′29.45484"	40Q	757874.593	2500061.349	Fossil coral reef with *Tridacna*	

easily distinguished lithofacies that alternate one another in two cycles (Fig. 2). The reef facies is a poorly consolidated carbonate sand (facies OT1). The other facies are massive boulder fanglomerates. Due to differences in the facies' ability to withstand erosion, an up to 4 m deep overhang has developed at parts of the cliff section (facies OT2). The cliff is the seaward edge of a coastal terrace that was described in detail by Hoffmann et al. (2020a). The authors have allocated the formation of the terrace surface to a sea-level highstand at MIS 5a according to an age model developed by cosmogenic nuclide and optically luminescence dating.

4.1.1. Sedimentology

Facies OT1 contains two layers of a white fine to medium gravelly sandstone that are interbedded with facies OT2. The layers stretch over the entire cliff and show no considerable variation in thickness (Fig. 2, upper part). Their surface is smoothened by erosion and displays a yellow weathering colour. The material is partially carbonate cemented. The sandstone is moderately sorted. Larger clasts, granules to cobbles, concentrate in lenses that display a shallow NW dip. All rock fragments are subrounded to well rounded, while fossils are mostly angular. Fossil debris content is high, consisting of broken gastropod and bivalve shells, sea urchins and corals. Embedded within the sandstone are in situ patch reefs and solitary corals (Fig. 2; Fig. 3 a). All corals belong to a single species within the genus *Porites* (Lars Reuning, University of Kiel, personal communication). One coral stock reaches a size of up to 1.2 m across. The individual corals are superimposed on one another and stretch over the entire thickness of the sandstone layers (up to 3 m). The material in between coral branches is poorly cemented white fine sand to silt (Fig. 3 c). It contains small, elongated, black components with uncertain origin. The material is coarsening upwards. The uppermost 0.4 to 0.5 m are enriched in echinoderm shells, coral fragments and other carbonate debris. The detected echinoderms belong to the species *Echinometra mathaei* (Fig. 3 f,g).

Facies OT2 consists of thick and massive boulder fanglomerates that are clast-supported (Fig. 3 b). Locally, lenses of matrix-supported material occur. Overall, this facies becomes more matrix rich towards the top of the profile. The matrix is coarse sand and calcite cement. The conglomerate is polymictic and very poorly sorted with clast sizes ranging from granules to boulders up to 1 m in diameter. The largest fraction of the grainsize accumulates in clusters. The clasts are subrounded limestone displaying various colours like dark grey, light grey, red or yellow. The top of the lower layer of this facies is partially encrusted by barnacles. In the lowermost part of the layer coral fragments and gastropod shells are observed (Fig. 3 d,e). Bioerosion is not evident at the clasts. The lower contact of the conglomerate layers are abrupt but conformable.

Facies OT3 consists of a few centimeter to decimetre thick layer of polymictic well-rounded pebbles and numerous mollusc shells.

4.1.2. Interpretation

The presence of an in situ *Porites* reef complex in facies OT1 serves as a significant indicator of a shallow marine environment within the photic zone as the zooxanthellae-bearing animals are tied to the availability of sun light for their metabolic processes (Dullo, 2005). The growth and morphological characteristics of corals are a consequence of several influential factors (Hibbert et al., 2016). Growth rates of *Porites* depend on the species and can reach up to 36 mm/y in shallow marine environments (Dullo, 2005 and references therein). The column-like structure exhibited by these *Porites* reflects a strategic adaptation to the environmental conditions and develops only under bright light conditions (Muko et al., 2000). One of the key environmental challenges that these corals faced was the continuous influx of sediment into their

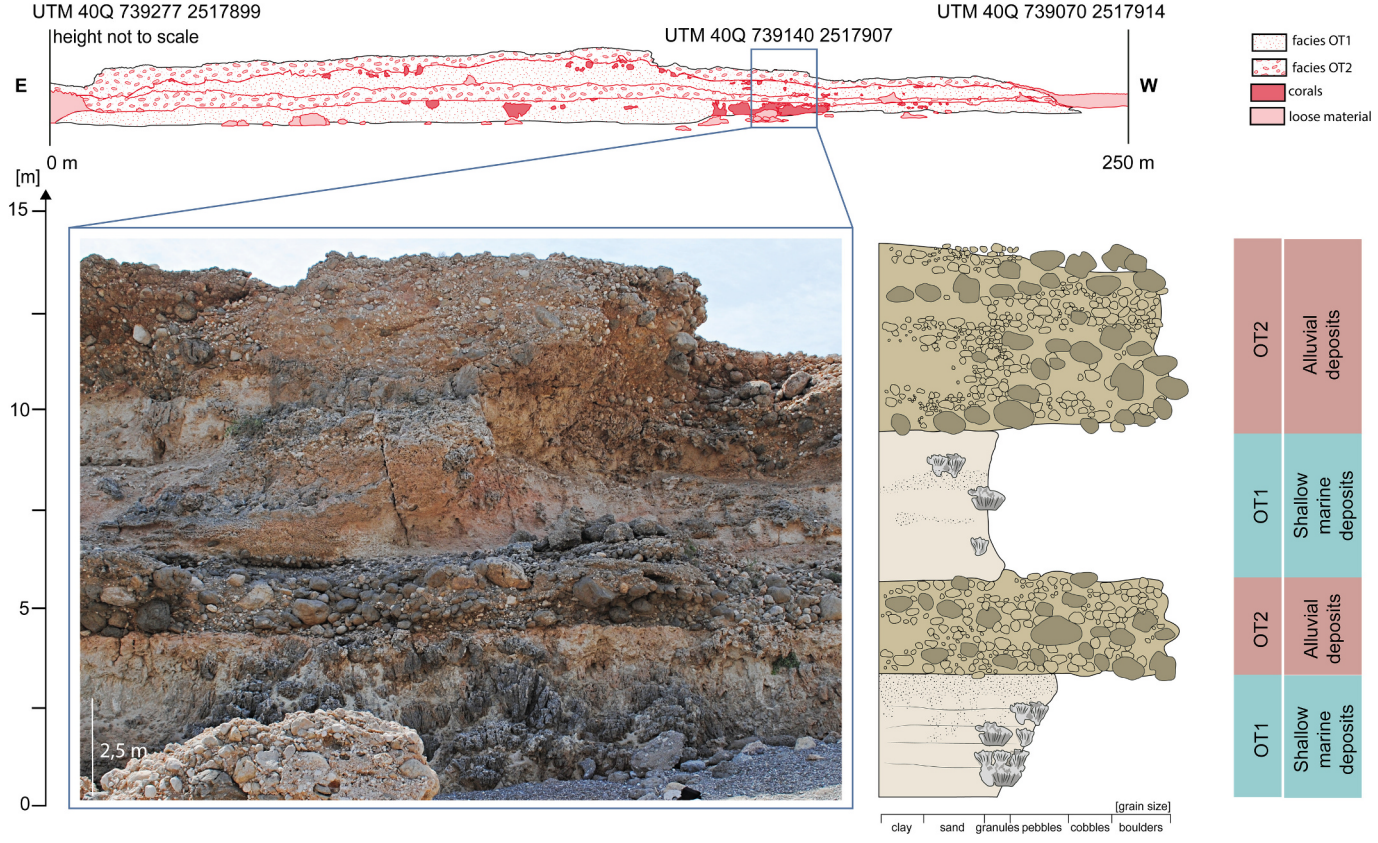

Fig. 2. Sketch, photo overview and a profile section of the coastal outcrop near Tiwi showing an intercalation of two cycles of an in situ coral reef and a very poorly sorted facies indicating a more terrestrial influence, most likely a debris flow within an alluvial fan. The top is an abrasional platform, and is part of the lowermost terrace of the marine terraces staircase in that area.

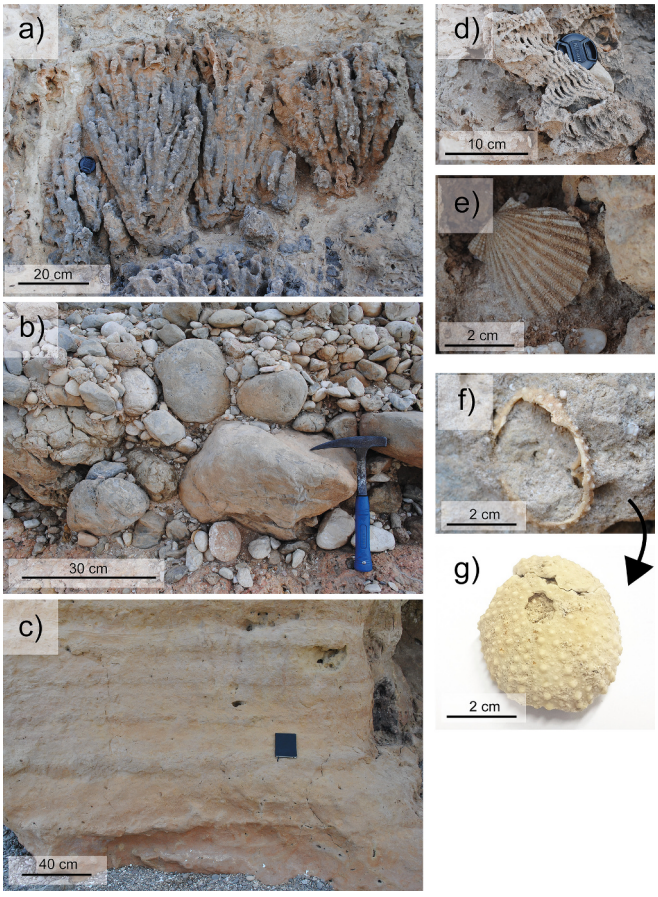

Fig. 3. Plate of specific features of the coastal outcrop near Tiwi, with a) facies OT1: fossil corals of a single species within the genus *Porites* (Lars Reuning, University of Kiel), the finger-like appearance of the corals reflect an adaptation to the influx of fine grain sediment that now is preserved as a light beige matrix, b) facies OT2, poorly sorted conglomerate c) fine-grained sediment, which can be found next to the patch reef and as a filling of the space between the corals (facies OT1), d) Ex situ fossil corals at the base of facies OT2, e) fossil *Pecte* bivalve shell at the base of facies OT2, f) & g) fossil echinoderm outer shell belonging to the species *Echinometra mathaei* (facies OT1).

habitat which is documented by void filling. The elongated columnar morphology of these *Porites* corals, therefore, appears to be an evolved response to mitigate the impact of sedimentation and maintain their position within the photic zone. The echinoderm *Echinometra mathaei* found in the upper part of OT1, lives in the littoral zone up to 30 m depth and is documented for the eastern Indian Ocean from the Late Pleistocene on (Philippe, 1998). The coarsening upwards of the matrix sediment indicates an ongoing change in environmental conditions.

In the geological sequence, the transition from facies OT1 to facies OT2 marks a significant shift in environmental conditions and sedimentary processes.

Facies OT2, which caps facies OT1 sharply, is characterized by distinctive characteristics like a very poor sorting and the presence of grain sizes of up to 1 m that suggest a deposition as a debris-flow with a high erosional energy. Debris flows are typically associated with terrestrial environments and are often triggered by heavy rain events or other factors that mobilize loose sediment and debris. The lack of bioerosional features support the terrestrial depositional environment. This sedimentation of facies OT2 led to the rapid burial and preservation of the underlying *Porites* reef facies OT1. Facies OT2 represents a terrestrial environment marked by periods of intense rainfall and erosional activity.

Facies OT3 depicts part of the lowermost terrace within the marine terraces stock in this area. It is an marine abrasion platform that worked up an older alluvial fanglomerate.

The alternation of a calm, shallow marine and a high energetic terrestrial facies clearly depicts an interaction of neotectonic uplift and sea-level oscillations. The marine terrace OT3 is referred by Hoffmann et al. (2020a) to a sea-level highstand at MIS 5a which gives a minimum age of 82.000 years to the sediments below. For these terraces Late Quaternary uplift rates of 0.01 to 0.89 mm, for Tiwi area 0.25–0.68 mm per year are documented by Hoffmann et al. (2020a). An ongoing recent uplift for this region is proven with uplift rates of ca. 1.3 mm per year (Pavlopoulos et al., 2023).

4.2. *Outcrop II: Ras ar Ru'ays*

Ras ar Ru'ays is located on the east coast of Oman (Fig. 1 II). The investigated outcrop is 6 m high and extends over ca. 280 m along the coast at the tip of Ras ar Ru'ays (Fig. 4). A total of five lithofacies are observed (OR1 to OR5). The lowermost facies OR1 and OR2 crop out at the southwestern end of the cliff and are discordantly overlain by the younger facies (Fig. 5a). While the layers of facies OR1 and OR2 are horizontal, the layers of OR3 to OR5 dip shallowly in a northwestern direction. As shown in Fig. 6, one log, comprising all observed lithofacies, is described from the southwestern section of the cliff. Furthermore, facies OR1 and OR2 were sampled for microfossil analyses.

4.2.1. *Sedimentology*

Facies OR1 occurs only at a 30 m wide section at the southwestern end of the cliff and shows a total thickness of 0.2 m. It is possible that the facies continues laterally, but is not visible due to the base of the outcrop is covered by the recent beach sediment. The facies consists of greenish-grey, silty clay and is horizontally laminated. The sediment contains organic material, that shows an orange-brown oxidation colour. The organic components are pebble-sized and scattered randomly throughout the layer. No macrofossils were observed.

Sample 1 (S1) was taken within this section in an elevation of 30 cm from the profile base (Fig. 4).

Facies OR2 is a 1.7 m thick, interbedded sandy silt and pebbly fine sand. It shows a colour alternation between light greenish beige of the silt to a more reddish orange of the sand. The sediment is semi consolidated and lamination varies between strictly horizontal, wavy and convoluted. Sandy layers often display ripple lamination. Facies OR2 crops out exclusively at the southwestern end of the cliff, where it can be traced for about 80 m. Pebbles occur randomly distributed but also concentrated in layers and lenses together with coarse sand. These layers and lenses are up to few centimetres thick. The facies is inversely graded – the occurrence of pebble layers increases towards the top. The material contains macroscopic fossils of molluscs (Fig. 5b). The facies shows different degrees of bioturbation. Some layers are bioturbated by single, vertical, 0.2 to 0.6 m wide and up to 0.47 m long burrows (Fig. 5c). The burrows show a consistent thickness, no branching, no lining and are infilled by sand. In these layers the bioturbation-index (bi) is low (1 or 2) so that overall bedding boundaries remain distinct. Some sand layers display very strong bioturbation (bi = 5 to 6) that masks all individual traces. White gypsum precipitation appears on top of greenish-orange clayey fine-sandy silt.

Sample 2 (S2) was taken within this section in an elevation of 160 cm from the foot of the profile (Fig. 4).

Facies OR3 is a at least 3.4 m thick, consolidated, matrix-supported conglomerate. It displays internal bedding with decimetre thick parallel layers that dip towards the NW at a low angle. The whole facies pinches out towards the southwest, where it appears as a thin bent layer of a few centimetres. At the northeastern end of the cliff it reaches a thickness of up to 5 m. The matrix is a light beige cemented fine-sandy coarse sand. Clasts are polymictic with an especially high diversity at the base of the facies. Clasts are, with decreasing abundance: granules to

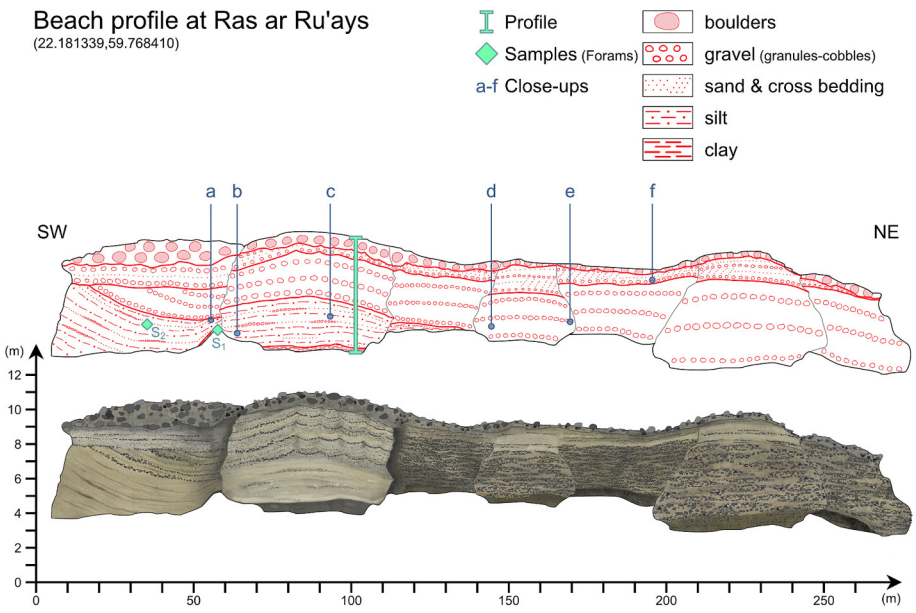

Fig. 4. Sketch and photo overview of the coastal outcrop near Ras ar Ru'ays, the green line indicates the location of the profile, the two green diamonds the sample locations for the foraminiferal investigation, the bluish a-f the locations of the close-up pictures in Fig. 5. (For interpretation of the references to colour in this figure legend, the reader is referred to the web version of this article.)

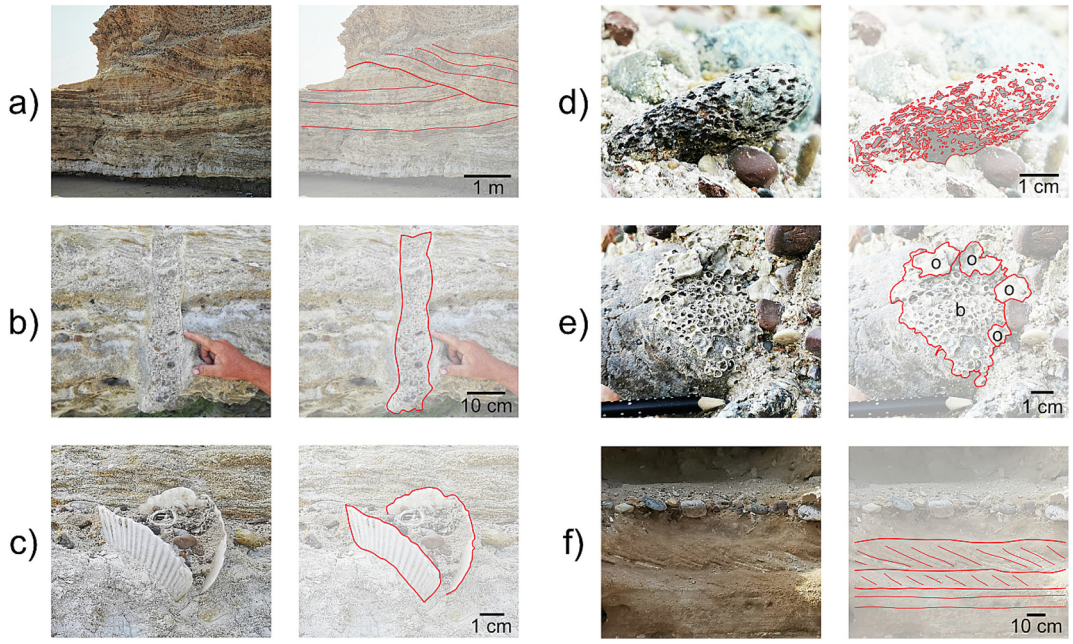

Fig. 5. Plate of specific features of the coastal outcrop near Ras ar Ru'ays with a) side view of the section showing cross bedding, b) bioturbation structure, filled with coarser sediment in facies OR2, c) still connected bivalve shells also in OR2, d) partly bioeroded pebble showing traces of the boring sponge *Cliona* (ichnogenus *Entobia*) that were created pre-depositional in facies OR3, e) remnants of barnacles (b) and oyster shells (o) also in OR3, f) cross bedding structures in facies OR4.

cobbles of grey, well-rounded limestones (45 %), pebbles of purple-red subrounded sandstone (20 %), pebbles of red subangular radiolarite (15 %) and pebbles of white/black rounded granite (10 %), others (10 %). Towards the top of the facies, the proportion of limestone increases significantly (up to 95 %) and replaces almost all other lithologies. The observed limestone clasts show traces of the boring sponge *Cliona* (ichnogenus *Entobia*) that were created pre-depositional (Fig. 5d). The matrix contains bivalve and gastropod shells. Additionally, some fossil oysters and barnacles are found on top of single clasts (Fig. 5e).

Facies OR4 (0.3 m thickness) shows a horizontally bedded interlayering of semi-consolidated sand and a consolidated, matrix-supported conglomerate. OR4 is similar to the base of OR3 but includes abundant reddish-beige fine-sand layers, varying in thickness of few centimetres up to ca. 0.8 m within the outcrop. Towards the northeastern part of the cliff, these sand layers partly show crossbedding structures (Fig. 5f). OR4 contains few limestone boulders up to 35 cm in diameter. The sandy layers are burrowed by vertical and oblique tubes of up to 5 cm in diameter and 15 cm in length. Some oyster shell remains can be found attached to clasts.

Facies OR5 is a 0.3 m thick, semi-consolidated, matrix-supported conglomerate. The conglomerate is polymictic with well to very well rounded limestone, granite and sandstone clasts that are mostly cobble

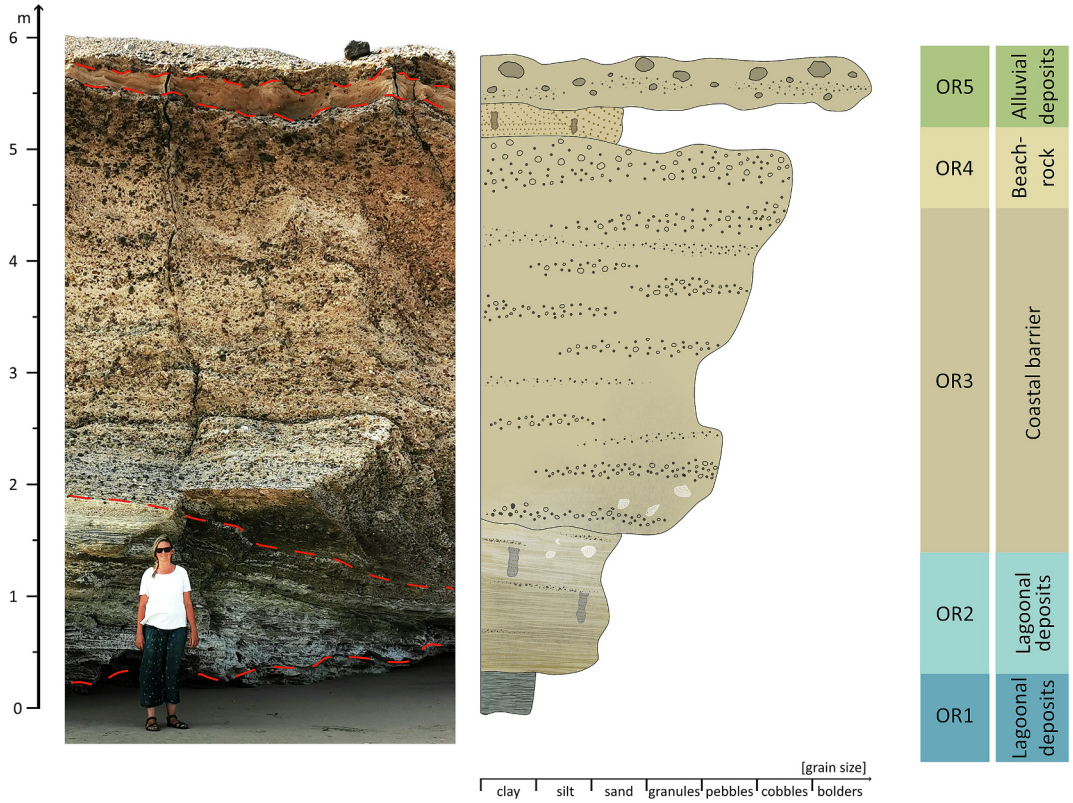

Fig. 6. Profile section of the coastal outcrop near Ras ar Ru'ays with the different facies ranging from marine to various terrestrial deposits.

sized. Granules, pebbles and boulders up to 35 cm in diameter also occur. The top of the layer is poorly consolidated. The matrix is light-beige.

4.2.2. *Microfossil analysis*

In Ras ar Ru'ays two samples were taken, one at an elevation of 30 cm (S1, Facies OR1) and one at 160 cm (S2, Facies OR2) (Fig. 4).

The microscopic examination of S1 of facies OR1 depicts a low content of foraminifera. Their shells, the tests, are badly preserved and thus unsuitable for species identification.

A total of 477 individual foraminifera were separated from S2 of facies OR2; 69 of these are badly preserved and unidentifiable. Species identification was done on the remaining 408 individuals. All of these are well preserved. Even tests of fragile specimen, e.g. *Pseudononion* sp., are found complete. The 408 individuals include 20 species and 13 genera (Table 2) (Fig. 7; Fig. 8). Most of the specimen are hyaline-perforate foraminifera (Fig. 9a). Of all specimens, only three are agglutinated and two are porcelaneous, most of these are unidentifiable. The Fisher-α-index gives a value of 4.5 (Fig. 9b). The Shannon-Weaver-index amounts to 2.63 (Fig. 9c).

Additionally to foraminifera, ostracods were detected in S2. Out of all ostracods ten specimen were found with articulated valves, plus 16 single ostracod valves.

4.2.3. *Interpretation*

At the Ras ar Ru'ays coastal site, the geological sequence distinctly reveals a transition from a marine depositional environment at the base to a more terrestrial one towards the top. A crucial aspect of reconstructing the depositional environment lies in the analysis of foraminiferal content within lithofacies OR1 and OR2 in the lowermost section.

In S1 of lithofacies OR1, the presence of foraminifera tests indicates a marine environment, although precise environmental analysis is hindered by the poor preservation of these tests in the sample. Conversely, in S2 of lithofacies OR2, foraminiferal tests are generally well-preserved, even the fragile *Pseudononion* sp. tests remain intact (Fig. 8d & e). This suggests minimal transport distance or implies that this fauna might be autochthonous.

While the position of S2 within the ternary diagram (Fig. 9a) suggests various possible environments, it does not singularly confirm the

Table 2
Foraminiferal species assemblage. In total 408 individuals were found, 20 different species were identified, belonging to 13 different genera.

No.	Genera		No.	Species	
	Name	Counted		Name	Counted
1	*Ammonia*	23	1	cf. *Ammonia* sp. 1	23
2	*Bolivina*	15		*Bolivina* indiff.	7
3	*Cibicides*	6	2	*Bolivina* sp. 1	3
4	*Elphidium*	115	3	*Bolivina* sp. 2	5
5	*Lobatula*	92	4	*Cibicides refulgens*	6
6	*Loxostomina*	5		*Elphidium* indiff.	51
7	*Neoconorbina*	11	5	*Elphidium* sp. 1	66
8	*Operculina*	7	6	*Elphidium* sp. 2	14
9	*Pararotalia*	8	7	*Elphidium* sp. 3	16
10	*Procerolagena*	1	8	*Elphidium* sp. 4	4
11	*Pseudononion*	43	9	*Elphidium* sp. 5	15
12	*Trochulina*	29		*Lobatula* indiff.	69
13	*Valvulina*	2	10	*Lobatula lobatula*	14
	Total:	**357**	11	cf. *Lobatula* sp. 1	9
			12	cf. *Loxostomina* sp. 1	5
				Neoconorbina indiff.	8
			13	*Neoconorbina marginata*	2
			14	*Neoconorbina multimarginata*	1
			15	*Operculina* cf. *ammonoides*	7
			16	*Pararotalia* sp. 1	8
			17	*Procerolagena* sp.1	1
			18	cf. *Pseudononion* sp. 1	43
			19	*Trochulina* sp. 1	29
			20	*Valvulina* sp. 1	2
				Total:	**408**

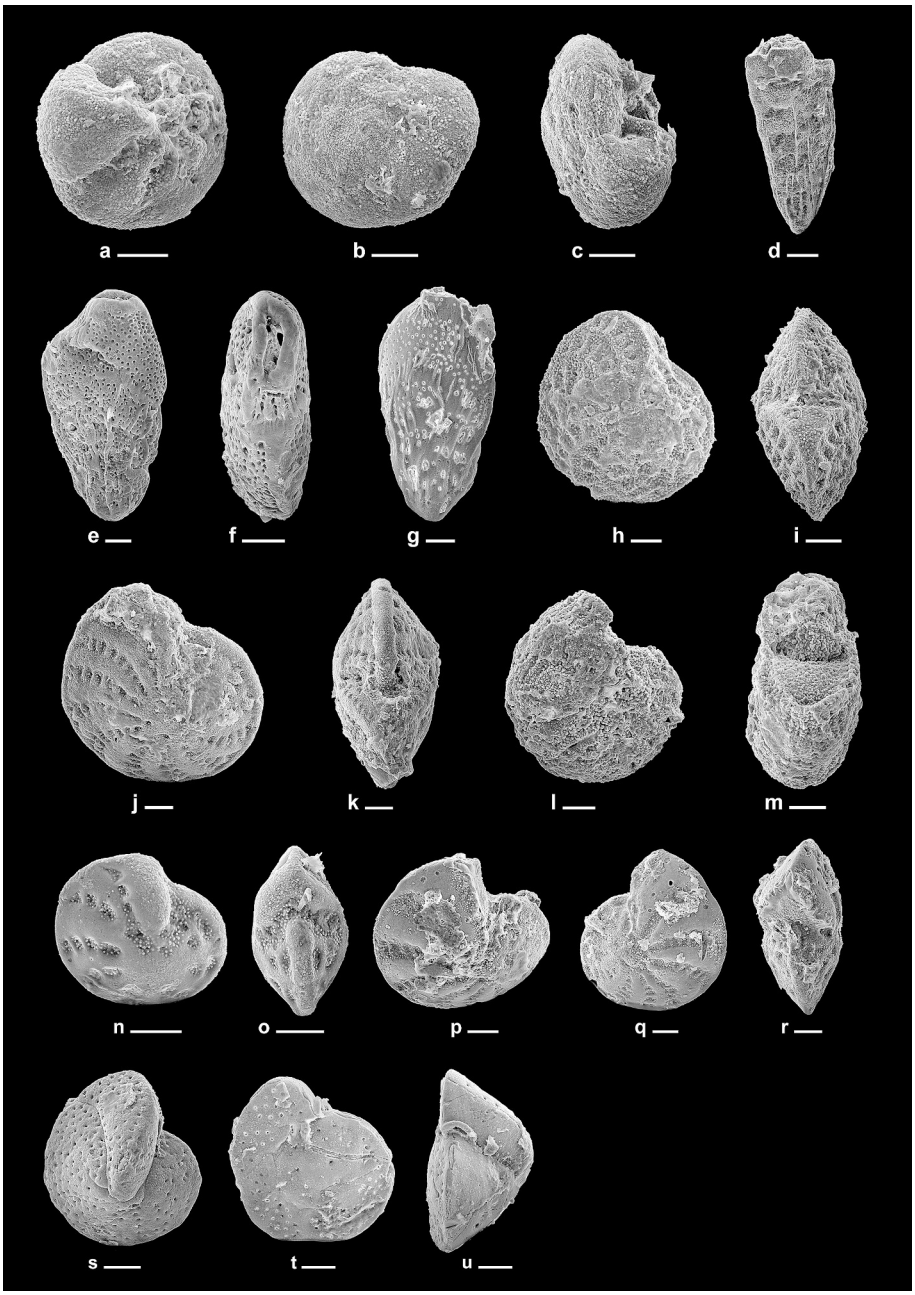

Fig. 7. Plate I, scale is 50 μm; a-c) cf. *Ammonia* sp. 1; d) cf. *Loxostomina* sp. 1; e,f) *Bolivina* sp. 1; g) *Bolivina* sp. 2; h,i) *Elphidium* sp. 1; j,k) *Elphidium* sp. 2; l,m) *Elphidium* sp. 3; n.o) *Elphidium* sp. 4; p-r) *Elphidium* sp. 5; s-u) *Cibicides refulgens*.

depositional background environment. The species assemblage in lithofacies OR2 includes abundant benthic and epifaunal species, like *Elphidium* sp. which preferably sits on algae, and also low-oxygen-tolerant species like *Ammonia* sp. This aligns with the deposition of fine-grained sediments resulting in low oxygen content within the sediment. The small grain size reflects a low-energy sedimentary setting while the presence of gypsum points to a shallow water body or tidal flat. This coincides with the appearance of sandy lenses and interlayers of pebbles in between which indicate the proximity to the coast.

Collectively, this sedimentary evidence paints a picture of a marine lagoon inhabited by algae and possibly mangroves, similar to today's Filim Lagoon west of Bar al Hikman. Such a specific environment is only suitable for a limited range of species. This is supported by the relatively low Fisher-α-index of 4.5 suggesting eutrophic conditions and a low biodiversity, commonly observed in muddy tidal flats rich in algae (Murray, 1991). The relationship between the Fisher-α-index and the Shannon-Weaver-index plots *Shelf* or *Normal marine to hypersaline lagoon*, the latter further supporting the lagoonal interpretation (Shannon and Weaver, 1949).

Notably absent are typical indicators of freshwater influence and typical reef indicators, with the exception of *Operculina*. The absence of larger foraminifera rules out an oligotrophic reef environment and a carbonate shelf. *Operculina* and *Pararotalia* however, point towards a nutrient-rich environment potentially influenced by upwelling processes, characteristic of Oman's east coast (McLachlan et al., 1998). Alternatively, nutrient enrichment could also be intensified by or result from the decay of algae or proximity to mangrove forests, with nutrient input from sources like crab fecal pellets and mangrove leaves.

Presently, oxygen content in the northern Indian Ocean is reported by the U.S. National Oceanographic Data Centre database to be <0,2 ml

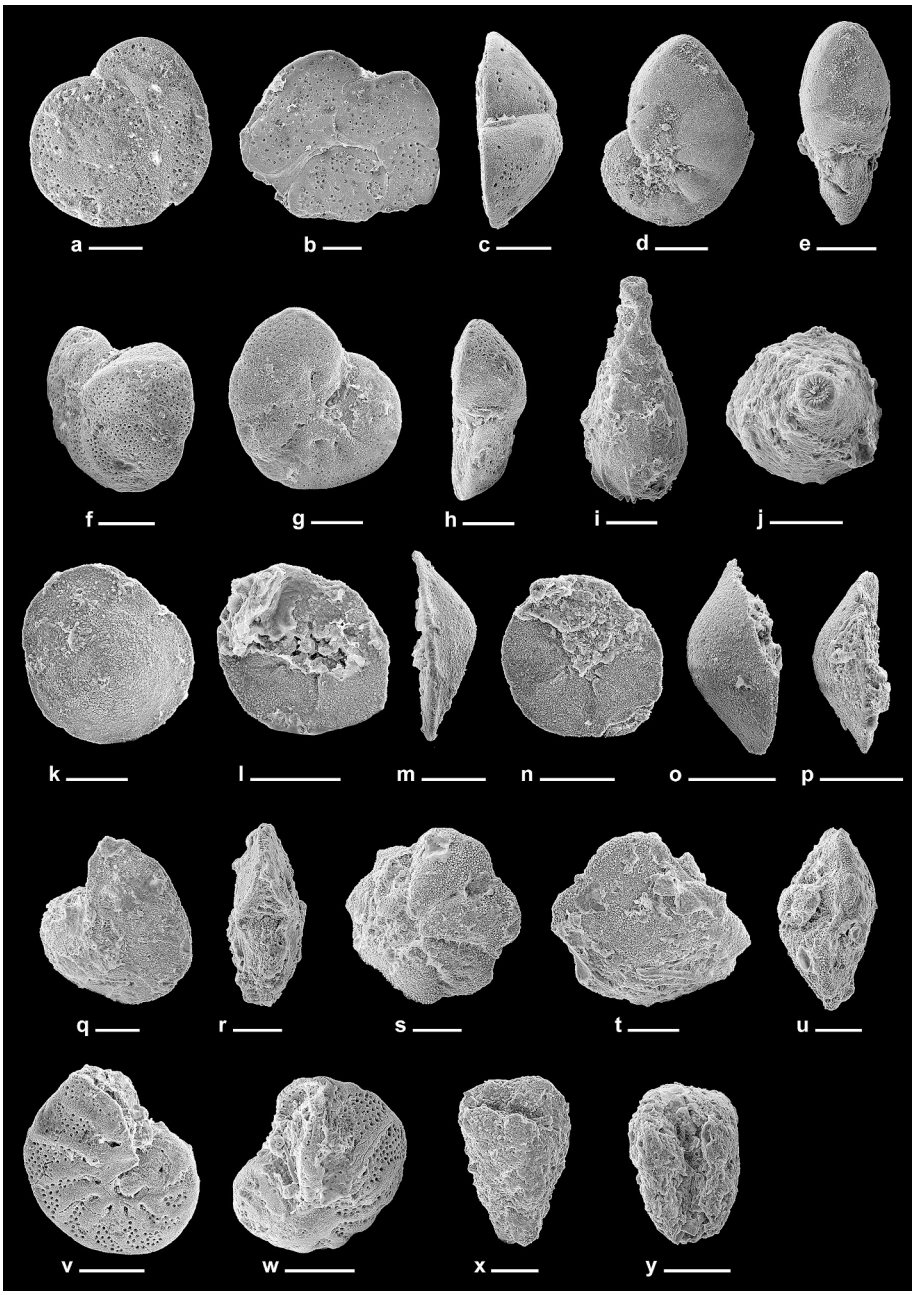

Fig. 8. Plate II, scale is 100 μm; a-c) *Lobatula lobatula* different tests of *Lobatula lobatula* are characterized by a different degree of deformation. (a) normal specimen – spiral side (b) moderately deformed specimen – spiral side; d,e) cf. *Pseudononion* sp. 1; f-h) cf. *Lobatula* sp. 1; i,j) *Procerolagena* sp.1; k-m) *Neoconorbina marginata*; n-p) *Neoconorbina multimarginata*; q,r) *Operculina* cf. *ammonoides*; s-u) *Pararotalia* sp. 1; v-w) *Trochulina* sp. 1; x-y) *Valvulina* sp. 1.

O_2/l, indicative of a dysoxic, microxic or even anoxic environment (Bernhard and Sen Gupta, 1999). The lack of freshwater input and the presence of oxygen-consuming organisms, including algae, likely exacerbated the reduction in oxygen content. This could have led to oxygen demand exceeding supply, rendering the sediment anoxic.

Lithofacies OR3, is interpreted as a coastal barrier overriding the lagoonal deposit, based on the typical landward dipping foresets overlaying the discordance at the top of OR2 and the shell content indicating marine influence. The clasts observed in OR3 indicate two distinct sediment sources, better rounded components are likely sourced along the southern flanks of the Hajar Mountains and transported to the coast via fluvial and/or alluvial processes, whereas poorly rounded radiolarite fragments stem from local bedrocks. Facies OR4 exhibits cross-bedding and bioturbation within some sandy portions indicating a beach or supratidal backshore setting. Overlying facies OR5 comprises gravel and rounded boulders, representing a fluvial setting and possibly a fanglomerate, formed during a sea-level regression.

In summary, the Ras ar Ru'ays coastal profile reveals a stratigraphy comprising a shallow marine lagoonal stage at the base, overridden by a coastal barrier that stabilised into a beach and, finally, a fanglomerate, indicating a terrestrial environment. This can be interpreted as transgression followed by a regressional phase. The position of the coastal barrier facies at roughly 4 m above pmsl coincides with the paleo shoreline at Sur Lagoon at a same height of 3.5 to 4 m above pmsl. In Sur, a bioerosion notch depicts the former sea level(Falkenroth et al., 2020) and is referred to MIS 5a sea-level highstand within the Last Interglacial by quartz U/Th datings of an associated beachrock deposit which revealed an age of 80 ± 3 ka (Mauz et al., 2015).

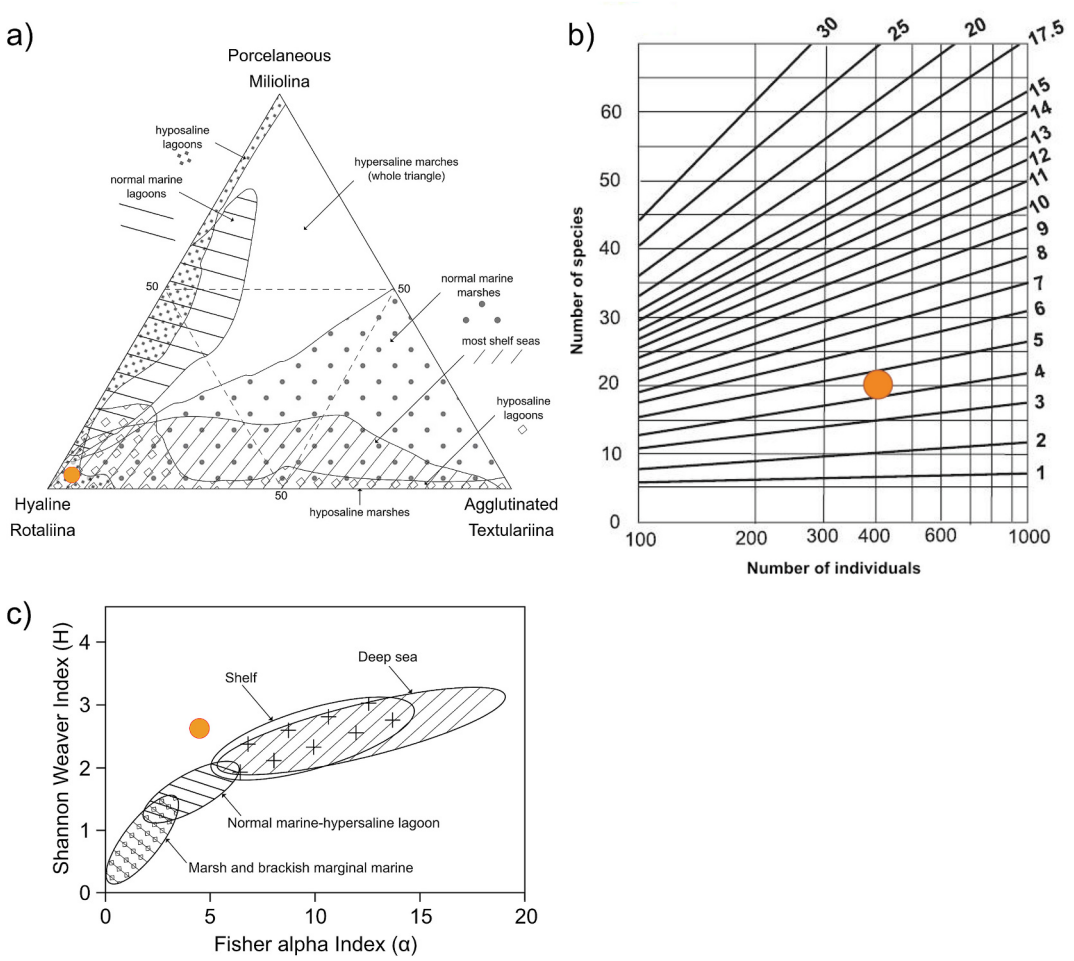

Fig. 9. The results of a comprehensive foraminiferal analysis. The sample of OR2, of the coastal profile at Ras ar Ru'ays is marked with an orange dot. a) A ternary diagram of the shell type ratio, differentiating between porcelaneous, hyaline and agglutinated tests, the sample's location in this diagram is not indicative for a specific environment (after Murray, 1991); b) The Fisher-α-index reflects the number of individuals against the number of species, the sample gives a value of 4.5 indicating eutrophic water conditions (after Murray, 1991); c) The Shannon-Weaver-index of the sample amounts to 2.63 and indicates a paleoenvironment of a shelf or lagoon (after Shannon and Weaver, 1949).

4.3. Outcrops III a and III b: Ras Madraka I and Ras Madraka II

In this study two coastal sections with marine facies were identified near Ras Madraka (Ras Madraka I and Ras Madraka II). Both show sandy sediments with some shell debris and molluscs ~4 m above pmsl. While Ras Madraka I is located sheltered inside a small lagoon, Ras Madraka II forms the tip of a headland and is exposed to the rough seaside of the Indian Ocean.

Outcrop Ras Madraka I is located ca. 100 m onshore. Outcropping rocks of the allochthonous Masirah-Ophiolite are unconformably overlain by several layers of consolidated sand, gravel and beachrock. The outcrop is approximately 30 m long and varies in thickness from 1.5 m on the seaward side to 2.5 m on the landward side. One log was measured on the seaward edge. Within this log, three distinct lithofacies (OM1 to OM3) are found overlaying the Ophiolite bedrock (Fig. 10).

Outcrop Ras Madraka II is located just besides the sea, the base of the hill consists of a micritic light grey limestone that belongs to the Miocene Warak Formation. The recent notch is formed within these rocks. This limestone is unconformably overlain by gravelly, sandy deposits. These deposits are attached as patches to the hill (Fig. 11). The limestone is partly covered with cemented rockfall at the base. The measured log at Ras Madraka II displays three distinct lithofacies (OM3 to OM5), one of which is also found at Ras Madraka I (OM3) (Fig. 12).

4.3.1. Sedimentology

Facies OM1 is a 0.65 m thick, clast-supported conglomerate. Clasts are 0.5 to 6 cm large, subangular and are mostly made up of ophiolite (95 %) and 5 % limestone. The clasts are embedded in a light-beige fine sandy silt-matrix, semi consolidated. Within the outcrop this facies shows few parts with cross-bedding-structures.

Facies OM2is 0.12 m thick and consists of a clast-supported semi-consolidated conglomerate. Clasts are pebble to cobble sized (0.5 to 8 cm diameter), whereas the largest clast fraction is only 5 % of the total. The clasts are rounded ophiolite (ca. 80 %) and shells of bivalves and gastropods (ca. 20 %). Further shell material occurs as debris and is thus impossible to identify. The matrix is a cemented off-white clay-silt.

This 0.1 to 1.1 m thick facies OM3 is a consolidated beige fine to middle sand with planar cross-bedding. Locally, the material contains 1 cm-thick bands of few cm-sized ophiolite clasts in Ras Madraka I. On the seaward side the facies is covered by patches of beachrock, 1 to 2 m in diameter, most likely few centimeter thick. In Ras Madraka I this facies shows one vertical bioturbation structure of ca. 1 cm in diameter. In Ras Madraka II this facies includes various vertical bioturbation structures of ca. 2 cm in diameter.

Facies OM4 is 0.15 to 0.5 m thick and consists of a beige consolidated middle sandy, gravelly coarse sand with rounded grains. The sediment is unsorted and chaotic and contains some incorporated shell debris. In the upper part OM4 includes shell debris and some embedded oyster shells.

Facies OM5 varies from 0.7 and 9.1 m in thickness. The facies

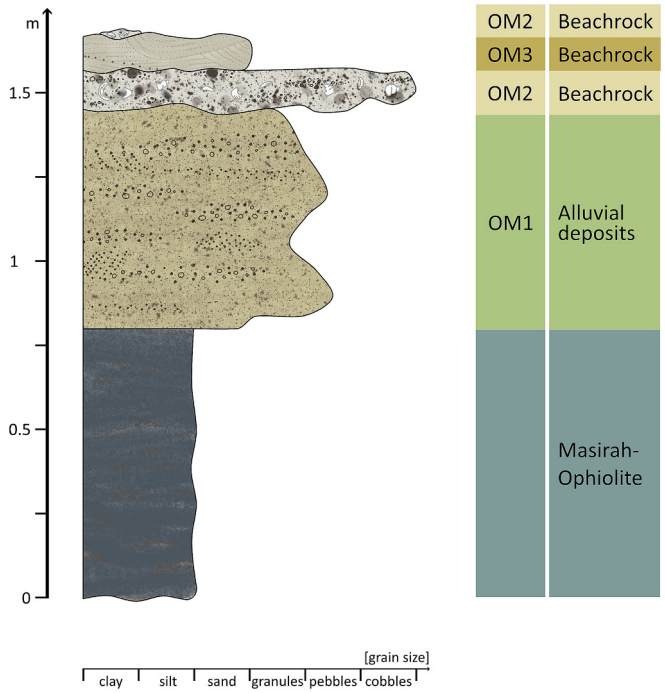

Fig. 10. Profile section of the coastal outcrop Ras Madraka I with the Masirah ophiolite at the base, discordantly overlain by alluvial sediments and various beachrock deposits.

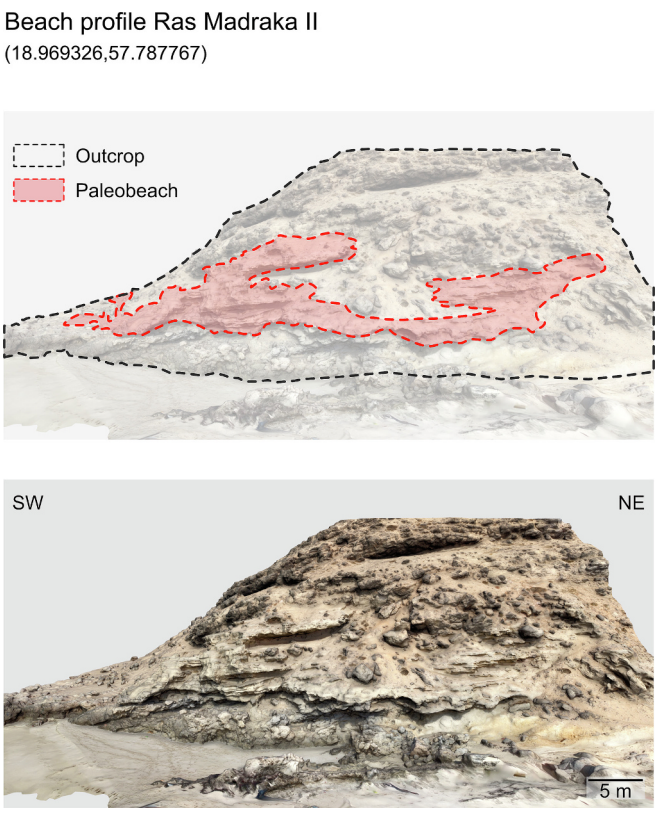

Fig. 11. Image taken from a 3D model (Grigowski, 2022) of the coastal outcrop Ras Madraka II; highlighted are the paleobeach findings.

consists of well-sorted, light beige, consolidated fine sandy middle sand with incorporated shell debris and isolated fully preserved mollusc shells. It is a congruent sediment layer showing distinctive features at

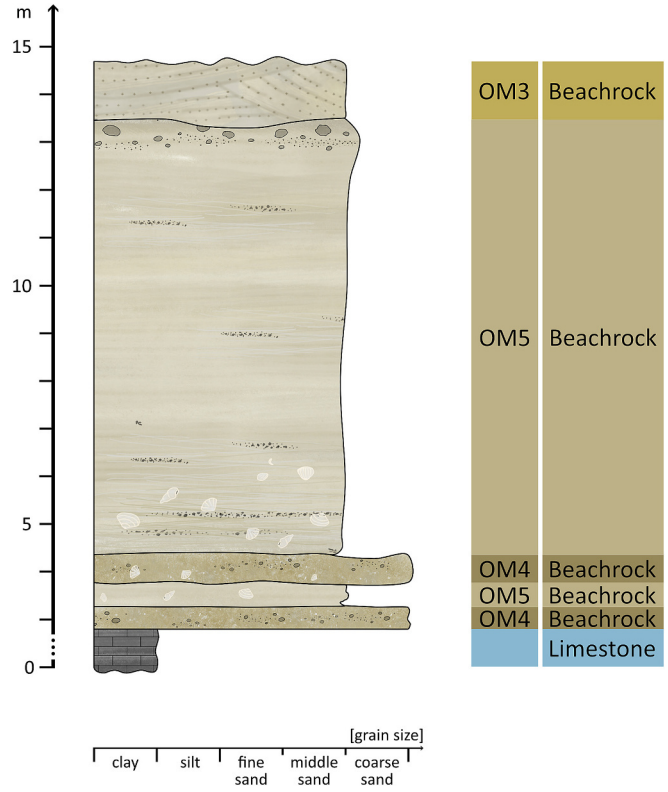

Fig. 12. Profile section of the coastal outcrop Ras Madraka II with various beachrock deposits discordantly overlying outcropping limestone.

different heights. At the base of the upper appearance of OM5, within the first 5 cm some bivalve shells are imbricated. The lower 30 cm show 3 lines of gravel and shells, each 2 cm in thickness. Such thin layers can be found occasionally throughout OM5 varying in composition with some consisting of few-cm-sized rock and shell debris and some only of rock clasts, e.g. at 5.9 m. From 7.3 m on the sediment is partly bioturbated. At an elevation of 13.4–13.7 m OM5 shows a high density (ca. 50 %) of incorporated angular, gravel-sized limestone debris that stretches over 30 cm of the profile.

4.3.2. Interpretation

Facies OM1 is a conglomerate formation found exclusively in Ras Madraka I. This facies is characterized by subangular clasts, primarily composed of ophiolithic material, which suggests a very short transportation distance. Such characteristics strongly support the interpretation of a fanglomerate deposition, indicating that these sediments likely originated from local or nearby sources, quickly accumulating in the area.

Facies OM2, found exclusively in Ras Madraka I, is characterized by an abundance of shells and shell debris, which distinctly identify it as a beachrock deposit. Beachrock formations typically form in intertidal or shallow subtidal zones where sediment is cemented by minerals like calcium carbonate, resulting in a solid, rocky structure. The occurrence of conglomerate within this facies indicates that the beach environment was subjected to either significant wave energy or notable fluvial influence.

Facies OM3 is encountered in both Ras Madraka I and II. This facies also represents a beachrock deposit. It exhibits notable features towards its upper layers, such as the presence of mollusc shells and bioturbation structures. These characteristics are indicative of a supratidal backshore environment, suggesting that this region has experienced fluctuations in sea level that allowed for the formation of beachrock structures under varying intertidal conditions.

Facies OM4 and OM5 are exclusive to Ras Madraka II and are both beachrock sediments. However, they represent different depositional environmental settings. OM4 exhibits a somewhat chaotic structure and contains shell debris but also intact shells including oyster shells. OM5, on the other hand, is characterized by finer-grained material, cross-bedding patterns, and an increased occurrence of bioturbation structures. This suggests distinct depositional conditions, with OM4 potentially reflecting more energetic wave conditions, while OM5 represents a quieter, fine-grained beachrock environment.

The presence of these contrasting sedimentary facies within the Ras Madraka region raises several observations:

Despite similar elevations, Ras Madraka I and II showcase differences in sediment characteristics, hinting at varying depositional environments. The coarser sediments in Ras Madraka I suggest the influence of an incoming wadi system, likely transporting larger, coarser materials to this bay. In contrast, Ras Madraka II features finer-grained sediments, suggesting a calm depositional environment within a rocky embayment with a different sediment source.

The presence of angular rock clasts in the upper part of OM5 may be interpreted as hillslope debris. Erosion and changes in coastal morphology might have been influenced by climatic changes, or have been associated with shifts in sea level or wave dynamics.

Both sites, Ras Madraka I and II, exhibit a transgressional conglomerate at their base, indicating a period of sea-level rise followed by highstand and regression. These sedimentary sequences hold valuable information about past sea-level fluctuations and the geological history of this coastal region.

4.4. Other outcrops

The following outcrops were not investigated in detail, but provide intriguing evidence of their marine origin, despite their elevation of up to ~4 m above msl.

4.4.1. Outcrop IV: Al Haddah

Close to Al Haddah at the eastern coastline of Oman (Fig. 1 IV), a 4 m high coastal cliff displays several semi consolidated marine and deltaic deposits discordantly overlaying the radiolarian mudstones and pelagic limestones of the Triassic Sal Formation (Peters et al., 2000) (Fig. 13). The profile has already been shortly described by Decker et al. (2021), but has been re-examined in March 2024 and is mentioned here again for completeness.

The base of the profile is made up by coarse sandstones interbedded with granule and pebble layers, that show steep seaward dipping foresets. The components are mostly angular radiolarites and shell fragments. These sandy layers are capped by a 25 cm thick, inversely graded

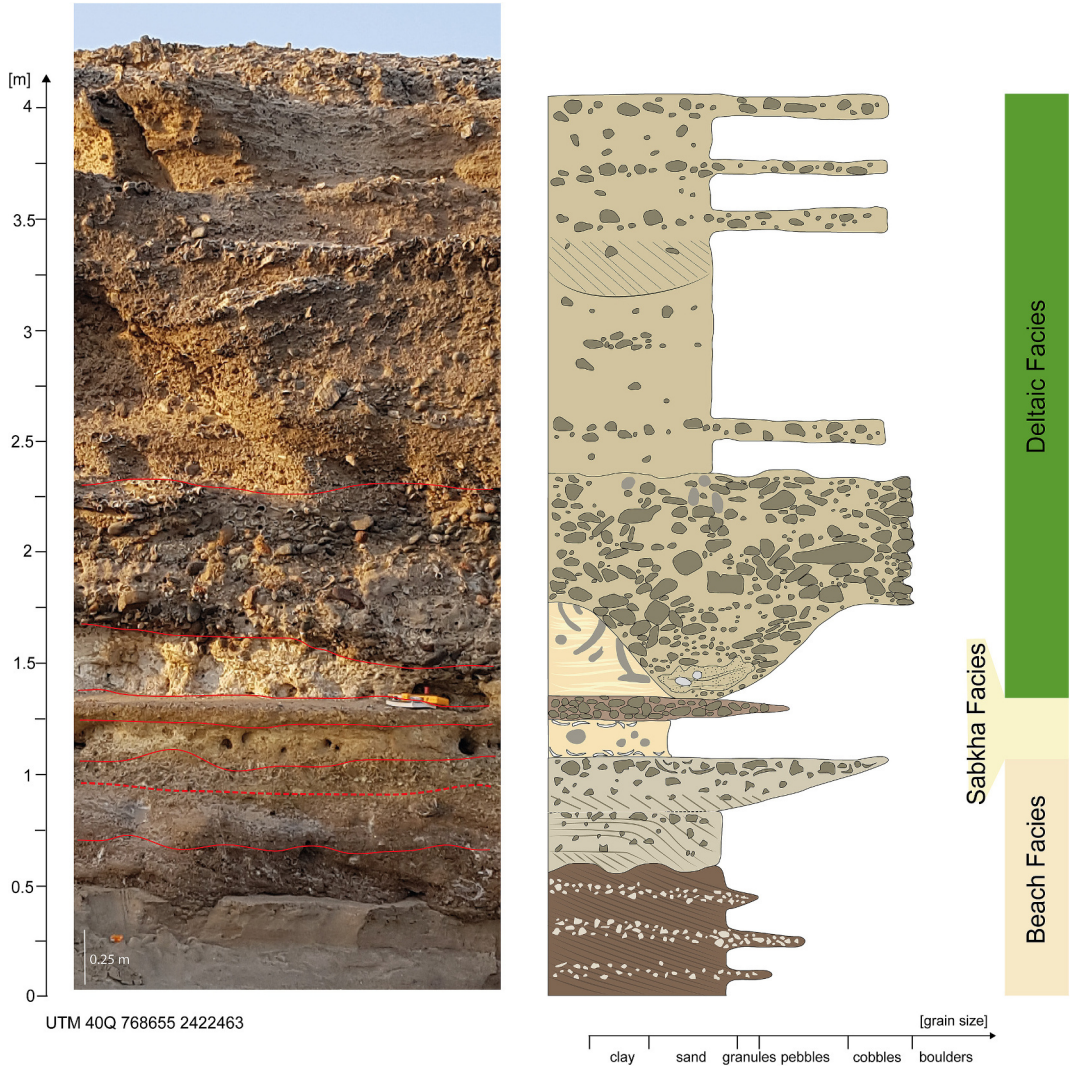

Fig. 13. Profile section of the coastal outcrop near Al Haddah, with different layers indicating beach facies deposits at the bottom, followed by sabkha facies deposits and deltaic deposits from ca. 1.5 m onwards towards the top. These deposits include findings of fossil *Crassostrea* oyster shells at various heights.

cobble conglomerate with a chaotic fabric that almost exclusively contains clasts of oyster shell fragments. A sharp but irregular contact is separating the conglomerate from a 0.5 m thick, fine to medium, light yellow sand showing parallel lamination and large burrows as well as a high content of evaporites (salt and gypsum) concentrated in individual laminae. This fine-grained layer is interrupted by another only 0.1 m thick pebble conglomerate with a high shell content. Finally, the upper part of the profile is made up of large cobble to boulder conglomerates that are mostly matrix supported but also display areas of clast supported fabric. The conglomerates show large scale trough cross bedding and channel structures. The clasts in these conglomerates are rounded and more variably than in the layers below containing limestones, ophiolites, radiolarites and large oyster shells of the genus *Crassostrea gryphoides* (Hoffmann et al., 2016).

Interpretation. The base of the profile is interpreted as a beach foreshore facies due to the sedimentary structures and clasts content that indicate an exclusively local source. These beach sands are overlain by sabkha deposits characterized by their fine grained sediments and evaporite content. Both the beach facies as well as the sabkha facies are interrupted by high energy events, possibly storms, that eroded an oyster reef and transported high amounts of the shell debris inland. The conglomerates at the top of the profile are interpreted as deltaic facies, based on their structure and clast content that show their connection to a larger feeder system transporting clasts from the southern side of the Al Hajar mountains to the coastline. A similar deltaic facies is also recorded in a nearby 2 m high coastal cliff next to As Sulayb (Decker et al., 2021) where it also contains a substantial quantity of well-preserved *Crassostrea gryphoides* (Hoffmann et al., 2016). The preservation of these shells makes them suitable candidates for dating. However, attempts to date one of the shells from the As Sulayb profile using radiocarbon dating yielded inconclusive results due to the age of the material exceeding the age limit of the method.

4.4.2. *Outcrop V: Daymaniyat Island Qafsiyyah*

The Daymaniyat Islands are located about 15 km north of the capital city, Muscat, within the Gulf of Oman (Fig. 1 V). The archipelago comprises three distinct islands: two characterized by stable bedrock formations and the third forming a complex of smaller rocky islands interconnected by sand spits. This intricate complex stretches over a distance of approximately 6.5 km. The islands predominantly consist of a micritic to brecciated reddish-beige Miocene limestone that belongs to the Sur Formation of the Fars Group (Wyns et al., 1992) and bears resemblance to the Jafnayn Formation that crops out at Ras al Hadd (Wyns et al., 1992).

On the middle island, Qafsiyyah Island, a notable beachrock outcrop is prominently located along the southern coast, situated at an elevation of approximately 4 m (Fig. 14a). It is located within a sheltered embayment, featuring a thickness of around 2.5 m, which tapers towards its edges, erosive processes created an overhang in the middle of the profile (Fig. 14b). This beachrock formation consists of yellowish-beige, cemented medium to coarse sand, often displaying characteristics such as cross-bedding and bioturbation structures (Fig. 14c). The latter are 1–3 cm in diameter, appear mostly unoriented and show a dark, inner lining (Fig. 14c). They are hollow or filled with coarse sand, differing from the surrounding material (Fig. 14d).

Interpretation. The beachrock deposits identified at an elevation of ~4 m on the Daymaniyat Island Qafsiyyah can be associated with a depositional environment within the lower backshore or upper foreshore, reflecting their position within the coastal zone (Falkenroth et al., 2019; Mauz et al., 2015).

4.4.3. *Outcrop VI: Ras al Hadd*

The village of Ras al Hadd is located on a bedrock that acts as a natural barrier separating a lagoon from the open ocean (Fig. 1 VI). The rock is a micritic beige, partly reddish Late Paleocene to Early Eocene limestone that belongs to the Jafnayn Formation (Wyns et al., 1992). The bedrock is prominently exposed in various locations around the perimeter of the Ras al Hadd lagoon. In this study, particular attention was given to an outcrop situated near the entrance of the Ras al Hadd lagoon. The outcrop is located on private ground. At this site, the bedrock cliff is 6–7 m high and 270 m wide.

The lowermost meter is covered by sessile intertidal organisms, namely oysters and barnacles (Fig. 15a). The barnacles can reach sizes of up to 5 cm in diameter, are found both on the surface and nestled within remnants of oyster shells. Above this overgrown area, an irregular coastal notch has developed (Fig. 15a, white arrow), it shows no signs of



Fig. 14. Plate of specific features of the paleobeach on the Daymaniyat Island Qafsiyyah; with a) an overview and the location of the outcrop at the beach, b) a side view of the paleobeach beachrock, c) & d) different bioturbation structures within the beige beachrock, the darker inner lining of the bioturbation channels is clearly visible.

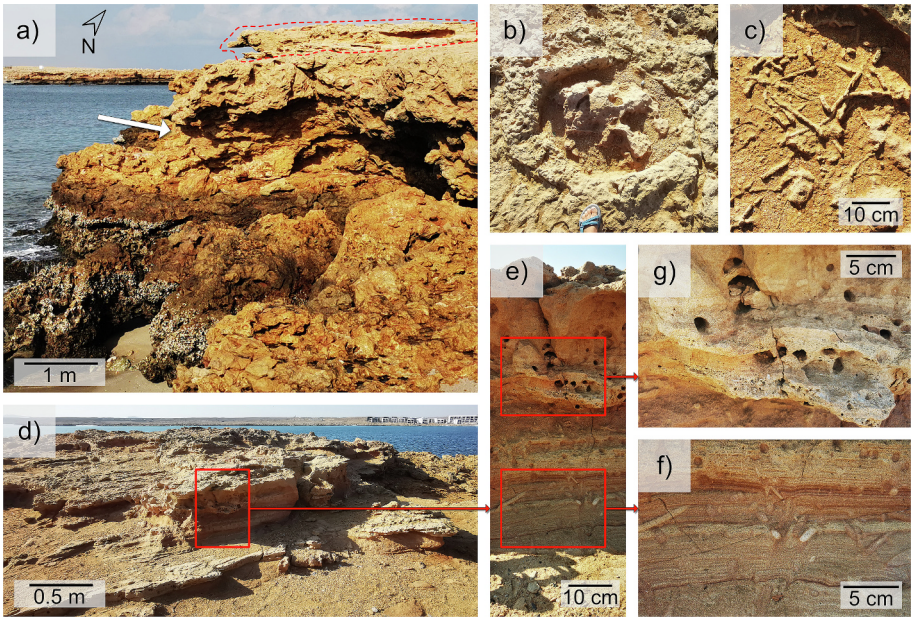

Fig. 15. Plate of specific features of the outcrop in Ras al Hadd (on private property, not freely accessible); with a) the recent notch (white arrow) and the location of the beachrock (red dashed line); b) surface: round structure, maybe altered coral; c) surface: mainly horizontal bioturbation structures; d) outcropping beachrock; e) profile of the beachrock; f) magnifying the lower part of the profile with many differently orientated sediment-filled bioturbation structures; g) magnifying the upper part of the profile with bore-hole structures. (For interpretation of the references to colour in this figure legend, the reader is referred to the web version of this article.)

bioerosion, suggesting abrasion as the primary formation process. The apex of this recent notch stands at an elevation of about 3.5 m above msl. The notch has a total height of 1.5 m and a symmetrical u-shaped configuration.

At an elevation of 2 m, the Eocene limestone is overlain by an 8-cm-thick matrix-supported conglomerate. This layer comprises rounded to subangular clasts ranging from 2 to 5 cm in size, featuring various lithologies, primarily limestone and red clay- to siltstone components.

The conglomerate is covered by a sandy beachrock deposit, measuring 1.4 m in thickness (Fig. 15a, red dashed line). The deposit exhibits a normal grading sequence, starting with beige medium to coarse sand at the base, transitioning to a beige to reddish medium sand towards the top. The layers are planar bedded, with a gentle dip of ca. 10° towards SW. The lower beds display distinct crossbedding structures, while the upper layers are characterized by extensive bioturbation (Fig. 15d-g). Tube-like trace fossils are predominantly oriented horizontally, with a few displaying vertical orientations. These trace fossils possess an average diameter of 1 cm, with the largest tube measuring 2 cm in diameter and extending to a length of 30 cm.

Interpretation. The coastal cliff at Ras al Hadd features a recent abrasional notch and a beachrock deposit that is ~3–4 m elevated above the

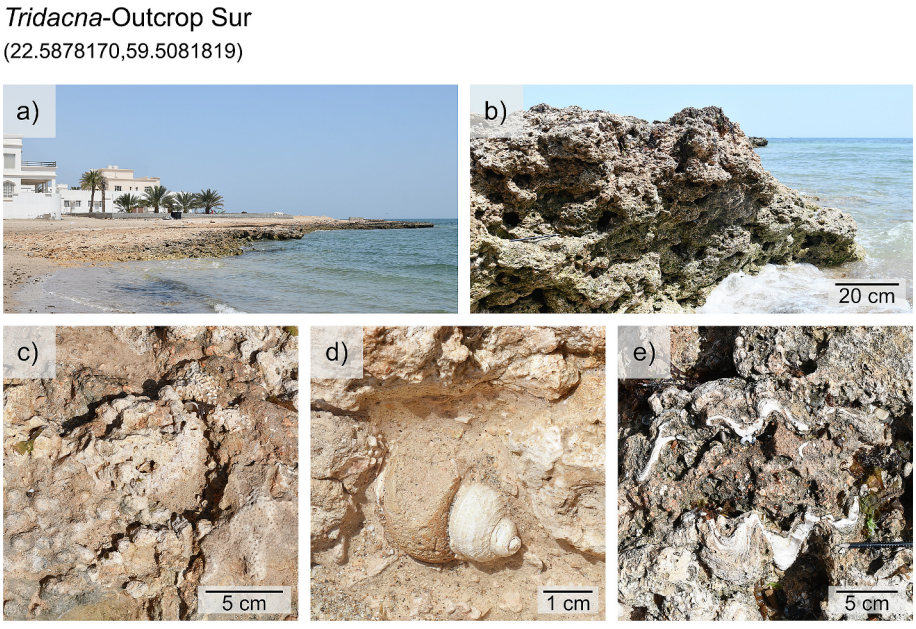

Fig. 16. Plate of specific features of the paleoreef in Sur; with a) an overview of the outcrop at the beach, b) picture of the section, c) a close up picture of in situ corals, d) a fossil gastropod shell with partly shell preservation, partly steinkern preservation and e) the fossil shell of an in situ *Tridacna* bivalve.

pmsl. The extensive bioturbation observed within this beachrock layer, along with the absence of marine shells, characterizes it as a beach facies situated within the Lower Backshore or Upper Foreshore zone.

4.4.4. Outcrop VII: Tridacna-outcrop Sur

In the city of Sur, located along the north eastern coastline, an ancient coral reef crops out and spans an area of approximately 900 m^2. This paleo reef is elevated to about 0.5 m above mean high tide, which means it is only submerged during spring tide conditions (Fig. 16a & b). It encompasses a diverse array of coral species and other reef-dwelling organisms (Fig. 16c & d). The most striking are shells of the giant clam *Tridacna*, which are found with articulated valves of up to 18 cm length (Fig. 16e). At the top of the fossil reef a wave-cut platform has developed. The upper surface of the platform experiences currently minimal abrasion, whereas the most seaside edge is eroded and undercut by waves.

Interpretation. The presence of *Tridacna* shells serves as an indicator of the original water depth, which ranged from 0 up to 20 m below sea level at its maximum (Hardy and Hardy, 1969). Today, the giant bivalve *Tridacna* inhabits shallow coral reef areas in the Indo-Pacific region, where it can be found either resting unattached on the seafloor or firmly anchored within coral reefs, using robust byssus threads (Hardy and Hardy, 1969). The latter situation aligns with our discoveries in Sur, where it is presumed that the ancient fossil reef formed within the Lower Shoreface Zone.

5. Discussion

There are two main points that need to be discussed: the question of a potential Mid Holocene sea-level highstand in the area and field evidence for older, most likely Late Pleistocene (MIS 5) coastal deposits.

In a global context, Mid Holocene sea-level highstands are reported (Mauz et al., 2022; Lambeck et al., 2002; Blum et al., 2001), however the spatial timing and amplitude of rsl-changes vary significantly worldwide (Li et al., 2023 and references therein). Khan et al. (2015) give an overview on global Holocene rsl-variations for near-field, intermediate-field and far-field regions. Though they do not provide site-specific data, neither for India nor the Arabian shoreline, comparable far-field regions like south-east Asia, southern China and South America provide evidence for a Mid-Holocene sea-level highstand. The timing ranges from 8 to 4 ka BP and the height from <1 to 6 m (Khan et al., 2015). Additionally, Holocene sea-level highstands are reported worldwide, e.g. from Australia (Lambeck et al., 2002), India (Bhatt and Bhonde, 2006; Nakada and Lambeck, 1987) and America (Blum et al., 2001). In Yemen, directly southwest of Oman, paleo notches and fossils like corals, indicate a Mid Holocene sea-level highstand which exceeded heights of approximately 0.5 to 1 m above pmsl; U-series chronology on in situ found *Porites* sp. and *Acropora* sp. corals dated these deposits to 5 to 5.4 ka (Al-Mikhlafi et al., 2021). A sea-level highstand of 1.6 ± 0.4 m is reported by Mauz et al. (2022) for the Arabian Gulf in the period 6.7–6.0 ka. A potential South Pacific eustatic Late Holocene highstand of 0.9 m above pmsl between 6 and 1.2 ka BP was postulated by Pirazzoli and Montaggioni (1986).

To our knowledge, no prior mapping focussing on deposits that indicate a Holocene sea-level highstand has been undertaken along the coastline of Oman. Nevertheless, some authors, such as Lézine et al. (2002) and Berger et al. (2020) have reported isolated, single findings that were interpreted as indicative of a Holocene sea-level highstand of 1–2 m (Lézine et al., 2002) or 9 m (Berger et al., 2020). Late Holocene marine deposits, approximately 1000 years old, at elevations of up to 15 m above pmsl in the Tiwi-area have been distinctly characterized as extreme wave deposits (Hoffmann et al., 2020b). As such, these deposits near Tiwi are not suitable for reconstructing Holocene rsl. Decker et al. (2021) reported on Holocene lagoonal deposits along the north eastern coast around Ras ar Ru'ays. These 6 ka old paleo mangrove environments are at an elevation above pmsl similar to recent mangrove habitats nearby, thereby excluding a Holocene sea-level highstand during the Mid-Holocene. The marine deposits described here support this, as there is currently no evidence for Holocene shorelines higher than that of the present level. More plausible is that the marine deposits described are associated with a Late Pleistocene sea-level highstand during MIS 5, which has been proven for the area around Sur (Falkenroth et al., 2020). The area is regarded as tectonically stable, an important requirement to disentangle the contributions of various processes (Lambeck et al., 2014, 2002).

We postulate that all coastal deposits described here are of Late Pleistocene age as there is no evidence for a Holocene sea-level highstand in the study area. Several factors support this hypothesis: (a) The coastal profile at Tiwi exhibits an abrasion platform as the uppermost facies, a marine terrace (MIS 5a (Hoffmann et al., 2020a)) belonging to the terraces of the Fins area. Consequently, all underlying layers are significantly older than 82 ka. The echinoderm shells of *Echinometra mathaei* suggest a maximum age of Late Pleistocene, as this is the oldest finding of that species in the eastern Indian Ocean area (Philippe, 1998). (b) In Sur, the paleo notch, along with the associated paleo beach, is located approximately 3.5 m above pmsl. Quartz grains of the paleo beachrock were dated using OSL, leading to an age of 80 ka ± 3 ka and their attribution to MIS 5e (Eemian) (Mauz et al., 2015). The *Tridacna* exposure at the beach lies just above the pmsl. *Tridacna* inhabits water depths ranging from 0 to 20 m (Hardy and Hardy, 1969). The relative elevation difference between the fossil coral reef with in-situ *Tridacnae* and the paleo notch with paleo beach permits the correlation of these exposures. Thus, the *Tridacna* exposure can be assigned to the Late Pleistocene sea-level highstand during MIS 5e. (c) Radiocarbon dating of the *Crassostrea* mussel shell from As Sulayb exceeds the dating method's age limit and therefore provides a minimum age of 45 ka. (d) The deltaic deposits in the upper outcrop areas in Al Haddah and As Sulayb and in the middle part of the outcrop in Ras ar Ru'ays can be correlated with similar facies in a nearby outcrop, studied by Berger et al. (2019). This conglomerate was OSL-dated to 437,983 ± 76,332 BCE and indicates a Pleistocene fluvial-deltaic formation. (e) This coastal section in north eastern Oman is considered tectonically stable, at least within the last 6000 years (Decker et al., 2021). Thus, the coastal profile at Ras ar Ru'ays indicates sea-level oscillations or uplift that must be considerably older than 6000 years.

Evidence of Last Interglacial sea-level highstands are reported worldwide (e.g. Rovere et al., 2023; Boyden et al., 2021; Pedoja et al., 2011; Banerjee, 2000). The results presented here contribute to the ongoing effort to identify new outcrops, develop approaches, investigate past sea-level changes and finally model sea-level scenarios (Chauveau et al., 2024b; Boyden et al., 2023; de Gelder et al., 2022). Such research aligns with initiatives such as the PALSEA project (PALeo constraints on SEA level rise) (Rovere and Dutton, 2021). Most notably amongst the project's outputs, is the recently launched WALIS Explorer database (World Atlas of Last Interglacial Shorelines), introduced by Rovere et al. (2022).

Future research in this area can use the findings from this study as a starting point. Most valuable would be a systematic dating of the sequences described. However, material suitable for dating is limited in this area due to depositional and climate conditions. In particular, recrystallization of primarily aragonitic corals has rendered Uranium-Thorium dating impractical (oral communications, Lars Reuning), as observed at the Tiwi cliff (refer to Section 4.1.), also Kellerhals (1998) encountered similar difficulties with dating in his study area south east of Tiwi. Radiocarbon dating of shells has proven unreliable due to the age of the material exceeding the dating method's limits which lie in the range of 40–45 ka BP (Törnqvist et al., 2015). This same issue was encountered by Moraetis et al. (2018) and Mattern et al. (2018) when endeavouring to establish an age model for the marine terraces near Fins. The dating and correlation of the marine terraces at Fins were

resolved by Hoffmann et al. (2020a), based on an age model using cosmogenic nuclides ^{10}Be and ^{36}Cl. The measurement of the nuclide concentrations reflects the surface exposure, the timespan since when the material, rock or coral, has been exposed to the sun (Ivy-Ochs and Kober, 2008). However, this dating method results in large uncertainties which will hamper its potential in rsl studies. OSL dating poses certain complexities due to the prevalent nature of carbonate deposits, which are the primary source materials for clastic sediments. An exception can be found along the coastline to the south of Ras al Hadd, where igneous source rocks supply quartz and feldspar that could potentially be suitable for OSL dating (Berger et al., 2020). Therefore, this area presents a promising prospect for future dating endeavours.

6. Conclusions

This study is a comprehensive coastal mapping effort covering the shoreline of northeastern Oman, ranging from the area around Muscat in the north to Ras Madraka in the south. The sedimentary deposits documented here, encompassing shallow marine to beach facies, represent coastal formations that are currently situated above mean sea level. These accumulations deviate from their expected locations under current sea-level conditions, suggesting influences such as eustatic sea-level oscillations, coastal uplift, or a combination of both.

In regions with tectonically stable coasts, particularly along the east coast, these deposits likely reflect eustatic sea-level oscillations. Notably, this pattern is observed in the outcrops around Sur, Ras al Hadd, Ras ar Ru'ays, and Ras Madraka. These outcrops provide evidence of an ancient sea-level highstand, approximately 3–4 m above present mean sea level. Dating these deposits proved difficult. Evidence for a Holocene sea-level highstand was not identified. We tentatively assign a Late Pleistocene age to the deposits and argue that they likely formed during MIS 5.

These descriptions serve as an initial orientation and localisation guide for these outcrops, highlighting the potential for further in-depth investigations. In subsequent projects or investigations, all outcrops should be surveyed using Differential Global Positioning System. Additionally, dating of sediments at these sites would provide valuable insights and allow to define sea-level index points. Hereby, these outcrops will become few of the many glimpses into past sea levels that are needed to obtain a verified view into sea-level history worldwide. Only through this we will understand processes and help to estimate future sea-level oscillations.

Funding

VD is grateful for a scholarship provided by the Studienstiftung des deutschen Volkes. Furthermore, this paper stands as a contribution to the IGCP projects 639 and 725.

CRediT authorship contribution statement

V. Decker: Writing – review & editing, Writing – original draft, Visualization, Conceptualization. **M. Falkenroth:** Writing – review & editing, Writing – original draft, Visualization. **G. Hoffmann:** Writing – review & editing, Writing – original draft, Conceptualization.

Declaration of Generative AI and AI-assisted technologies in the writing process

Statement: During the preparation of this work the authors used ChatGPT in order to improve the language and readability. After using this tool/service, the authors reviewed and edited the content as needed and takes full responsibility for the content of the publication.

Declaration of competing interest

The authors declare that they have no known competing financial interests or personal relationships that could have appeared to influence the work reported in this paper.

Data availability

All data used for this work have been collected and processed by ourselves. Additional data related to this article can be found at (https://data.mendeley.com/datasets/6yx52x7cvv/1), an open source online data repository hosted at Mendeley Data.

Acknowledgements

Prof. Dr. Martin Langer (University of Bonn) is thanked for his invaluable assistance in conducting foraminiferal analyses, which includes species identification and interpretation. We are also grateful for his provision of technical support and access to essential equipment. Our acknowledgment extends to Olaf Dülfer (University of Bonn) for his indispensable contributions in the laboratory.

Special thanks are due to Martha Berens (University of Bonn), whose support in the realm of REM pictures and visual preparation has been crucial to this paper. Additionally, we express our gratitude to Edouard Grigowski (University of Bonn) who skillfully processed the 3D model for Ras Madraka II.

Our heartfelt appreciation goes to the Golden Highlands team in Oman for their exceptional logistic support during our field campaigns. We extend our thanks to Kim Hußmann for her tireless efforts and invaluable assistance in managing the fieldwork.

Clare Bamford is gratefully thanked for the English review.

We thank three anonymous reviewers for their time and effort and their critical comments that helped to improve the quality and readability of the manuscript significantly.

References

Al-Farraj, A., 2005. An evolutionary model for sabkha development on the north coast of the UAE. J. Arid Environ. 63 (4), 740–755.

Al-Mikhlafi, A.S., Hibbert, F.D., Edwards, L.R., Cheng, H., 2021. Holocene relative sea-level changes and coastal evolution along the coastlines of Kamaran Island and As-Salif Peninsula, Yemen, southern Red Sea. Quat. Sci. Rev. 252, 106719.

Banerjee, P.K., 2000. Holocene and late Pleistocene relative sea level fluctuations along the east coast of India. Mar. Geol. 167 (3–4), 243–260.

Bange, H.W., Bathmann, U., Behrens, J., Dahlke, F., Ebinghaus, R., Ekau, W., Emeis, K.-C., et al., 2017. Coasts – A Vital Habitat Under Pressure. World Ocean Review: Living with the Oceans 5. Maribus, Hamburg, Germany.

Barlow, N.L., McClymont, E.L., Whitehouse, P.L., Stokes, C.R., Jamieson, S.S., Woodroffe, S.A., Sanchez-Montes, M.L., 2018. Lack of evidence for a substantial sea-level fluctuation within the last Interglacial. Nat. Geosci. 11 (9), 627–634.

Béchennec, F., Le Métour, J., Platel, J.P., Roger, J., 1993. Geological Map of the Sultanate of Oman. Scale 1: 1.000. 000, with Explanatory Notes. Directorate General of Minerals, Oman Ministry of Petroleum and Minerals.

Berger, J.F., Charpentier, V., Crassard, R., Martin, C., Davtian, G., López-Sáez, J.A., 2013. The dynamics of mangrove ecosystems, changes in sea level and the strategies of Neolithic settlements along the coast of Oman (6000–3000 cal. BC). J. Archaeol. Sci. 40 (7), 3087–3104.

Berger, J.F., Guilbert-Berger, R., Marrast, A., Munoz, O., Guy, H., Barra, A., Béarez, P., 2020. First contribution of the excavation and chronostratigraphic study of the Ruways 1 Neolithic shell midden (Oman) in terms of Neolithisation, palaeoeconomy, social-environmental interactions and site formation processes. Arab. Archaeol. Epigr. 31 (1), 32–49.

Bernhard, J.M., Sen Gupta, B.K., 1999. Foraminifera of oxygen-depleted environments. In: Sen Gupta, B.K. (Ed.), Modern Foraminifera. Kluwer Publishers, Great Britain, pp. 201–216.

Bhatt, N., Bhonde, U., 2006. Geomorphic expression of late Quaternary Sea level changes along the southern Saurashtra coast, western India. J. Earth Syst. Sci. 115, 395–402.

Blum, M.D., Misner, T.J., Collins, E.S., Scott, D.B., Morton, R.A., Aslan, A., 2001. Middle Holocene Sea-level rise and highstand at +2 m, Central Texas coast. J. Sediment. Res. 71 (4), 581–588.

Bosworth, W., Taviani, M., 1996. Late Quaternary reorientation of stress field and extension direction in the southern Gulf of Suez, Egypt: evidence from uplifted coral terraces, mesoscopic fault arrays, and borehole breakouts. Tectonics 15 (4), 791–802.

Boyden, P., Weil-Accardo, J., Deschamps, P., Oppo, D., Rovere, A., 2021. Last interglacial sea-level proxies in East Africa and the Western Indian Ocean. Earth Syst. Sci. Data 13, 1633–1651. https://doi.org/10.5194/essd-13-1633-2021.

Boyden, P., Stocchi, P., Rovere, A., 2023. Refining patterns of melt with forward stratigraphic models of stable Pleistocene coastlines. Earth Surf. Dyn. 11 (5), 917–931. https://doi.org/10.5194/esurf-11-917-2023, 2023.

Brasier, M.D., 1980. Microfossils. Allen & Unwin, London.

Burns, S.J., Fleitmann, D., Matter, A., Neff, U., Mangini, A., 2001. Speleothem evidence from Oman for continental pluvial events during interglacial periods. Geology 29 (7), 623–626.

Cerrone, C., Vacchi, M., Fontana, A., Rovere, A., 2021a. Last Interglacial Sea-level proxies in the western Mediterranean. Earth Syst. Sci. Data 13, 4485–4527. https://doi.org/10.5194/essd-13-4485-2021.

Cerrone, C., Ascione, A., Robustelli, G., Tuccimei, P., Soligo, M., Balassone, G., Mormone, A., 2021b. Late Quaternary uplift and sea level fluctuations along the Tyrrhenian margin of Basilicata-northern Calabria (southern Italy): New constraints from raised paleoshorelines. Geomorphology 395, 107978.

Chauveau, D., Authemayou, C., Pedoja, K., Molliex, S., Husson, L., Scholz, D., Aster Team, 2021. On the generation and degradation of emerged coral reef terrace sequences: first cosmogenic 36Cl analysis at Cape Laundi, Sumba Island (Indonesia). Quat. Sci. Rev. 269, 107144. https://doi.org/10.1016/j.quascirev.2021.107144.

Chauveau, D., Pastier, A.M., de Gelder, G., Husson, L., Authemayou, C., Pedoja, K., Cahyarini, S.Y., 2024a. Unravelling the morphogenesis of coastal terraces at Cape Laundi (Sumba Island, Indonesia): Insights from numerical models. Earth Surf. Process. Landf. 49 (2), 549–566. https://doi.org/10.1002/esp.5720.

Chauveau, D., Georgiou, N., Cerrone, C., Dean, S., Rovere, A., 2024b. Sea-level oscillations within the last Interglacial: insights from coral reef stratigraphic forward modelling. Quat. Sci. Rev. 336, 108759. https://doi.org/10.1016/j.quascirev.2024.108759.

Church, J.A., Gregory, J.M., Huybrechts, P., Kuhn, M., Lambeck, K., Nhuan, M.T., Woodworth, P.L., 2001. Changes in sea level. In: Houghton, J.T., Ding, Y., Griggs, D. J., Noguer, M., Van der Linden, P.J., Dai, X., Maskell, K., Johnson, C.A. (Eds.), Climate Change 2001: The Scientific Basis: Contribution of Working Group I to the Third Assessment Report of the Intergovernmental Panel, pp. 639–694.

de Gelder, G., Husson, L., Pastier, A.M., Fernández-Blanco, D., Pico, T., Chauveau, D., Pedoja, K., 2022. High interstadial sea levels over the past 420 ka from the Huon Peninsula, Papua New Guinea. Commun. Earth Environ. 3 (1), 256.

De Giosa, F., Scardino, G., Vacchi, M., Piscitelli, A., Milella, M., Ciccolella, A., Mastronuzzi, G., 2019. Geomorphological signature of late Pleistocene Sea level oscillations in Torre Guaceto marine protected area (Adriatic Sea, SE Italy). Water 11 (11), 2409.

De Santis, V., Scardino, G., Scicchitano, G., Meschis, M., Montagna, P., Pons-Branchu, E., Ortiz, J.E., Sánchez-Palencia, Y., Caldara, M., 2023. Middle-late Pleistocene chronology of palaeoshorelines and uplift history in the low-rising to stable Apulian foreland: Overprinting and reoccupation. Geomorphology 421, 108530.

Decker, V., Falkenroth, M., Lindauer, S., Landgraf, J., Al-Lawati, Z., Al-Rahbi, H., Franz, S.O., Hoffmann, G., 2021. Collapse of Holocene mangrove ecosystems along the coastline of Oman. Quat. Res. 100, 52–76.

Decker, V., Gee, C.T., Schucht, P.J., Lindauer, S., Hoffmann, G., 2022. Life on the edge: a powerful tsunami overwhelmed indian ocean mangroves one millennium ago. Forests 13 (6), 922.

Decker, V., Falkenroth, M., Hoffmann, G., 2024. Dataset for sedimentological evidence of Pleistocene shorelines in Oman. Mendeley Data V1. https://doi.org/10.17632/6yx52x7cvv.1.

Deiana, G., Antonioli, F., Moretti, L., Orrù, P.E., Randazzo, G., Lo Presti, V., 2021. MIS 5.5 highstand and future sea level flooding at 2100 and 2300 in tectonically stable areas of Central Mediterranean Sea: Sardinia and the Pontina Plain (Southern Latium), Italy. Water 13 (18), 2597. https://doi.org/10.3390/w13182597.

Dullo, W.C., 1990. Facies, fossil record, and age of Pleistocene reefs from the Red Sea (Saudi Arabia). Facies 22 (1), 1–45.

Dullo, W.C., 2005. Coral growth and reef growth: a brief review. Facies 51 (1), 33–48. https://doi.org/10.1007/s10347-005-0060-y.

Dumitru, O.A., Dyer, B., Austermann, J., Sandstrom, M.R., Goldstein, S.L., D'Andrea, W. J., et al., 2023. Last interglacial global mean sea level from high-precision U-series ages of Bahamian fossil coral reefs. Quat. Sci. Rev. 318, 108287. https://doi.org/10.1016/j.quascirev.2023.108287.

Dutton, A., Lambeck, K., 2012. Ice volume and sea level during the last interglacial. Science 337 (6091), 216–219.

Dyer, B., Austermann, J., D'Andrea, W.J., Creel, R.C., Sandstrom, M.R., Cashman, M., et al., 2021. Sea-level trends across the Bahamas constrain peak last interglacial ice melt. Proc. Natl. Acad. Sci. USA 118 (33), e2026839118. https://doi.org/10.1073/pnas.2026839118.

Engel, M., Matter, A., Parker, A.G., Parton, A., Petraglia, M.D., Preston, G.W., Preusser, F., 2017. Lakes or wetlands? A comment on 'The middle Holocene climatic records from Arabia: Reassessing lacustrine environments, shift of ITCZ in Arabian Sea, and impacts of the southwest Indian and African monsoons' by Enzel et al. Glob. Planet. Chang. 148, 258–267.

Enzel, Y., Quade, J., Kushnir, Y., 2017. Response to Engel et al.(in press): Lakes or wetlands? A comment on "the middle Holocene climatic records from Arabia: reassessing lacustrine environments, shift of ITCZ in Arabian Sea, and impacts of the southwest Indian and African monsoons" by Enzel et al. 2015. Glob. Planet. Chang. 100 (148), 268–271.

Enzel, Y., Kushnir, Y., Quade, J., 2015. The middle Holocene climatic records from Arabia: Reassessing lacustrine environments, shift of ITCZ in Arabian Sea, and impacts of the southwest Indian and African monsoons. Glob. Planet. Chang. 129, 69–91.

Erlandson, J.M., 2017. Coastlines, Marine Ecology, and Maritime Dispersals in Human History. Human Dispersal and Species Movement: From Prehistory to Present. Cambridge University Press, Cambridge, pp. 147–163.

Ermertz, A., Kázmér, M., Adolphs, S., Falkenroth, M., Hoffmann, G., 2019. Geoarchaeological evidence for the decline of the medieval city of Qalhat, Oman. Open Quat. 5 (8), 1–14.

Falkenroth, M., Schneider, B., Hoffmann, G., 2019. Beachrock as sea-level indicator–a case study at the coastline of Oman (Indian Ocean). Quat. Sci. Rev. 206, 81–98.

Falkenroth, M., Adolphs, S., Cahnbley, M., Bagci, H., Kázmér, M., Mechernich, S., Hoffmann, G., 2020. Biological indicators reveal small-scale sea-level variability during MIS 5e (Sur, Sultanate of Oman). Open Quat. 6 (1), 1–20. https://doi.org/10.5334/oq.72.

Grigowski, E., 2022. 3D Model Ras Madraka 2023. https://sketchfab.com/3d-models/ras-madraka-dcf50a64861747188ae7b15556822548 (Last access 10th December 2023).

Haigh, I.D., Wahl, T., Rohling, E.J., Price, R.M., Pattiaratchi, C.B., Calafat, F.M., Dangendorf, S., 2014. Timescales for detecting a significant acceleration in sea level rise. Nat. Commun. 5 (1), 3635. https://doi.org/10.1038/ncomms4635.

Hardy, J.T., Hardy, S.A., 1969. Ecology of tridacna in Palau. Pac. Sci. 23, 467–472.

Harrison, J.V., 1941. Coastal makran. Geogr. J. 97 (1), 1–15.

Heidarzadeh, M., Satake, K., 2017. A combined earthquake–landslide source model for the tsunami from the 27 November 1945 M w 8.1 Makran Earthquake. Bull. Seismol. Soc. Am. 107 (2), 1033–1040.

Hibbert, F.D., Rohling, E.J., Dutton, A., Williams, F.H., Chutcharavan, P.M., Zhao, C., Tamisiea, M.E., 2016. Coral indicators of past sea-level change: a global repository of U-series dated benchmarks. Quat. Sci. Rev. 145, 1–56.

Hijma, M.P., Engelhart, S.E., Törnqvist, T.E., Horton, B.P., Hu, P., Hill, D.F., 2015. A protocol for a geological sea-level database. Handbook Sea-level Res. 536–553.

Hoffmann, G., Rupprechter, M., Al Balushi, N., Grützner, C., Reicherter, K., 2013. The impact of the 1945 Makran tsunami along the coastlines of the Arabian Sea (Northern Indian Ocean) – A review. Z. Geomorphol. 57 (4), 257–277.

Hoffmann, G., Meschede, M., Zacke, A., Al Kindi, M., 2016. Field Guide to the Geology of Northeastern Oman.

Hoffmann, G., Schneider, B., Mechernich, S., Falkenroth, M., Dunai, T., Preusser, F., 2020a. Quaternary uplift along a passive continental margin (Oman, Indian Ocean). Geomorphology 350, 106870.

Hoffmann, G., Grützner, C., Schneider, B., Preusser, F., Reicherter, K., 2020b. Large Holocene tsunamis in the northern Arabian Sea. Mar. Geol. 419, 106068.

Imbrie, J., Imbrie, J.Z., 1980. Modeling the climatic response to orbital variations. Science 207 (4434), 943–953.

Imbrie, J., Hays, J., Martinson, D., McIntyre, A., Mix, A., Morley, J.J., Pisias, N., Prell, W., Shackleton, N., Berger, A., Kukla, G., Saltzman, B., 1984. In: Milankovitch, Climate, Berger, A., et al. (Eds.), The Orbital Theory of Pleistocene Climate: Support from a Revised Chronology of the Marine d18O Record. Kluwer Academic Publishers (Nato ASI Ser. C), Dordrecht, pp. 269–305.

IPCC, 2023. Sections. In: Core writing Team, Lee, H., Romero, J. (Eds.), Climate Change 2023: Synthesis Report. Contribution of Working groups I, II and III to the Sixth. Assessment Report of the Intergovernmental Panel on climate Change. IPCC, Geneva, Switzerland, pp. 35–115. https://doi.org/10.59327/IPCC/AR6-9789291691647.

Ivy-Ochs, S., Kober, F., 2008. Surface exposure dating with cosmogenic nuclides. E&G Quat. Sci. J. 57 (1/2), 179–209.

Kellerhals, P., 1998. Ice Age Related Erosional and Depositional Processes. Examples from the Late Proterozoic and Quaternary, Sultanate of Oman.

Khan, N.S., Ashe, E., Shaw, T.A., Vacchi, M., Walker, J., Peltier, W.R., Kopp, R.E., Horton, B.P., 2015. Holocene relative sea-level changes from near-, intermediate-, and far-field locations. Curr. Clim. Chang. Rep. 1, 247–262.

Kukowski, N., Schillhorn, T., Flueh, E.R., Huhn, K., 2000. Newly identified strike-slip plate boundary in the northeastern Arabian Sea. Geology 28 (4), 355–358.

Kwarteng, A.Y., Dorvlo, A.S., Vijaya Kumar, G.T., 2009. Analysis of a 27-year rainfall data (1977–2003) in the Sultanate of Oman. Int. J. Climatol. 29, 605–617.

Lajoie, K.R., 1986. Coastal tectonics. Active Tecton. 95–124.

Lambeck, K., Esat, T.M., Potter, E.K., 2002. Links between climate and sea levels for the past three million years. Nature 419 (6903), 199–206.

Lambeck, K., Rouby, H., Purcell, A., Sun, Y., Sambridge, M., 2014. Sea level and global ice volumes from the last Glacial Maximum to the Holocene. Proc. Natl. Acad. Sci. 111 (43), 15296–15303.

Lézine, A.M., Saliège, J.F., Mathieu, R., Tagliatela, T.L., Mery, S., Charpentier, V., Cleuziou, S., 2002. Mangroves of Oman during the late Holocene; climatic implications and impact on human settlements. Veg. Hist. Archaeobotany 11, 221–232.

Lézine, A.M., Ivory, S.J., Braconnot, P., Marti, O., 2017. Timing of the southward retreat of the ITCZ at the end of the Holocene Humid Period in Southern Arabia: Data-model comparison. Quat. Sci. Rev. 164, 68–76.

Li, T., Chua, S., Tan, F., Khan, N.S., Shaw, T.A., Majewski, J., Horton, B.P., 2023. Glacial Isostatic Adjustment modelling of the mid-Holocene Sea-level highstand of Singapore and Southeast Asia. Quat. Sci. Rev. 319, 108332.

Mattern, F., Moraetis, D., Abbasi, I., Al Shukaili, B., Scharf, A., Claereboudt, M., Looker, E., Al Haddabi, N., Pracejus, B., 2018. Coastal dynamics of uplifted and emerged late Pleistocene near-shore coral patch reefs at fins (eastern coastal Oman, Gulf of Oman). J. Afr. Earth Sci. 138, 192–200.

Mauz, B., Vacchi, M., Green, A., Hoffmann, G., Cooper, A., 2015. Beachrock: a tool for reconstructing relative sea level in the far-field. Mar. Geol. 362, 1–16.

Mauz, B., Shen, Z., Alsuwaidi, M., Melini, D., Spada, G., Purkis, S.J., 2022. The mid-Holocene sea-level change in the Arabian Gulf. Holocene 32 (11), 1173–1183. https://doi.org/10.1177/09596836221114291.

McGranahan, G., Balk, D., Anderson, B., 2007. The rising tide: assessing the risks of climate change and human settlements in low elevation coastal zones. Environ. Urban. 19 (1), 17–37. https://doi.org/10.1177/0956247807076960.

McLachlan, A., Fisher, M., Al-Habsi, H.N., Al-Shukairi, S.S., Al-Habsi, A.M., 1998. Ecology of sandy beaches in Oman. J. Coast. Conserv. 4, 181–190.

Milankovitch, M.M., 1941. Canon of insolation and the iceage problem. Koniglich Serbische Akademice Beograd Special Publ. 132.

Milne, G.A., 2009. Using models to inform the field community: Far-field Sea level data applications. AGES News 17 (2), 56–57.

Milne, G.A., Mitrovica, J.X., 2008. Searching for eustasy in deglacial sea-level histories. Quat. Sci. Rev. 27 (25–26), 2292–2302.

Mitrovica, J.X., Milne, G.A., 2002. On the origin of late Holocene Sea-level highstands within equatorial ocean basins. Quat. Sci. Rev. 21 (20−22), 2179–2190.

Mitrovica, J.X., Peltier, W.R., 1991. On postglacial geoid subsidence over the equatorial oceans. J. Geophys. Res. Solid Earth 96 (B12), 20053–20071.

Moraetis, D., Mattern, F., Scharf, A., Frijia, G., Kusky, T.M., Yuan, Y., El-Hussain, I., 2018. Neogene to Quaternary uplift history along the passive margin of the northeastern Arabian Peninsula, eastern Al Hajar Mountains, Oman. Quat. Res. 90, 418–434.

Muko, S., Kawasaki, K., Sakai, K., Takasu, F., Shigesada, N., 2000. Morphological plasticity in the coral Porites sillimaniani and its adaptive significance. Bull. Mar. Sci. 66 (1), 225–239.

Murray, J.W., 1991. Ecology and Paleoecology of Benthic Foraminifera. Longman, Harlow, p. 397.

Nakada, M., Lambeck, K., 1987. Glacial rebound and relative sea-level variations: a new appraisal. Geophys. J. Int. 90 (1), 171–224.

Normand, R., Simpson, G., Herman, F., Biswas, R.H., Bahroudi, A., Schneider, B., 2019. Dating and morpho-stratigraphy of uplifted marine terraces in the Makran subduction zone (Iran). Earth Surf. Dyn. 7 (1), 321–344.

Oppenheimer, M., Glavovic, B.C., Hinkel, J., van de Wal, R., Magnan, A.K., Abd-Elgawad, A., Cai, R., Cifuentes-Jara, M., DeConto, R.M., Ghosh, T., Hay, J., Isla, F., Marzeion, B., Meyssignac, B., Sebesvari, Z., 2019. Sea level rise and implications for low-lying islands, coasts and communities. In: Pörtner, H.-O., Roberts, D.C., Masson-Delmotte, V., Zhai, P., Tignor, M., Poloczanska, E., Mintenbeck, K., Alegría, A., Nicolai, M., Okem, A., Petzold, J., Rama, B., Weyer, N.M. (Eds.), IPCC Special Report on the Ocean and Cryosphere in a Changing Climate. Cambridge University Press, Cambridge, UK and New York, NY, USA, pp. 321–445. https://doi.org/10.1017/9781009157964.006.

Oveisi, B., Lavé, J., van der Beek, P., 2007. Rates and processes of active folding evidenced by Pleistocene terraces at the central Zagros front (Iran). In: Thrust Belts and Foreland Basins: From Fold Kinematics to Hydrocarbon Systems. Springer, Berlin Heidelberg, pp. 267–287.

Paillard, D., 2010. Climate and the orbital parameters of the Earth. Compt. Rendus Geosci. 342 (4–5), 273–285. https://doi.org/10.1016/j.crte.2009.12.006.

Parker, J.H., Gischler, E., Eisenhauer, A., 2012. Biodiversity of foraminifera from late Pleistocene to Holocene coral reefs, South Sinai, Egypt. Mar. Micropaleontol. 86, 59–75.

Pavlopoulos, K., Moraetis, D., Foumelis, M., Scharf, A., Mattern, F., Forman, S., Papageorgiou, E., de Gelder, G., 2023. Uplift dynamics of the obducted northeastern continental margin of the Arabian Peninsula, Sultanate of Oman. Geochem. Geophys. Geosyst. 24 (11), e2023GC011054. https://doi.org/10.1029/2023GC011054.

Pedoja, K., Husson, L., Regard, V., Cobbold, P.R., Ostanciaux, E., Johnson, M.E., Delcaillau, B., 2011. Relative Sea-level fall since the last interglacial stage: are coasts uplifting worldwide? Earth Sci. Rev. 108 (1–2), 1–15. https://doi.org/10.1016/j.earscirev.2011.05.002.

Pedoja, K., Husson, L., Johnson, M.E., Melnick, D., Witt, C., Pochat, S., Garestier, F., 2014. Coastal staircase sequences reflecting sea-level oscillations and tectonic uplift during the Quaternary and Neogene. Earth Sci. Rev. 132, 13–38. https://doi.org/10.1016/j.earscirev.2014.01.007.

Peltier, W.R., 1999. Global sea level rise and glacial isostatic adjustment. Glob. Planet. Chang. 20 (2–3), 93–123.

Peters, T., Battashy, M.A., Bläsi, H., Hauser, M., Immenhauser, A., Moser, L., Rajhi, A.A., 2000. Geological Map of SUR and AL ASHKHARAH. Expanatory Notes. Sultanate of Oman, Ministry of Commerce and Industry, Directorate General of Minerals.

Petraglia, M.D., Parton, A., Groucutt, H.S., Alsharekh, A., 2015. Green Arabia: Human prehistory at the crossroads of continents. Quat. Int. 382, 1–7.

Philippe, M., 1998. Les Échinides Miocènes du bassin du Rhône: révision systématique. Première partie. Publ. du musée des Confluences 36 (1), 3–241.

Pirazzoli, P.A., 1993. Global sea-level changes and their measurement. Glob. Planet. Chang. 8 (3), 135–148.

Pirazzoli, P.A., Montaggioni, L.F., 1986. Late Holocene Sea-Level changes in the Northwest Tuamotu Islands, French Polynesia1. Quat. Res. 25 (3), 350–368.

Pirazzoli, P.A., Reyss, J.L., Fontugne, M., Haghipour, A., Hilgers, A., Kasper, H.U., Radtke, U., 2004. Quaternary coral-reef terraces from Kish and Qeshm Islands, Persian Gulf: new radiometric ages and tectonic implications. Quat. Int. 120 (1), 15–27.

Preusser, F., Radies, D., Driehorst, F., Matter, A., 2005. Late Quaternary history of the coastal Wahiba sands, Sultanate of Oman. J. Quat. Sci.: Publ. Quat. Res. Assoc. 20 (4), 395–405.

Reyss, J.L., Pirazzoli, P.A., Haghipour, A., Hatte, C., Fontugne, M., 1999. Quaternary marine terraces and tectonic uplift rates on the south coast of Iran. Geol. Soc. Lond. Spec. Publ. 146 (1), 225–237.

Rohling, E.J., Hibbert, F.D., Grant, K.M., Galaasen, E.V., Irvalı, N., Kleiven, H.F., Yu, J., 2019. Asynchronous Antarctic and Greenland ice-volume contributions to the last interglacial sea-level highstand. Nat. Commun. 10 (1), 5040. https://doi.org/10.1038/s41467-019-12874-3.

Rose, J.I., Usik, V.I., Marks, A.E., Hilbert, Y.H., Galletti, C.S., Parton, A., Roberts, R.G., 2011. The Nubian complex of Dhofar, Oman: an African middle stone age industry in southern Arabia. PLoS One 6 (11), e28239.

Rovere, A., Dutton, A., 2021. PALSEA: 13 years of ice-sheet and sea-level science. Past Global Changes Magazine 29 (1), 18–20. https://doi.org/10.22498/pages.29.1.18. https://pastglobalchanges.org/publications/pages-magazines/pages-magazine/13246.

Rovere, A., Raymo, M.E., Vacchi, M., Lorscheid, T., Stocchi, P., Gomez-Pujol, L., Hearty, P.J., 2016a. The analysis of last Interglacial (MIS 5e) relative sea-level indicators: Reconstructing Sea-level in a warmer world. Earth Sci. Rev. 159, 404–427.

Rovere, A., Stocchi, P., Vacchi, M., 2016b. Eustatic and relative sea level changes. Curr. Clim. Chang. Rep. 2, 221–231.

Rovere, A., Ryan, D.D., Vacchi, M., Dutton, A., Simms, A., Murray-Wallace, C., 2022. Introducing WALIS, the World Atlas of last Interglacial Shorelines Version 1.0. In EGU General Assembly Conference Abstracts (pp. EGU22-2489).

Rovere, A., Ryan, D.D., Vacchi, M., Dutton, A., Simms, A.R., Murray-Wallace, C.V., 2023. The world atlas of last interglacial shorelines (version 1.0). Earth Syst. Sci. Data 15 (1), 1–23.

Saber, M., Kantoush, S.A., Sumi, T., Ogiso, Y., Alharrasi, T., Koshiba, T., Hadidi, A., 2022. Integrated Study of Flash Floods in Wadi Basins considering Sedimentation and climate Change: An International Collaboration Project. Wadi Flash Floods: Challenges and Advanced Approaches for disaster Risk Reduction, 401-422. In: Sumi, T., et al. (Eds.), Wadi Flash Floods, Natural Disaster Science and Mitigation Engineering: DPRI Reports. Springer. https://doi.org/10.1007/978-981-16-2904-4_15.

Sana, A., Chitrakar, P., Baawain, M., Al-Mamun, A., 2023. Baseline Measurements of Waves and Currents along the Coast of Oman. J. Marine Sci. Eng. 11 (9), 1711. https://doi.org/10.3390/jmse11091711.

Shannon, C.E., Weaver, W., 1949. The Mathematical Theory of Communication. The University of llinois Press, Urbana, p. 117.

Small, C., Nicholls, R.J., 2003. A global analysis of human settlement in coastal zones. J. Coast. Res. 584-599. https://doi.org/10.2307/4299200.

Spada, G., 2017. Glacial isostatic adjustment and contemporary sea level rise: an overview. Integr. Study Mean Sea Level Comp. 155–187.

Steffen, H., Wu, P., 2011. Glacial isostatic adjustment in Fennoscandia—a review of data and modeling. J. Geodyn. 52 (3–4), 169–204.

Törnqvist, T.E., Rosenheim, B.E., Hu, P., Fernandez, A.B., 2015. Radiocarbon dating and calibration. Handbook Sea-Level Res. 347–360.

Williams, A.H., Walkden, G.M., 2002. Late Quaternary highstand deposits of the southern Arabian Gulf: a record of sea-level and climate change. Geol. Soc. Lond. Spec. Publ. 195 (1), 371–386.

Wyns, R., Le Métour, J., Roger, J., Chevrel, S., 1992. Geological Map of Sur 1:250,000, Sheet NF 40–08, Explanatory Notes. Ministry of Petroleum and Minerals, Directorate General of Minerals, Muscat, Oman, p. 80.

Yokoyama, Y., Purcell, A., 2021. On the geophysical processes impacting palaeo-sea-level observations. Geosci. Lett. 8, 13. https://doi.org/10.1186/s40562-021-00184-w.

6. Resumée

6.1 Discussion

Evidence of Quaternary climate variations and of significant sea-level fluctuations over the past 130,000 years was identified along the coastlines of northeastern Oman. Sea-level fluctuation appear as long-term and short-term water-level changes. Long-term relative sea-level changes result from a combination of interacting processes, including insolation- and climatic-driven eustatic variations, isostatic adjustments and vertical tectonic movements (Rovere et al. 2016b; Lambeck 2002). Climatic dynamics influence oceanographic dynamics and generate a complex, spatially and temporally variable sea-level signal (Lambeck 2002). Consequently, it is crucial to consider all these local, regional, and global drivers while collecting data on past sea-level records and interpreting them. These studies examine the Last Interglacial (LIG) transgression during MIS 5e, approximately 130–120 ka BP, and consider a debated transgression within the timeframe of 8–6 ka BP. Hereby, mainly sedimentological techniques were used. Especially, the investigations on LIG shorelines is based on the identification and detailed sedimentological description of coastal outcrops in northeastern Oman. Eight locations were identified with deposits that clearly indicate lithogenesis associated with a marine environment. The distinct sedimentary units were classified into lithofacies, representing depositional environments ranging from shallow marine intertidal flats to sections of a typical coastal profile, including beach facies from the backshore and upper foreshore, as well as remnants indicative of lower foreshore and shoreface conditions. At Ras Ar Ru'ays on the east coast, for example, the sediment profile contains a foraminiferal fauna with species that clearly indicate a shallow marine, intertidal environment. These species are considered epibenthic, living attached to substrates such as algae. Beach facies were found as beachrocks in both the north, on the Daymaniyat Islands, and in the southeast near Ras Madraka. In the east, at Ras Al Hadd, beachrock is also present, though here it is heavily bioturbated and contains rounded structures, such as corals in the upper layers, suggesting deposition in an intertidal to subtidal setting. Fossil intertidal to subtidal facies are also exposed in Sur, where *Tridacna* shells are embedded in a fossil coral reef. Dating of these deposits showed difficulties. The attempt to 14C-date one *Crassostrea*-mollusc shell proved the marine deposits older than 45 ka. Falkenroth et al. (2020) examined a notch in Sur Lagoon and could prove a LIG sea-level highstand to 3.93 ± 0.12 m above pmsl. This area around Sur and along the east coast is considered tectonically stable (Decker et al. 2021; Falkenroth et al. 2020).

The identified paleo-marine deposits are located 3–4 m above pmsl. Assuming similar depositional processes, these deposits are attributed to the last verified sea-level highstand during MIS 5e. Although robust chronological control and precise altimetric measurements are still lacking and require further investigation, the findings already represent a valuable contribution to the ongoing global effort to document LIG shorelines (Rovere et al. 2023; 2022).

In addition to the transgression phase during the Late Pleistocene, around 130 ka ago, evidence of an Early to Mid-Holocene global sea-level highstand has been reported (Khan et al. 2015; Lambeck et al. 2002). A climatic optimum followed the LGM, marking the onset of the Holocene. With the rise in global temperatures, the melting of continental ice sheets led to a significant eustatic sea-level rise, primarily between ca. 16.5 ka BP and 8.2 ka BP. This rise continued at a much slower and

gradually declining rate until around 2.5 ka BP (Lambeck et al. 2014). During and after the glacial melting, GIA processes became increasingly relevant (Lambeck 2002). When investigating relative sea-level changes globally, the impact of forebulge dynamics is considered, and regions are classified based on their distance from the former northern hemisphere ice sheet margins into near-, intermediate-, and far-field zones (Nakada et al. 2016; Lambeck et al. 2014). The study area in question falls within the intermediate-field, similar to regions such as Indonesia and Central America (Nakada et al. 2016). According to Lambeck et al. (2014), there is no compelling evidence for a global eustatic sea-level highstand exceeding pmsl by more than minor oscillations of 15-20 cm. However, some studies do suggest the existence of a relative Holocene highstand above present levels (Tian et al. 2025; Mannaa & Jones 2024; Clement et al. 2016). For the coastlines of Oman, a Holocene sea-level highstand occurring between approximately 8 and 6 ka BP is under active scientific debate. Highstands of up to 9 m above pmsl (Berger et al. 2013), a highstand of 2 to 3 m (Teillet et al. 2025) or a “slight seawater incursion” (Lézine et al. 2002) are discussed.
Regarding Early to Mid-Holocene climate, geological records prove a shift to a warm and wet period in the tropics and subtropics (Axelsson 2024; Lüning & Vahrenholt 2018; Fleitmann et al. 2007). The pluvial period is attributed to a shift and intensification of the ISM belt (Axelsson 2024; Lüning & Vahrenholt 2018). But it is unsure how far northward the ITCZ has shifted and how much more precipitation was received (Fleitmann et al. 2022; 2007 and references therein). The shift back to the recent ITCZ position and the associated climate change is not finally understood, some records suggest a gradual transition, some a rather abrupt change to the recent more arid climate in this region (Lézine et al. 2014).
Decker et al. (2021) address both the debated question of a potential Holocene sea-level highstand and the broader research on Holocene climate fluctuations. The approach employed a novel proxy, paleo-mangroves, due to their dual value: their sensitivity to soil salinity makes them effective precipitation indicators, while their strict growth limitation to the intertidal zone renders them reliable sea-level indicators.
Research results published in Decker et al. (2021) built upon the palynological work of Lézine et al. (2002), who revealed that during the Early to Mid-Holocene, mangrove-fringed lagoons existed along the eastern Omani coastline near Ras Ar Ru’ays. Importantly, two mangrove species were identified: *Rhizophora mucronata* and *Avicennia marina*. The more salinity-sensitive *R. mucronata* became locally extinct during the Mid-Holocene, while *A. marina* populations declined significantly and survived at relict sites in Oman. Taking this into account, the paleo-lagoon near Ras Ar Ru’ays was investigated and additional paleo-mangrove sites along the northern and eastern coasts of Oman were identified. The investigations reveal the spatial changes in distribution through time and altimetric Differential GPS measurements determine the elevation of former mangrove stands. These elevations were found to be comparable to modern mangrove elevations in relation to pmsl. Assuming negligible sediment compaction, as supported by sedimentological and geochemical evidence, sea level appears to have remained relatively stable since the Early to Mid-Holocene, with possible fluctuations limited to the centimeter scale. This contradicts other studies that, based on various proxies and factors, suggest a Mid-Holocene sea-level highstand, with estimated elevations varying considerably, from marginally above pmsl, to 2–3 m, up to 8–9 m (Teillet et al. 2025; Berger et al. 2013; Lézine et al. 2002). Sedimentological, geochemical, and granulometric analyses conducted in the study of Decker et al. (2021) reveal that these former lagoons were

abruptly infilled by aeolian sands, leading to a rapid transition to sabkha environments. This instant shift likely occurred over just a few decades, representing a tipping point that led to the collapse of local mangrove ecosystems.
Archaeological evidence, such as coastal shell middens, confirms that humans inhabited the Omani coastline during this time. This suggests that human activity interacted with these ecosystems and may have played a role in the decline of the mangroves. These communities utilized mangroves for various purposes: hunting grounds, firewood, and later charcoal production, yet there is no indication that they overexploited these resources. (Decker et al. 2019; Cleuziou & Tosi 2007). Additionally, the near-synchronous collapse of mangrove ecosystems across the region, coupled with the survival of the more salinity-tolerant species, suggests that human activity was not the primary driver of ecosystem decline.
In conclusion, neither sea-level regression nor anthropogenic influence appears to have driven the widespread mangrove decline around 6 ka BP. Instead, aridification processes likely reached a critical threshold at this time, triggering a regional mangrove collapse.

During the fieldwork campaigns several coastal outcrops along the northern and eastern margins of Oman were identified that reflect a former sea-level highstand. However, all evidence suggests these outcrops correspond to the LIG highstand rather than to the Holocene. Given the absence of Holocene-specific indicators, the hypothesis of a significant Holocene sea-level highstand in northeastern Oman is rejected (Decker et al. 2024, 2021). This conclusion aligns with the findings of Lambeck et al. (2014), who argue that in the last 6,000 years, prior to the onset of anthropogenic sea-level rise approximately 100–150 years ago, there is no evidence for eustatic sea-level fluctuations lasting longer than ca. 200 years or exceeding amplitudes of 15–20 cm.
The findings contribute to the global effort to better understand GIA processes in near-, intermediate- and far-field areas by providing new data from an intermediate-field region.

The third time window provides insight into a very recent and short-lived sea-level change. It concerns a sediment layer in the lagoon of Sur, previously interpreted as tsunamigenic, however, its age had not yet been securely constrained (Donato et al. 2009, 2008). Attempts at dating relied on mollusc shells, which are problematic due to the potential influence of marine reservoir effects, an uncertainty not always quantifiable (Douka 2017). The investigations revealed elongated wood fragments associated with the tsunami layer, measuring several decimeters in length and a few centimeters in diameter. These fragments were aligned in a NNW orientation, toward the MSZ, the likely tsunami source (Decker et al. 2022). Radiocarbon dating of the wood, which is generally more comfortable than shell dating, yielded an age of approximately 1,000 y BP. This places the deposits in temporal correlation with the tsunamigenic boulders and imbricated deposits described by Hoffmann et al. (2020a).

The findings enabled the first definitive dating of the previously identified tsunamigenic layer within the Sur lagoon. Furthermore, it was hypothesized that the recovered wood fragments originated from mangroves, a proposition verified through anatomical analysis of their internal structure. After 1,000 years of preservation in brackish water, the wood was extremely fragile, requiring significant methodological adaptation for histological sectioning, as existing preparation

protocols proved partly inadequate. Consequently, this methodological contribution may benefit future studies facing similar challenges in sample preparation. Microscopic analysis identified the wood as *Avicennia marina*, confirming the presence of mangrove stands in Sur around 1,000 years ago. This represents an important paleo-ecological record, as data on historical mangrove distribution in Oman remains scarce and is limited to palynological analyses (Lézine et al. 2014; Lézine 2009). Understanding the past distribution of mangroves also informs current discussions on their resilience to climate change and sea-level rise, processes whose impact on Oman's mangroves remains poorly understood. Contemporary measurements indicate that *Avicennia marina* in Oman exhibits a vertical accretion rate of 0–1 mm per year (Saintilan et al. 2020). In contrast, the global average sea-level rise currently stands at approximately 4.2 mm per year (IPCC 2023). Whether this rate already exceeds the adaptive threshold of natural mangrove systems in Oman - and may eventually lead to their decline - remains a subject of active debate.

6.2 Conclusions

The aim of this thesis was to investigate the northeastern coastline of Oman for archives of past climate variability and sea-level oscillations.
The study area extends from the Daymaniyat Islands in the north, across Ras Al Hadd, to Ras Madraka in the southeast. The research outcomes aim to improve our understanding of geological processes and contribute to more robust projections of future environmental scenarios.
This aim has been achieved, and the main conclusions of this thesis can be summarized as follows:

- **Several coastal outcrops along northeastern Oman indicate a paleo-sea-level highstand of approximately 3–4 meters above present mean sea level tentatively assigned to the Last Interglacial period (ca. 125,000 years ago, Marine Isotope Stage 5e).** These outcrops were identified, geologically and sedimentologically described, and in some cases further analyzed using micropaleontological methods. A radiocarbon dating attempt on one sample revealed that the material was beyond the ^{14}C dating limit (> 45,000 years BP). Based on regional correlation with previously dated facies, these deposits are attributed to the Last Interglacial.

- **Investigations of paleo-lagoonal environments containing paleo-mangrove horizons suggest that sea level during the Mid-Holocene (ca. 6,000 years ago) was near present-day levels.** This conclusion is based on radiocarbon (^{14}C) dating, combined with sedimentological and geochemical analyses, as well as centimetre-precise elevation measurements of the paleo-mangrove horizons using a Differential GPS. These elevation data were compared to the modern intertidal distribution of *Avicennia marina* in the study area. A previously proposed Mid-Holocene sea-level highstand is not supported by the findings and can thus be refused.
  The sedimentological records reveals a distinct and relatively abrupt shift in depositional conditions, from lagoonal systems to coastal sabkha environments. Potential drivers of this transition include sea-level fluctuation, anthropogenic influence and climate change. A sea-level fluctuation can be excluded by these findings. Human populations inhabited that

region at that time and utilized mangrove resources, though, there is no evidence for overexploitation. **Thus, the explanation for the sudden decline of the mangrove ecosystems 6,000 years ago is a climatic shift. Increasing aridity likely pushed the ecosystems beyond a critical threshold, ultimately leading to their collapse.**

- **In the Sur Lagoon, a previously described but undated sediment layer interpreted as tsunami-related was successfully dated and attributed to a tsunami event approximately 1,000 years ago.** Likely triggered by seismic activity within the Makran Subduction Zone in the Gulf of Oman, this event generated a wave estimated to reach up to 15 meters in height, causing widespread coastal destruction. The tsunami left a ca. 10 cm thick shell debris layer in the lagoon. The lower part of this deposit includes woody axes suitable for radiocarbon dating. **Histological analyses identified the wood as *Avicennia marina*, thus confirming the presence of a mangrove stand at this site ca. 1,000 years ago.**

6.3 Future research directions

The research conducted between 2017 and 2024 yielded valuable insights into Late Quaternary climate variability and sea-level fluctuations along the northeastern coast of Oman. The investigations identified promising sea-level proxies and opened up further research questions, with several outcrops showing potential for more detailed analysis.

A major challenge remains the chronological classification of some key sedimentary sequences. This is particularly true for the outcrops described in Decker et al. (2024), where absolute dating proved inconclusive. Although sufficient for the present study, which centered on detection of such deposits and their sedimentologically desciption, it leaves room for future research. The difficulty lies in the lack of suitable dating material. The deposits are presumed to belong to the LIG (ca. 125,000 years ago), for which OSL dating would be the appropriate method. However, these sediments are notably poor in quartz, necessitating the identification of sites with suitable mineralogical composition for reliable OSL analysis.

As part of the investigation of paleo-lagoonal systems with mangrove horizons, a preliminary survey was carried out on the Bar al Hikman Peninsula. A trench approximately 3 m long and 1.35 m deep was excavated and described in detail. The promising results were included in the Bachelor's thesis of Vivian Henke (University of Bonn, 2020) and a student research project at GUtech (German University of Technology in Muscat, Oman, 2020). Although the area today represents a coastal sabkha environment, the trench revealed fossil *Cerithidea cingulata* and, across the deflation surface, *Terebralia palustris* shells, both of which are well-known mangrove-associated gastropods (Tomlinson 2016; Bosch et al. 1995). A radiocarbon date from organic material at 75 cm depth yielded an age of 7,133-7,006 cal y BP. Previous work on Bar al Hikman has focused on various aspects: Lézine et al. (2017) examined pollen to reconstruct the retreat of the ITCZ, Charpentier et al. (2012) studied archaeological sites and paleo-shorelines and Teillet et al. (2025) recently investigated the local carbonate systems. However, the position of the Holocene paleo-shoreline remains ambiguous, and further multidisciplinary research is needed.

Reconstructing the dynamics of the ITCZ remains a complex task, but the palynological approach is particularly valuable. More data are needed to better understand the north–south transition of the

ITCZ. Recent insights from Horisk et al. (2023) for the Dhofar region demonstrate the potential of this approach. This mangrove project also initiated a cooperation with Prof. Hermann Behling (Head of the Department of Palynology and Climate Dynamics, University of Göttingen, Germany) with the aim of supplementing the current dataset through additional pollen analyses to achieve a more comprehensive reconstruction of past vegetation dynamics. Unfortunately, time constraints delayed the processing and evaluation of these samples, leaving this as a potential future research direction. A comparative study along a north–south transect along the west coast of India would also be valuable. Such a comparison would be particularly insightful given the correlations between the eastern coast of Oman and the western coast of India, in terms of monsoonal dynamics as well as in sea-level histories. Both regions have been affected by short-term events, such as tsunamis originating from the Makran Subduction Zone (Prizomwala et al. 2018; Hoffmann et al. 2013a). Additionally, the coastlines along the Indian Ocean represent a valuable research area for long-term sea-level changes, as they lie within the understudied intermediate-field distance from the margins of the Pleistocene ice sheets.
Further work on sedimentological and micropaleontological features is ongoing. In 2025, Hannah Wiesenthal (TU Darmstadt, Germany) completed a Bachelor's thesis under the supervision of Dr. Michaela Falkenroth (co-author on two of the publications in this thesis). The Bachelor's thesis provides a detailed description of the coastal profile at Ras Ar Ru'ays, focusing on bioturbation structures and fine-scale sedimentary features and reconstructs the diagenetic context to interpret the paleo-environment. Thin-section analysis confirmed the presence of foraminifera in all analyzed layers. Given their value as indicators of paleo-environmental parameters, foraminiferal analysis represents a promising opportunity for future research here. Outcrops at the Daymaniyat Islands, Bar al Hikman, and Ras Madraka have also shown high potential for micropaleontological analysis and should be further investigated in terms of their foraminiferal content.

Oman is shaped by dynamic climatic and sea-level histories and is exposed to various natural hazards, including tsunamis and tropical cyclones. The country now faces growing challenges: while population and urbanization increase and living standards improve, ongoing aridification and more frequent extreme weather events are making life increasingly difficult. In a world experiencing accelerating sea-level rise and intensifying weather extremes, exacerbated by anthropogenic climate change, sustained geological research is essential. Such research enhances our ability to assess future changes and deepens our understanding of the interconnected processes within the geosphere, biosphere, hydrosphere and asthenosphere, thereby helping to preserve or restore the capacity to respond and adapt effectively - because everything is linked.

7. Acknowledgements

This work marks the end of a long and winding road. Looking back on that meandering path, I wouldn't want to miss a single bend. It was a long, but no lonesome road. So many people and experiences lit the way, and the very most of them were truly wonderful. Here, I'd like to acknowledge the most meaningful travel mates I had along the way.

My deepest gratitude goes to Gösta Hoffmann for being my mentor and for teaching me how to read landscapes, as well as how to apply for funding and publish scientific papers. Thank you, Gösta, for making my dream come true and giving me the opportunity to travel the world - without spending too much money. Thank you also for always encouraging your research group to attend conferences and for making sure we felt like part of the scientific community. It was incredible to experience, even as a student, what it means to be valued and to truly belong to a research team. Thank you as well for showing me that sometimes dogs are cats, and for allowing Dita and Joscha to join me on so many amazing excursions. The most important lessons you've taught me are to radiate confidence in crucial moments - I hope that works out during the exam - and to make sure you only do what brings you joy. If you follow that latter advice, no day is ever wasted.

My honest thanks go to Peter Kukla for being my second supervisor. Thank you for all your support and also for the wonderful times and memorable evenings we shared in Oman at the campfire. I am deeply grateful for your unwavering support and your steadfast belief in me that this thesis would be completed.

Thank you to my wonderful family, especially, to Mama and Papa, my sister Juliana and my aunt Franziska for their unwavering support. After initially being a bit stunned that I chose such an unconventional field of study like geoscience, you grew more and more interested. I'm so happy that you now support what I'm doing and what I love. Thank you for believing in me and, over the past few years, at least most of the time, in my ability to finish this work.

My heartfelt thanks go to Kim, my very best friend from day one of the university introduction. Even back then, the champagne tasted perfect together. Thank you for all the wonderful moments we've shared and the unforgettable excursions - in Germany, across Europe, and in Oman. I am deeply grateful for all your help and support, also during the tougher times. Thank you for always being there for me.

As well, I'd like to thank my friend Michi for the amazing times in Oman - our girls' fieldwork trip will always remain unforgettable. Thank you for your scientific support with research, writing, and publishing, as well as for your psychological support during those moments when the scientific side of things became too burdening.

A huge thank you to our fantastic OutcropWizard workgroup, especially Eddi, Bine and Martha. Without the 30 Geotope^3 project, this thesis would probably have been finished two years earlier, but I wouldn't know how to fly a drone or edit videos - and we would have missed out on so much along the way.

I also thank all the wonderful people I met at conferences or during fieldtrips and fieldwork, those who inspired me and with whom I had a great time, mostly spent over a beer or a G&T. Special thanks go to Klaus Reicherter, who gave me the chance to catch a glimpse of the Indian mangroves and to learn how tsunami modelling works. Further thanks go to our Oman fieldwork group, especially to those who went on to write their Bachelor's and Master's theses with us: Zahra, Huda, Jessica and Vivian – you not only contributed to this research project but also to the great atmosphere within the group.

I am thankful to have had the opportunity to meet Jean Thein, the first professor during my studies who demonstrated that one doesn't have to be confined by narrow scientific views but can, and should, have an interdisciplinary interest. For the best start to a scientific career one could imagine, I thank my primary school teacher, Uta Schneider-Rüth, for her patience, clarity and joy.

I am grateful for a three-year scholarship and travel grants from the Studienstiftung des deutschen Volkes, for travel grants from IGCP project 639 and for the financial support from the DFG for our project. I also want to thank the team of Golden Highlands, especially Mansoor al Shabibi, for all their support, particularly for the wonderful camp setup with outdoor catering during our fieldwork, and special Shukrans to Hamed for the extraordinary prawns at Fins Beach.

Last but not least, my final thanks go to all the people without whom this thesis probably would not have been finished by now. These include my friends and neighbours in our small village, Bahnhof Kottenforst, especially Claudia and Michael, my bosses at the veterinary practice, Kerstin and Jörg, my wonderful colleagues, and many participants in our fabulous field trips to Oman, especially Eberhard: Thank you all for continuously nudging me to finish this work.

8. References

Abdel-Fattah, M., Kantoush, S. A., Saber, M. & Sumi, T. (2018). Rainfall-runoff modeling for extreme flash floods in wadi samail, oman. *Journal of Japan Society of Civil Engineers, Ser. B1 (Hydraulic Engineering)*, *74*(5), I_691-I_696.

Al-Habsi, Z., Hereher, M., El-Hussain, I., Omira, R., Baptista, M. A., Deif, A., Al-Awadhi, T. & Al-Nasiri, N. (2022). Tsunami hazard and risk zoning for Qurayyat in northeast Oman coast: Worst-case credible scenarios along the Makran Subduction Zone, Western Asia. *Journal of Asian Earth Sciences: X*, *8*, 100103.

Al Harrasi, M. & Labib, A. (2022). Stakeholders management in rainfall enhancement project of Oman. *Journal of Weather Modification*, *53*(1).

Al-Kalbani, M. S., John, C. & Martin, F. P. (2015). Recent Trends in Temperature and Precipitation in Al Jabal Al Akhdar, Sultanate of Oman, and the Implications for Future Climate Change. *Journal of Earth Science & Climatic Change*, *6*(8). doi:10.4172/2157-7617.1000295

Al-Marshudi, A. S. (2007). The falaj irrigation system and water allocation markets in Northern Oman. *Agricultural Water Management*, *91*(1-3), 71-77.

Al-Maskari, J. (2012). How the National Forecasting Centre in Oman dealt with tropical cyclone Gonu. *Tropical Cyclone Research and Review*, *1*(1), 16-22.

Al-Zaabi, S. & Al-Zadjali, S. (2022). Qualitative analysis of early warning: A case study from Oman. *International Journal of Disaster Risk Reduction*, *68*, 102731.

Ali, M. Y., Aidarbayev, S., Searle, M. P. & Watts, A. B. (2018). Subsidence history and seismic stratigraphy of the western Musandam peninsula, Oman–United Arab Emirates mountains. *Tectonics*, *7*, 154–181. https://doi.org/10.1002/2017TC004777

Aguirre-Ayerbe, I., Martínez Sánchez, J., Aniel-Quiroga, Í., González-Riancho, P., Merino, M., Al-Yahyai, S., González, M. & Medina, R. (2018). From tsunami risk assessment to disaster risk reduction–the case of Oman. *Natural Hazards and Earth System Sciences*, *18*(8), 2241-2260.

Anderson, D. G., Maasch, K. A., Sandweiss, D. H. & Mayewski, P. A. (2007). Climate and culture change: exploring Holocene transitions. In: Anderson, D. G., Maasch, K. A. & Sandweiss, D. H. (eds.), Climate Change and Cultural Dynamics. Academic Press.

Arceo-Carranza, D., Chiappa-Carrara, X., Chávez López, R. & Yáñez Arenas, C. (2021) Mangroves as Feeding and Breeding Grounds. In: Rastogi, R. P., Phulwaria, M. & Gupta, D. K. (eds.), Mangroves: Ecology, biodiversity and management. Springer, Berlin. https://doi.org/10.1007/978-981-16-2494-0_1

Armitage, S. J., Jasim, S. A., Marks, A. E., Parker, A. G., Usik, V. I. & Uerpmann, H. P. (2011). The southern route “out of Africa”: evidence for an early expansion of modern humans into Arabia. *Science*, *331*(6016), 453-456.

Arrivabene, H. P., Souza, I., Có, W. L. O., Rodella, R. A., Wunderlin, D. A. & Milanez, C. R. (2014). Functional traits of selected mangrove species in Brazil as biological indicators of different environmental conditions. *Science of the Total Environment*, *476*, 496-504.

Auriemma, R. & Solinas, E. (2009). Archaeological remains as sea level change markers: a review. *Quaternary International*, *206*(1-2), 134-146.

Axelsson, J. (2024). Interglacial climates in proxies and models: Utilizing sampled oxygen isotopes and model simulations to understand past Indian summer monsoon variability. (Doctoral dissertation, Institutionen för naturgeografi, Stockholms universitet).

Auriemma, R. & Solinas, E. (2009). Archaeological remains as sea level change markers: a review. *Quaternary International*, *206*(1-2), 134-146.

Azzarà, V. M. (2009). Domestic architecture at the Early Bronze Age sites HD-6 and RJ-2 (Jaʿalān, Sultanate of Oman). In *Proceedings of the Seminar for Arabian Studies* (pp. 1-15). Archaeopress.

Bange, H. W., Bathmann, U., Behrens, J., Dahlke, F., Ebinghaus, R., Ekau, W., Emeis, K.- C., et al. (2017). Coasts – A Vital Habitat Under Pressure. World Ocean Review: Living with the Oceans 5. Maribus, Hamburg, Germany.

Berger, J. F., Charpentier, V., Crassard, R., Martin, C., Davtian, G. & López-Sáez, J. A. (2013). The dynamics of mangrove ecosystems, changes in sea level and the strategies of Neolithic settlements along the coast of Oman (6000–3000 cal. BC). *Journal of Archaeological Science*, 40(7), 3087-3104.

Beyer, R. M., Krapp, M., Eriksson, A. & Manica, A. (2021). Climatic windows for human migration out of Africa in the past 300,000 years. *Nature Communications*, *12*(1), 4889.

Biagi, P. (1994). An Early Palaeolithic site near Saiwan (Sultanate of Oman). *Arabian archaeology and epigraphy*, *5*(2), 81-88.

Biagi, P. & Nisbet, R. (1999). The shell-midden sites of RH5 and RH6 (Muscat, Sultanate of Oman) in their environmental setting. *Archaeologia Polona*, 37, 31-47.

Blasco, F., Saenger, P. & Janodet, E. (1996). Mangroves as indicators of coastal change. *Catena*, *27*(3-4), 167-178.

Bretzke, K., Preusser, F., Jasim, S., Miller, C., Preston, G., Raith, K., Underdown, S. J., Parton, A. & Parker, A. G. (2022). Multiple phases of human occupation in Southeast Arabia between 210,000 and 120,000 years ago. *Scientific reports, 12*(1), 1600.

Bosch, D. T. , Dance, S. P., Moolenbeek, R. G. & Oliver, P. G. (1995). Seashells of Eastern Arabia. Motivate Publishing, Dubai. ISBN 1-873544-64-2., pp. 296.

Bradley, R. S. (1999). Paleoclimatology: reconstructing climates of the Quaternary, Second Edition. Harcourt Academic Press; Burlington, London.

Burns, S. J., Fleitmann, D., Matter, A., Neff, U. & Mangini, A. (2001). Speleothem evidence from Oman for continental pluvial events during interglacial periods. *Geology*, *29*(7), 623-626.

Burns, S. J., Matter, A., Frank, N. & Mangini, A. (1998). Speleothem-based paleoclimate record from northern Oman. *Geology*, *26*(6), 499-502.

Cerrone, C., Vacchi, M., Fontana, A. & Rovere, A. (2021). Last Interglacial sea-level proxies in the Western Mediterranean. *Earth System Science Data Discussions*, *2021*, 1-93.

Chakraborty, R. (2012). Centuries old aflaj irrigation system in Oman. *Proceedings of the Institution of Civil Engineers-Engineering History and Heritage*, *165*(2), 73-80.

Chambers, R., Beare, S., Peak, S. & Al-Kalbani, M. (2016). Using ground-based ionisation to enhance rainfall in the Hajar Mountains, Oman. *Arabian Journal of Geosciences*, *9*, 1-16.

Charpentier, V., Berger, J. F., Crassard, R., Lacaze, M. & Davtian, G. (2012). Prehistory and palaeo-geography of the coastal fringes of the Wahiba Sands and Bar al-Hikman, Sultanate of Oman. *Proceedings of the Seminar for Arabian Studies* (pp. 57-78). Archaeopress.

Chen, K., Axelsson, J., Zhang, Q., Li, J. & Wang, L. (2022). EC-Earth simulations reveal enhanced inter-hemispheric thermal contrast during the Last Interglacial further intensified the Indian monsoon. *Geophysical Research Letters, 49*, e2021GL094551. https://doi.org/10.1029/2021GL094551

Chen, L., Wang, W., Li, Q. Q., Zhang, Y., Yang, S., Osland, M. J., Huang, J. & Peng, C. (2017). Mangrove species' responses to winter air temperature extremes in China. *Ecosphere*, *8*(6), e01865.

Clarke, P. J. (1993). Dispersal of grey mangrove (*Avicennia marina*) propagules in southeastern Australia. *Aquatic Botany*, *45*(2-3), 195-204.

Clemens, S., Prell, W., Murray, D., Shimmield, G. & Weedon, G. (1991). Forcing mechanisms of the Indian Ocean monsoon. *Nature*, *353*(6346), 720-725.

Clement, A. J., Whitehouse, P. L. & Sloss, C. R. (2016). An examination of spatial variability in the timing and magnitude of Holocene relative sea-level changes in the New Zealand archipelago. *Quaternary Science Reviews*, *131*, 73-101.

Cleuziou, S. & Tosi, M. (2007). In the Shadow of the Ancestors. The Prehistoric Foundations if the Early Arabian Civilization in Oman. Ministry of Heritage and Culture, Muscat, Oman.

Cohen, K. M., Finney, S. C., Gibbard, P. L. & Fan, J.-X. (2013) The ICS International Chronostratigraphic Chart. Episodes 36: 199-204.

Cremaschi, M., Degli Esposti, M., Fleitmann, D., Perego, A., Sibilia, E. & Zerboni, A. (2018). Late Holocene onset of intensive cultivation and introduction of the falaj irrigation system in the Salut oasis (Sultanate of Oman). *Quaternary Science Reviews*, *200*, 123-140.

Cremaschi, M. & Negrino, F. (2005). Evidence for an abrupt climatic change at 8700 14C yr BP in rockshelters and caves of Gebel Qara (Dhofar-Oman): Palaeoenvironmental implications. *Geoarchaeology: An International Journal*, *20*(6), 559-579.

Curci, A., Carletti, M. & Tosi, M. (2014). The camel remains from site HD-6 (Ra's al-Hadd, Sultanate of Oman): an opportunity for a critical review of dromedary findings in eastern Arabia. *Anthropozoologica*, *49*(2), 207-224.

Decker, V., Falkenroth, M. & Hoffmann, G. (2024). Sedimentological evidence of Late Pleistocene Shorelines in Oman. *Marine Geology*, *477*, 107407. https://doi.org/10.1016/j.margeo.2024.107407

Decker, V., Falkenroth, M., Lindauer, S., Landgraf, J., Al-Lawati, Z., Al-Rahbi, H., Franz, S. O. & Hoffmann, G. (2021). Collapse of Holocene mangrove ecosystems along the coastline of Oman. *Quaternary Research*, *100*, 52-76. https://doi.org/10.1017/qua.2020.96 [2]

Decker, V., Gee, C. T., Schucht, P. J., Lindauer, S. & Hoffmann, G. (2022). Life on the Edge: A Powerful Tsunami Overwhelmed Indian Ocean Mangroves One Millennium Ago. *Forests, 13*(6), 922. https://doi.org/10.3390/f13060922

DeMenocal, P., Ortiz, J., Guilderson, T., Adkins, J., Sarnthein, M., Baker, L. & Yarusinsky, M. (2000). Abrupt onset and termination of the African Humid Period: rapid climate responses to gradual insolation forcing. *Quaternary science reviews*, *19*(1-5), 347-361.

DeMets, C., Gordon, R. G. & Argus, D. F. (2010). Geologically current plate motions. *Geophysical journal international*, *181*(1), 1-80.

Donato, S. V., Reinhardt, E. G., Boyce, J. I., Pilarczyk, J. E. & Jupp, B. P. (2009). Particle-size distribution of inferred tsunami deposits in Sur Lagoon, Sultanate of Oman. *Marine Geology, 257*, 54–64.

Donato, S. V., Reinhardt, E. G., Boyce, J. I., Rothaus, R. & Vosmer, T. (2008). Identifying tsunami deposits using bivalve shell taphonomy. *Geology, 36*, 199–202.

Donato, D. C., Kauffman, J. B., Murdiyarso, D., Kurnianto, S., Stidham, M. & Kanninen, M. (2011). Mangroves among the most carbon-rich forests in the tropics. *Nature geoscience*, *4*(5), 293-297.

Douka, K. (2017). 22. Radiocarbon dating of marine and terrestrial shell. *Molluscs in Archaeology: Methods, Approaches and Applications*, 381.

Duque-Villegas, M., Claussen, M., Kleinen, T., Bader, J. & Reick, C. H. (2025). Pattern scaling of simulated vegetation change in northern Africa during glacial cycles. *Climate of the Past*, *21*(4), 773-794.

Engel, M., Matter, A., Parker, A. G., Parton, A., Petraglia, M. D., Preston, G. W. & Preusser, F. (2017). Lakes or wetlands? A comment on 'The middle Holocene climatic records from Arabia: Reassessing lacustrine environments, shift of ITCZ in Arabian Sea, and impacts of the southwest Indian and African monsoons' by Enzel et al. *Global and Planetary Change*, *148*, 258-267.

Enzel, Y., Kushnir, Y. & Quade, J. (2015). The middle Holocene climatic records from Arabia: Reassessing lacustrine environments, shift of ITCZ in Arabian Sea, and impacts of the southwest Indian and African monsoons. *Global and Planetary Change*, *129*, 69-91.

Enzel, Y., Quade, J. & Kushnir, Y. (2017). Response to Engel et al.(in press): Lakes or wetlands? A comment on" The middle Holocene climatic records from Arabia: Reassessing lacustrine environments, shift of ITCZ in Arabian Sea, and impacts of the southwest Indian and African monsoons" by Enzel et al.(2015). *Global and Planetary Change*, *148*, 268-271.

[2] This publication was extended by a Corrigendum: *Quaternary Research*, *100*, 260–262. https://doi.org/10.1017/qua.2021.6

Erlandson, J. M. (2017). Coastlines, marine ecology, and maritime dispersals in human history. *Human Dispersal and Species Movement: From Prehistory to Present, Cambridge University Press, Cambridge*, 147-163.

Faheem, H., Ji, Y. F., Zhu, W. L., Qu, R., Zhu, Y. & Yoshioka, S. (2025). Subduction thermal state, slab metamorphism, and seismicity in the Makran Subduction Zone. *Earth Planet. Phys., 9*(2), 1–13. http://doi.org/10.26464/epp2025004

Falkenroth, M., Adolphs, S., Cahnbley, M., Bagci, H., Kázmér, M., Mechernich, S. & Hoffmann, G. (2020). Biological indicators reveal small-scale sea-level variability during MIS 5e (Sur, Sultanate of Oman). *Open Quaternary*, *6*(1).

Falkenroth, M., Schneider, B. & Hoffmann, G. (2019). Beachrock as sea-level indicator–a case study at the coastline of Oman (Indian Ocean). *Quaternary Science Reviews*, *206*, 81-98.

Fleitmann, D., Burns, S. J., Mangini, A., Mudelsee, M., Kramers, J., Villa, I., Neff, U., Al-Subbary, A. A., Buettner, A., Hippler, D. & Matter, A. (2007). Holocene ITCZ and Indian monsoon dynamics recorded in stalagmites from Oman and Yemen (Socotra). *Quaternary Science Reviews*, *26*(1-2), 170-188.

Fleitmann, D., Burns, S. J., Matter, A., Cheng, H. & Affolter, S. (2022). Moisture and seasonality shifts recorded in Holocene and Pleistocene speleothems from southeastern Arabia. *Geophysical Research Letters*, *49*(16), e2021GL097255.

Fleitmann, D. & Matter, A. (2009). The speleothem record of climate variability in Southern Arabia. *Comptes Rendus. Géoscience*, *341*(8-9), 633-642.

Fratini, S., Vigiani, V., Vannini, M. & Cannicci, S. (2004). Terebralia palustris (Gastropoda; Potamididae) in a Kenyan mangal: size structure, distribution and impact on the consumption of leaf litter. *Marine Biology*, *144*, 1173-1182.

Fritz, H. M., Blount, C. D., Albusaidi, F. B. & Al-Harthy, A. H. M. (2010). Cyclone Gonu storm surge in Oman. *Estuarine, Coastal and Shelf Science*, *86*(1), 102-106.

Ghazanfar, S. A., Böer, B., Al Khulaidi, A. W., El-Keblawy, A. & Alateeqi, S. (2019). Plants of Sabkha Ecosystems of the Arabian Peninsula. In: Gul, B., Böer, B., Khan, M., Clüsener-Godt, M., Hameed, A. (eds.), Sabkha Ecosystems – Vol. VI Asia/Pacific, Tasks for Vegetation Science, 49. Springer, Cham. https://doi.org/10.1007/978-3-030-04417-6_5

Glennie, K. W., Boeuf, M. G. A., Clarke, M. H., Moody-Stuart, M., Pilaar, W. F. H. & Reinhardt, B. M. (1973). Late Cretaceous nappes in Oman Mountains and their geologic evolution. *American Associated Petroleum Geologists Bulletin*, *57*(1), 5-27. https://doi.org/10.1306/819A4240-16C5-11D7-8645000102C1865D

Goldberg, L., Lagomasino, D., Thomas, N. & Fatoyinbo, T. (2020). Global declines in human-driven mangrove loss. *Global change biology*, *26*(10), 5844-5855.

Hadidi, A., Holzbecher, E. & Molenaar, R. E. (2020). Flood mapping in face of rapid urbanization: a case study of Wadi Majraf-Manumah, Muscat, Sultanate of Oman. *Urban Water Journal*, *17*(5), 407–415. https://doi.org/10.1080/1573062X.2020.1713172

Haggag, M. & Badry, H. (2012). Hydrometeorological modeling study of tropical cyclone Phet in the Arabian Sea in 2010. *Atmospheric and Climate Sciences*, *2*, 174-190. http://dx.doi.org/10.4236/acs.2012.2201

Haider, R., Ali, S., Hoffmann, G. & Reicherter, K. (2023). A multi-proxy approach to assess tsunami hazard with a preliminary risk assessment: A case study of the Makran Coast, Pakistan. *Marine Geology*, *459*, 107032.

Haider, R., Ali, S., Hoffmann, G. & Reicherter, K. (2024). Tsunami inundation and vulnerability analysis on the Makran coast, Pakistan. *Natural Hazards and Earth System Sciences*, *24*(9), 3279-3290.

Hannah, L., Lovejoy, T. E. & Schneider, S. S. (2005). Biodiversity and Climate Change in Context. In: Lovejoy, T. E. & Hannah, L. (eds.), Climate Change and Biodiversity. Yale University Press, New Haven & London.

Hansman, R. J., Ring, U., Scharf, A., Glodny, J. & Wan, B. (2021). Structural architecture and Late Cretaceous exhumation history of the Saih Hatat Dome (Oman), a review based on existing data and semi-restorable cross-sections. *Earth-Science Reviews*, *217*, 103595.

Hansman, R. J., Ring, U., Thomson, S. N., den Brok, B. & Stübner, K. (2017). Late Eocene uplift of the Al Hajar Mountains, Oman, supported by stratigraphy and low-temperature thermochronology. *Tectonics*, *36*(12), 3081-3109.

Heidarzadeh, M. & Satake, K. (2014). Possible sources of the tsunami observed in the northwestern Indian Ocean following the 2013 September 24 M w 7.7 Pakistan inland earthquake. *Geophysical Journal International*, *199*(2), 752-766.

Heine, K. (2024). Climate Archives. In: Heine (ed.), The Quaternary in the Tropics – A Reconstruction of the Paleoclimate. Springer Textbooks in Earth Sciences, Geography and Environment. Springer, Cham. https://doi.org/10.1007/978-3-031-31921-1_4

Hijma, M. P., Engelhart, S. E., Törnqvist, T. E., Horton, B. P., Hu, P. & Hill, D. F. (2015). A protocol for a geological sea-level database. *Handbook of sea-level research*, 536-553.

Hoffmann, G., Grützner, C., Reicherter, K. & Preusser, F. (2015a). Geo-archaeological evidence for a Holocene extreme flooding event within the Arabian Sea (Ras al Hadd, Oman). *Quaternary Science Reviews*, *113*, 123-133.

Hoffmann, G., Grützner, C., Schneider, B., Preusser, F. & Reicherter, K. (2020a). Large Holocene tsunamis in the northern Arabian Sea. *Marine Geology*, *419*, 106068.

Hoffmann, G., Meschede, M., Zacke, A. & Al Kindi, M. (2016). Field Guide to the Geology of Northeastern Oman. Borntraeger Science Publishers, Stuttgart.

Hoffmann, G. & Reicherter, K. (2014). Reconstructing Anthropocene extreme flood events by using litter deposits. *Global and Planetary Change*, *122*, 23-28.

Hoffmann, G., Rupprechter, M., Al Balushi, N., Grützner, C. & Reicherter, K. (2013a). The impact of the 1945 Makran tsunami along the coastlines of the Arabian Sea (Northern Indian Ocean)–a review. *Zeitschrift für Geomorphologie*, *57*(4), 257-277.

Hoffmann, G., Rupprechter, M. & Mayrhofer, C. (2013b). Review of the long-term coastal evolution of North Oman-subsidence versus uplift. *Zeitschrift der Deutschen Gesellschaft für Geowissenschaften*, *164*(2), 237-252.

Hoffmann, G., Rupprechter, M., Rahn, M. & Preusser, F. (2015b). Fluvio-lacustrine deposits reveal precipitation pattern in SE Arabia during early MIS 3. *Quaternary International*, *382*, 145-153.

Hoffmann, G., Schneider, B., Mechernich, S., Falkenroth, M., Dunai, T. & Preusser, F. (2020b). Quaternary uplift along a passive continental margin (Oman, Indian Ocean). *Geomorphology*, *350*, 106870.

Horisk, K. E., Ivory, S. J., McCorriston, J., McHale, M., Al Mehri, A., Anderson, A., Anderson, R. S. & Al Kathiri, A. A. (2023). Vegetation dynamics in Dhofar, Oman, from the Late Holocene to present inferred from rock hyrax middens. *Quaternary Research*, *116*, 12-29.

IPCC, 2023. Sections. In: Core writing Team, Lee, H., Romero, J. (eds.), Climate Change 2023: Synthesis Report. Contribution of Working groups I, II and III to the Sixth. Assessment Report of the Intergovernmental Panel on climate Change. IPCC, Geneva, Switzerland, pp. 35–115. https://doi.org/10.59327/IPCC/AR6-9789291691647.

Islam, M. N., Ratul, S. B., Sharmin, A., Rahman, K. S., Ashaduzzaman, M. & Uddin, G. M. N. (2019). Comparison of calorific values and ash content for different woody biomass components of six mangrove species of Bangladesh Sundarbans. *Journal of the Indian Academy of Wood Science*, *16*, 110-117.

Jagiella, C. & Kürschner, H. (1987). Atlas der Hölzer Saudi Arabiens. Die Holzanatomie der Wichtigsten Bäume und Sträucher Arabiens mit Einem Holzanatomischen Bestimmungsschlüssel; *Beihefte zum Tübinger Atlas des Vorderen Orients, Reihe A, 20*. Ludwig Reichert: Wiesbaden, Germany.

Karl, T. R. & Trenberth, K. E. (2005). What is Climate Change?. In: Lovejoy, T. E. & Hannah, L. (eds.), Climate Change and Biodiversity. Yale University Press, New Haven & London.

Kathiresan, K. (2021). Mangroves: Types and Importance. In: Rastogi, R. P., Phulwaria, M. & Gupta, D. K. (eds.), Mangroves: Ecology, biodiversity and management. Springer, Berlin. https://doi.org/10.1007/978-981-16-2494-0_1

Kemp, A. C., Horton, B. P., Donnelly, J. P., Mann, M. E., Vermeer, M. & Rahmstorf, S. (2011). Climate related sea-level variations over the past two millennia. *Proceedings of the National Academy of Sciences*, *108*(27), 11017-11022.

Khan, N. S., Ashe, E., Shaw, T. A., Vacchi, M., Walker, J., Peltier, W. R., Kopp, R. E. & Horton, B. P. (2015). Holocene relative sea-level changes from near-, intermediate-, and far-field locations. *Current Climate Change Reports*, *1*, 247-262.

Knight, J. (2023). The African Humid Period and the 'Green Sahara'. In: Knight, J., Merlo, S. & Zerboni, A. (eds.), Landscapes and Landforms of the Central Sahara. World Geomorphological Landscapes. Springer, Cham. https://doi.org/10.1007/978-3-031-47160-5_15

König, P. (2016) Vegetation of Oman. *In:* Hoffmann, G., Meschede, M., Zacke, A., & Al Kindi, M. (authors), Field Guide to the Geology of Northeastern Oman. Borntraeger Science Publishers, Stuttgart.

Kukowski, N., Schillhorn, T., Flueh, E. R. & Huhn, K. (2000). Newly identified strike-slip plate boundary in the northeastern Arabian Sea. *Geology*, *28*(4), 355-358.

Kuhlmann, H., Meggers, H., Freudenthal, T. & Wefer, G. (2004). The transition of the monsoonal and the N Atlantic climate system off NW Africa during the Holocene. *Geophysical Research Letters*, *31*(22).

Kwarteng, A. Y., Dorvlo, A. S. & Vijaya Kumar, G. T. (2009). Analysis of a 27-year rainfall data (1977-2003) in the Sultanate of Oman. *International Journal of Climatology*, *29*(4), 605.

Lambeck, K. (2002). Sea level change from mid Holocene to recent time: an Australian example with global implications. *Ice sheets, sea level and the dynamic earth*, *29*, 33-50.

Lambeck, K., Esat, T. M. & Potter, E. K. (2002). Links between climate and sea levels for the past three million years. *Nature, 419*(6903), 199-206.

Lambeck, K., Rouby, H., Purcell, A., Sun, Y. & Sambridge, M. (2014). Sea level and global ice volumes from the Last Glacial Maximum to the Holocene. *Proceedings of the National Academy of Sciences*, *111*(43), 15296-15303.

Lézine, A. M. (2009). Timing of vegetation changes at the end of the Holocene Humid Period in desert areas at the northern edge of the Atlantic and Indian monsoon systems. *Comptes Rendus Geoscience*, *341*(8-9), 750-759.

Lézine, A. M., Bassinot, F. & Peterschmitt, J. Y. (2014). Orbitally-induced changes of the Atlantic and Indian monsoons over the past 20,000 years: New insights based on the comparison of continental and marine records. *Bulletin de la Société Géologique de France*, *185*(1), 3-12.

Lézine, A. M., Ivory, S. J., Braconnot, P. & Marti, O. (2017). Timing of the southward retreat of the ITCZ at the end of the Holocene Humid Period in Southern Arabia: Data-model comparison. *Quaternary Science Reviews*, *164*, 68-76. http://doi.org/10.1016/j.quascirev.2017.03.019.

Lézine, A. M., Saliège, J. F., Mathieu, R., Tagliatela, T. L., Mery, S., Charpentier, V. & Cleuziou, S. (2002). Mangroves of Oman during the late Holocene; climatic implications and impact on human settlements. *Vegetation History and Archaeobotany*, *11*, 221-232.

Li, B., Nychka, D. W. & Ammann, C. M. (2010). The value of multiproxy reconstruction of past climate. *Journal of the American Statistical Association*, *105*(491), 883-895. https://doi.org/10.1198/jasa.2010.ap09379

Lüning, S. & Vahrenholt, F. (2018). Holocene climate development of North Africa and the Arabian Peninsula. In: Bendaoud, A., Hamimi, Z., Hamoudi, M., Djemai, S. & Zoheir, B. (eds.), The Geology of the Arab World---An Overview (pp. 507-546). Cham: Springer International Publishing. https://doi.org/10.1007/978-3-319-96794-3_14

Lyakhovsky, V., Ben-Avraham, Z. & Achmon, M. (1994). The origin of the Dead Sea rift. *Tectonophysics*, *240*(1-4), 29-43.

Lynas, M., Houlton, B. Z. & Perry, S. (2021). Greater than 99% consensus on human caused climate change in the peer-reviewed scientific literature. *Environmental Research Letters*, *16*(11), 114005.

Macreadie, P. I., Anton, A., Raven, J. A., Beaumont, N., Connolly, R. M., Friess, D. A., ... & Duarte, C. M. (2019). The future of Blue Carbon science. *Nature communications*, *10*(1), 3998.

Maier, J., Burdanowitz, N., Schmiedl, G. & Gaye, B. (2025). Spatial and temporal variability in sea surface temperatures and monsoon dynamics in the northwestern Arabian Sea during the last 43 kyr. *Climate of the Past*, *21*(1), 279-297.

Mannaa, A. & Jones, B. G. (2024). Holocene sea-level highstand evidence from beachrock and carbonate terraces along the Saudi Arabian Red Sea coast. In *Rifting and Sediments in the Red Sea and Arabian Gulf Regions* (pp. 312-323). CRC Press.

Martinez-Alier, J. (2001). Ecological conflicts and valuation: mangroves versus shrimps in the late 1990s. *Environment and Planning C: Government and Policy*, *19*(5), 713-728.

Matter, A., Neubert, E., Preusser, F., Rosenberg, T. & Al-Wagdani, K. (2015). Palaeo-environmental implications derived from lake and sabkha deposits of the southern Rub'al-Khali, Saudi Arabia and Oman. *Quaternary International*, *382*, 120-131. http://dx.doi.org/10.1016/j.quaint.2014.12.029

McLachlan, A., Fisher, M., Al-Habsi, H. N., Al-Shukairi, S. S. & Al-Habsi, A. M. (1998). Ecology of sandy beaches in Oman. *Journal of Coastal Conservation, 4*, 181–190.

Milankovitch, M. K. (1941). Kanon der Erdbestrahlung und seine Anwendung auf das Eiszeitenproblem. Royal Serbian Academy Special Publication, 133, 1-633.

Mitrovica, J. X. & Peltier, W. R. (1991). On postglacial geoid subsidence over the equatorial oceans. *Journal of Geophysical Research: Solid Earth*, *96*(B12), 20053-20071.

Morton, R. A., Gelfenbaum, G. & Jaffe, B. E. (2007). Physical criteria for distinguishing sandy tsunami and storm deposits using modern examples. *Sedimentary Geology*, *200*(3-4), 184-207. https://doi.org/10.1016/j.sedgeo.2007.01.003

Murdiyarso, D., Purbopuspito, J. Kauffman, J. B., Warren, M. W., Sasmito, S. D., Donato, D. C., Manuri, S., Krisnawati, H., Taberima, S. & Kurnianto, S. (2015). The potential of Indonesian mangrove forests for global climate change mitigation. *Nature climate change*, *5*(12), 1089-1092.

Murty, T. S. & Rafiq, M. (1991). A tentative list of tsunamis in the marginal seas of the north Indian Ocean. *Natural Hazards*, *4*, 81-83.

Najah, A., Merwe, R. van der & Al Shehhi, M. R. (2024). Review of tropical cyclones impacting the Western Arabian Sea and Oman. *Journal of Operational Oceanography*, 1–19. https://doi.org/10.1080/1755876X.2024.2444753

Nakada, M., Okuno, J. I. & Yokoyama, Y. (2016). Total meltwater volume since the Last Glacial Maximum and viscosity structure of Earth's mantle inferred from relative sea level changes at Barbados and Bonaparte Gulf and GIA-induced J̇ 2. *Geophysical Journal International*, *204*(2), 1237-1253.

Nirgi, T., Rosentau, A., Habicht, H.-L., Hang, T., Jonuks, T., Jõeleht, A., Kihno, K., Kriiska, A., Mustasaar, M., Risberg, J., Suuroja, S., Talviste, P. & Tõnisson, H. (2020). Holocene relative shore-

level changes and Stone Age palaeogeography of the Pärnu Bay area, eastern Baltic Sea. *The Holocene*, *30*(1), 37-52. https://doi.org/10.1177/0959683619865603

Oppenheimer, M., Glavovic, B. C., Hinkel, J., Wal, R. van de, Magnan, A. K., Abd-Elgawad, A., Cai, R., Cifuentes-Jara, M., DeConto, R. M., Ghosh, T., Hay, J., Isla, F., Marzeion, B., Meyssignac, B. & Sebesvari, Z. (2019). Sea Level Rise and Implications for Low-Lying Islands, Coasts and Communities. In: Pörtner, H.-O., Roberts, D. C., Masson-Delmotte, V., Zhai, P., Tignor, M., Poloczanska, E., Mintenbeck, K., Alegría, A., Nicolai, M., Okem, A., Petzold, J., Rama, B. & Weyer, N. M. (eds.), IPCC Special Report on the Ocean and Cryosphere in a Changing Climate. Cambridge University Press, Cambridge, UK and New York, NY, USA, pp. 321-445. https://doi.org/10.1017/9781009157964.006.

Otto-Bliesner, B. L., Marshall, S. J., Overpeck, J. T., Miller, G. H., Hu, A. & CAPE Last Interglacial Project members. (2006). Simulating Arctic climate warmth and icefield retreat in the last interglaciation. *science*, *311*(5768), 1751-1753.

Otto-Bliesner, B. L., Rosenbloom, N., Stone, E. J., McKay, N. P., Lunt, D. J., Brady, E. C. & Overpeck, J. T. (2013). How warm was the last interglacial? New model–data comparisons. *Philosophical Transactions of the Royal Society A: Mathematical, Physical and Engineering Sciences*, *371*(2001), 20130097.

Overpeck, J., Cole, J. & Bartlein, P. (2005). A "Paleoperspective" on Climate Variability and Change. In: Lovejoy, T. E. & Hannah, L. (eds.), Climate Change and Biodiversity. Yale University Press, New Haven & London.

Parton, A., Farrant, A. R., Leng, M. J., Schwenninger, J. L., Rose, J. I., Uerpmann, H. P. & Parker, A. G. (2013). An early MIS 3 pluvial phase in Southeast Arabia: climatic and archaeological implications. *Quaternary International*, *300*, 62-74.

Parton, A., Farrant, A. R., Leng, M. J., Telfer, M. W., Groucutt, H. S., Petraglia, M. D. & Parker, A. G. (2015). Alluvial fan records from southeast Arabia reveal multiple windows for human dispersal. *Geology*, *43*(4), 295-298. doi:10.1130/G36401.1

Penney, C., Tavakoli, F., Saadat, A., Nankali, H. R., Sedighi, M., Khorrami, F., Sobouti, F., Rafi, Z., Copley, A., Jackson, J. & Priestley, K. (2017). Megathrust and accretionary wedge properties and behaviour in the Makran subduction zone. *Geophysical Journal International*, *209*(3), 1800-1830.

Petraglia, M. D. (2003). The Lower Paleolithic of the Arabian Peninsula: occupations, adaptations, and dispersals. *Journal of World Prehistory*, *17*(2), 141-179.

Pilarczyk, J. E. & Reinhardt, E. G. (2012). Testing foraminiferal taphonomy as a tsunami indicator in a shallow arid system lagoon: Sur, Sultanate of Oman. *Marine Geology*, *295*, 128-136.

Pimple, U., Leadprathom, K., Simonetti, D., Sitthi, A., Peters, R., Pungkul, S., Pravinvongvuthi, T., Dessard, H., Berger, U., Siri-on, K., Kemacheevakul, P. & Gond, V. (2022). Assessing mangrove species diversity, zonation and functional indicators in response to natural, regenerated, and rehabilitated succession. *Journal of Environmental Management*, *318*, 115507.

Pourkerman, M., Marriner, N., Amjadi, S., Lak, R., Hamzeh, M., Mohammadpor, G., Lahijani, H., Tavakoli, M., Morhange, C. & Shah-Hosseini, M. (2023). The impacts of Persian Gulf water and

ocean-atmosphere interactions on tropical cyclone intensification in the Arabian Sea. *Marine Pollution Bulletin*, *188*, 114553.

Preusser, F. (2009). Chronology of the impact of Quaternary climate change on continental environments in the Arabian Peninsula. *Comptes Rendus. Géoscience*, *341*(8-9), 621-632.

Preusser, F., Radies, D., Driehorst, F. & Matter, A. (2005). Late Quaternary history of the coastal Wahiba sands, Sultanate of Oman. *Journal of Quaternary Science: Published for the Quaternary Research Association*, *20*(4), 395-405.

Prizomwala, S. P., Gandhi, D., Bhatt, N., Winkler, W., Kumar, M. R., Makwana, N. & Bhatt, N. (2018). Geological evidence for AD 1008 tsunami along the Kachchh coast, Western India: Implications for hazard along the Makran Subduction Zone. *Scientific reports*, *8*(1), 16816.

Ragavan, P., Kathiresan, K., Kumar, S., Nagarajan, B., Jayaraj, R. S. C., Mohan, P. M., Sachithanandam, V., Mageswaran, T. & Rana, T. S. (2021). Biogeography of the Mangrove Ecosystem: Floristics, Population Structure, and Conservation Strategies. In: Rastogi, R. P., Phulwaria, M. & Gupta, D. K. (eds.), Mangroves: Ecology, biodiversity and management. Springer, Berlin. https://doi.org/10.1007/978-981-16-2494-0_1

Ramírez-Herrera, M. T. & Coca, O. (2024). A global database of tsunami deposits. *Geoscience Data Journal*, *11*(4), 974-994. https://doi.org/10.1002/gdj3.270

Rodrigues, P., Behling, H., Hoffmann, G., & Bauer, W. (2023). Effects of the Indian Ocean Monsoon oscillation during the Pleistocene-Holocene transition on the palinomorphic records in the NW Arabian Sea. In *EGU General Assembly Conference Abstracts* (pp. EGU-11475).

Rohling, E. J., Hibbert, F. D., Grant, K. M., Galaasen, E. V., Irvalı, N., Kleiven, H. F., Marino, G., Ninnemann, U., Roberts, A. P., Rosenthal, Y., Schulz, H., Williams, F. H. & Yu, J. (2019). Asynchronous Antarctic and Greenland ice-volume contributions to the last interglacial sea-level highstand. *Nature Communications*, *10*(1), 5040.

Rosenberg, T. M., Preusser, F., Blechschmidt, I., Fleitmann, D., Jagher, R. & Matter, A. (2012). Late Pleistocene palaeolake in the interior of Oman: a potential key area for the dispersal of anatomically modern humans out-of-Africa?. *Journal of Quaternary Science*, *27*(1), 13-16.

Rosenberg, T. M., Preusser, F., Fleitmann, D., Schwalb, A., Penkman, K., Schmid, T. W., Al-Shanti, M.A., Kadi, K. & Matter, A. (2011). Humid periods in southern Arabia: windows of opportunity for modern human dispersal. *Geology*, *39*(12), 1115-1118.

Rovere, A. & Dutton, A. (2021). PALSEA: 13 years of ice-sheet and sea-level science. *Past Global Changes Magazine 29* (1), 18–20. https://doi.org/10.22498/pages.29.1.18. https://pastglobalchanges.org/publications/pages-magazines/pages-magazine/ 13246.

Rovere, A., Raymo, M .E., Vacchi, M., Lorscheid, T., Stocchi, P., Gomez-Pujol, L. & Hearty, P. J. (2016a). The analysis of last Interglacial (MIS 5e) relative sea-level indicators: Reconstructing Sea-level in a warmer world. *Earth-Science Reviews*, *159*, 404-427.

Rovere, A., Stocchi, P. & Vacchi, M. (2016b) Eustatic and relative sea level changes. *Current Climate Change Reports*, *2*, 221-231.

Rovere, A., Ryan, D. D., Vacchi, M., Dutton, A., Simms, A. & Murray-Wallace, C. (2022). Introducing WALIS, the World Atlas of last Interglacial Shorelines Version 1.0. In EGU General Assembly Conference Abstracts (pp. EGU22-2489).

Rovere, A., Ryan, D. D., Vacchi, M., Dutton, A., Simms, A. R. & Murray-Wallace, C. V. (2023). The world atlas of last interglacial shorelines (version 1.0). *Earth System Science Data 15*(1), 1–23.

Saenger, P., Ragavan, P., Sheue, C. R., López-Portillo, J., Yong, J. W. & Mageswaran, T. (2019). Mangrove biogeography of the Indo-Pacific. In: Gul, B., Böer, B., Khan, M., Clüsener-Godt, M., Hameed, A. (eds.), Sabkha Ecosystems – Vol. VI Asia/Pacific, Tasks for Vegetation Science, 49. Springer, Cham. https://doi.org/10.1007/978-3-030-04417-6_5

Saintilan, N., Khan, N. S., Ashe, E., Kelleway, J. J., Rogers, K., Woodroffe, C. D. & Horton, B. P. 2020. Thresholds of mangrove survival under rapid sea level rise. *Science 368*(6495), 1118-1121. doi: 10.1126/science.aba2656

Sandilyan, S. & Kathiresan, K. (2014). Decline of mangroves–a threat of heavy metal poisoning in Asia. *Ocean & coastal management*, *102*, 161-168.

Scharf, A., Mattern, F., Al-Wardi, M., Frijia, G., Moraetis, D., Pracejus, B., Bauer, W. & Callegari, I. (2021). Chapter 5 Tectonic evolution of the Oman Mountains. *Geological Society, London, Memoirs*, *54*(1), 67-103. https://doi.org/10.1144/M54.5

Scharf, A., Mattern, F., Moraetis, D., Callegari, I. & Weidle, C. (2019). The Semail Gap Fault Zone of the Oman Mountains and its postobductional evolution. In *Geophysical Research Abstracts* (Vol. 21).

Searle, M. P. (2007). Structural geometry, style and timing of deformation in the Hawasina Window, Al Jabal al Akhdar and Saih Hatat culminations, Oman Mountains. *GEOARABIA-MANAMA-*, *12*(2), 99.

Sefton, J., Woodroffe, S. & Ascough, P. (2021). Radiocarbon dating of mangrove sediments. In *Dynamic Sedimentary Environments of Mangrove Coasts* (pp. 199-215). Elsevier.

Segev, A., Wetzler, N. & Schattner, U. (2024). When did the Dead Sea fault become a transform?. *Tectonophysics*, *892*, 230543.

Shah-hosseini, M., Morhange, C., Beni, A. N., Marriner, N., Lahijani, H., Hamzeh, M., & Sabatier, F. (2011). Coastal boulders as evidence for high-energy waves on the Iranian coast of Makran. *Marine Geology*, *290*(1-4), 17-28.

Sirocko, F., Sarnthein, M., Lange, H. & Erlenkeuser, H. (1991). Atmospheric summer circulation and coastal upwelling in the Arabian Sea during the Holocene and the last glaciation. *Quaternary Research*, *36*(1), 72-93.

Small, C. & Nicholls, R. J. (2003). A global analysis of human settlement in coastal zones. *Journal of coastal research*, 584-599.

Teillet, T., Homewood, P., Mettraux, M., Bois, P., Melini, D., Spada, G., Petrovic, A., Khanna, P. & Vahrenkamp, V. (2025). Development and factors controlling tropical carbonate barrier island systems—Bar Al Hikman; mid-late Holocene, Oman. *Sedimentology*, doi: 10.1111/sed.70017

Terry, J., Al Ruheili, A., Boldi, R., Gienko, G. & Stahl, H. (2022). Cyclone Shaheen: the exceptional tropical cyclone of October 2021 in the Gulf of Oman. *Weather*, *77*(10), 364-370.

Tian, Y., Fleitmann, D., Zhang, Q., Sha, L., Wassenburg, J. A., Axelsson, J., Zhang, H., Li, X., Hu, J., Li, H., Zhao, L., Cai, Y., Ning, Y. & Cheng, H. (2023). Holocene climate change in southern Oman deciphered by speleothem records and climate model simulations. *Nature Communications*, *14*(1), 4718.

Tian, L., Vermeersen, B. L., Wang, F., Li, J. & Wang, H. (2025). Holocene sea-level history from the southern Bohai Sea coast, China: Far-field GIA processes and an associated mid-Holocene sea-level highstand. *Quaternary Science Reviews*, *351*, 109166.

Tomlinson, P. B. (2016). The Botany of Mangroves, 2nd ed.; Cambridge University Press: New York, NY, USA.

Walsh, T. (2013). Walking through History – Oman's World Heritage Sites. Al Roya Press and Publishing House. Muscat, Oman.

Wilkinson, J. C. (2002). The origins of the aflāj of Oman. In: Production and the exploitation of resources – The Formation of the Classical Islamic World, Volume XI [Morony, M. G. (ed.)], pp. 285-302.

Wirabuana, P. Y., Baskorowati, L., Pamungkas, B., Mulyana, B., South, J., Purnobasuki, H., Andriyono, S. & Hasan, V. (2025). Mangroves, fauna compositions and carbon sequestration after ten years restoration on Flores Island, Indonesia. *Scientific Reports*, *15*(1), 4866.

Woods, W. W. & Imes, J. L. (1995). How wet is wet? Precipitation constraints on late Quaternary climate in the southern Arabian Peninsula. *Journal of Hydrology*, *164*(1-4), 263-268.

Woor, S., Thomas, D. S., Parton, A. & Leenman, A. (2023). Morphology and controls of the mountain-front fan systems of the Hajar Mountains, south-east Arabia. *Earth-Science Reviews*, *237*, 104316.

Yokoyama, Y. & Esat, T. M. (2011). Global climate and sea level: Enduring variability and rapid fluctuations over the past 150,000 years. *Oceanography*, *24*(2), 54-69.

Zaki, A. S., Delaunay, A., Baby, G., Haghipour, N., Blanchet, C., Dallmeyer, A., Sternai, P., Woor, S., Wani, O., Khalil, H., Schuster, M., Petraglia, M., Sylvestre, F., Peyrotty, G., Ali, M., Van Buchem, F., Afifi, A. M. & Castelltort, S. (2025). Monsoonal imprint on late Quaternary landscapes of the Rub'al Khali Desert. *Communications Earth & Environment*, *6*(1), 255.

Zarins, J. (1978). The camel in ancient Arabia: a further note. *Antiquity*, *52*(204), 44.

Zekri, S. (2020). Oman Water Policy. In: Zekri, S. (ed.), Water Policies in MENA Countries. Global Issues in Water Policy, 23. Springer, Cham. https://doi.org/10.1007/978-3-030-29274-4_6

APPENDIX

I. LIST OF PUBLICATIONS

Decker, V., Falkenroth, M., Lindauer, S., Landgraf, J., Al-Lawati, Z., Al-Rahbi, H., Franz, S. O., & Hoffmann, G. (2021). Collapse of Holocene mangrove ecosystems along the coastline of Oman. Quaternary Research, 100, 52–76.
https://doi.org/10.1017/qua.2020.96 [3]

Decker, V., Gee, C. T., Schucht, P. J., Lindauer, S., & Hoffmann, G. (2022). Life on the Edge: A Powerful Tsunami Overwhelmed Indian Ocean Mangroves One Millennium Ago. Forests, 13(6), 922.
https://doi.org/10.3390/f13060922

Decker, V., Falkenroth, M., & Hoffmann, G. (2024). Sedimentological evidence of Late Pleistocene shorelines in Oman. *Marine Geology*, *477*, 107407.
https://doi.org/10.1016/j.margeo.2024.107407

II. PERSONAL CONFERENCE CONTRIBUTIONS

Decker, V., Grigowski, E., Hoffmann, G. 2022. Digital Outcrops as 3D Models: Their Scientific and Geotouristic Outreach Potential. – 16th European Geoparks Conference I 46th EGN Coordination Committee Meeting. Verbania, Italy. 26-30 September 2022.

Decker, V., Lindauer, S., Landgraf, J., Hoffmann, G. 2019c. Late Holocene silting up of paleolagoons along the coastline of Oman: climate or sea-level forcing? – IGCP Project 639 Annual meeting. Xiamen, China. 13.-19. October 2019.

Decker, V., Landgraf, J., Lindauer, S., Hoffmann, G. 2019b. Sedimentological analyses of paleomangroves reveal Holocene climate and sea-level variations in Oman. – INQUA Congress. Dublin, Ireland. 25-31 July 2019.

Decker, V., Lindauer, S., Landgraf, J., Hoffmann, G. 2019a. Holocene mangrove ecosystems indicate climate variations in Oman. – AMK 37th Annual Meeting. Cologne, Germany. 09-10 May 2019.

Decker, V., Lindauer, S., Landgraf, J., Hoffmann, G. 2018d. Reconstruction of spatial distribution and floral association of Holocene mangrove forests in Oman. – IGCP Project 639 Annual meeting. Taranto, Italy. 16.-23. September 2018.

Decker, V., Lindauer, S., Landgraf, J., Hoffmann, G. 2018c. Paleolagoonal archives along the Arabian Sea reveal Holocene climate and sea-level variability. GeoBonn Conference. Bonn, Germany. 02.-06. September 2018.

Decker, V., Lindauer, S., Landgraf, J., Hoffmann, G. 2018b. Mangrove ecosystems as paleoclimate archives. IGCS Summer School. Aachen, Germany. 14.-25. July 2018.

[3] This publication was extended by a Corrigendum: *Quaternary Research, 100,* 260–262. https://doi.org/10.1017/qua.2021.6

Decker, V., Lindauer, S., Landgraf, J., Hoffmann, G. 2018a. Holocene mangrove forests in Oman: paleo-archives for climate & sea-level variations. ECSM Annual Meeting. Hannover, Germany. 08.-09. June 2018.

Decker, V., Lindauer, S., Landgraf, J., Hoffmann, G. 2017. Mangrove ecosystems as a key to understand Holocene climate and sea-level changes. IGCS Workshop. Chennai, India. 23.-26. October 2017.